Indira Gandhi Centre for Atomic Research

Annual Report 2025

Government of India
Department of Atomic Energy
Indira Gandhi Centre for Atomic Research
Kalpakkam - 603 102

Contents

Address for Correspondence

Shri J. Rajan
Chairman, Editorial Committee
Head, Scientific Information & Networking Division
Indira Gandhi Centre for Atomic Research
Kalpakkam - 603 102
Phone : +91-44-27480281
Email : rjn@igcar.gov.in

e-Copy available at: http://www.igcar.gov.in

Published by
Planning & Human Resource Management Division
Safety, Quality & Resource Management Group
Indira Gandhi Centre for Atomic Research, Kalpakkam - 603 102

Foreword

Dear Colleagues,

I am delighted to release the IGCAR Annual report of 2025. The report highlights accomplishments in R&D pertaining to fast reactor and associated fuel cycle technologies as well as in the frontier areas of basic and applied research.

The Fast Breeder Test Reactor (FBTR), which is the flagship reactor of the second stage of our nuclear power programme, continued to operate at its design power of 40 MWt. During the current 34th irradiation campaign of FBTR, the cumulative thermal energy generated was 32,590 MWth, and the total electrical energy delivered to the grid was 6.355 million units.

As a step forward towards achieving net zero emission, works related to integrating the Copper–Chlorine thermo-chemical cycle based hydrogen production facility at FBTR has commenced, and the required steel structure with platforms and staircases has been fabricated, erected and installation of equipment is in progress, it is expected that we may be able to demonstrate production of nuclear hydrogen by the end of Jan 2026.

IGCAR has been consistently supporting various milestone activities of PFBR. Last year, there was a major setback with the transfer pot of the Inclined Fuel Transfer Machine (IFTM) facing an obstruction and could not reach the bottom. Investigations using a specially designed “Under Sodium Ultrasonic Scanner” revealed that one of the two 31° tilting rails in the Primary Tilting Mechanism (PTM) was dislocated. To address this, a direct fuel loading system was conceived, designed, fabricated, erected and commissioned through the dedicated efforts of colleagues from IGCAR and BHAVINI. For retrieval of the displaced rail, a full-scale mock-up facility was created at BHAVINI, where teams from BHAVINI and BARC successfully developed and tested the required tools. It is heartening that fuel loading into the reactor core for the First Approach to Criticality has commenced and is progressing smoothly and around 35% core loading has been completed.

Simultaneously, the NDE inspection module of the DISHA-V2 in-service inspection vehicle, consisting of eight ultrasonic transducers and one eddy current probe for inspecting the dissimilar weld between the main vessel and the roof slab, has been successfully deployed at PFBR after qualification at high-temperatures and inspection in one of the sectors has been completed.

The ^{233}U fuelled Kalpakkam Mini Reactor (KAMINI) is continuing its successful operation for testing of various neutron detectors, Neutron Activation Analysis (NAA), Neutron radiography of fresh & irradiated fuels and Shielding experiments.

In-principle approval has been obtained from the Atomic Energy Commission (AEC) for a 100-120 MWth FBTR-II, along with associated facilities for metal fuel fabrication, post-irradiation examination, and pyro-processing of metal fuel. The primary objective of FBTR-II will be the development and testing of metal fuel at a one-to-one scale for a 500/1000 MW fast reactor. Secondary objectives include green hydrogen production, isotope production (both strategic and commercial), material irradiation studies, and minor actinide burning studies.

A conceptual physics design for the 100-120 MWth FBTR-II core has been completed. The design is based on driver carbide fuel and test metal fuel. In addition, approval has also been obtained for sodium intermediate heat exchanger (IHX) and pump test facilities to support the large-scale expansion of the fast reactor programme.

A large experimental sodium test facility has been commissioned at the Sodium Technology Complex. The facility, constructed with Austenitic Stainless Steel 316L(N), includes major sodium handling systems such as test vessels, storage tanks, a heater vessel, heat exchangers, an electro-magnetic pump, and a full purification circuit. Sodium flow has been established in all paths, and the facility will serve as a test bed for design optimization and provide valuable inputs for future Fast Breeder Reactors.

In 2025, significant progress was achieved in our Reprocessing Programme with 67th campaign completing successfully and initiation of 68th campaign at Compact Reprocessing of Advanced Fuels in Lead Cells (CORAL) facility. CORAL continues to achieve high recovery and decontamination rates and remains a unique facility for reprocessing high burn-up carbide fuels.

At the Demonstration Fast Reactor Fuel Reprocessing Plant (DFRP), four campaigns for processing FBTR spent fuel with a burnup of 155 GWd/ton were successfully completed, since its hot commissioning in April 2024. The fifth campaign is currently in progress.

In addition, recovery of Neptunium-237 (^{237}Np) from the PUREX

process stream has been successfully demonstrated, with approximately 1,800 mg separated from the uranium product stream. ^{237}Np can be used to produce Plutonium-238, which serves as a source material for Radioisotope Thermoelectric Generators (RTGs). Curium-244 (^{244}Cm) has also been successfully isolated from the PUREX process stream.

Towards development of Pyro-Processing, fresh 2 kg U-Zr sodium bonded fuel pin was cut, sodium was distilled out and loaded in the electro refiner. After electro refining about 1.6 kg of uranium was retrieved. Towards R&D related to metal fuel irradiation studies, Irradiation of different composition (Pu/U+Zr) of metallic fuel pins is in progress at FBTR. The maximum burnup attained till date is 37.6GWd/t for 23%Pu-19%EnU-6%Zr fuel pin.

R&D activities in other areas are also progressing well. Notable work includes the development of uniaxial and biaxial fatigue test systems for generating location-specific material properties, completion of long-term performance assessment of SS304HCu and Alloy 617M tubes after 30,000 hours of exposure in the Fireside Corrosion Test Rig at Dadri, and the development of high-performance reinforced green concretes suitable for coastal nuclear plant environments, which have shown excellent resistance to chloride ingress and corrosion.

I am happy to share that the indigenously developed hydrogen sulphide sensors were tested in Heavy Water Plant, at Manuguru. The performance of in-house developed sensor was found to be comparable with the imported sensor functioning already in the plant.

A significant breakthrough has been achieved in the field of quantum communication; IGCAR is developing an alternative to Quantum Key Distribution, called the Quantum Secure Direct Communication.

A new facility, the In-situ Ion Irradiation and Imaging System with FESEM (i4-FESEM), has been established by integrating a field-emission scanning electron microscope with the 1.7 MV Tandetron accelerator beamline. This facility enables real-time observation of micro-structural evolution under ion-irradiation and is the first of its kind in India and only the third such facility worldwide.

In the areas of safety, environment, and health, several important developments were achieved during the year. The site acceptance testing of Wind Profiler involving performance of radar sub-systems, software, data products and its validation using GPS Sonde experiments were completed. Height coverage under different weather conditions was evaluated and the system was made fully operational. The “Remote Sensing-enabled Chemical Emergency Response System (ROCERS Ver 1.0),” developed collaboratively by IGCAR and NRSC-ISRO for the Department of Factories and Boilers, Government of Kerala, was formally inaugurated on 11th October 2025 during the Surakshitam 3.0 International Conclave on Occupational Safety and Health. Additionally, sustained efforts in CdZnTe single-crystal growth for room-temperature gamma spectrometry applications have resulted in achieving an energy resolution of 2.6% (FWHM) for the 667 keV Cs-137 peak, marking a significant enhancement in detector performance.

Our green energy initiatives have been further strengthened with the installation of the “Thermal Energy Storage System” at the North Plant Site. This smart energy management solution shifts air-conditioning (AC) load from peak to off-peak hours by storing thermal energy as latent heat using Phase Change Material (PCM), which freezes and melts to absorb or release energy efficiently. In addition, a major solar PV plant of 2.29 MWp capacity has been installed, raising the total installed solar capacity at the Centre to 3.1 MWp.

The DAE Incubation Centre at IGCAR, registered as AIC-IGCAR-FAST Foundation, continued its activities during the year. In 2025, MoUs were established with HBNI, Startup TN, and AIC-PECF (Puducherry). An IGCAR-patented technology, remotely operated self-locking fixture for wall-mounted equipment in contaminated enclosures was transferred to a start-up firm during November, 2025

In this year, we had celebrations and commemorations for achievement of key milestones. Fortieth anniversary of the Fast Breeder Test Reactor (FBTR) achieving first criticality was celebrated on 18th October, 2025 with Shri K. N. Vyas, Homi Bhabha Chair Professor and former Chairman, Atomic Energy Commission & Secretary, DAE, gracing the day as our Guest. A commemorative Coffee Table Book on FBTR was formally released during the event. Senior dignitaries and former associates of FBTR were present, and their contributions to the reactor’s development and sustained performance were acknowledged.

A significant scientific achievement announced during the event was the successful in-house separation of Phosphorus-32 (^{32}P) from irradiated Strontium Sulphate ($SrSO_4$) pellets in FBTR for the first time. The separated ^{32}P was formally handed over to the Chief Executive, BRIT, marking an important milestone in radioisotope production for societal applications. A photo exhibition depicting major milestones in the evolution of FBTR was also inaugurated.

Swachhata Pakhwada-2025 was observed with the same excitement to include, “Shramdaan”, a beach cleaning drive with students from schools and a cleanliness drive in Sadras Village, alongside systematic cleaning and weeding of records at IGCAR. A Nisargruna bio gas-plant of 500kg capacity was established at IGCAR to transform biodegradable canteen waste into clean biogas. As part of "World Environment Day 2025", tree plantation was carried out at north DAE campus during July 2025. As part of the Swachhata Hi Seva-2025 campaign, various activities have been carried out at IGCAR under “Swachhotsav” theme: - ‘Ek Ghanta, Ek Din, Ek Saath’. As part of National Science Day, the Brilliant Bharath Hackathon was conducted, encouraging UG, PG students, and researchers to propose innovative solutions to real-world challenges.

Our flagship Summer Training in Physics and Chemistry (STIPAC) programme was also successfully conducted, offering valuable academic enrichment to 70 M.Sc. students. In addition, 20 M.Sc. students from various engineering and science colleges across Tamil Nadu took part in the Summer

Training Programme in Physics (STPP-2025), organized in collaboration with Science City, Department of Higher Education, Government of Tamil Nadu.

The 32nd Prof. Brahm Prakash Memorial Materials Quiz (BPMMQ), a national event was conducted to promote awareness among high school students about the vital role of materials in nation-building, particularly in the peaceful applications of atomic energy. Ninety students participated in this event

Further, in alignment with national capacity-building initiatives, a three-day training programme was conducted as part of the Capacity Building Commission's Rashtriya Karmayogi - Large Scale Jan Seva Programme, aimed at fostering a spirit of public service (Seva Bhaav). As part of its outreach activities, Anu Awareness Yatra-2025 was organized in collaboration with professional bodies. The yatra commenced from Kalpakkam, Tamil Nadu, and concluded at Kaiga, Karnataka, covering over 1,100 km and many educational institutions, with the active participation of nearly 10,000 students and 500 faculty members and teachers.

Our Centre continues to attract a large number of visitors every year. This year about over 2,800 students and faculty from various schools and colleges, along with 770 visitors including members of the public and VIPs, had visited our centre. Apart from this, more than 150 students have pursued their postgraduate or undergraduate projects at the Centre. As part of OCES outreach programme, Placement Officers Meet was organized at IGCAR on 8ww January, 2025. Around 27 placement officers from various colleges across Tamil Nadu actively participated in this meet.

The IGC Lecture Series, which commenced in July 2024 continued this year with a total of 62 lectures completed so far, on diverse topics, highlighting achievements, challenges overcome, and the Centre's preparedness to meet the Amrit Kaal vision targets.

An online portal has been developed in-house and launched for booking online appointment with the specialist doctors in DAE hospitals at Kalpakkam, Anupuram, IMSc (Chennai) and Pallavaram (Chennai). This digital platform was made available to the serving and retired employees of all the DAE units being served by GSO Hospital, Kalpakkam, to enable them to book appointments for themselves and for their dependant family members.

As we look ahead to 2026, in addition to ongoing R&D and routine activities across various groups of IGCAR, our focus will remain on several key areas. These include supporting the integrated commissioning activities of PFBR towards the First Approach to Criticality, operating DFRP with spent fuel from fast reactors and ensuring the recovery of strategic materials, sustaining the operation of FBTR at 40 MWt with irradiation of advanced FBR structural materials, isotope production, metal fuel irradiation, and hydrogen production activities, and advancing activities such as detailed project report towards realizing the conceptualized FBTR-II along with its proposed front-end and back-end facilities.

The accomplishments achieved so far reflect the hard work and commitment of all our colleagues, and I look forward to your continued support in the coming year to achieve further professional growth, productivity, and sustained progress across all our endeavors.

I look forward to your support and co-operation in the coming year 2026!

(Shri C. G. Karhadkar)
Distinguished Scientist &
Director, IGCAR

Our Primary Mission

To conduct a broad based multidisciplinary programme of scientific research and advanced engineering development, directed towards the establishment of the technology of Sodium Cooled Fast Breeder Reactors (FBR) and associated fuel cycle facilities in the Country. The mission includes the development and applications of new and improved materials, techniques, equipment and systems for FBRs, pursue basic research to achieve breakthroughs in Fast Reactor technology.

Editor's Desk

Dear Reader,

I am delighted to present the Annual Report of IGCAR for 2025 as the Editorial Committee Chairman.

This year, the annual report has 103 technical articles. A significant portion of this report reflects the progress in mission-specific activities of IGCAR concerning FBTR, PFBR, R&D on Fast Breeder Reactors, and the Fuel Cycle. The rest of the chapters indicate the basic research essential for sustained growth in research and development, technology transfers and societal benefit programs. Other developmental activities are part of the chapter on infrastructure and resource management.

The articles have gone through numerous editing stages to ensure correctness and readability. I convey my sincere thanks to the Editorial Committee for their dedicated efforts in successfully bringing out the Annual Report.

Chapter I on Fast Breeder Test Reactor has articles that focus on the 40 years of safe and sucessful operation of FBTR, Installation and Commissioning of Seismically Qualified 48 V DC Class-I Power Supply Charger at FBTR, Carrier-free ^{32}P Production in FBTR, Separation and Quality Control at multi-Curie Activity Levels, Periodic Safety Review (PSR) for KAMINI Reactor etc.

Chapter II on Prototype Fast Breeder Reactor highlights the commissioning status of PFBR. Articles on design of Portable Sub-Assembly Handling Flask for PFBR Initial Fuel Loading, design of Permanent Transfer Pot in IVTP for PFBR Vertical Fuel Handling Scheme, Under Sodium Ultrasonic Imaging of the Internals of the Primary Tilting Mechanism (PTM) of Inclined Fuel Transfer Machine (IFTM) of PFBR etc. discuss the challenges faced during fuel loading and how were they overcome.

Chapter III on R&D for FBR has articles about the centre's efforts to develop indigenous technology for future nuclear reactor programs. There are various articles on R&D for FBR namely feasibility study of Gas based Reactor Vault Cooling System for FBTR-2, Conceptual Design and Preliminary Sizing of Primary Sodium Pump for FBTR-2, Design Qualification of Indigenously Developed Sodium Service Valves for Indian FBRs etc.

Chapter IV on Fuel Cycle consists of articles that showcase the latest development carried out towards recovery and purification of Strontium-90 from FBTR Reprocessing Waste and Production of Carrier-Free Yttrium-90, recovery of Neptunium-237 from spent nuclear fuel discharged from FBTR etc.

Chapter V on Basic Research contains articles on influence of Thermo-mechanical Treatment on Creep Properties of Austenitic 316LN Stainless Steel, establishment of Neutron Reference Fields for Calibration of Neutron-Measuring Instruments etc.

Chapter VI on Infrastructure and Resource Management that highlights the efforts and augmentation of essential services, public awareness, and infrastructure management. Article on Construction & Commissioning of Nisargruna Biogas Plant at IGCAR: Creation of Wealth from Waste, DAE Hospital Kalpakkam – Online Hospital Appointment System etc. are discussed.

Chapter VII has details on the publications, the events, awards, organization, and a summary of the activities of various groups of IGCAR.

We welcome feedback from readers concerning the quality of the presentation and the technical content therein. We thank the Group Directors for their support and the enthusiastic authors for providing quality articles in the stipulated time. I take this opportunity to thank the editorial team and Dr. Vidya Sundararajnan, Associate Director, SQRMG in bringing out the Annual Report in expected quality.

The committee sincerely thanks Shri C. G. Karhadkar, Director, IGCAR, for his keen interest, continued guidance and support towards bringing out the publication in its present form.

Shri. J. Rajan,
Chairman, Editorial Committee &
Head, Scientific Information & Networking Division

Chapter - I

Fast Breeder Test Reactor

I-01 40 Years of Safe & Successful Operation of FBTR

Fast Breeder Test Reactor (FBTR) continues to be the flagship of the second stage of the Indian nuclear power program. It continues to spearhead India's advancement in fast reactor technology. Operating at its full design capacity of 40 MWt for the last five successive power campaigns, with TG connected to grid delivering ~10 MWe, FBTR plays a pivotal role in serving as a dynamic test bed for advanced reactor fuels, structural materials, testing the indigenously developed neutron detectors in a high-flux fast neutron environment and production of radioisotopes such as Strontium-89 & Phosphorus-32 etc.

Beyond research, it serves as a vital training ground for the next generation of fast reactor operators, reinforcing India's leadership in sustainable nuclear energy.

FBTR achieved the major milestone of 40 years of safe & successful operation on 18th October 2025. To commemorate the momentous occasion, the 40th Anniversary of First Criticality of FBTR was celebrated in a grand manner.

Evolution of FBTR Reactor Core to the Target Power of 40 MWt

FBTR is a 40 MWt, sodium-cooled, loop-type fast reactor with indigenously developed MK-I fuel assembly having 70% PuC & 30% UC as the driver fuel, and achieved its first criticality on 18th October 1985 at 22:10 h, marking a historic milestone in India's nuclear energy program. It attained criticality with 22 MK-I FSAs. Initially, the reactor was operated at 10.5 MWt. After gaining sufficient confidence in the performance of indigenously developed carbide fuel, reactor power was progressively increased from 10.5 MWt to 32 MWt by expanding the core by adding fresh SAs.

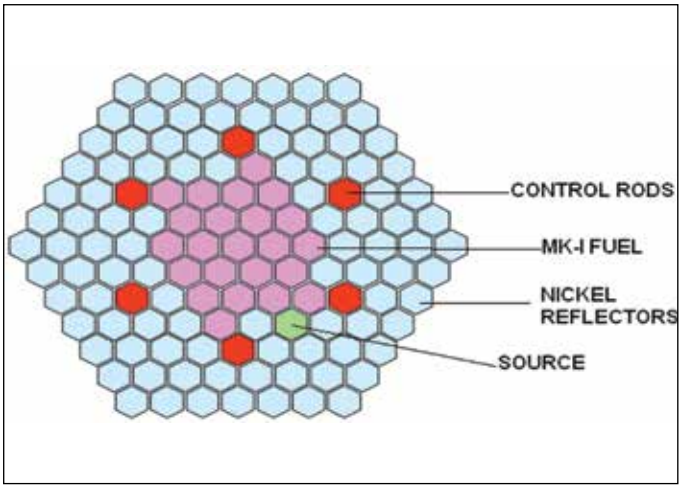

Fig. 1: Core configuration at first criticality in 1985

FBTR achieved its rated design power of 40 MWt on 7th March 2022 in the 30th irradiation campaign with 68 Mark-I FSAs & by adding four B_4C poison (enriched 50% in B^{10}) subassemblies in the reactor core to ensure adequate shutdown margin. Subsequently, three more mission-based campaigns were successfully completed at 40 MWt, and currently, the 34th irradiation campaign is in progress.

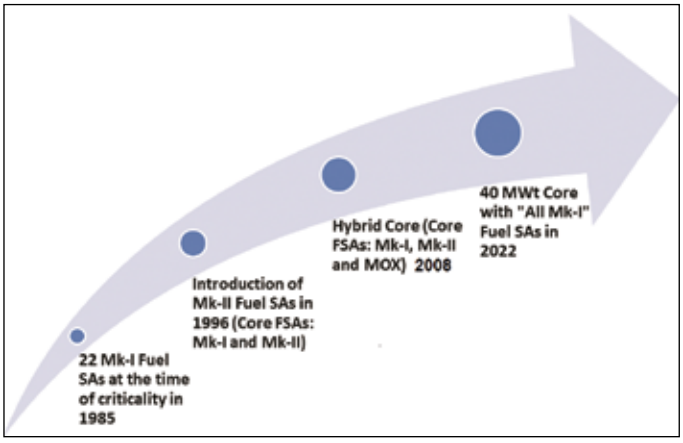

Fig. 2: Evolution of reactor core from 1985

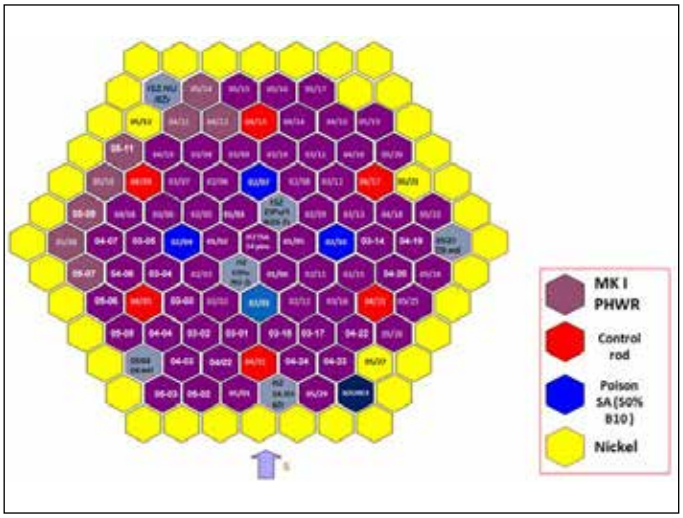

Fig. 3: Core configuration during the 30th campaign in March 2022 (40 MWt operation)

Operational Experience

With over forty years of operation, FBTR has achieved the following major milestones:-

- Excellent performance of Carbide fuel & closure of Carbide fuel cycle with a lead Mark -1 FSA reaching 165 GWd/t & more than 2000 fuel pins reaching 155 GWd/t.
- Irradiation of various binary & ternary sodium bonded metallic fuel pins and advanced structural materials such as D9, IFAC-1, Gr. 91, and 9Cr-ODS steels.

- Irradiation of PHWR structural materials, PFBR test MOX SA up to a burnup of 112 GWd/t.
- Development of a radioisotope production programme, yielding Strontium-89 and Phosphorus-32 for medical and industrial applications.
- Testing and calibration of High-Temperature Fission Chambers (HTFCs), Neutron Detectors, and other in-core sensors for PFBR and future FBRs.
- Sufficient confidence has been obtained for the smooth manual power control in FBTR.
- Optimization of reactor trip parameters to achieve the maximum availability without compromising the safety of the reactor.
- Cumulative electrical energy generated so far is 156 Million Units.
- High reliability of sodium systems, maintaining excellent sodium purity for over four decades.
- Excellent performance of centrifugal Sodium pumps- (Cumulative hours of operation: around 11 Million Hours).
- Performance of Steam Generators satisfactory (Cumulative hours of operation: 54678 Hours) (One minor tube leak event & minor leak from the thermal baffle joint in the shell side).
- Satisfactory performance of the Triplicated SG Leak Detection System (SGLDS).
- Satisfactory performance of ED-20 Central Data Processing System.
- Impeccable safety record - no radiological incidents since commissioning.

Fig. 4: Shri K. N. Vyas, Homi Bhabha Chair Professor & former Chairman AEC & Secretary, DAE addressing the gathering

Fig. 5: Shri C.G. Karhadkar, Distinguished Scientist & Director IGCAR addressing the gathering

Fig. 6: Shri S. Sridhar, Outstanding Scientist & Director RFG addressing the gathering

Fig. 7: Dignitaries of the department gracing the 40th anniversary celebrations

Celebration of 40th anniversary of first criticality of FBTR

I-02 Operation of FBTR at 40 MWt in the 34th Irradiation Campaign

Introduction

The Fast Breeder Test Reactor (FBTR), the flagship facility of the Indira Gandhi Centre for Atomic Research (IGCAR), continues to fulfil its mission of testing advanced reactor fuels, including metallic fuels, structural materials, indigenously developed neutron detectors, and the production of radioisotopes for societal applications in a fast neutron flux environment. FBTR also serves as an important training facility for future fast reactor operators.

FBTR Operational History

The indigenously developed MK-I fuel assembly, consisting of 70% PuC & 30% UC, serves as the driver fuel for FBTR. Initially, the reactor operated at 10.5 MWt. After gaining operational experience and confidence in fuel performance, the reactor power was progressively increased from 10.5 MWt to 32 MWt by expanding the core through the addition of fresh sub-assemblies (SAs). To enhance the Shut Down Margin (SDM), four poison subassemblies containing B_4C enriched with 50% B^{10} were introduced in the second ring. Following this modification, the reactor was successfully operated at the design power of 40 MWt with 68 MK-I fuel subassemblies during the 30th irradiation campaign. Subsequently, three more mission-based campaigns were successfully completed at 40 MWt.

The 34th irradiation campaign commenced on 05th June 2025. After operating the reactor for 34 Effective Full Power Days (EFPDs) at 40 MWt, the campaign was interrupted for taking up the integration of the Cu-Cl facility to the FBTR sodium system for producing clean Hydrogen. After installation and commissioning of Cu-Cl facility, 34th campaign will be resumed to complete the remaining 20 EFPDs of reactor operation.

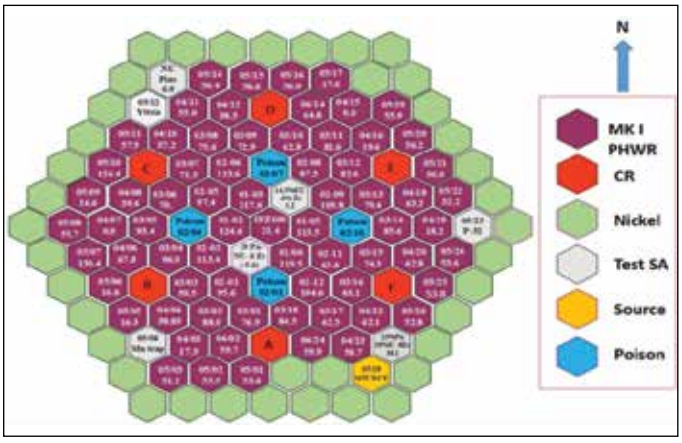

Fig. 1: Core configuration for 34th Irradiation Campaign (40 MWt operation)

Reactor Operation in 34th Campaign

After completing the 33rd irradiation campaign, necessary core changes were made for the 34th irradiation campaign. The core of the 34th campaign has 69 Mark-I FSAs (Fig. 1), one special FSA (IFZ-100) at the core centre, four poison SAs in the second ring, four ISZ-100 SAs with metal fuel pins (i.e. two SAs in first ring & two SAs in fifth ring), two ISZ carrier SAs with Yttrium Oxide pins and Strontium Sulphate pins in the fifth ring for producing Sr^{89} and P^{32} respectively, and steel carrier subassembly containing nickel foil for trapping Mn^{54} in the primary sodium system.

Following are the major missions of the recent irradiation campaigns at 40 MWt:

1) Continued irradiation of the various sodium bonded metallic fuel pins:

- Ternary fuel-1 (23%Pu-19%EU-6%Zr).
- Ternary fuel-2 (19%Pu-Nat U-6%Zr).
- Binary fuel-1 (14.8%EU-6%Zr).
- Binary fuel-2 (Nat U-6%Zr).

2) Irradiation of Yttrium Oxide for the production of Sr^{89} medical radioisotope.

3) Irradiation of Strontium Sulphate for the production of P^{32} medical radioisotope.

4) Irradiation of advanced core structural materials (D9, IFAC-1, Gr. 91 and 9Cr-ODS steels) in a capsule locked in special fuel subassembly IFZ-100.

The 34th irradiation campaign at a target power of 40 MWt with 69 MK-I FSAs core was commenced on 5th June 2025 with startup criticality. After low power physics experiments such as measurement of control rod worth & isothermal temperature coefficient of reactivity, and calibration of Steam Generator Leak Detection System (SGLDS), reactor power was gradually raised with measurement of power coefficient of reactivity at each MWt stabilization.

TG was rolled and synchronized to the grid at 24.0 MWt after obtaining super-heated steam at the outlet of Steam Generator. After stabilizing the reactor parameters for 24 h at 90% of the target power, thermal balance was done and actual power was computed. Also, neutronic channels were normalized with respect to the thermal power. On

22nd July 2025, reactor power was raised to 40 MWt & TG output was raised to 10 MWe. After a cumulative 34 EFPDs of reactor operation at 40 MWt, on 23rd August 2025, reactor was brought to shutdown state. Subsequently, Yttrium Oxide and Strontium Sulphate carrier SAs were removed from core & both were sent to RML to retrieve the capsules. They will be further processed in RCL for the recovery of Sr^{89} and P^{32} radioisotopes. In the vacant slots of the core, two fresh carrier SAs with Yttrium Oxide and Strontium Sulphate pins will be loaded for irradiating the remaining 20 EFPDs of 34th irradiation campaign. The reactor physics and thermal parameters observed in the 34th irradiation campaign at 40 MWt are as follows.

Reactor Physics Parameters	
Parameters	Value
Temperature Coefficient of Reactivity	-3.80 pcm/°C
Power Coefficient of Reactivity	-6.98 pcm/MWt
Burn up Coefficient of Reactivity	-0.64 pcm/MWd
Shutdown margin at BOC (at 180 °C)	6933.0 pcm
Total CR worth	9624.0 pcm

Thermal Parameters	
Parameters	Value
Reactor Power/TG Power	40 MWt/10 MWe
Beginning of the campaign	05.06.2025
End of the Campaign date	23.08.2025
Effective Full Power Days (EFPD)	34
Reactor inlet/outlet sodium temperature	380/480 °C
Central SA outlet temperature	517 °C
Primary sodium loop flow (each)	650 m^3/h
Secondary sodium loop flow (each)	345 m^3/h
SG inlet/outlet sodium temperature	191/456 °C
Feed water flow	72 m^3/h
SG inlet/outlet pressure	135/120 kg/cm^2

I-03 Replacement of Control Rod Outer Sheath based on Fluence Limit

In FBTR, six boron (B_4C - 90% enriched in B^{10}) carbide control rods (Fig. 1) are used for reactor shutdown, regulation of reactor power and for burn-up compensation. These six control rods are placed symmetrically in the core in the 4th ring. The hindrance-free movement of these control rods is therefore essential for the safe operation of the reactor. The control rod assembly consists of:

- The support sleeve on the grid plate.
- The outer sheath in which control rod moves.
- The control rod containing boron carbide.

The outer sheath of the control rod is made of three parts namely foot, hexagonal sheath and handling sleeve welded together. In addition to guiding the control rod, it also houses the labyrinth orifice at the entry to limit the flow to the required value. To prevent the lifting of the outer sheath due to sodium pressure and movement of the control rod, the foot of the outer sheath is locked in the sleeve by a Bayonet -type locking arrangement. The outer sheath is made of stainless steel AISI 316L. The foot has a stellited conical shoulder to provide seating surface for the control rod when it is disengaged from the drive mechanism. Guiding the control rod is achieved by close fit between the cylindrical hole just below the conical cylinder and the long stem of the control rod.

The residence time of the control rod and its outer sheath in the core is limited by the neutron fluence seen by them. The technical specification limits on the fluence are:

- Control rod - 1.14×10^{23} nvt
- Outer sheath - 2.43×10^{23} nvt

At the end of 33rd campaign, it was estimated that the fluence limit on the outer sheath of Control rod-C was approaching the Technical specification limit. Hence, it was planned to be replaced before commencing the 34th Irradiation Campaign.

A detailed special procedure was prepared and the same was submitted and discussed in committee for review of Block Pile Handling Procedures (CRBHP) for approval.

Procedure for Replacement of Control Rod Outer Sheath

In order to create vacancy around the control rod-C for unlocking of outer sheath, the surrounding six Mk-I fuel subassemblies were transferred to periphery. Control rod-C was transferred from its location to control rod storage location in the core periphery and by this transfer operation, the storage location for the control rod was qualified for the first time. Before lifting the outer sheath of control rod from its location, it was rotated by 60 degrees in anti-clockwise direction to unlock it from its supporting sleeve. The outer sheath was discharged and stored in discharge pot kept in the transfer block area of RCB using the discharge flask. Similarly, during charging, the outer sheath of the control rod was rotated by 60 degrees in clockwise direction to lock it to its supporting sleeve provided in the grid plate. After replacing the outer sheath of control rod, the control rod and six subassemblies around the control rod were brought back to their original positions from the peripheral locations.

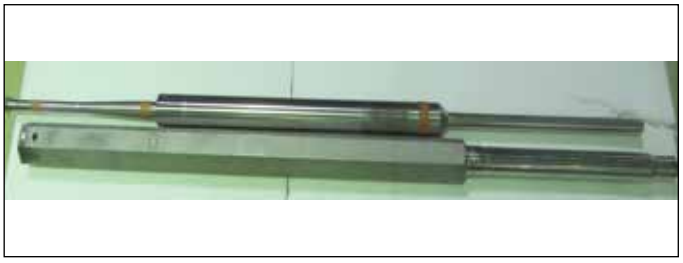

Fig. 1: Control rod and its outer sheath

I-04 Installation and Commissioning of Seismically Qualified 48 V DC Class-I Power Supply Charger at FBTR

The 48 V DC class-I power supply system of FBTR consists of 2 nos. of 48 V DC, 325 A main chargers and 1 no. of standby charger of identical capacity. The 48 V DC control power supply is used for control logic relays of various systems, annunciations, indication lamps (excluding those of 6.6 kV and 415 V switch gear) and solenoid valves. It also supplies the excitation power to DC motor and DC generator field circuit of primary and secondary sodium pumps. Given its role in ensuring decay heat removal, the integrity and reliability of the 48 V DC system are of critical safety significance.

The old chargers were of M/s Forbes & Campbell make, manufactured in the year 1976 and were in continuous service for the past 49 years. As a part of ageing management and post Fukushima retrofits, it was planned to replace the old chargers with state of the art seismically qualified chargers.

In the first phase, one prototype 48 V DC, 325 A charger was seismically qualified in IGCAR SML lab as per the approved test procedure based on the IEEE Standard for Seismic Qualification of Equipment for Nuclear Power Generating Stations, IEEE Std 344-2013.

Originally, these chargers are located in the inverter room, (+4525 mm from FFL) of FBTR fixed by welding the panel base channel to the existing structural framework made of ISMC 125 mm channels. The structural integrity and functional operability of battery charger was confirmed using Review Basis Ground Motion (RBGM) spectra with 5% damping ratio taken as Required Response Spectrum (RRS) . The test matrix consisted of resonance search tests followed by one Safe Shutdown Earthquake (SSE) test for the floor response spectra.

To simulate the site condition, battery charger panel was welded to base channels. The base channels were then welded to base plate bolted to the shake table as shown in Fig. 1. The floor response spectrum for SSE is shown in Fig. 2.

Fig. 1: Prototype 48 V DC charger in shake table

To measure the acceleration responses, four tri-axial accelerometers were used. Towards measuring the structural damage of the panel, seven bi-axial strain gauges were pasted at critical locations. Functional test of the charger was carried out before and after the seismic test and found OK. DC output voltage and current were continuously

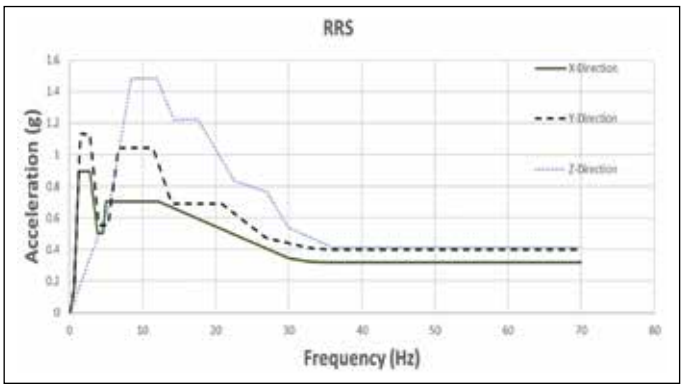

Fig. 2: Floor response spectrum for SSE

recorded during the seismic test and no variations were observed. After successful seismic qualification of the prototype charger, the fabrication of the two main chargers and the standby charger were completed, and the associated I&C works were carried out at FBTR. Fig. 3 shows the old chargers that were in service, and Fig. 4 presents the newly installed chargers at FBTR.

Fig. 3: Old chargers at FBTR

Fig. 4: New chargers installed at FBTR

I-05 Ageing Management of 10 MVA, 33 kV/6.6 kV Main Incomer Transformer 2 at FBTR

At FBTR, there are two 10 MVA incomer transformers (TMtb001 and TMtb002) fed from the 33 kV Central Sub Station through two independent 400 sq mm, XLPE insulated underground power cables. These transformers supply to the 6.6 kV bus sections HTtb100A and HTtb100B, respectively.

These two oil-cooled transformers, manufactured in 1977, have been in continuous operation for the past 45 years with regular preventive maintenance. As part of the ageing management and life-extension programme, major overhauls are carried out every 20 years. The most recent overhaul for both transformers was conducted in 2002.To ensure continued reliability and extend service life, it was decided to perform a complete overhaul of both the 10 MVA transformers. The overhauling of the first transformer (TMtb-001) and its reinstallation at site was successfully completed in 2021. Subsequently, in 2024, the overhauling of second transformer (TMtb-002) was also undertaken and successfully completed.

The technical details of the transformer are given in the following table.

Capacity	10000 kVA
Voltage	33/6.6/3.3 kV
Current	175/875/337 A
Frequency	50 Hz
Type of cooling	Natural Oil Cooling
Tapings (ON load)	+10% to -10% in 17 equal steps (HV side)
Vector Group	YYO(d1)
% Impedence	11.55
Volume of Oil	9000 Ltrs

Fig. 1: Loading on to the truck

The overhaul works were carried out by Voltech Engineering Services Pvt. Ltd., Chennai. The transformer was first isolated, and the oil was drained down to the transportation level. All accessories were then dismantled, and the transformer, along with its components, was safely transported to their facility. Before initiating the overhaul, pre-overhaul tests were conducted at their works in the presence of the department engineer. The core-coil assembly was carefully removed from the tank and subjected to hot-oil washing and vacuum drying to ensure complete removal of moisture from the paper insulation.

The 33 kV side bushings were replaced due to obsolescence and the presence of minor surface cracks. The On-Load Tap Changer (OLTC) was also overhauled. All major accessories—including the Winding Temperature Indicator (WTI), Oil Temperature Indicator (OTI), Buchholz relay, and valves—were replaced with fresh units. After completion of internal work, the core–coil assembly was re-tanked, and the transformer was filled with fresh oil. All routine tests, including high-voltage tests, were carried out, and the results were found satisfactory. The transformer, along with its accessories, was then transported back to site and installed in its designated location. The oil was topped up and circulated, and all commissioning tests were successfully completed, after which the transformer was put back into service.

After 15 days of transformer loading, an oil sample was tested for Dissolved Gas Analysis (DGA), and the results were recorded for future reference.

This overhauling would extend the life of the transformer by 15 more years.

Fig. 2: Vacuum drying of core-coil assembly

Fig. 3: Reinstallation of transformer after overhauling

I-06 COMS – A Web-based Integrated System for Scheduling FBTR Operation and Maintenance Activities

Precise scheduling is crucial for operational efficiency and effective resource management. The Fast Breeder Test Reactor (FBTR) requires meticulous scheduling for co-ordinating operation and maintenance activities involving multiple agencies, necessary approvals, and adherence to safety and surveillance mandates.

To streamline and digitize the monthly scheduling and planning of tasks and activities for FBTR, KAMINI, and IFSB, the Computerized Online Monthly Scheduling (COMS) system was developed and implemented as a secure, web-based solution.

The web-based COMS application provides a clean and responsive user interface for entering, editing, viewing, and updating schedule status. Spring Boot manages the workflow rules, validations, and communication with the database. MySQL stores schedule details, agency information, pre-assigned tasks, and audit trails. Role-Based Access Control (RBAC) ensures that only authorized users can perform specific actions based on their roles. Email services are used to send automated notifications during workflow transitions.

Major functions of COMS are as follows:

a) Manage job schedules for plant systems.

b) Manage predefined schedules such as PM/YPM/ HYPM & Surveillance activities.

c) Manage PRIS(G) & Alarm activities.

d) Manage ECN, FCN and Task Force activities.

e) Manage Civil Works.

With a pre-defined workflow, COMS enables co-ordinated planning, job schedule tracking, and effective communication across multiple agencies and making it ideal for handling complex, collaborative jobs requiring inputs from multiple agencies.

COMS WORKFLOW

The monthly scheduling process begins with updating the reactor state by the Operation Section. Based on plant availability, the Supervisor or System Engineer of each section plans and schedules their activities. The system provides options to create new tasks, carry forward pending work from previous months, include pre-assigned tasks planned for the current or upcoming months, and reinstate cancelled schedules from the last month if required. For new activities, users enter the details in COMS (Fig. 1).

The schedule then moves to the Section Head for approval. Once approved, it reaches the Planner, who coordinates

Fig. 1: User interface for creating schedule in COMS

the job entries from all sections. The combined monthly schedule is then submitted to the Reviewer to ensure completeness and correctness. Finally, the schedule goes to the Approver, who has the final authority to approve and release it (refer Fig. 2).

Fig. 2: Released schedule in COMS

Once released, users can update the status of scheduled work during the month.

COMS improves overall efficiency by reducing manual collation and enabling faster monthly consolidation, while complete audit trails provide clear traceability for every schedule and decision. The availability of historical schedules also supports analysis of overall plant and section-wise performance, enabling data-driven planning and better resource allocation.

Fig. 3: Statistics overview as shown in COMS

I-07 RWPS – A Web-based Integrated Radiological Work Permit System for RML

The Radiological Work Permit (RWP) system followed in RML is a critical administrative control system designed to ensure radiological safety while carrying out work activities in radioactive areas. To bring this process online, the Computerized Online Radiological Work Permit System (RWPS) was developed and implemented as a secure, web-based platform tailored for RML's operational needs.

RWPS digitizes the entire permit lifecycle—from the creation and review of the work permit to its approval, execution, and closure—replacing manual paperwork with a streamlined digital workflow. This enables faster permit issuance, improved planning, real-time tracking, and enhanced regulatory compliance across all radiological work activities.

The web-based RWPS application provides a clean and responsive user interface. Built on the Spring Boot framework and backed by a MySQL database, RWPS securely manages user profiles, permit records, active areas, work types, and comprehensive audit trails. The system implements Role-Based Access Control (RBAC), ensuring that only authorized personnel can perform specific actions based on their designated roles, thereby safeguarding data integrity and operational safety.

RWPS offers a complete suite of integrated features:

a) Managing radiological permit for active areas.
b) Generating compliance and operational reports.
c) Managing TLD dose for users & contractors.
d) Maintaining and updating active areas.
e) Managing permitted types of work.
f) Administering users and roles.
g) Documentation and auditing.

The system enforces a predefined, multi-level approval workflow that supports coordinated planning and clear communication among radiation safety officers, work supervisors, and management. This structured approach is especially effective for complex tasks requiring approvals at multiple levels and ensures safety without compromising operational efficiency.

The RWP predefined workflow begins when the permit holder completes all required fields (Fig. 1), including the designated working area, types of work, applicable area-specific checklist, detailed work description, anticipated radiological and non-radiological hazards, and the list of personnel or contractors involved. Upon submission, the system assigns a unique RWP number and initiates a structured approval sequence:

Fig. 1: User interface for creating permit in RWPS

a. **Level-1 (Shift-in-Charge):** Verifies operational readiness (e.g., ventilation, power, access).
b. **Level-2 (Area-in-Charge):** Validates the safety checklist and confirms area suitability
c. **Level-2A (Head of Division):** Validation is required for high-risk tasks (e.g., hot-cell entry).
d. **Level-3 (Health Physicist):** Assesses radiological conditions, verifies shielding & contamination controls, ensures safety compliance and populates HP-specific fields. Only then, work permit is activated and work may commence.

At any stage, reviewers may return the permit for corrections or cancel it outright if safety, operational, or regulatory concerns exist.

Upon task completion, the permit holder surrenders the permit. The Health Physicist logs actual DRD doses, and the Area-in-Charge verifies all post-work checklist items. Once both are recorded, the permit is formally closed by the permit holder.

This end-to-end digital trail in RWPS ensures complete traceability, accountability, and strict adherence to radiological safety protocols throughout the entire work cycle. It provides easy tracking of permit status (Fig. 2) and improves overall efficiency by reducing manual collation. Ultimately, RWPS strengthens RML's commitment to protecting personnel, the environment and facility integrity, setting a benchmark for modern, technology-driven radiation safety governance.

Fig. 2: RWPS dashboard

I-08 Periodic Safety Review (PSR) for KAMINI Reactor

The KAMINI reactor is a U^{233}-fuelled, BeO-reflected, and DM-water-moderated research reactor. Its first criticality was achieved in October 1996. In 2015, after completing the first comprehensive PSR, the plant was granted operating licence for five years. After the submission of the Application for Renewal of Authorization (ARA) in 2020, the plant was relicensed as per the AERB safety guidelines for renewal of the operating licence up to June 2025. As part of the relicensing process beyond 2025, a comprehensive PSR was carried out for the KAMINI reactor as per the AERB Safety Guide No. AERB/SG/O-12. The objective of the PSR is to ensure that KAMINI continues to operate safely and provides a high level of protection to the public and the environment.

PSR involves a detailed review of the plant design with respect to current codes and guides; the performance of safety systems and safety support systems; the status of SSCs important to safety; the effects of system modifications; ageing management; results of In-Service Inspection (ISI); safety analysis; the use of operating experience from other NPPs and research findings; manpower and training; radiological protection practices; leadership and management for safety; human factors; emergency preparedness; and pending regulatory issues, etc. The focus areas are divided into 14 safety factors, and their review observations and findings are addressed in individual Safety Factor (SF) reports, as listed below:

PSR Safety Factors as per AERB guide	Description
01	Plant Design
02	Actual Condition of SSCs
03	Equipment Qualification
04	Ageing Management
05	Utilization
06	Deterministic Safety Analysis
07	Hazard Analysis
08	Operational Safety Performance
09	Use of Experience from other NPPs & Research Findings
10	Leadership and Management for Safety
11	Procedures
12	Human Factors
13	Emergency Planning
14	Radiological Impact on Environment

Design compliance with present practices was also reviewed. One of the major tasks undertaken was the residual life assessment of plant equipment as part of ageing management for non-replaceable components such as the neutron beam tubes and the reactor vessel. Since KAMINI operates at low temperature and pressure, the fuel and structural materials are not subjected to harsh conditions, except for irradiation effects from neutron flux. The irradiation effect on the reactor vessel and beam tubes is very low, and sufficient residual life remains for these components. Several modifications have been implemented based on operational experience, equipment obsolescence, and maintenance convenience to enhance safety, reliability, and performance during reactor operation. Major refurbishment activities—such as the replacement of neutronic channels, replacement of the Safety Control Plate (SCP) drive mechanism, development of the Integrated Control and Information System (ICIS), and the installation of UPS units—have contributed to increased availability and a reduction in reactor trips.

Being a research reactor, the plant continues to serve as a national facility for neutron activation analysis, neutron radiography, detector testing, shielding experiments, and reactor physics experiments.

In 2012, one of the fuel SAs (at core position B1), which was contributing to increased water activity, was removed from the core, and a spare Pu–Al SA was loaded in its place.

The visual examination of the removed fuel SA revealed distinct de-bonding and was sent to BARC for PIE. Subsequently, all core FSAs were photographed using a remote high-resolution camera, and image analysis indicated de-bonding of the clad at the top of the fuel plates

Fig. 1: KAMINI core

of the FSAs at positions B2, C2, and C1. Considering that the defective FSAs are only gas leakers, operation of the KAMINI reactor has been continued with the three de-bonded fuel subassemblies, with a water activity limit of 600 Bq/ml, after obtaining safety clearance from AERB.

As part of the development of new fuel to replace the existing fuel, various options are being explored for revamping the KAMINI reactor core. After carrying out a detailed review in KORC and incorporating its comments, the PSR document covering 14 Safety Factor (SF) chapters was submitted to AERB for the renewal of the plant licence beyond July 2025. Following a multi-tier safety review by AERB, the operating licence for the KAMINI reactor was renewed up to 30th June 2030. Based on the safety assessment carried out, the plant can be operated safely without undue risk to the facility, working personnel, the public, or the environment.

I-09 Level-1 Full Power Internal Events PSA of FBTR

Fast Breeder Test Reactor (FBTR), is a 40 MWt sodium cooled loop type reactor located at Kalpakkam, Tamil Nadu. FBTR is in operation since 1985 with different core configurations. FBTR uses mixed carbide fuel (PuC/UC).

Level-1 Probabilistic Safety Assessment (PSA) has been performed for FBTR. The scope of the analysis covers modeling of internal events at full power operation of the reactor with core as the source of radioactivity. Various elements of level-1 PSA such as initiating event (IE) analysis, system analysis, accident sequence models development, Common Cause Failure (CCF) analysis, Human Reliability Analysis (HRA) and uncertainty analysis are addressed. This study considers 68 IEs grouped into 39 event groups. The front line systems considered are shutdown system (LOR and SCRAM modes) for reactivity control and shutdown, decay heat removal through normal heat transport path, pre-heating and emergency cooling system and biological shield cooling system. In addition to the front line systems, different support systems such as electrical power supply system (class-I, II & III), compressed air system and service water system are also considered in the analysis. For system modelling, fault tree with immediate cause approach is used. The event progression given the occurrence of an IE is modelled through event trees. Small event tree large fault tree approach is used in this analysis.

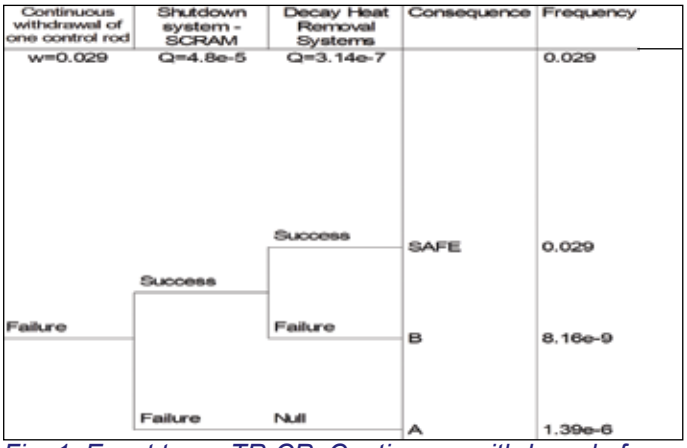

Fig. 1: Event tree - TR-CR: Continuous withdrawal of one control rod

The modelling has been performed using the software ISOGRAPH WORKBENCH v-10.2. One example event tree is shown in Fig. 1. HRA has been performed for various safety critical human actions. α, β factor models are used to model CCF of redundant safety equipment. Input data for this analysis is based on FBTR operating experience and generic sources like IAEA TECH DOCs. Uncertainty in the input data are propagated through the logic models in uncertainty analysis. The primary sources of information for this PSA are design reports, plant safety analysis reports and technical specifications.

The results of the study comprises of statement of Core Damage Frequency (CDF) along with uncertainty bounds, identification of important accident sequences, and list of importance measures for all basic components. The estimated energetic CDF (category-A) is ~2.0E-05 /y and non-energetic CDF (category-B) is ~9.28E-05/y. The total CDF (both energetic & non-energetic) is ~1.13E-04 /y. The 5% lower bound total CDF is estimated to be 8.26E-06 /y and the 95% upper bound value is 2.49E-04 /y. As observed in Fig. 2, the IE groups LOF-SEC-2 (Loss of both secondary sodium loops) and TR-RT-1 (Reactivity Transients) contribute significantly to the estimated CDF of FBTR.

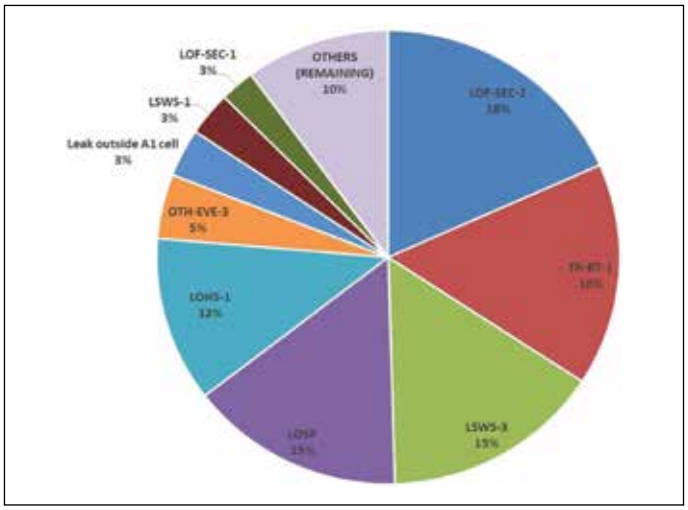

Fig. 2: Contribution of different IE Groups to CDF

I-10 Carrier-free ^{32}P Production in FBTR: Separation and Quality Control at multi-Curie Activity Levels

^{32}P is a pure beta emitter with β_{max} energy of 1.71 MeV and decays with a half-life of 14.28 d. ^{32}P is extensively used for tagging biomolecules, labeled nucleotides and molecular biology kits and being supplied nationwide for advanced research in biology, agriculture, healthcare and genetic engineering. High specific active and carrier free ^{32}P can be produced in FBTR through $^{32}S(n,p)^{32}P$ reaction. 110 numbers of strontium sulphate ($SrSO_4$) pellets having weight of 1 g each were encapsulated in double walled SS 316 clad and enclosed in a steel carrier sub-assembly. The $SrSO_4$ pellets were irradiated in 5th ring of FBTR at 40 MWt power for 33 days. The pellets were transferred to RCL Hotcells after their cutting at RML Hotcells.

Fig. 1 Dissolution and processing of FBTR irradiated $SrSO_4$ target inside Hot cell and Ion-exchange purification of ^{32}P.

25 Pellets of irradiated $SrSO_4$ were dissolved in titanium vessel inside Hotcell using boiled sodium carbonate solution for 24 h to form $SrCO_3$ residue and Na_2SO_4 solution. The ^{32}Phosphate is present in both $SrCO_3$ residue and Na_2SO_4 solution. The residue $SrCO_3$ after its filtration was dissolved in hydrochloric acid and subsequently added with $FeCl_3$ and ammonia solution. This makes the phosphate to co-precipitate along with $Fe(OH)_3$ precipitate. Similarly, the ^{32}Phosphate in Na_2SO_4 solution was co-precipitated independently with $Fe(OH)_3$. The precipitate obtained in both cases was dissolved in 1M HCl and mixed. The solution was conditioned to 0.1 M HCl, which was subjected to cation-exchange chromatography to hold the Fe(III) and Sr(II) ions. The ^{32}P was eluted as phosphate using 0.1 M HCl and was further purified using anion-exchange chromatography to purify the anion impurities such as sulphate. The ^{32}P was eluted using 0.01M HCl in

Fig. 2 ^{32}P source sealing in vials and final package for dispatching to BRIT-RC, Hyderabad

about 20 mL and the sulphate was held inside the resin. The final eluted ^{32}P solution was repeatedly evaporated with the addition of Millipore Bio-Pak water under an IR lamp to reduce the volume and then adjusted to a small volume at pH 6. The purified ^{32}P fraction was subjected to routine quality control protocols.

The radionuclidic purity was carried out using alpha and gamma spectrometric techniques and found to contain no alpha and gamma emitting impurities. Liquid scintillation counting was carried out to determine the total ^{32}P activity separated and followed decay kinetics to monitor its half-life. The ^{32}P was quantified to be about 1.2 Ci as on separation date and found to be free from any other beta impurities as the half-life determined to be about 14.2 days which is in good agreement with literature value. The radiochemical quality control was tested using Thin Layer Chromatography (TLC) method and found to have more than 95% radiochemical purity (RCP). Chemical impurities were found to be less than detection limits of ICP-OES instrument for the elements like Al, Ti, Ca, Mg, Fe, Sr, P and Pb. Specific activity of ^{32}P source was determined using spectrophotometry and found to be 6000-8000 Ci/mmol as on separation date.

The total activity of ^{32}P produced at the end of irradiation for 33 days was calculated to be around 40 Ci / 100 g of $SrSO_4$ target. The present ^{32}P source separated from 25 g batch was made in to 3 doses of 150 mCi each and supplied to BRIT-RC, Hyderabad for quality assurance of the ^{32}P source.

I-11 Core Physics Studies on Feasibility of Pu-238 Production in FBTR-40 Core

Pu-238 is an important heat source used in Radioisotope Thermoelectric Generators (RTG) with preferable properties of suitable half-life (88 y), high specific power and (0.56 W/g) and minimum shielding requirements. Purity of Pu-238 is stringent (>85% Pu-238) with minimum impurities (Pu-236 <2 ppm). The isotope can be produced in nuclear reactors with suitable neutron spectrum. The feasibility of Pu-238 production by the irradiation of Np-237 in FBTR is investigated. The fast spectrum of FBTR is tailored for better Pu-238 yield with the help of neutron moderator ZrH.

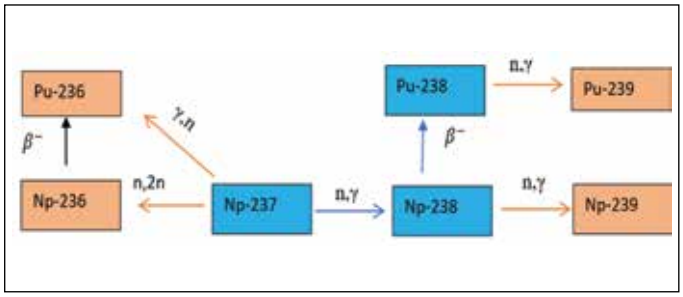

Fig. 1: Pu-238 production path from Np-237 target

FBTR core is modelled with Monte-Carlo code and study is performed with latest ENDF data and depletion code ORIGEN. The irradiation location is optimized with requirements of maximum neutron flux and minimum increase in core reactivity and associated LHR.

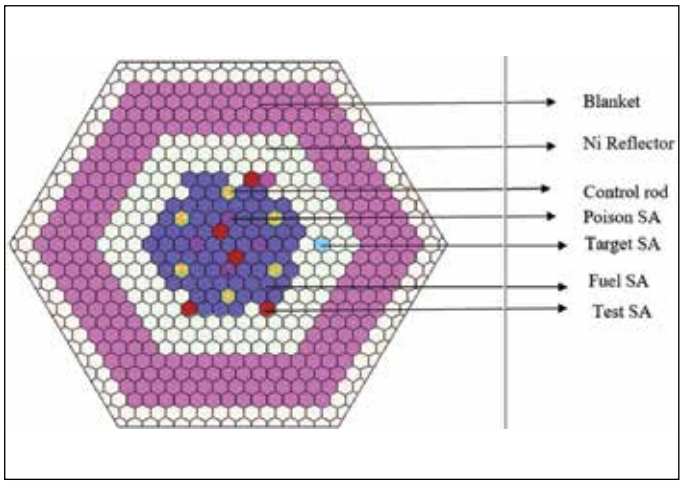

Fig. 2: Radial cross-section of FBTR core modelled in Monte-Carlo

The irradiation target is planned to be in an irradiation capsule inside the special sub-assembly ISZ-100. Capsule have an outer diameter of 20 mm and an inner diameter of 18 mm and inserted into the bore. Within the irradiation capsule, a pin with an outer diameter of 6.6 mm is positioned at the centre. This pin contains three pellets each with 5 mm length constitutes the irradiation target. It is surrounded by a layer of moderator.

The study has been carried out as a function of moderator thickness, irradiation time and self-shielding. To reduce self-shielding and to improve yield, a dispersed target of Al_2O_3 (70 vol%) + NpO_2 (20 vol%) is considered.

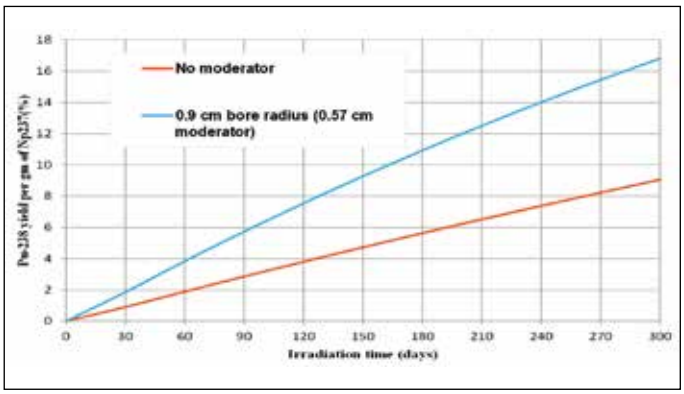

Fig. 3: Yield of Pu-238 for NpO_2 target with and without moderator flux

The Pu-238 vector degrades with increasing irradiation time. The study reveals that for current ISZ100 SA containing optimum moderator size, the vector does not fall down the limit even after 300 days.

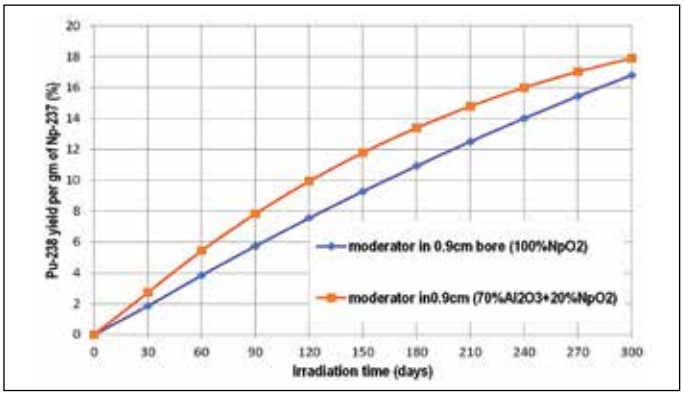

Fig. 4: Pu-238 Yield comparison for dispersed target NpO_2 and 100% NpO_2

The amount of impurity Pu-236 produced is also studied as a function of irradiation time and moderator thickness. Pu-236 impurity is found to more without moderator.

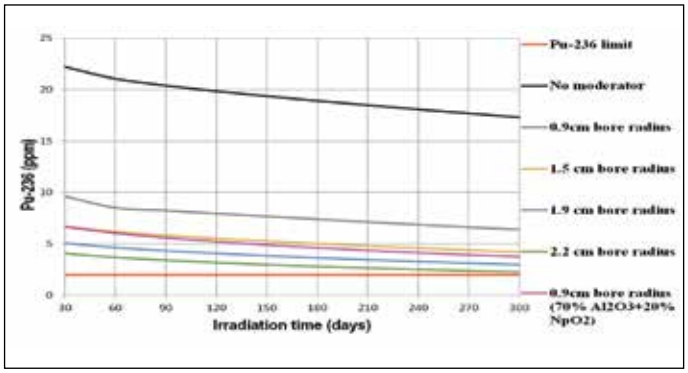

Fig. 5: Pu-236 production from (n.2n) reaction

I-12 Thermal Stress Analysis to Confirm the Design of the Thermolysis Chemical Reactor for Hydrogen Production at FBTR

The production of clean hydrogen using the thermal energy of the FBTR secondary sodium system is being pursued through the integration of the Copper-Chlorine (Cu-Cl) thermochemical cycle. The Cu-Cl cycle, consisting of Hydrolysis-Thermolysis-Electrolysis-Crystallization steps, operates at significantly lower temperatures than other cycles. For the thermolysis step, heat input at operating temperatures of 325 °C and 500 °C is required. Based on the preliminary mechanical design of the thermolysis reactor, finite element analysis (axi-symmetric model) is carried out to evaluate the stress levels across the critical sections and verify the thickness adequacy and the allowable number of cycles as per RCC-MRx.

The reactor assembly consists of three concentric shells: inner, intermediate, and outer, with helium-filled double envelope around the inner shell and secondary sodium flowing through the outermost shell. All shells are fabricated from Inconel-625, while the sodium piping connected to the reactor nozzles is made of SS-316.

An axi-symmetric finite element model incorporating geometric details, nozzles, discontinuities, and shell-to-shell interconnections is developed. Mechanical stress analysis under internal and external pressures confirms that peak stresses (~12 MPa) are significantly lower than allowable limits. Thermal analysis is performed considering differential temperature conditions (maximum ΔT of 100 °C during fault scenarios such as helium leakage). The maximum thermal peak stress (~648 MPa) occurs at the fillet near the inner–outer shell junction (shown in Fig. 1). However, combined mechanical and thermal stress levels remain below the allowable $2\sigma_y$ limit (666 MPa at 500 °C), indicating no concern of progressive strain accumulation.

Inconel-625 creep behaviour is negligible below 600 °C, and fatigue assessment (conservatively based on SS-316 properties) yields an allowable 187 cycles against an expected 100 operating cycles, ensuring structural safety.

A dissimilar metal weld between Inconel-625 and SS-316, located 100 mm away from the reactor shell, is also assessed. Differential thermal expansion generates local discontinuity stresses (~199 MPa), which are secondary

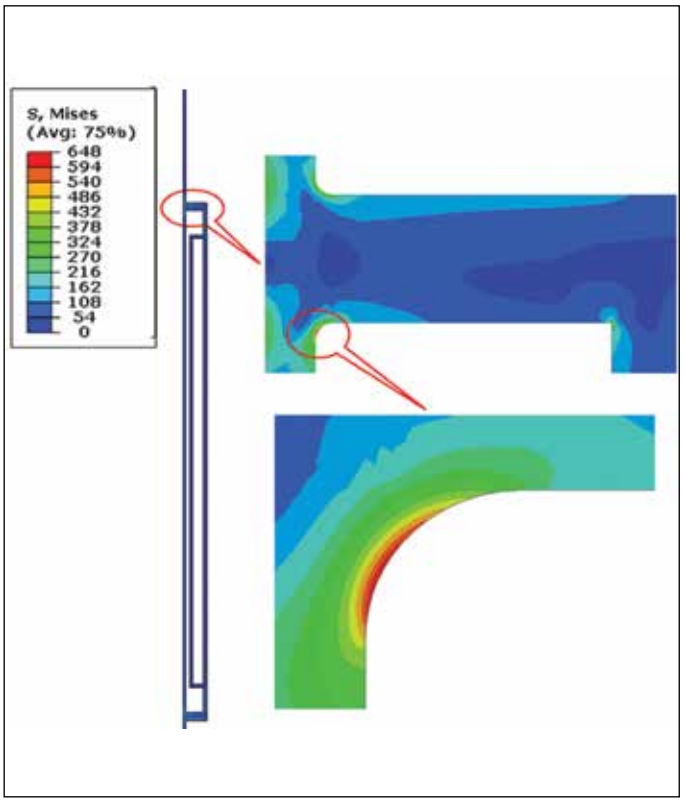

Fig. 1: Equivalent stress distribution (in MPa) under thermal loading in thermolysis reactor

in nature and well below the code-specified limits. Fatigue damage is insignificant in this region.

Thermal shock during initial sodium filling is analysed using codal guidelines. Several preheating scenarios are evaluated for sodium at 480 °C. To avoid surface yielding, a preheating temperature of ~454 °C is required. However, considering fatigue criteria, preheating temperatures of ~275 °C for weld metal and ~242 °C for base metal are adequate for 100 operational cycles. Creep is negligible over the anticipated 10,000 h operational duration.

In summary, the stress analysis confirms the structural adequacy of the thermolysis reactor and associated piping under mechanical, thermal, fatigue, and discontinuity stresses. Established safe preheating requirements, ensuring long-term operational reliability of the thermochemical loop when coupled to FBTR secondary sodium for hydrogen production.

I-13 The Effect of Shuffling on the Residence Time in FBTR Thoria Subassemblies

Thoria Subassemblies (SAs) are used in FBTR as radial blankets. The SA consists of ThO_2 pellets contained within a Stainless-steel clad tube. The SAs are placed in the ninth and tenth rows of the core. During reactor operation, these SAs tend to absorb neutrons and convert Thorium-232 to Uranium-233 leading to increase in the SA Power and temperature. With linear increase in the SA power, the 9th ring SAs are seen to reach the operational limit of clad hotspot temperature of 650 °C (Fig. 1), in about 44,000 hrs (5 years) of operation, which is reached since the time of their loading into the core. This necessitates their removal from the core. At the same time, the 10th ring Thoria SAs have operated in the benign conditions compared to the 9th ring SAs (Fig. 1). Following the slope of line II (Fig. 1), it is seen that the 10th ring SA will take about 23 years (from Beginning of Life (BOL)) to reach its DSL limit. Thus, the 10th ring SA still possesses considerable margins over DSL. Since fresh SAs to replace in the 9th ring locations are not readily available, the effect of interchanging the 9th and 10th ring SAs became necessary to study in order to extend the irradiation life of the present SAs. Hence, a study was undertaken to quantify the effect of interchanging the 9th and 10th ring SAs so that the present 9th ring will be continued to irradiate in the 10th ring positions, where the flux and temperature are lower.

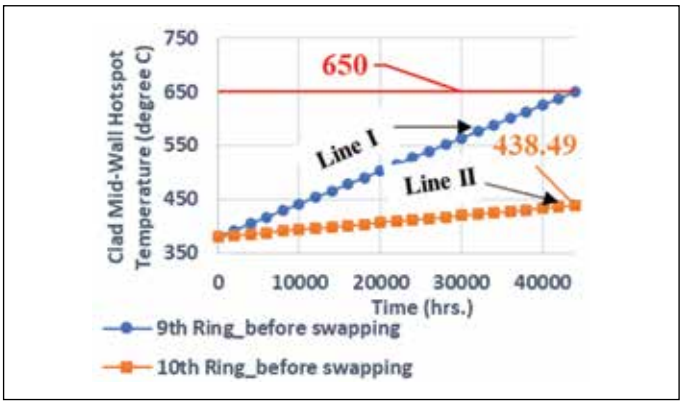

Fig. 1: Variation of clad temperature before shifting

To find the change in residence time due to such shifting, it is assumed that the rate of variation of power (hence, temperature) with time (slope) remains constant for a particular ring.

Thus, when the 9th ring SA is shifted into the 10th ring, its power reduces and it starts following the slope of 10th ring subsequently (obtained from Fig. 1). This is shown in Fig. 2. Similarly, when the 10th ring SA is shifted into the 9th ring, its power increases and it starts following the slope of 9th ring (obtained from Fig. 1). This is shown in Fig. 3.

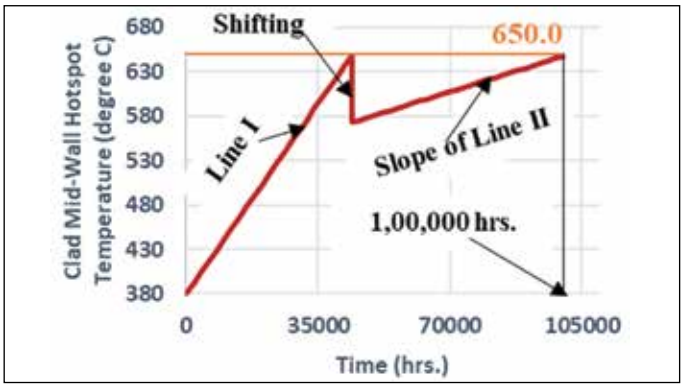

Fig. 2: Temperature variation of 9th ring after shifting to 10th ring

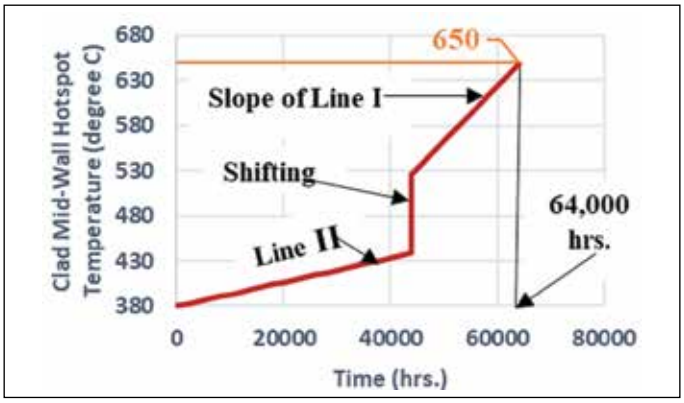

Fig. 3: Temperature variation of 10th ring after shifting to 9th ring

As the slope of 10th ring is lesser than that of the 9th ring, for reaching the DSL temperature, the shifted 9th ring SA will take (Fig. 2) another six years (1,00,0000 hrs – 44,000 hrs) to reach the DSL of 650 °C. Whereas, the shifted 10th ring SA to 9th ring will take another two years (64,000 hrs – 44,000 hrs) (Fig. 3) to reach the DSL of 650 °C. Thus, from the above study, it is concluded that the shuffling operation of the SAs between the 9th and 10th rings can extend the residence time of the Thoria SAs in the FBTR core.

Chapter - II

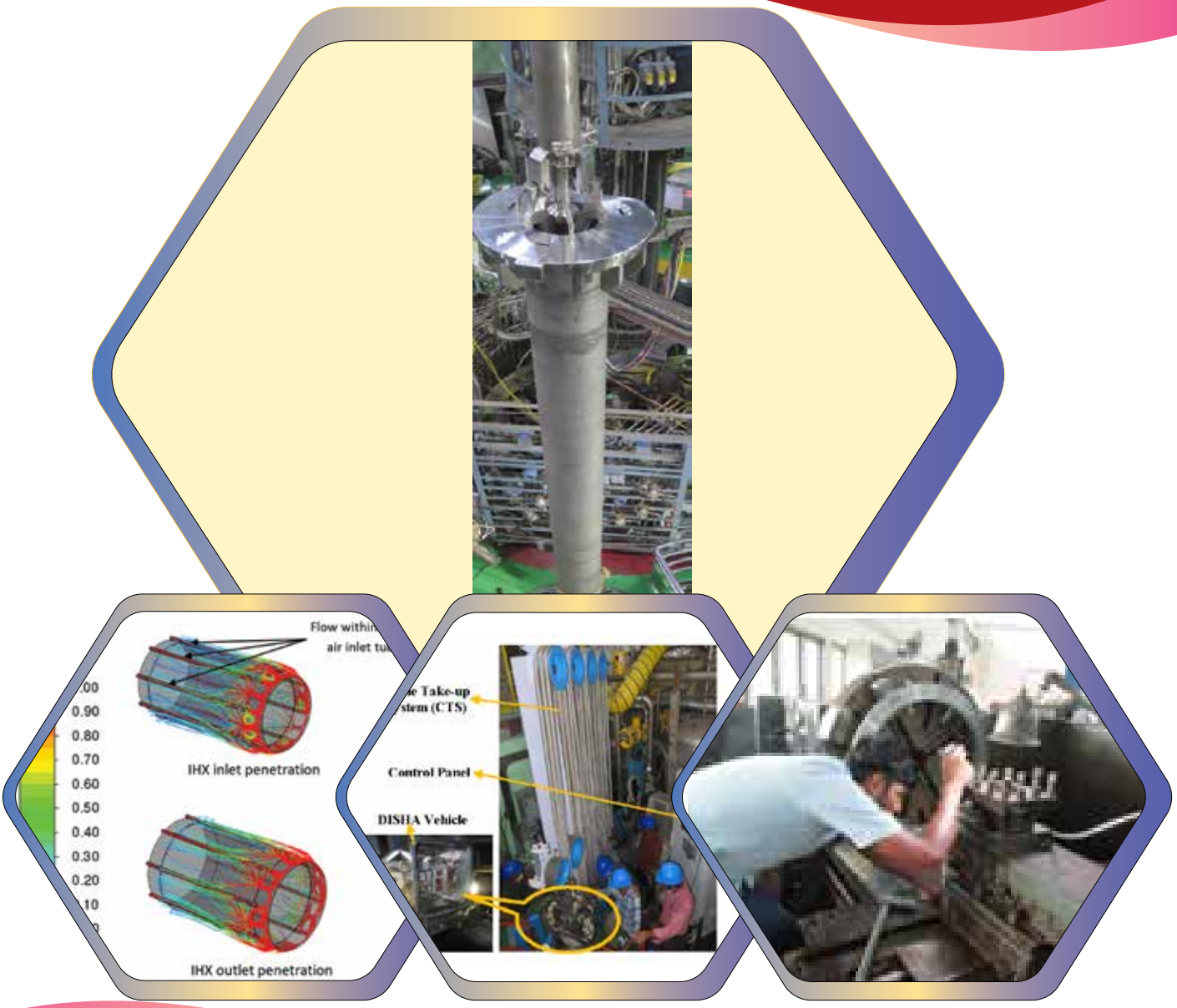

Prototype Fast Breeder Reactor

II-01 Design of Portable Sub-Assembly Handling Flask for PFBR Initial Fuel Loading

In the proposed scheme of initial fuel loading in PFBR, loading of fresh fuel SA & unloading of dummy SA from reactor core is planned to be carried out through IVTP port in LRP by a dedicated flask called Portable Sub-Assembly Handling Flask (PSAHF). Since transfer pot cannot be brought to IVTP through Inclined Fuel Transfer Machine, a separate pot is permanently mounted over the PTM body at IVTP for receiving fresh & dummy SA during transfer. PSAHF works at three work posts namely IVTP port on LRP, SA Preheating Facility (SPF) and Dummy SA Discharge Facility (DSDF) supported on the decontamination vessel-1 in RCB.

The PSAHF consist of Flask body, bottom isolation valve, gripper assembly, gripper hoisting mechanism, lifting attachments and pulley assembly.

The PSAHF is designed to facilitate coupling of the flask with various work-post like IVTP, DSDF and SPF. Special argon circuits are provided for flushing of the interspace between the work-post valve and flask valve. The bottom isolation valve also takes care of the dripping sodium from the dummy sub-assembly. Various safety features and interlocks are provided to meet the design & safety requirements. Gripped and un-gripped position of the gripper is indicated by an indication rod. Mechanical fail-safe feature is provided in the gripper to prevent the release of core SA at the un-intended elevations in addition to electrical interlocks. Sufficient shielding is provided in the flask to limit the dose on contact and at 1 meter distance less than 2 mSv/h & 100 µSv/h respectively. The flask internals are maintained in inert atmosphere to avoid exposure of sodium wetted parts to air during handling. The gripper hoisting mechanism is provided with single failure proof design features to avoid dropping of SA being handled.

The overall length of the flask is ~17 m and weight is ~5.5 ton. For lifting the flask using RCB crane for its transfer between the work-post, dedicated lifting lugs are designed using ASMR BTH code.

The gripper assembly is manufactured and tested for its operation in sodium for 15 cycles and later it is tested with transfer pot and guide tube in integrated manner. Handling of 55 mm bowed SA using PSAHF gripper is also demonstrated.

A prototype bottom isolation valve is manufactured and tested for 300 cycles. Based on the testing, a new valve is designed, manufactured, tested and deployed with the PSAHF in PFBR.

All the components of PSAHF are manufactured inhouse in IGCAR and BHAVINI. Component level testing of all the PSAHF components is carried out before assembly at site. After assembly integrated testing of the Flask is completed. Qualification trials required based on the regulatory requirements were also completed. At present the PSAHF is deployed in PFBR as ex-vessel handling machine for initial fuel loading.

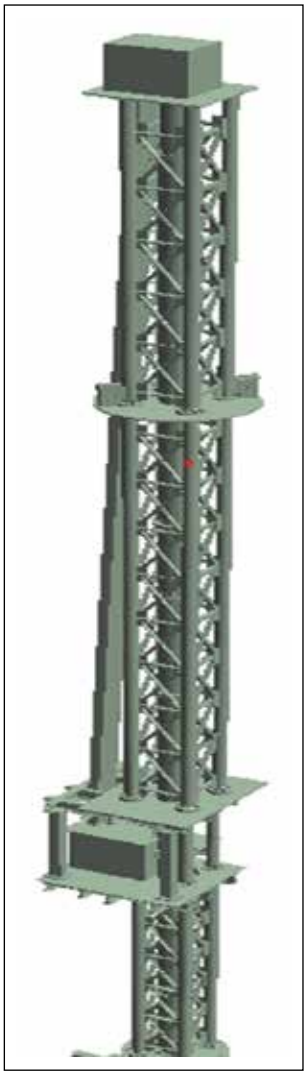

Fig. 1: 3D model of PSAHF

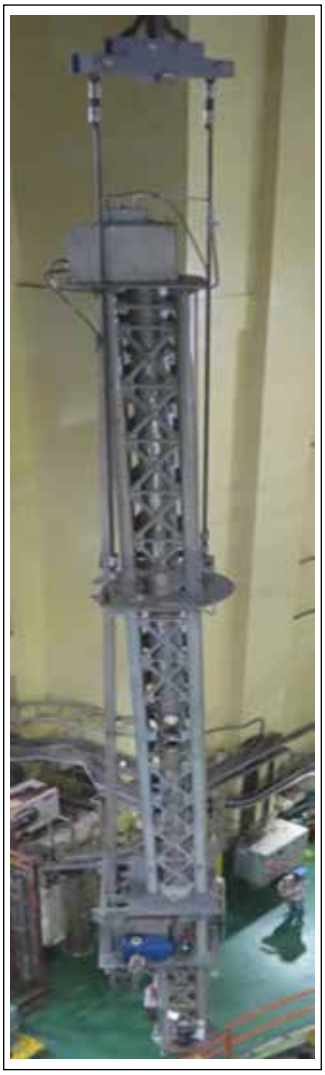

Fig. 2: Handling of PSAHF with RCB crane

II-02 Design of Permanent Transfer Pot in IVTP for PFBR Vertical Fuel Handling Scheme

An alternative fuel handling scheme based on ex-vessel Flask-type transfer is developed for PFBR in the absence of IFTM. As part of it, a new fixed Transfer Pot (TP) was designed, manufactured, tested, and installed in the reactor. The transfer pot is designed to house the Core Subassembly (CSA) during Fuel Handling. The TP is parked at the In-Vessel Transfer Position (IVTP) and receives the fresh CSA through IVTP from the Portable Subassembly Handling Flask. The CSA is subsequently transferred to its corresponding in-core position using the Transfer Arm. Similarly, TA loads the irradiated subassembly to the TP, which is further handled by the Subassembly Transfer Flask/Shielded Transfer Flask. The transfer pot has challenging design requirements, like self-aligning provisions, to enable precise remote positioning of TP from a distance of approximately 10m, maintaining the verticality of the pot in the absence of machined support location, and restraining in-plane movements during operations.

The TP is introduced into the reactor through the IVTP port in the large rotatable plug. The TP is suspended vertically from the top surface of the Primary Tilting Mechanism (PTM) body. It comprises a top support, a main body, and a bottom guide. The PTM main body is designed to swing freely around the top support, ensuring vertical alignment regardless of the flatness and horizontality of the PTM top surface. The TP top support is equipped with guiding features to ensure self-alignment of the TP with respect to the PTM body and precise positioning during lowering. It also locks the TP against the PTM body and rail in the rest position. These features enabled the remote positioning of the TP within 5 mm of the IVTP axis. The TP's bottom end is guided by the cylindrical feature near the PTM base to prevent unwanted lateral movement during fuel handling.

The main pot body is made of 250NB pipe. The TP is provided with the top guide and bottom housing to support and guide the CSA. Disc springs are provided in the housing to accommodate any shock load during subassembly transfer.

The guide and support locations of TP are hard-faced with RNiCr-B. The TP is equipped to accommodate both straight and bowed subassemblies. The TP is permanently fixed inside the sodium, hence it is open to sodium at both ends. However, TP can be removed if required. The TP is designed for elevated temperature during reactor operation. The structural components of the TP are manufactured using SS 316LN/SS 316 L, except for the disc springs, which are fabricated from Inconel X-750 due to its high-temperature resilience and mechanical properties.

A prototype transfer pot was made, and the design was validated through testing at the PRPTM test facility. A reactor-grade transfer pot was successfully manufactured and tested for remote installation and operation. Handling of straight and bowed subassemblies was demonstrated. The transfer pot was successfully installed remotely in the reactor, and smooth CSA handling was accomplished.

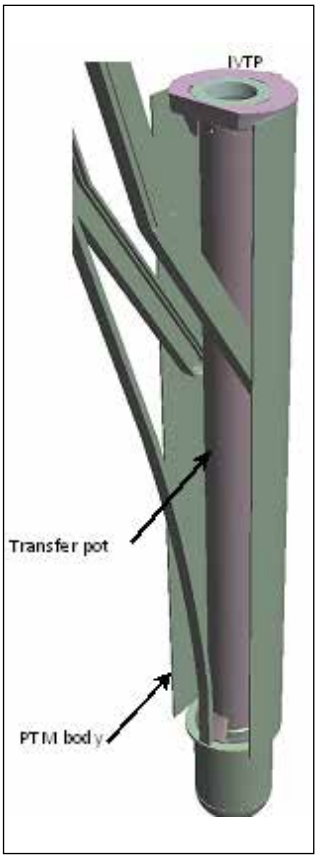

Fig. 1: Permanent transfer pot in IVTP

Fig. 2: TP Lowering through IVTP access port

II-03 Design of Fuel Cell based Hydrogen Management System for in-situ Regeneration of Secondary Cold Trap of PFBR

Cold trap of Secondary Sodium Purification Circuit (SSPC) needs to be regenerated if it becomes inoperable due to impurity loading and reaching its saturation limit. Major impurity expected in secondary sodium circuit of PFBR is hydrogen, which is continuously diffused into sodium through the SG tubes during its operation. Estimation of diffusion rate of hydrogen through SG tubes at reactor in full power operation indicates that cold trap will saturate with NaH in 4.5 years. The estimated hydrogen load into secondary cold trap for every 4.5 years is 93.2 kg. It is planned that after every 4.5 years, PFBR secondary cold trap would be regenerated in-situ by vacuum decomposition method for removing the sodium hydride.

The scheme for in-situ regeneration of secondary sodium cold trap of PFBR is shown in Fig. 1. A Proton Exchange Membrane Fuel Cell (PEMFC) based Hydrogen Management System (HMS) has been designed for connecting to the secondary cold trap during regeneration for safe management and accounting of hydrogen released during the regeneration process. PEMFC converts hydrogen into water vapour safely by electrochemically reacting with oxygen present in air and generates electric power and heat. The electric power generated is fed to a load bank. The current generated is used to quantify the amount of hydrogen liberated during cold trap regeneration. Hydrogen Management System (HMS) consists of oil free diaphragm vacuum pump, PEMFC, hydrogen meter, mass flow controllers, vacuum gauge, flow control valves and associated process control system.

During secondary cold trap regeneration, cold trap will be isolated from the sodium system by using frozen seal loop, sodium column of 2.65 m will be maintained and the surface heaters provided at the bottom dished end will be used to heat sodium upto 400 °C. HMS is connected to the cold trap through sodium vapour condenser and sodium vapour trap. Sizing of components and equipment layout is arrived in consonance with site space. There are two secondary cold trap in secondary sodium system of PFBR. HMS will be portable and it is common for both secondary cold traps of PFBR.

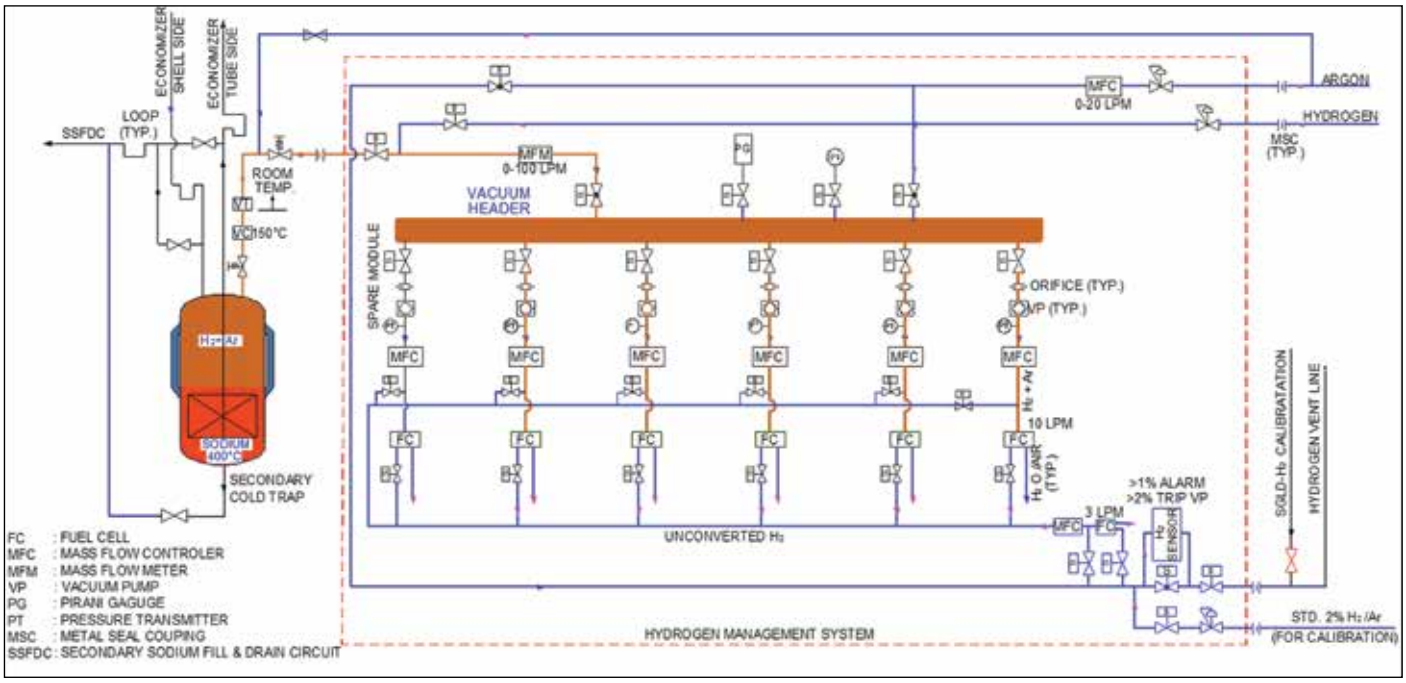

Fig. 1: Flow sheet for in-situ regeneration of secondary cold trap

II-04 Space Time Kinetics Transient Study of a Control Rod Withdrawal Incident in PFBR with Doppler Feedback

The coupled neutronics-thermal hydraulics code PREDIS, which is currently being used for transient analyses of PFBR, uses a point kinetics model for simulating the core dynamics. This is a valid model since PFBR is a tightly coupled core. However, in a severe accident scenario where core disruption can occur, a space time kinetics model may be more appropriate. Towards this purpose a space time kinetics code named SPARTA (Space dependent Reactor Transient Analysis) is developed. The code uses finite difference method in 3-D triangular/hexagonal geometry. Backward Euler method is used for time marching. Sparse matrix algebra is used along with BiCGSTAB algorithm for solving the linear system of equations at every time step. It was validated using the AER-DYN-001 numerical benchmark problem. The results predicted by SPARTA were found to match with that of other international codes such as DYN-3D, KIKO-3D and REDAC. A heat transfer model identical to that of PREDIS code is also implemented in SPARTA along with a Doppler feedback model.

For testing the code's usability in actual reactor transients, an unprotected single CSR withdrawal incident in PFBR is simulated. A hypothetical rod withdrawal speed of 20 mm/s is assumed. The transient starts from cold critical state with 100 KW power. To reduce the computational burden, a condensed 6 energy group structure is used. It should be noted that this is just a test study to assess the performance of the code rather than an actual UTOPA calculation of PFBR.

Variation of total power with time is shown in Fig. 1. Peak fuel, steel and sodium temperatures with time are shown in Fig. 2. The CSR withdrawal lasts up to 24 seconds. The power is found to increase rapidly at the beginning due to lack of feedback effects at low power. However, as power

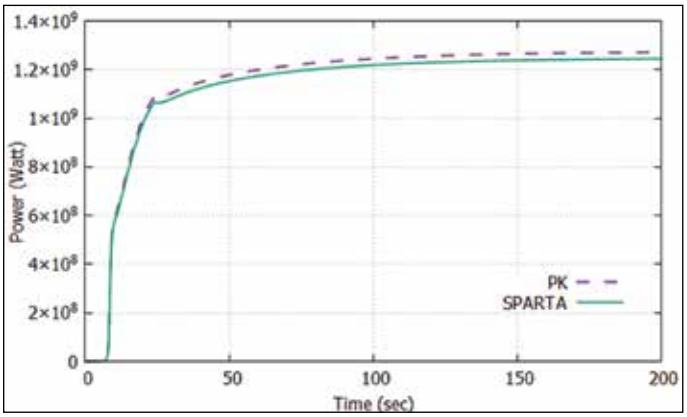

Fig. 1: Variation of total power with time

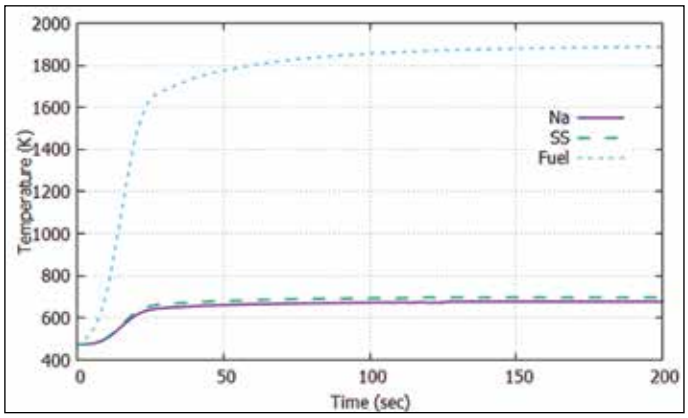

Fig. 2: Variation of peak temperatures with time

and fuel temperature increases, Doppler feedback kicks in and the power is found to stabilize at 1250 MW within 200 seconds.

The variation in total power predicted by point kinetics model is within 2% of that predicted by SPARTA code. However, SPARTA code is able to calculate the spatial variation in power density due to the CSR withdrawal which is not possible with a point kinetics model which assumes the initial power distribution throughout the transient. The normalized power distribution is found to peak at the SAs close to the withdrawn CSR compared to the initial power distribution as shown in Fig. 3.

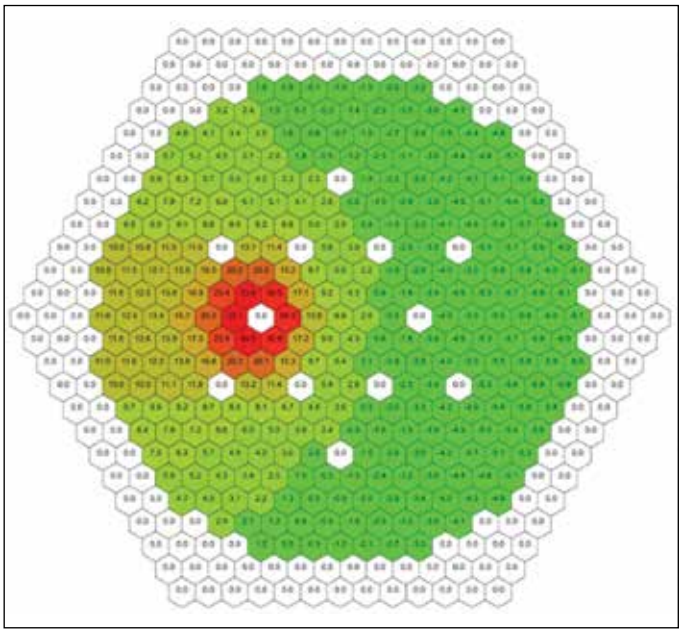

Fig. 3: Difference in power density predicted by STK and PK models. Red and green indicates positive and negative deviations respectively

II-05 Thermal Analysis of Portable Sub-Assembly Handling Flask Gripper Assembly of PFBR

A Portable Sub-Assembly Handling Flask (PSAHF) is designed as an alternative of transfer pot to load fresh fuel sub-assemblies (SA) vertically into reactor core. The gripper of PSAHF moves into the main vessel through a guide tube. In top shield, the guide tube passes through the In-Vessel Transfer Port (IVTP) in Large Rotatable Plug (LRP). During the SA loading into the core, the gripper bottom end is dipped in primary sodium pool, which is at a temperature of 200 °C. The gripper fingers are envisaged to be operated manually using a handling wheel at the top of the gripper. Temperature at the handling wheel should be less than 60 °C to enable manual operation. The guide tube and gripper get heated up due to primary sodium pool and hot argon cover gas. It is indirectly cooled at the top shield by the top shield cooling system. Since the gripper handling wheel is not cooled directly, it might be at a higher temperature, which will make it difficult during its handling. To check whether the handle wheel temperature is below 60 °C, a steady state thermal analysis has been carried out. The gripper is expected to attain maximum temperature when it is at its lowest elevation and a major portion is in primary sodium.

A 2-D axi-symmetric model is chosen for the analysis considering symmetry of the domain. The model consists of gripper assembly, guide tube, guide tube support in top shield, argon within the guide tube, portion of the gripper above sodium surface is modeled. Gripper and guide tube submerged in sodium pool is considered to be at sodium pool temperature and a constant temperature boundary of 200 °C is used. Height of argon cover gas during SA handling is 1.4 m. A radial distance of 1 m from guide tube outer surface is considered to simulate natural circulation heat transfer from argon at the guide tube outer surface. Top of argon cover gas faces steel thermal shield and top shield bottom plate which is cooled by air. These are modeled implicitly by giving overall heat transfer coefficient at the argon surface.

The gripper handling wheel is located at an elevation above top shield and below working platform (the enclosure). Temperature of enclosure as measured from plant (~35 °C) is used for convective boundary condition. Total height of guide tube considered in the model is 19.2 m from the sodium pool surface. The domain is discretized in to ~15 lakh meshes. Steady state analysis is carried out using commercial CFD code. Temperature distribution in gripper at handling wheel region is shown in Fig. 1. It is seen that predicted average temperature at handling wheel is 40 °C. Temperature varies from 41 °C to 38 °C from the lower end to the higher end of the hand wheel. Thus, even at 200 °C sodium pool temperature, fuel handling by manual rotation of the gripper is not a concern. Fig. 2 shows argon velocity at the handling wheel region. The argon removes heat from the gripper inner surfaces and flows in upward direction near the handling wheel and gets cooled when by the gripper outer shell and flows downwards. Maximum velocity is 0.052 m/s, which represents a weak natural convection flow.

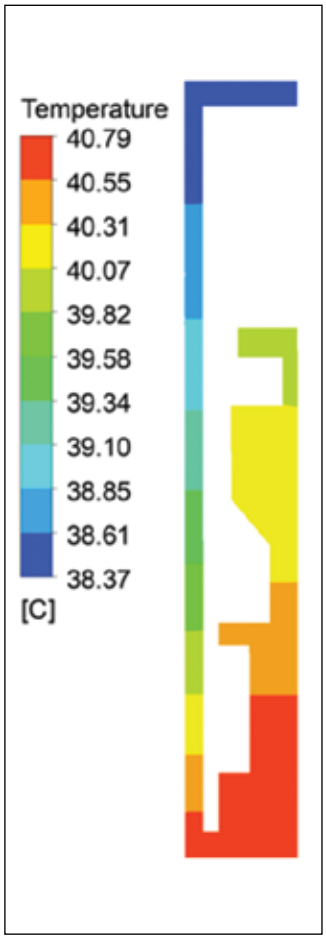

Fig. 1: Temperature distribution in gripper at handling wheel region

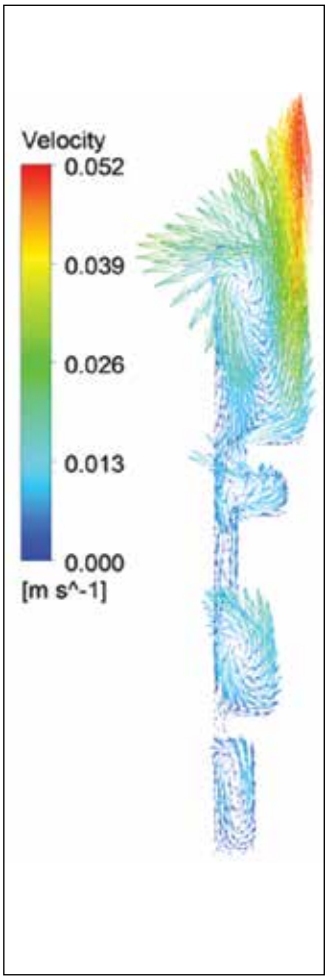

Fig. 2: Argon velocity profile

II-06 Protective Relay Co-ordination Study for PFBR As Built 6.6 kV and 415 V Power Supply Systems Using ETAP Software

Electrical Power Systems are the source of power for reactor control, safety instrumentation, reactor coolant pumps and other auxiliaries during normal operation, as well as for the protection system and engineered safety systems during normal and accident conditions. Electrical protection systems are essential for ensuring the safe and reliable operation of NPPs. This work focused on performing an earth fault and overcurrent protective relay coordination study for the PFBR as-built 6.6 kV and 415V system feeders.

PFBR Electrical Power Supply system was modelled using As-Built drawings, load lists, and factory test reports. Load flow studies were conducted to arrive at the voltage profile and power flow during the plant's steady-state operating conditions. Short-circuit analysis was conducted at various Buses to arrive at the maximum and minimum fault currents and the effects of these faults on connected bus voltages during fault conditions. Then the Relay coordination studies for Overcurrent (51) and Earth Fault (51N) relays were performed using load flow and short circuit studies results (shown in Table 1), incorporating the time grading principles with a discrimination time interval of 0.25 s through ETAP simulation software. The Time Current Characteristic (TCC) curves were obtained (shown in Fig. 2) from the relay coordination study (shown in Fig. 1) for both Overcurrent and Earth fault elements and are thoroughly analyzed and adjusted to mitigate unnecessary outages and equipment damage, by ensuring the protective relays operate in the optimal sequence (shown in Fig. 1). The below table shows the results from Load Flow, Short circuit Studies.

The below table shows the results from Overcurrent relay coordination study with current seen by each feeder during fault scenario.

Bus	Voltage (%)	Current (A)	Active Power (MW)	Reactive Power (MVAR)	Short circuit current (kA)
Unit Bus 1	100.1	1669	16.4	9.81	35.7
Unit Bus 2	101.7	1154	11.8	6.36	34.5
Station Bus 1	102.5	855.9	8.85	4.26	35.7
Station Bus 2	101.4	1262	12.5	6.96	34.5
HVBeb52-100A	99.8	702.4	7.23	3.48	33.4
HVBeb52-100B	102.5	532.5	5.63	2.4	33.8
HVBeb52-200A	101.5	620.2	6.53	3.04	32.7
HVBeb52-200B	101.2	584.1	6.07	2.63	32.8
HVBsb52-300A	99.77	104.6	1.06	0.54	27.9
HVBsb52-300B	101.42	81.7	0.84	0.43	23.8

Incomer to	Rated/ Load flow current	Fault current seen (kA)	Pickup setting (51)	TMS Setting	Relay curve
Unit Bus 1	2929	18.919	0.74	0.425	IEC SI
Unit Bus 2	2929	18.87	0.74	0.425	IEC SI
Station Bus 1	2929	19.959	0.74	0.45	IEC SI
Station Bus 2	2929	16.527	0.74	0.4	IEC SI
HVBeb52-100A	1395.3	22.183	0.77	0.45	IEC SI
HVBeb52-100B	1275.2	21.605	0.73	0.45	IEC SI
HVBeb52-200A	1230.6	19.98	0.68	0.425	IEC SI
HVBeb52-200B	1254	20.455	0.69	0.45	IEC SI
HVBsb52-300A	174.8	24.733	1.6	0.275	IEC SI
HVBsb52-300B	176.1	20.795	1.6	0.275	IEC SI

Fig. 1: Protective relay coordination of feeders

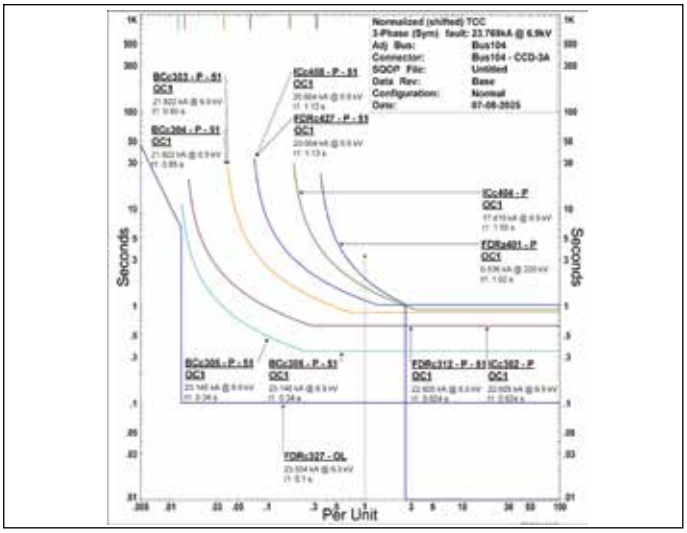

Fig. 2: TCC curve showing relay responses on fault

II-07 Thermal Analysis of Secondary Sodium Piping Penetrations in Reactor Containment Building – Validation Against Isothermal Testing Results

Among the several penetrations in the Reactor Containment Building (RCB) walls for routing heat transport and other process systems, those for secondary sodium piping are particularly critical due to the large diameter and high temperature of the sodium carried by these lines. During normal operation, the cold leg carries sodium at 355 °C to IHX (IHX inlet pipe) and the hot leg carries sodium at 525 °C from IHX (IHX outlet pipe) to the steam generators. Both of these lines have guard pipes over them when they fall inside the RCB wall, and the guard pipes are provided with a layer of thermal insulation. Furthermore, special embedded parts are provided in these penetrations to ensure the leak-tightness of the RCB. A carbon steel liner is embedded in the RCB wall on the inner surface of the concrete penetration. This liner is connected to the guard pipe through an SS conical sleeve. The annulus between the guard pipe and sleeve is supplied with cooling air through eight cooling pipes, each with a diameter of 32 mm. The temperature of the RCB wall is to be limited to a maximum of 90 °C.

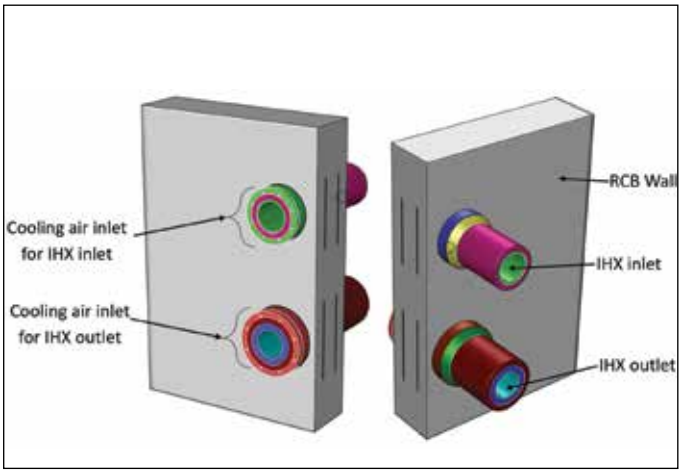

Fig. 1: CFD model of penetration cooling system

The required air flow rate to maintain the RCB wall within the allowed temperature limits is estimated using a detailed three-dimensional CFD model (Fig. 1). As part of the present study, a detailed validation exercise is carried out against field readings of concrete temperatures recorded during isothermal testing. The tests were performed at various sodium temperatures in the IHX inlet and outlet pipelines, and measurements from two sodium temperature conditions, viz. 200 °C and 400 °C, were used for the exercise.

The exercise involved isolating and studying the influence of several important parameters, such as cooling flow rates and temperatures, ambient conditions, and material properties, and optimizing these with respect to the modeling approach. The intricate velocity patterns within the cooling chambers are shown in Fig. 2. A good match was obtained for the maximum concrete temperature at an isothermal sodium temperature of 400 °C, with estimated temperatures being within 3 °C of the measured values, which were higher than the estimated values. Using the validated model, cooling air flows required to limit concrete temperatures to prescribed limits during normal operation and power failure conditions are re-estimated. The estimated concrete temperatures of the RCB wall for normal operation are shown in Fig. 3 (maximum temperature of 86 °C).

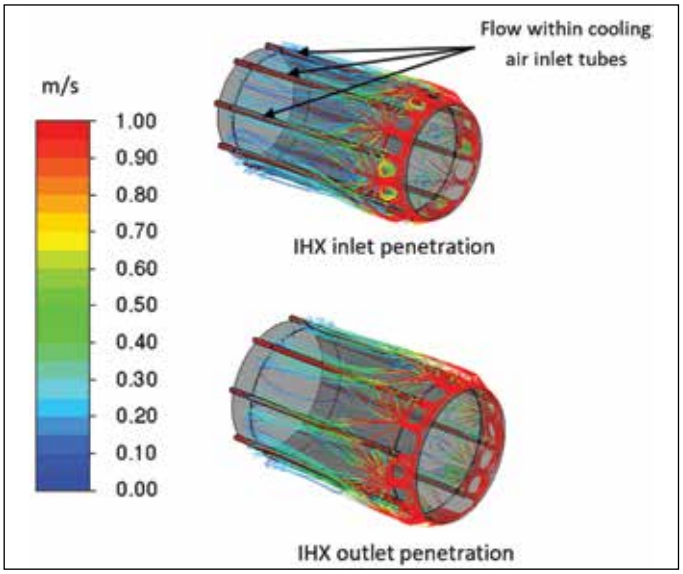

Fig. 2: Pathlines of cooling air flow

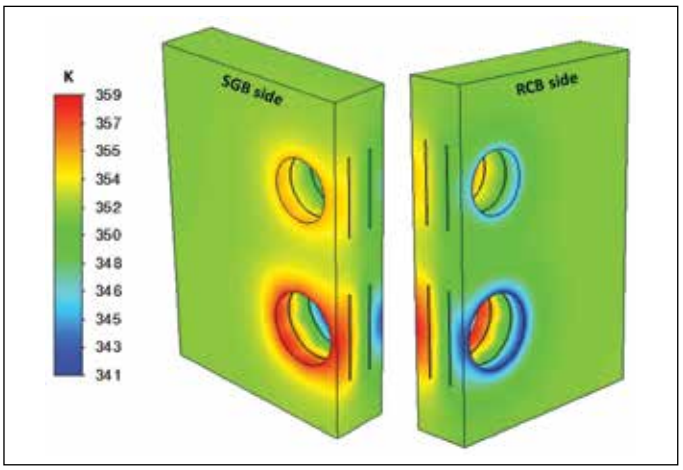

Fig. 3. Contours of concrete temperatures for normal operation

II-08 Welding Qualification for Plugging of Suspected Tubes of the Intermediate Heat Exchanger of PFBR

IHX (Intermediate Heat Exchanger) is a large-sized shell-and-tube type heat exchanger in the PFBR. Its primary function is to transfer heat from radioactive primary sodium to the non-radioactive secondary sodium. PFBR is equipped with four IHXs, each consisting of 3600 tubes. These tubes measure 8 meters in length, have an outer diameter of 19 mm, and a wall thickness of 0.8 mm. Each tube is connected to the top and bottom tube sheets at both ends. The tubes are arranged in a circular configuration, creating a tube bundle with a diameter of 1.85 meters. The total height of the heat exchanger is 18 meters, and it is constructed from SS 316LN material. In this system, radioactive primary sodium circulates on the shell side, while non-radioactive secondary sodium flows through the tube side at a higher pressure for safety reasons.

In the event of any performance deviation in the IHX, it is essential to identify and isolate the suspected tubes by

Fig. 1: A spring loaded portable internal tube cutter

Fig.2: Sealweld removal tool

plugging them as a corrective measure. Consequently, a methodology for the qualification of plug welding has been developed for use whenever required. A mock-up welding qualification is performed to optimize the geometry and process of the plug weld. Initially, suspected tubes are identified through eddy current testing. Subsequently, these tubes will be isolated from the flow path by cutting them at both ends with a spring-loaded portable internal tube cutter (Fig. 1). Following this, the existing seal weld between the tube and the tubesheet will be removed using a seal weld removal tool (Fig. 2). The seal weld before and after its removal is illustrated in (Fig. 3). and sealing them with welded plugs. The isolation process included meticulous inner diameter (ID) measurements with an accuracy of 1 micron to identify variations in thickness and profile at the tube-to-tube sheet locking areas, the fabrication of plugs with close tolerance, and their precise dimensional assessments. Adequate fusion at the weld joint root was

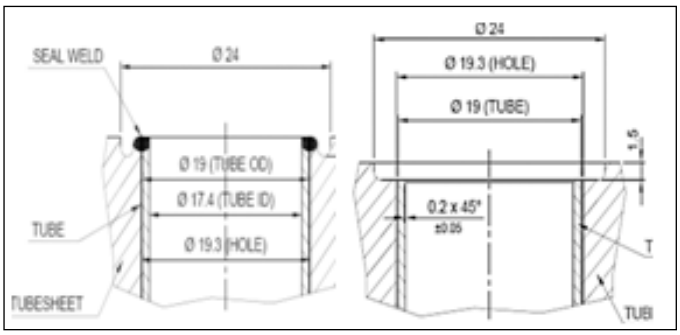

Fig. 3 TTS Joint before and after seal weld removal

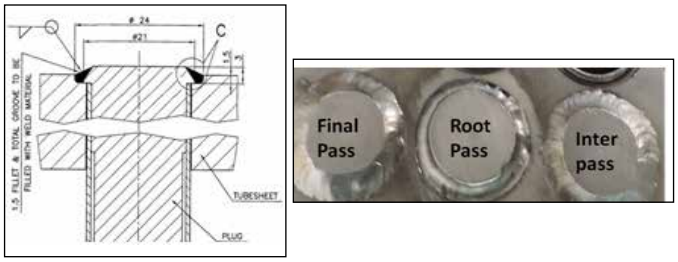

Fig.4: Welding of plug (Schematic and mock up welding)

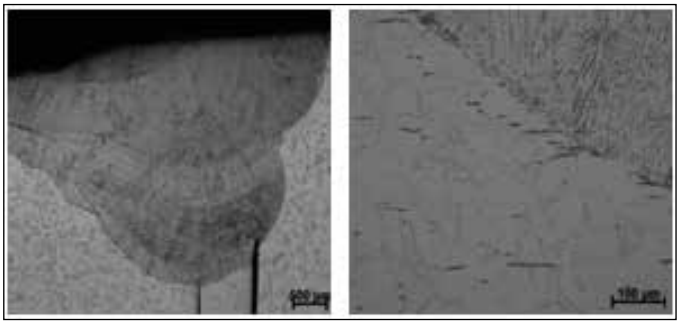

Fig.5: Micro examination of plug weld

ensured by qualification and optimisation of the welding procedure. Visual inspection, along with fluorescent liquid penetrant examination (LPE), will be performed, followed by pneumatic testing and helium leak testing to ensure weld quality, integrity, leak tightness and long-term operational reliability.

A plug is placed into the tube, and plug welding is executed in three passes, as illustrated in (Fig. 4). After the welding process, the three welds are severed, and a micro-examination is carried out at the four cut edges of the two weld plugs (Fig. 5).

Finally, sufficient fusion at the root of the weld joint was achieved through the qualification and optimization of the welding procedure. A visual inspection, in conjunction with fluorescent liquid penetrant examination (LPE), was conducted to verify the integrity of the welds and ensure long-term operational reliability.

II-09 Development & Qualification of High-Temperature Camera in Sodium Environment for IFTM Rail Inspection

The PFBR fuel handling system comprised the Inclined Fuel Transfer Machine (IFTM) and the Transfer Arm for transferring fresh and irradiated Subassemblies (SA). During preparatory operations for PFBR fuel-handling activities, a requirement arose to carry out a detailed visual inspection of the rails inside the Primary Ramp and Primary Tilting Mechanism (PR&PTM). To meet this requirement, a specialized PR&PTM Rail Visual Inspection System was developed using a High-Temperature (HT) camera capable of reliable operation in a 200 °C sodium aerosol environment.

The HT camera module was developed using a 4m long 3" Sch. 40 stainless-steel pipe containing a hose-in-pipe with argon cooling line surrounded by ceramic-wool insulation. A specially designed camera enclosure was incorporated, which included Teflon insulation to minimize heat transfer and a blend-off arrangement through four vent holes to prevent sodium aerosol deposition on the quartz window. The enclosure housed a CCD camera, four 3 W LED lamps for illumination, a quartz glass viewing window, a thermocouple for real-time temperature monitoring. The qualification trials were carried out in Test Vessel-2 (TV-2) of LCTR, a 2 m diameter sodium facility equipped with heaters, leak detectors and cover-gas instrumentation as shown in Fig.1. The HT camera module was lowered into the vessel through a 400-mm top opening using the high-bay crane. Continuous argon sweeping prevented air ingress during insertion.

Fig.1 Lowering of HT camera assembly in TV2

Sodium aerosol behavior on the quartz window was evaluated during two hours of exposure at 200 °C. LED illumination and template visibility remained clear throughout the exposure period, confirming effective optical performance. Cooling-flow optimization confirmed that an argon flow rate of 200 LPM (12 m^3/h) was required to maintain a stable camera housing temperature of about 60 °C. A dedicated argon manifold, temporary cylinder header, and control panel were used for regulated gas flow, pressure and temperature monitoring, along with live video display during operation, as shown in Fig. 2.

Fig. 2 Real time camera view inside TV2

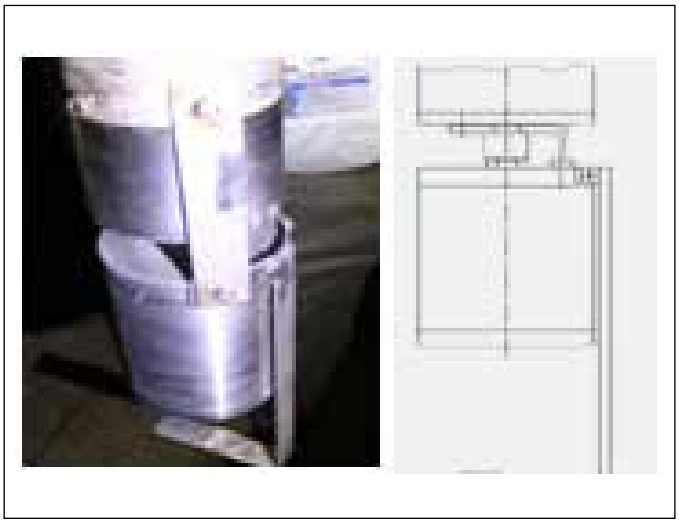

Fig.3 Camera assembly after HT trials

In a loss-of-coolant scenario, a test was carried out by cutting off the argon flow. The camera housing temperature reached approximately 85 °C within 30 minutes, thereby defining the safe withdrawal time during emergency conditions. Post-test inspection revealed no significant sodium aerosol deposition on the quartz window, with only minor smudges that were easily cleaned using alcohol, as shown in Fig. 3. The HT camera system was thus fully qualified for deployment in PFBR, enabling reliable visual inspection of PR&PTM rails under high-temperature sodium aerosol environments.

II-10 Successful deployment of DISHA and completion of Pre-Service Inspection of 7.3 m of dissimilar weld through 152° ISI port in PFBR

Dissimilar weld between the main vessel (MV) and roof slab shell is one of the critical welds in PFBR, which requires periodic in-service inspection (ISI) to ascertain its structural integrity throughout the lifetime of the reactor. For this, a remotely operated inspection vehicle (DISHA) was developed, tested, qualified and successfully demonstrated in the reactor during the pre-commissioning of PFBR in 2022. Following this reactor deployment, due to as-built site constraints, design modification was envisaged for the unhindered motion of the vehicle over Anti Convection Barrier(ABC).

Redesigned DISHA with increased undercarriage clearance (DISHA-V2) (Fig.1) has been successfully tested and qualified at 120 °C in the mock-up test facility. A novel safety guide roller design has been implemented in DISHA-V2 for safe handling of DISHA during emergency conditions.

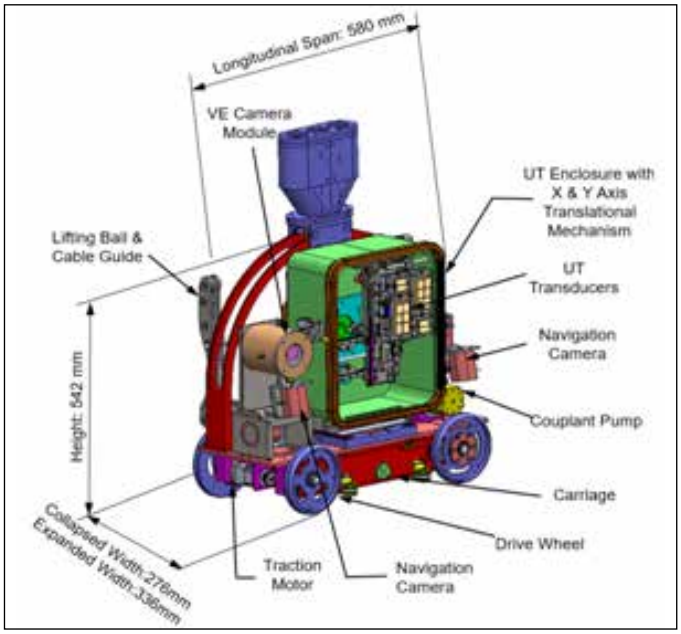

Fig.1: CAD Model of DISHA-V2 depicting the important modules

DISHA is designed to operate 120 °C and move over the ACB to perform visual examination (VE) and ultrasonic testing (UT) of the dissimilar weld. DISHA is a four-wheeled vehicle, where the wheels are oriented to follow the fixed curvature of MV without active steering mechanism.

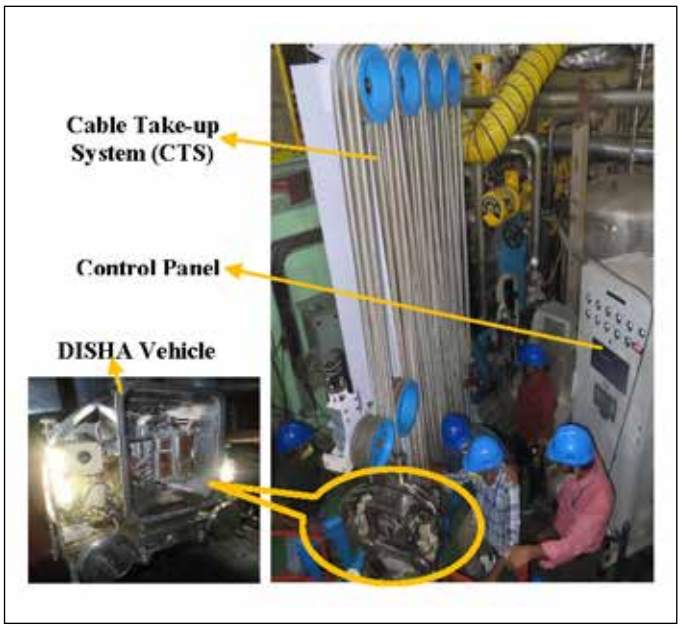

Fig.2 DISHA-V2 with CTS at 152° ISI port for performing the PSI of dissimilar weld

On-board cooled cameras aid in navigating the vehicle over ACB.

Tethered control is employed between DISHA and the dedicated control unit through cable take-up/release system (CTS).

After the mandatory qualification for reactor deployment and as part of pre-service inspection (PSI), DISHA-V2 (Fig.2) was deployed through 152° ISI port in the reactor to inspect the dissimilar weld at 120 °C ambient state. The visual examination of the 7.3 m dissimilar metal weld has been carried out as DISHA traversed 3.8 m in the clockwise (CW) direction and 3.5 m in the counter-clockwise (CCW) direction using two independent safety guide roller designs, customized for the respective movement directions due to as-built constraints on either side of ACB. Subsequently, UT of the dissimilar weld was performed with 65 scans, each scan covering 120 mm of weld length with a 20 mm overlap between consecutive scans. With these UT scans, the PSI data through UT has been generated for 6.56 m of the weld at the 152° ISI port location. No visible and volumetric defects were observed during the inspection of the dissimilar weld. DISHA-V2 was deployed at high temperature and PSI of 7.3 m of the weld was successfully performed under challenging conditions.

II-11 Performance testing and qualification of Portable Sub assembly Handling Flask gripper for reactor application

In PFBR, to transfer core Sub Assemblies (SAs) in and out of the main vessel, a new machine called Portable Subassembly Handling Flask (PSHF) is persuaded. PSHF consists of straight pull type gripper assembly (Fig. 1), which is the critical part of the machine, has the design features similar to the Transfer Arm gripper except the offset arm. Length of the griper assembly is around 10 m and through this, hoisting and lowering of core SAs into and from the vessel is carried out. The gripper assembly consists of concentric tubes i.e. outer tube and inner tube, conical ended finger holder and three numbers of fingers hinged at 120° apart to the holder. A manually operated screw-nut mechanism is provided for actuation of the fingers via inner tube to grip or un-grip the core SAs. After detailed design and manufacturing of the griper assembly, performance tests were carried out to assess the finger actuation and overall functionality under simulated PFBR fuel handling conditions.

The testing was carried in the Test vessel-5 (TV-5) of Large Component Test Rig in Hall-III. The test setup comprised a leak-tight shell assembly positioned above TV-5, equipped with a vessel isolation valve, glove ports for manual operation, and argon flushing provisions to maintain an inert atmosphere during testing. The arrangement enabled gripper finger actuation under both sodium and argon environments simulating PFBR fuel handling conditions. The testing sequence involved gripper finger actuation in sodium at 200°C, followed by lifting and re-positioning of the gripper subassembly in the leak-tight shell maintained under argon. In the argon environment, finger actuation tests were carried out at temperatures ranging from 45°C to 100°C.

Prior to sodium testing, ambient tests were completed outside TV-5 using a dummy SA head, to verify gripper finger positioning and torque were recorded. Subsequent hot argon testing at 393 K for five cycles in TV-5 confirmed torque within acceptable limits. Then, the vessel was filled with sodium to simulate 4m gripper submergence, and 15 cycles of testing were carried out. Torque remained consistent through fourteen cycles, with a minor increase observed in the last cycle, attributed to progressive sodium oxide deposition on the gripper finger surfaces (Fig.2).

After the test cycles, the gripper subassembly was taken out from TV-5 and the finger region (Fig.3) was cleaned using alcohol which simulates the removal of sodium deposits in case of finger actuation jamming in the reactor. After three hours cleaning, actuation torque returned to ambient levels, and five post-cleaning cycles confirmed stable performance. Then water vapor–CO_2 cleaning effectively removed residual sodium. Post-cleaning, load testing of gripper subassembly with a 645 kg load (twice the blanket subassembly weight) confirmed structural integrity with no deformation or surface cracks observed. With this successful completion of performance testing and qualification, gripper assembly was sent to BHAVINI for installation in the reactor.

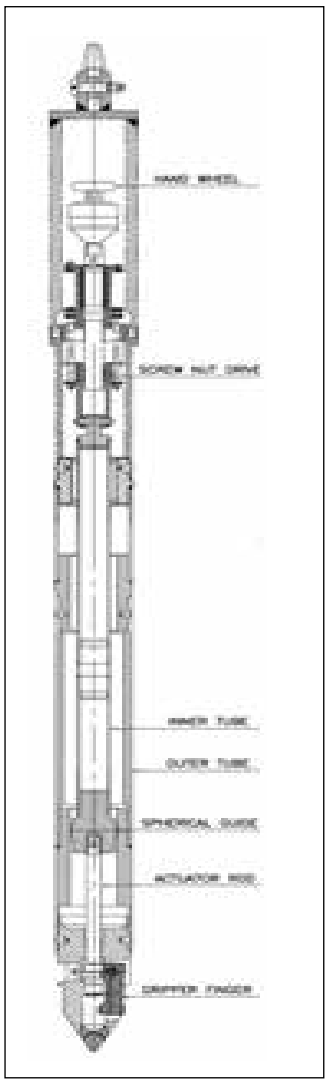

Fig.1 gripper subassembly

Fig.2 Sodium oxide deposition on the gripper finger region

Fig.3 Gripper finger region cleaned using alcohol

II-12 Performance validation of ultrasonic transducers in Revamped USUSS of PFBR

Under Sodium Ultrasonic Scanner System (USUSS) is used in PFBR to ensure the safe startup of fuel handling operations. Before fuel handling begins, it is essential to verify that no sub-assembly (SA) or other structures protrude through the 100 mm gap between the core top and the bottom of the core support structure, as such projections may obstruct fuel-handling operations. During the revamping of the USUSS, four Side Viewing Transducers (SVTs) and four Down Viewing Transducers (DVTs) were newly fabricated in-house, assembled, and mounted on the revamped scanner. The MI cables of all transducers were routed through the spinner tube and terminated at the upper part of the scanner assembly. The alignment of both SVTs and DVTs was carried out systematically, as the performance and accuracy of the USUSS depend significantly on the directional orientation of its ultrasonic transducers. Any deviation in angular positioning can lead to beam misalignment, resulting in inaccurate localization of protrusions.

Fig.1 Retroreflector

For the SVTs, the inclination with respect to the horizontal plane must be zero, meaning they are aligned parallel to the horizontal reference. Retroreflectors, as shown in Fig. 1, were employed to achieve this alignment. Four retroreflectors were mounted inside a large water tank of size 8 m × 2.5 m × 1.5 m located in Hall III, FRTG, at distances of 5985 mm, 1220 mm, 1000 mm, and 880 mm from the USUSS mounted in the tank. The degree of misalignment of each SVT was determined by performing (Fig. 2)B-scan imaging of all retroreflectors along the z-axis in 1 mm steps. An in-house developed Python-based software was used to analyze the B-scan data and determine the degree of misalignment. The analysis revealed that each of the four SVTs exhibited an initial upward inclination of approximately 1°. To correct this, thin stainless steel washers were inserted under the transducer mounting screws to push the transducers downward and minimize the inclination.

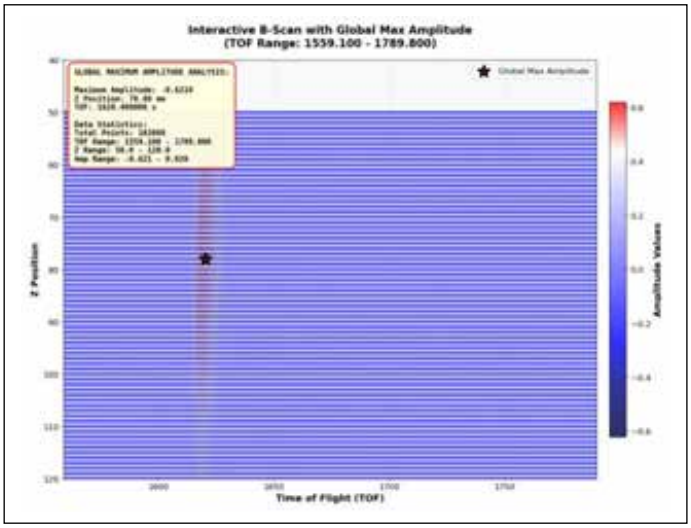

Fig. 2 Typical B-scan of retroreflector

Subsequent verification using the retroreflectors confirmed that the final misalignment was reduced to less than 0.2°. After achieving the required alignment, the transducers were permanently fixed in position by tack-welding.

The alignment of the DVTs was carried out in a smaller water setup using a stainless steel target plate placed 110 mm below the transducers. By making slight angular adjustments, the position corresponding to the maximum echo amplitude was identified, and each transducer was then fixed in this position using tack-welding. Post-alignment functionality tests of the USUSS were conducted by performing C-scans of simulated subassembly clusters and B-scans of subassembly heads. The results confirmed reliable side-viewing and downward-viewing performance of the revamped USUSS, thereby marking the successful completion of fabrication, assembly, alignment, and verification of the ultrasonic transducers.

II-13 Experimental determination of Instantaneous Sodium combustion in RCB during HCDA in PFBR

In case of a Hypothetical Core Disruptive Accident (HCDA) in PFBR, sodium can leak into the Reactor Containment Building (RCB) through the interspaces between the Roof Slab (RS) and rotating plugs during the expansion of core bubble. Previous studies indicate that sodium ejection would last ~ 0.6 seconds, releasing about 100 kg through RS–LRP (Large Rotating Plug) leak path of 11 mm wide, 21 m in circumference. The ejected sodium undergoes combustion leading to increase in RCB pressure and temperature.

An experimental study has been conducted at SED to assess the extent of instantaneous combustion of the sodium ejected during such scenario. The experimental test setup comprises a sodium vessel, a duct featuring the leak path, a timer actuated pneumatic valve and a Sodium Collection Tray (SCT) as shown in Fig.1. The duct comprises a rectangular outlet (11 mm opening, 300 mm wide) to simulate a sector of the actual exit of the RS-LRP leak path. Based on the scaling ratio of the leak path between the model and prototype, the amount of the sodium ejection is arrived at ~1.5 kg in 0.6 s. The SCT is provided with a quick closure lid and nitrogen injection system for collecting the leaked sodium and quick nitrogen flooding to avoid combustion in pool mode. Thermocouples were also positioned in the SCT for monitoring the sodium temperature.

Initially, experiments were carried out with water and the driving pressure and valve opening time required for generating the sodium ejection rate of 2.5 kg/s were found to be 3 bar and 1.4 s respectively. Subsequently sodium experiments were carried out. The first experiment involved ejecting 1.5 kg of sodium at 500 °C. The resulting spray fire was confirmed visually using a video camera (Fig. 2) and thermally by the duct outlet temperature, which reached ~700 °C. After 0.6 s of release, the SCT lid was closed and the chamber was flooded with nitrogen. The second experiment followed the same procedure, except the release duct was maintained at 120 °C to simulate the temperature conditions expected at the RS–LRP gap.

Following each experiment, the SCT was allowed to cool before opening it to collect the frozen sodium samples (Fig. 3). Samples from various locations were analysed using wet chemical methods to determine the fraction of unburned sodium. The first and second experiments yielded instantaneous combustion fractions of 18.7 wt% and 18.1 wt%, respectively, indicating that spray-mode combustion was far lower than the theoretical value of 100%.

The experiments also showed that the ejected sodium eventually forms a pool and continues to burn in pool-fire mode, resulting in slower energy release and lower peak temperatures and pressures. These observations indicate that complete instantaneous combustion of the sodium released into the RCB does not occur.

Fig.1. Experimental Setup

Fig.2. Sodium ejection during the experiment

Fig. 3: Frozen sodium in the collection tray

II-14 Under Sodium Ultrasonic Imaging of the Internals of the Primary Tilting Mechanism (PTM) of Inclined Fuel Transfer Machine (IFTM) of PFBR

After receiving regulatory approvals for fuel loading in PFBR, it was observed that the transfer pot did not reach its lowest intended elevation in the PTM and stopped approximately 950 mm above the required level during a trial operation. As the PTM is fully submerged in opaque sodium, under-sodium ultrasonic imaging was performed to visualize the PTM internals to investigate the cause of the obstruction. A manual scanner with a 13.8 m long

spinner tube and a 8.4 m guide tube was designed and fabricated in-house to acquire encoded under sodium ultrasonic signals using four sodium-compatible high temperature ultrasonic transducers in a specially designed and fabricated hermetically sealed housing mounted at the bottom of the spinner tube. The transducers were connected via Mineral Insulated (MI) cables to an 8-channel ultrasonic system, enabling simultaneous acquisition of signals from multiple transducers. Two of the transducers provided horizontal side views, one was inclined at ~17° and one provided downward viewing, offering redundant and diverse inspection angles. Before taking up the under-sodium ultrasonic imaging, underwater mock-up trials were performed in a spare PTM filled with water to optimize the scanning setup, encoder system and data-processing workflow. Circumferential and vertical scan data were acquired using rotary and linear encoders with a sprocket–chain arrangement for angle encoding (Fig. 1). A specific software was developed in Python for processing ultrasonic signals and to generate 3D visualization of the internals of the PTM using the ultrasonic data superimposed on its 3D model (Fig. 2).

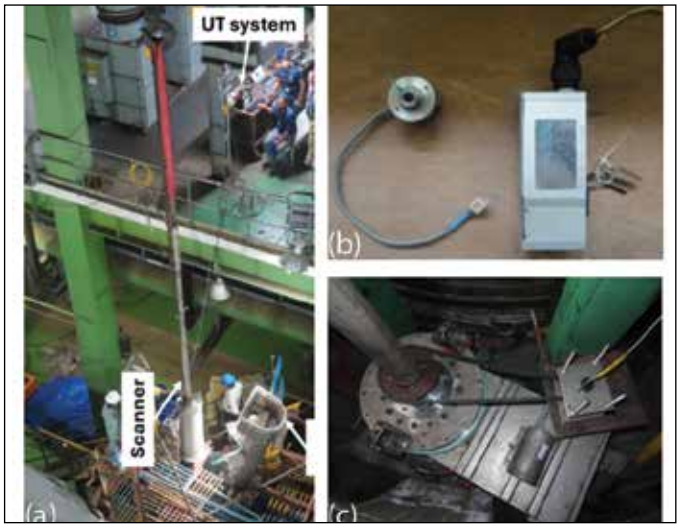

Fig. 1: Photographs showing (a) the spare PTM experimental setup with scanner and ultrasonic inspection system at turbine building in BHAVINI, (b) rotary & linear encoders and (c) sprocket & chain set-up used for encoded data acquisition

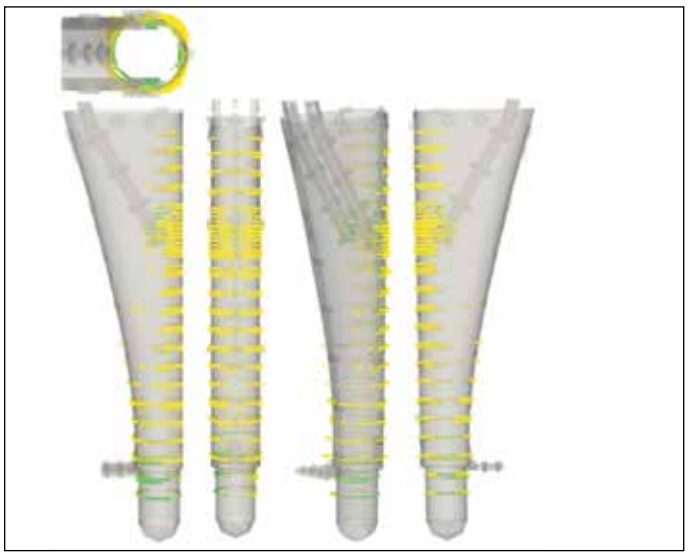

Fig. 2: Visualization of the internals of the spare PTM using the ultrasonic scan data, with corresponding 3D CAD model superimposed for reference

The developed scanner was mounted in the In-Vessel Transfer Port (IVTP) of PFBR and under sodium ultrasonic imaging of the PTM was performed by scanning ~4.4 m of the PTM at multiple elevations. Sector scan data were acquired at every 10 mm vertical steps in the top ~2 m of the PTM to precisely image the 31° tilting rails at 90° and 270° positions and at 200 mm steps in the lower region for geometry mapping, complemented by 560 mm vertical scans at both the rail positions.

Ultrasonic imaging in PFBR revealed that one of the 31° tilting rails in the PTM was dislodged causing an obstruction in the movement of transfer. The positions of the dislodged rail visualized in the ultrasonic image was also confirmed by dislodging a rail in the spare PTM. Based on the comprehensive 3D ultrasonic image generated, the dislodged rail could be extracted from the PTM without draining the sodium and the fuel loading could be initiated using an in-house developed vertical fuel loading system.

II-15 Manufacturing of Portable Sub-Assembly Handling Flask for PFBR Fuel Loading Through IVTP Port

Following malfunctioning of PFBR IFTM after loading of the blanket sub-assemblies, PFBR fuel loading was decided to be carried out directly through the In-Vessel Transfer Port (IVTP) on the Large Rotatable Plug (LRP). Accordingly, Reactor Design Group (RDG) designed a direct fuel loading machine, which was named as Portable Sub-Assembly Handling Flask (PSAHF) and Central Workshop Division (CWD) was entrusted to manufacture the PSAHF in mission mode in parallel to the design activities so that PFBR fuel loading could be resumed in minimum possible time. CWD rose to the occasion and manufacturing of the PSAHF and delivered in minimum possible time.

For the direct fuelling machine PSAHF, CWD manufactured

and delivered ten different assemblies and components, namely 1) Support structure, 2) Gripper assembly, 3) Guide tube assembly, 4) Flask support structure, 5) Transfer Pot, 6) Air Lock, 7) Leak tight housing, 8) Sensor pipes, 9) Drum Shaft and 10) Flask valve, which were assembled at site by BHAVINI. Being a very tall leak tight machine of about 14.5 m height over the reactor pile, the overall tolerances for verticality, concentricity, parallelism and leak tightness for the individual assemblies and components were very stringently specified and same were achieved by CWD through precision machining, fabrication and welding followed by thorough stage-wise and final inspections by the BHAVINI QA team. Salient points of a few major assemblies are described in the following.

The Ø 273.1mm x 6.35mmWT x 14541 mm height Leak tight housing made of SS 316L is an important class III component meant for holding the gripper and the SA. It consists of leak tight pipes, top pipe, flanges and two interface shells with glove ports and viewing windows. The Ø 720mm x 7732mm overall height leak tight Guide Tube Assembly made of SS 316L connects the overhead PSAHF to the fixed transfer port for fuel loading. It consists of top support plate, top flange, Guide Tube, Guide Sleeve, bottom guide, Plug, and Sensor Pipe Housing. All the flanges in both leak tight housing and guide tube assembly has double dovetail grooves for installation of silicone seals for leak tightness. Inevitable Weld distortion was ably controlled by adopting sequential welding methods.

The transfer pot (TP) is fixed at the bottom of the IFTM PTM coaxially to the IVTP port centre-line to receive the SA while loading into as well as unloading from the reactor core. The overall size of the TP is OD 273mm x 4083mm long with the bottom housing of OD 424mm and consists of top cover, guide, top support plate, pot body, bottom housing, sub-assembly seating block, conical cover, bottom guide block, cylindrical pins and disc springs. To avoid inevitable wear and tear due to repeated ingress and extraction of SAs, five parts of the TP, namely guide, top support plate, bottom housing, sub-assembly seating block, and bottom guide block were hardfaced with Ni-based Colmonoy 5 coating. Pre-machining of the hardfaced parts were done at CWD and hardfacing followed by final machining was done by outsourcing. The TP was fully assembled and qualified at CWD and delivered to BHAVINI for installation.

Totally, for manufacturing all the assemblies and components

Fig. 1 Guide Support

Fig. 2 Guide Tube

Fig. 3 Leak Tight Housing, Intermediate Shell

Fig. 4 Machining of Double Dovetail Grooves on Flange

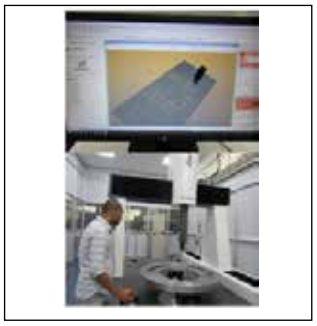

Fig. 5 CMM Inspection of PSAHF Component

Fig. 6 Gripper Assembly

Fig. 7 Hardfaced Parts of Transfer Pot and Final Assembled Transfer Pot

Fig. 8 Erection of PSAHF at PFBR Site

Fig. 9 Site Assembled and Erected PFBR PSAHF

Fig. 10 Trial Movement of PFBR PSAHF within RCB

the PFBR PSAHF meant for direct fuel loading without the IFTM, CWD processed 75 nos. of drawings, each of which further covered 5 to 10 different kinds/sizes of components based the design requirements. Works were executed in parallel wherever possible and all the items were delivered sequentially to BHAVINI in about 7 months, which enabled resumption of PFBR fuel loading. A few pictures of on-site erection and testing of the PSAHF are shown in Fig. 9 to 11.

II-16 Instrumentation & Control for Portable SA Handling Flask of Alternate Fuel Handling Scheme

Alternate Fuel Handling (FH) Scheme:

An alternate FH route with a vertical handling of subassembly through IVTP access port was considered as a promising option for PFBR after thorough analysis subsequent to the non-availability of IFTM-primary-ramp for FH operations.

Portable SA Handling Flask (PSAHF):

PSAHF is used to transfer the preheated SA from SA Preheating facility in RCB to IVTP and the sodium wetted dummy SA from IVTP to Dummy SA Discharge Facility in RCB. The overall height of the flask is ~16m. Lower portion of the flask has an isolation valve to be coupled with the roof slab isolation valve at IVTP access port. The gripper assembly has a manual operated actuator mechanism at the centre. Dual wire rope hoisting mechanism is provided for lowering and lifting the gripper assembly along with SA.

Instrumentation of PSAHF:

Flask is provided with reed, proximity and limit switches for discrete position sensing, draw-wire & absolute rotary encoders for continuous position sensing and two loadcells for continuous load measurement. Apart from these, pressure monitoring of flask is also provided.

Control system of PSAHF:

Fig.1 shows the context of control system of flask. A relay based control system housed in Local Control panel (LCP) is used for controlling the flask operations.

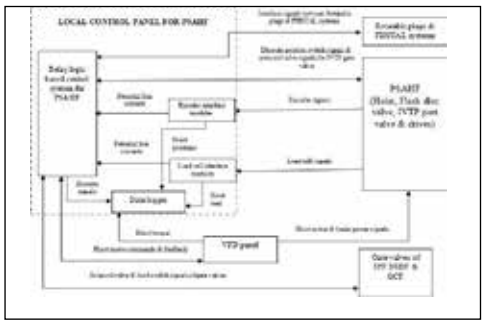

Fig. 1: Context of Control System of PSAHF

Fig. 2: Local Control Panel & VFD Panel of PSAHF

The signals of all instruments are included as safety interlocks in the control logic. A VFD is provided to move the flask hoist in two different speeds. LCP operations include hoist raising & lowering and IVTP gate valve opening & closing. Manual operations include gripper finger operation, transfer pot sensor rod operation and flask disc valve opening & closing operations. LCP is provided with necessary controls (Pushbuttons, selector switches & key switches), lamp indications, hooter, etc. to aid the operator. Data logger is provided to log essential signals of the system for future analysis. Safety interlocks have been incorporated for the interface between HCR controls & LCP operations through key switch authorisation. Similarly, safety is taken care between LCP and manual operations of flask through key switches & administrative approvals at multiple levels.

Challenges:

Once the proposal was conceived, in a minimum possible duration, the I&C requirements were decided, suitable instruments with their mounting methodologies were finalised, control system was designed with the required control schemes for LCP & VFD panel, necessary instruments were procured, design documents & control schemes were internally reviewed, presented to various safety committees & obtained clearances and the control system was made ready.

Outcome:

With the control scheme implemented at PFBR site, the system was successfully commissioned, required number of trial operations were carried out at site with & without subassembly. All operations were confirmed with the requirements specification. PSAHF with the control system is being used successfully for fuel loading operations of PFBR. Fig.2 shows the LCP & VFD panel at site.

II-17 Quality Assurance and Inspection Challenges during Modification of Under Sodium Ultrasonic Scanner of PFBR

Under Sodium Ultrasonic Scanner (USUSS) installed at Prototype Fast Breeder Reactor (PFBR) is utilized to detect and locate any protrusions of fuel sub-assemblies to ensure that they are in correct positions prior to fuel handling operations. In order to increase primary sodium temperature during commission tests, USUSS (Fig. 1a) was taken out of pile and was found to have deformation of the Transducer Holder (TH) and the bottom of the Spinner Tube (ST). This deformation was suspected to the interaction of bottom portion of USUSS with the transfer pot. It was decided to replace deformed transducer holder along with Side Viewing Transducers (SVTs), Downward Viewing Transducers (DVTs) and spinner tube with newly fabricated components at Engineering Hall 3 of FRTG after sodium cleaning. TH assembly consists of housing to hold 4 nos. SVT and 4 nos. DVT, bush and split sleeves. The assembly is made of austenitic stainless steel material and fabricated as per the approved drawing with stringent dimensional tolerances and geometric features. TH having outside diameter of Ø 404 mm holds 4 nos. of SVT and 4 nos. of DVT probes is to be aligned concentrically with the axis of ST and bolted to perform its smooth translational and rotational functions with positional accuracies.

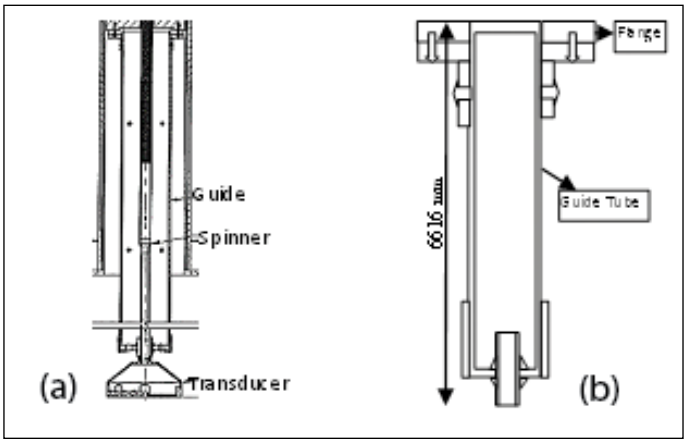

Fig.1: (a) USUSS, (b) Guide tube

Quality Assurance Division (QAD) conducted inspections during the above refurbishment works to ensure compliance with PFBR specifications. Key tasks includes visual examinations, welding stage inspections, liquid penetrant examinations, close tolerance dimensional inspections and alignment inspections using optical instruments at various steps of refurbishment process.

Initially, all structural weld joints of guide tube (Fig. 1b) were inspected for soundness by visual and Liquid Penetrant Examination (LPE).

Levelling of ST flange was checked using optical levelling instrument and ensured the variation of less than 20 microns. At each inspection stages such as fit-up, LPE after root, intermediate & final weld passes during welding between Flange and ST (Fig. 2a), Run out (Fig. 2b) was measured on bottom of hard chrome plated ST diameter (Ø 70 e7) at each 10 mm intervals

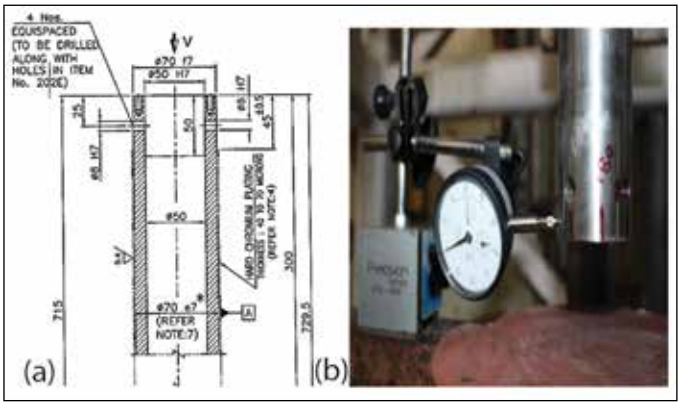

Fig. 2: (a) Spinner tube, (b) Run-out measurement

from bottom upto 160 mm height. The variations was found to be less 90 microns. After mounting SVT & DVT probes (Fig. 3a) with TH and TH to ST, The positions of SVT, Horizontality of TH (Fig. 3b) was measured using optical tilting level at every 60 degree orientation for both clockwise (CW) and anticlockwise (ACW) directions by rotating ST. The horizontality variations noted from the above measurements are plotted as in Fig. 4 and found to be less than 0.9 mm.

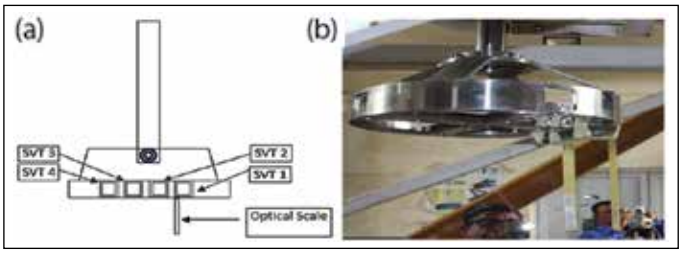

Fig. 3: (a) SVT position in TH, (b) Horizontality check using optical tilting level

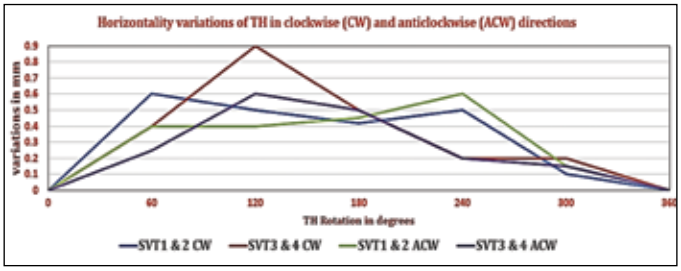

Fig. 4: The systematic QA and inspection activities resulted in successful performance of USUSS in PFBR.

II-18 Machining of Enriched Boron Carbide (B_4C) pellets with 90% 10B for Absorber rods of 40 MWt FBTR & DSRDM, CSRDM of PFBR

In FBTR, the safety shutdown systems strongly rely on neutron absorbers to rapidly terminate the chain reaction whenever required. For this purpose, the absorber rods are packed with enriched Boron Carbide (EB_4C) pellets. Boron carbide is selected due to several favourable characteristics: the Boron-10 isotope (^{10}B) possesses an exceptionally high neutron absorption cross-section; B_4C also offers excellent thermal and mechanical stability, with a high melting point >2450 °C and strong resistance to radiation-induced degradation. However, natural boron contains only about 19.9% ^{10}B and approximately 80.1% ^{11}B, the latter of which has significantly lower neutron absorption cross section. Typical properties of EB_4C are given in the following table:

Property	90% Enriched Boron Carbide (^{10}B isotope)
Chemical Formula	B_4C
Density (theoretical)	2.38 g/cm^3
Hardness (Vickers)	30–38 GPa
Elastic Modulus	450 GPa
Fracture Toughness	2–3 MPa·m½
Thermal Conductivity	30–45 W/m·K
Electrical Resistivity	$10^5 – 10^6$ Ω·cm
Melting Point	~2,450°C

As per IGCAR requirements, Heavy Water Plant (HWP), Manuguru had manufactured and delivered EB_4C pellets with an enrichment of 90%. Random lot of pellets were selected for testing to determine chemical composition and evaluate the physical and mechanical properties. Accordingly, specimens of appropriate dimensions as per the applicable standards had to be manufactured from the pellets for different tests and Central Workshop Division (CWD) was entrusted to manufacture the same. Machining & fabrication of EB_4C pellets are a challenging task, as the material is extremely brittle, possesses a very high hardness (above 9 on the Mohs) and strength but low electrical and thermal conductivity. Despite these challenges, CWD successfully machined the pellets by using wire cut electric discharge machining (WEDM) process with innovative custom designed fixtures and optimized processing parameters through extensive trials and delivered specimens of specified geometry, dimensions and tolerances (GD&T). Trial 1 established a preliminary machining window for enriched B_4C pellets through parameter optimization for WEDM, but highlighted persistent edge peel-off issues. Trial 2 demonstrated that fixture design and job holding are equally important as process parameters in controlling the edge quality. The custom designed fixtures and the WEDM process flow is shown in Fig. 1.

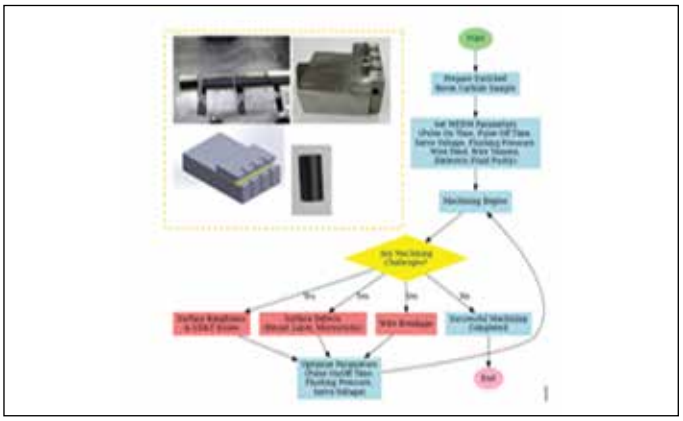

Fig.1. Custom Designed Fixture and Process Flow for WEDM of enriched B4C pellets.

Fig. 2. Enriched boron specimens after machining from the pellets by WEDM sensors.

The combination of optimized WEDM parameters and improved fixturing has enabled the successful machining of enriched B_4C pellets with GD&T maintained within ±10 microns. These results confirm that machining of enriched B_4C requires not only multi-parameter optimization but also a system-level approach, where both process parameters and fixturing strategies are integrated.

Optimization of WEDM parameters for enriched B_4C requires careful adjustment of pulse on time, pulse off time, and flushing pressure values. EB_4C has very poor machinability due to its very high strength and poor electrical and thermal conductivity, which restrict efficient utilization of spark-discharge energy, resulting in unstable discharges, higher surface roughness, and the formation of micro-cracks. Smoother surfaces can be achieved using short pulse-on durations and moderate flushing, but the material removal rate (MRR) decreases sharply, causing significantly longer machining cycles.

II-19 Manufacturing of In-Sodium Collapsible Machine for Remote Retrieval of the Dislodged IFTM Rail from PFBR

In PFBR, one of the rails on which the core sub-assembly (SA) transfer pot moves inside the inclined fuel transfer machine (IFTM) got dislodged from its holding brackets and resulted in complete halt in the initial fuel loading operations after loading of the blanket SAs. For loading fuel through an alternate path, this dislodged rail had to be removed from the IFTM sodium pool, either by draining the sodium or ideally without draining. The later was chosen for overall operational ease.

Already the exact coordinated and position of the rail was determined by using a remotely operated ultrasound scanner manufactured by Central Workshop Division (CWD) and based on this input, Reactor Technology Division (RTD) of BARC designed a remotely operated machine. CWD was entrusted to manufacture this machine. The machine was designed in three assemblies consisting of more than 300 precision parts in total and finally assembled on the PFBR core. To reduce overall weight of the machine, most of the parts were made from long hollows and plates of different thickness. Diameter and center position accuracies for the holes on the guide plates were very critical for achieving overall axial tolerances, being a very tall structure made in three transportable stages. The works included manufacturing of components, assembly, mock testing and load testing. BARC adopted sequential design concept to reduce overall manufacturing time and also to utilize the resources available in CWD optimally. In the process of sequential design and manufacturing, only after successful manufacturing of a predecessor sub-assembly, the next connected sub-assembly design was finalized based on the tolerances achieved and released to CWD for manufacturing. Thus, 205 drawing were released to CWD in the series. Most of the parts manufactured using CNC abrasive water jet cutting as well as precision machining processes, followed by assembly and joining by welding or fasteners as applicable. In each stage, the parts and the assemblies were checked for the geometrical tolerances using computer coordinate measuring (CMM) machine to finalize the dimensions for the next stage. CWD executed the manufacturing of the custom made machine in unique way by parallelizing wherever possible and completed the task in 55 days. About 15% of the components of the machine were manufactured at CDM, BARC before handing over the manufacturing works to CWD. The dislodged rail was removed successfully from the PFBR sodium pool using this machine in the very first attempt and the fuel path was cleared for installation and operation of an alternate direct portable fueling machine, also manufactured by CWD.

Fig.1 Parts and Assemblies of the PFBR IFTM Rail

Chapter - III

R&D for Breeder Reactor

III-01 Feasibility Study of Gas based Reactor Vault Cooling System for FBTR-2

The Reactor Vault Cooling System (RVCS) removes radiant heat from the reactor to protect the concrete structure. In PFBR, FBTR, and MAPS, the RVCS uses embedded pipes carrying forced-circulation DM water, but these systems are prone to corrosion-induced leaks; several have occurred in FBTR and a few in PFBR. Because the embedded pipes are inaccessible during operation, remote chemical sealing is used, though only effective for small leaks. Due to the leak-prone nature of water-based cooling, a study was initiated to evaluate a gas-based alternative, which also reduces water use inside the RCB. The proposed active RV cooling concept circulates nitrogen through the annular space between the CS liner and SV insulation to remove radiant heat, entering at the bottom and exiting at the top (Fig. 1).

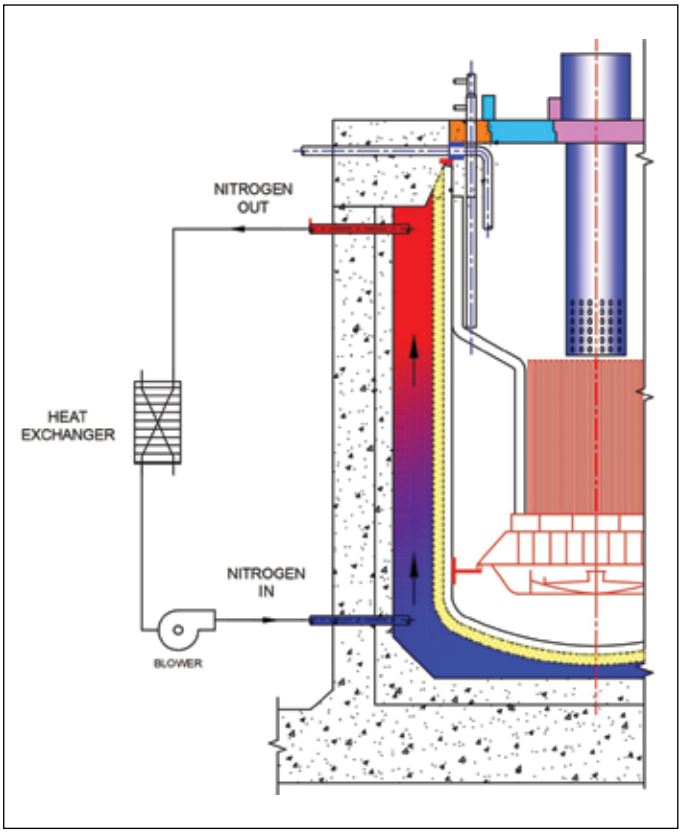

Fig. 1: Schematic of active RVCS

Heat transfer in the RVCS involves coupled natural convection, forced convection, and radiation. Neutron-induced heating of the concrete is excluded in this preliminary study and can be added after shielding calculations. A simplified 1-D design code was developed for initial optimization, with the model schematic shown in Fig. 2.

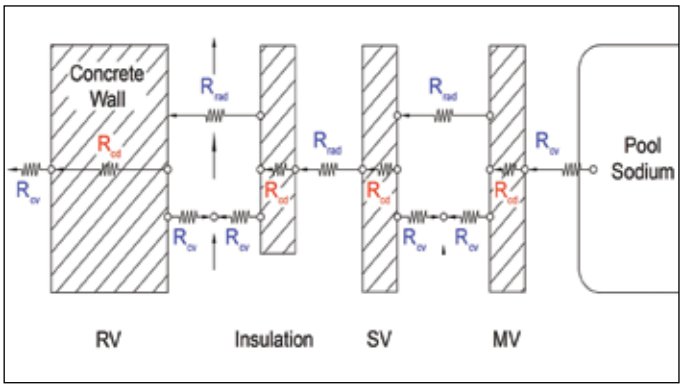

Fig. 2: Equivalent heat transfer circuit

Figs. 3 & 4 show liner temperature variation with flow rate for four supply temperatures. The lateral shield temperature drops rapidly at low flows and then tapers off, requiring at least 6000 CMH to meet limits at 25 °C supply. The bottom shield temperature is largely insensitive to flow and depends mainly on supply temperature, and remains acceptable at 25 °C. This preliminary study indicates that a gas-based system could be a viable alternative to the water-based RVCS, subject to detailed 3D analysis and experimental validation.

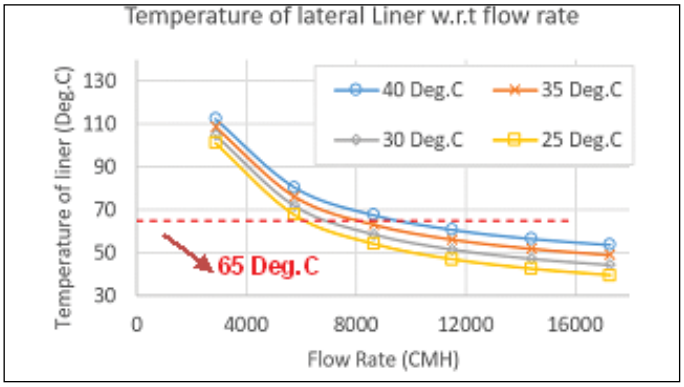

Fig. 3: Temperature variation of lateral shield w.r.t flow rate

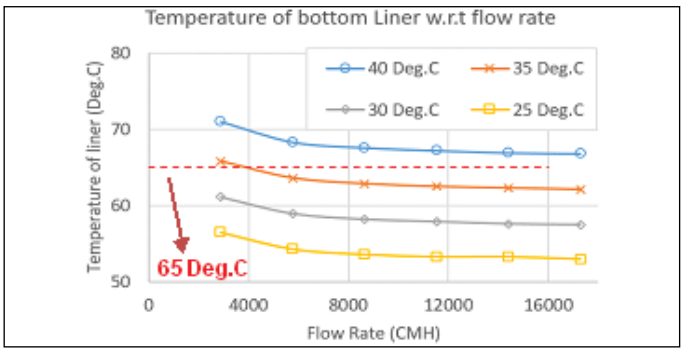

Fig. 4: Temperature variation of bottom shield w.r.t flow rate

III-02 Seismic Qualification Tests for 200 kVA DG Set and Radiation Monitors for Onsite Emergency Support Centre (OESC)

A beyond design basis external event may disable all the facilities available at the NPP site. It may also result in physical isolation of the site such that it may not be possible to receive outside help for a considerable period of time. Emergency facility, known as On-site Emergency Support Centre (OESC) is planned at all Indian NPP sites, which is designed to remain functional under such conditions. The OESC will have adequate radiation shielding and all systems are seismically qualified. The seismic qualification of major equipments of OESC has been qualified using 100 Ton high-capacity shake table at Structural and Fluids Dynamics Division (SFDD) of RDG/IGCAR.

Fig. 1: 200 kVA DG set for Onsite Emergency Support Centre (OESC)

Seismic qualification test for the 200 kVA DG set has been carried out using 100 Ton shake table as per the approved test procedure. The Diesel Generating (DG) set comprises of V-8 Internal Combustion Diesel engine, Alternator with Terminal Box, AVR (Automatic Voltage Regulator), DG local Control panel, Radiator, Battery, Diesel tank, Anti vibration mount etc. Enveloped Floor Response Spectra (FRS) of Auxiliary DG room floor of Onsite Emergency Support Centre (OESC) Building at all existing PHWR station sites (except NAPS) and at 4 No of DEC DG room for TAPS-1&2, TAPS-3&4, KGS-3&4 & RAPS-5&6 has been taken as Required Response Spectra (RRS) with 5% damping. Test matrix consists of sine sweep tests in X, Y and Z directions followed by tests for 5 OBE & 1 BDBE conditions.

Based on the observations from pre-seismic test, during-seismic test & post-seismic test inspections, the 200 kVA DG set met the required seismic qualification criteria and it has been qualified.

Seismic qualification tests for High Range Area Radiation Monitor (HRARM), Low Range Area Radiation Monitor (LRARM), Frisker and Hand & Foot contamination radiation monitors also have been performed using 100 Ton shake table as per the approved test procedure. The floor response spectra of applicable floors of OESC building for MAPS, KAPS, RAPS, KGS and TAPS, are enveloped and broadened which has been taken as Required Response Spectra (RRS) with 5% damping ratio. Test matrix consists of sine sweep tests in X, Y and Z directions followed by tests for 5 OBE & 1 BDBE conditions. Test Response Spectra (TRS) are generated such that TRS envelops the RRS in each direction for OBE & BDBE. The LRARM, HRARM, Frisker and Hand & Foot contamination Radiation monitor was mounted on the shake table and tested. To assess the dynamic amplification and structural damage of the test equipment, the accelerometer and strain gauges are pasted at critical locations and readings are captured and analyzed. Based on the observations from pre-seismic test, during seismic test & post-seismic test inspections, the LRARM, HRARM, Frisker and Hand & Foot contamination radiation monitors met the required seismic qualification criteria and it have been qualified.

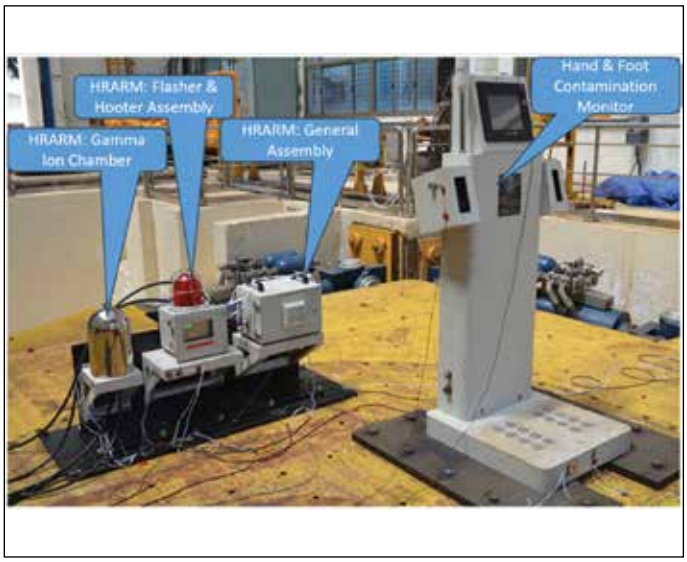

Fig. 2: Radiation Monitors for Onsite Emergency Support Centre (OESC)

III-03 Design & Analysis of Experimental Set-Up for Qualification of Indigenously Developed Large Diameter Inflatable Seals

In PFBR, rotatable plugs are provided with a sealing arrangement consisting of two inflatable seals and a backup seal which act as a leak-tight barrier between the radioactive primary cover gas, laden with sodium aerosols and RCB air. At present, imported inflatable seals are used in these rotatable plugs. To encourage import substitution and promote self-reliance, indigenous development of these large-diameter inflatable seals is in progress.

To qualify these indigenously developed seals for reactor application, it shall be tested under simulated operating conditions as in reactor. For this purpose, a full-scale (1:1) experimental setup was designed, analyzed, fabricated & installed. In this setup, critical operating conditions such as rotation speed, temperature, fluid medium inside & between the seals & pressure experienced by the seals in the PFBR etc. are simulated. The test rig comprises an outer stationary shell fitted with Teflon plates on inner surface & an inner rotating shell. The inflatable seals are mounted in grooves on the inner shell and are designed to interact with the Teflon surface of the outer shell during rotation. The inner shell is reinforced with multiple beams & channels and is connected to a central shaft, which is supported at the bottom by a thrust bearing.

To ensure full functionality of the seal test rig, support structures for the inner and outer shells, along with a hydraulic jack system and guide mechanism for raising/ lowering the outer shell to facilitate seal installation and inspection, were designed. A gearbox support structure with strict deflection control and a drive mechanism for the inner shell were also designed. Additional systems include surface heaters on both the shells, an argon supply system for pressurizing the inflatable seals and inter-seal space, and a cable drag chain to prevent entanglement of cables during rotation, were designed. A control panel was designed to operate the heaters and display real-time data such as pressure, temperature, shell gap, and rotation count.

Fig. 1: Large diameter inflatable seal test rig installed in ITSTF

Static structural analysis of the gear box support structure, inner shell & outer shell supports of large diameter inflatable seal test rig was carried out. Carbon steel (Young's Modulus − 200 GPa & Poisson's ratio − 0.3) was used as material of construction. Torque generated by seal friction, self-weight and load due to cable drag chain were applied with suitable boundary conditions. The resultant stresses & deflection were found to be within limits.

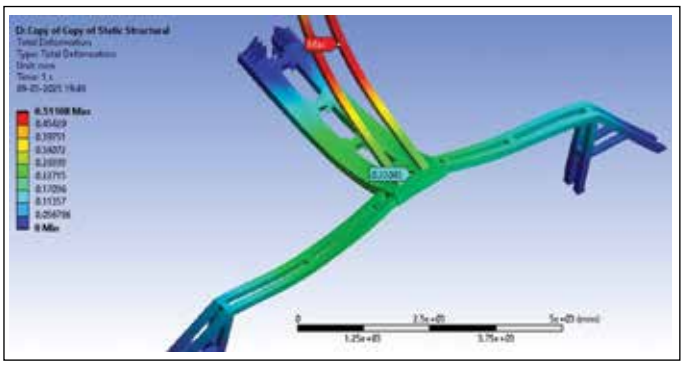

Fig. 2: FE analysis of gear box support structure

Fig. 3: Overall bending stress distribution in the inner shell

Fig. 4: Von mises stress distribution of outer shell support

III-04 Code Development for Column Separation Water Hammer in Water Piping

Water hammer is a banging or vibration that can occur in the water service pipe. The water hammer can cause pipes to burst if a weakness exists in the pipe work. It can also cause pipes to move if they are not well secured, resulting in fatigue cracks or friction holes or breakage of fixed support.

Single phase water hammer occurs in condensate and feed water systems, due to single phase water and steam pressure transients respectively while column separation water hammer occurs, if the pressure during a low pressure period for a liquid filled pipe reaches the vapour pressure and the water starts to evaporate. This evaporation will form vapour bubbles and cavities. A subsequent increase in pressure will cause the bubbles to collapse. This phenomenon is also referred to as cavitation. The model for column separation in single phase liquid flow was developed using Discrete Vapour Cavity Model (DVCM).

The water hammer phenomenon is fully described by the continuity and momentum equations. These equations are solved by the Method of Characteristics (MOC). The discretization and implementation of MOC is shown in Fig. 1. The model assumes that all the vapour in each reach is present in a single pocket at the node causing the wave speed to be constant and identical to the wave speed for a single phase system between each node. In deriving DVCM Equation, it is assumed that there is no free gas in the system, and that at steady state, and when the pressure is above the vaporization pressure, there is no vapour present in the system.

The developed model is validated with experiments from literature.

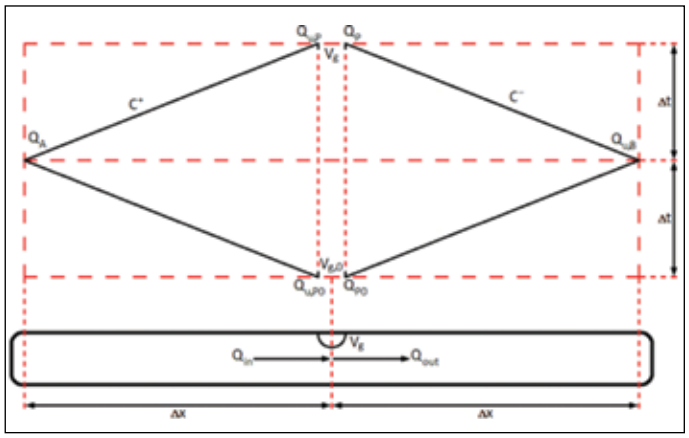

Fig. 1: Grid for two phase Method of Characteristics (MOC)

The experimental study conducted by Bergant et al. as reported in “A Discrete Gas-Cavity Model that Considers the Friction Effects of Unsteady Pipe Flow” in Journal of Mechanical Engineering, Jan 2005, pages 692 to 710, uses a 37.22 m straight copper pipe with an inner diameter of 22.1 mm and a wall thickness of 1.63 mm. The test section has a pressurized tank at the upstream and the downstream end of the pipe. To generate the transient, a fast closing valve is placed at the downstream end of the pipe. The pipe has an inclination of 3.12. The experiment was conducted with an initial velocity of 0.30 m/s which resulted in column separation. The closure time of the valve for the experiments in 0.009 s and the head at the upstream pressurized tank is 22 m. Water is the working fluid at room temperature. The measured results and code result are in agreement with each other as shown in Fig. 2 and Fig. 3 respectively.

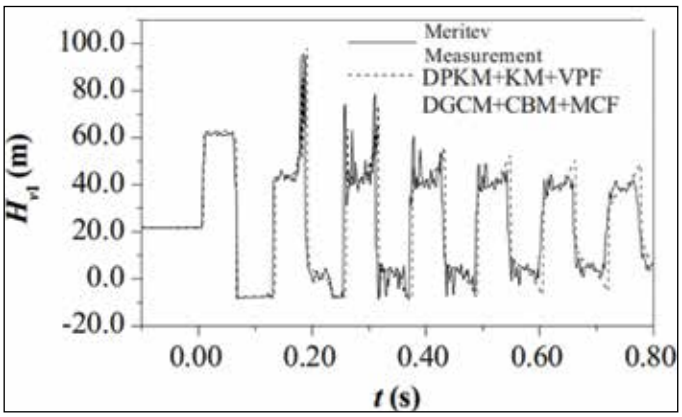

Fig. 2: Pressure evolution at the valve by Bergant et al. column separation occurring at ~0.2 s

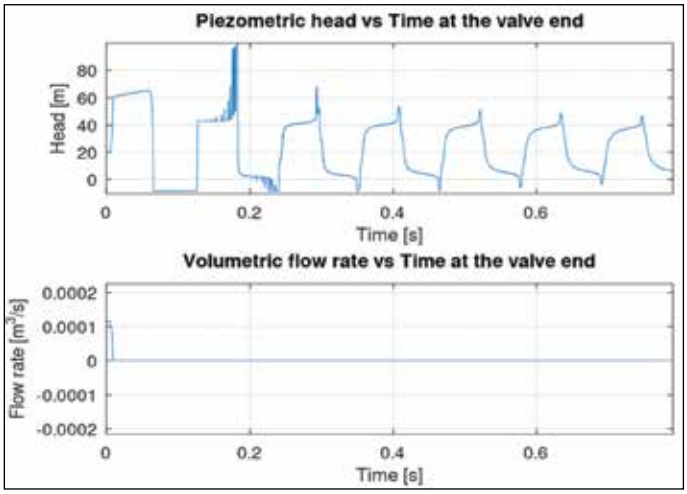

Fig. 3: Flow and pressure evolution at the valve from developed code for by Bergant et al.

III-05 Conceptual Design of Primary Sodium Main System for FBTR-2

FBTR-2 is a 100 MWt (40 MWe) metal fueled, sodium cooled, loop type fast reactor. It consists of two Primary Sodium Main Circuits (PSMCs) and two Secondary Sodium Main Circuits (SSMCs).

Each PSMC includes one Primary Sodium Pump (PSP) and one Intermediate Heat Exchanger (IHX), connected to the Main Vessel (MV) through the Primary Sodium Main Piping (PSMP). Both PSMCs are located in shielded cells inside the Reactor Containment Building (RCB). A schematic of a typical primary loop is shown in Fig. 1.

The primary sodium piping draws sodium from the hot pool and is routed above the free sodium level, passing through the argon cover gas space and through the reactor vault before entering the IHX. This elevated routing is unique compared to existing loop type fast reactors. Hot primary sodium enters the shell side of the IHX through the inlet plenum, transfers heat to the secondary sodium, and exits from the lower end. The cold sodium then flows to the PSP suction and is pumped back into the MV grid plate plenum through the sodium piping. From Grid plate plenum, sodium enters radially to fuel sub-assemblies, flows upward through the core and returns to the hot pool. The outlet line from the PSP enters the cover gas space and then passes through the stand pipe in hot pool and joining the grid plate.

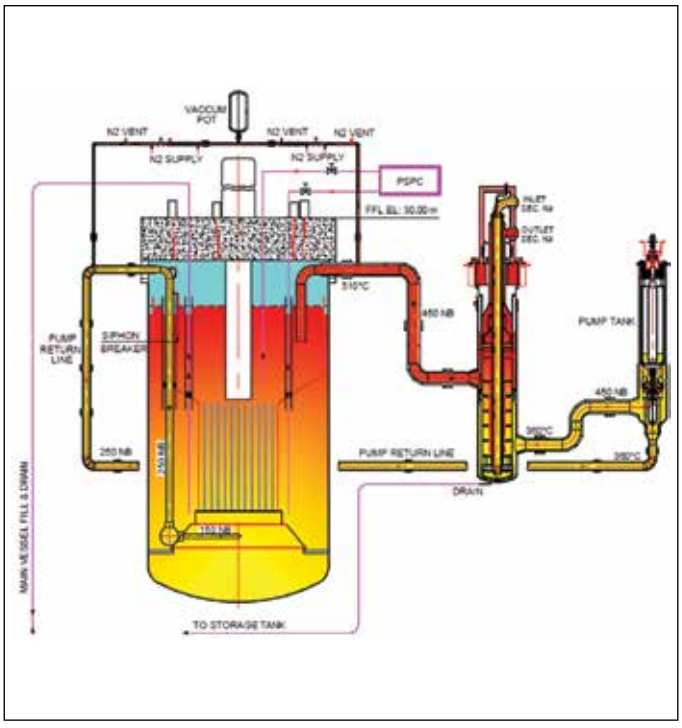

Fig. 1: Schematic of primary sodium main system in FBTR-2

Table 1: Operating plant parameter

Parameters	Value
Reactor Power	100 MWt
Primary sodium inlet/outlet temp.	360/510 °C
Primary sodium flow rate/loop	291 kg/s
Secondary sodium temp.	318/480 °C
Sec. sodium flow rate/loop	241 kg/s
Pipe diameter from hot pool to IHX	450 NB
Pipe diameter from IHX to PSP	450 NB
Pipe diameter from PSP to grid plate	300 NB
No. of IHX & PSP per loop	1 & 1 per loop

Key process parameters are listed in Table 1. All PSMC pipes outside main vessel are enclosed within the guard pipe. The guard pipe is compartmentalized for effective leak detection in case of sodium leak. Each compartment has a bellows to accommodate differential thermal expansion, and the annular space between the main pipe and guard pipe is inerted with low pressure nitrogen. Each compartment is provided with sodium leak detector and sodium drain line.

Since the PSMC piping rises above the hot pool sodium free level, initial filling of this elevated section requires a dedicated vacuum-pulling system. Two separate vacuum lines, one connected to the IHX inlet line and the other to the pump outlet line are connected to the vacuum pulling system of each primary loop. Once these lines are filled with sodium, they will be isolated using sodium freeze seal along with isolation valve to ensure leak tight sealing.

To avoid uncovering of core from primary sodium in MV in case of an accidental pipe break event outside MV, a siphon break line is provided for sodium return line to main vessel. Termination of siphon break line and sodium outline are considered at same elevation which is sufficiently below free sodium level to avoid gas entrainment for all plant conditions. Purity of the radioactive primary sodium is maintained and monitored by a dedicated primary sodium purification circuit with adequate shielding against its activity level.

III-06 Conceptual Design and Preliminary Sizing of Primary Sodium Pump for FBTR-2

Fast Breeder Test Reactor-II is being designed with metallic fuel pins, leading to longer fuel subassemblies and consequently a higher pressure drop across the core. The higher pressure drop in the primary sodium circuit with relatively low flow rate results in the design of Primary Sodium Pumps (PSPs) operating in the low specific speed regime, i.e., radial-type pumps as the preferred choice.

To determine the permissible operating speed of the pump, several design constraints must be satisfied: the critical speed margin (ratio of critical speed to operating speed) must exceed 1.3, the cavitation margin (ratio of NPSHA to NPSHR) must be greater than 1.5, and the ratio of pump diameter in the hollow region to that in the solid region must remain below 3.

Two design options are explored considering PSP in loop-type and pool-type reactor configuration. The pump shaft is supported by two radial bearings. The top bearing location is selected at/near to the pump support flange. In loop type and pool type designs, the pump is supported at EL 28000 and EL 30000 respectively. The position of the impeller and sodium bearing are based on the (a) elevation of hot pool, (b) pressure drop from hot pool to pump tank and (c) submergence required during rated flow rate condition. Based on these factors, the elevation of sodium bearing is estimated as EL 23290 and EL 24640 for loop type and pool type design respectively.

With these bearing positions and shaft power to be transmitted as input parameters, a preliminary shaft design is arrived. Considering pump hydraulics parameters such as cavitation margin and suction specific speed, upper limit on shaft speed is obtained as 1400 rpm. Critical speed analysis is carried out using Rayleigh-Ritz method and FEM method, considering it as a dry rotor. The diameter of the hollow portion of the shaft is progressively increased until either the limit on hollow-to-solid diameter ratio or critical speed margin is reached. The speed selected for loop and pool type design are 1400 rpm and 1200 rpm respectively.

Based on speed, the impeller diameter is estimated and diffuser-type pump is selected, as it is necessary to accommodate the Non-Return Valve (NRV) integrated into the pump assembly. The overall dimensions such as diameter and height of the PSP are established for both loop-type and pool-type configurations of FBTR-II. The key parameters are presented in Table 1 and a schematic of PSP is shown in Fig. 1.

Table 1: Parameters of PSP for FBTR-II

S. No.	Details of PSP	Loop type	Pool type
1	Flow rate (m^3/hr)	1200	1200
2	Head (mlc)	120	110
3	Speed (rpm)	1400	1200
4	Dia of impeller (m)	0.65	0.72
5	Dia of PSP top flange (m)	1.40	1.52
6	Total height (m)	8.5	9.2

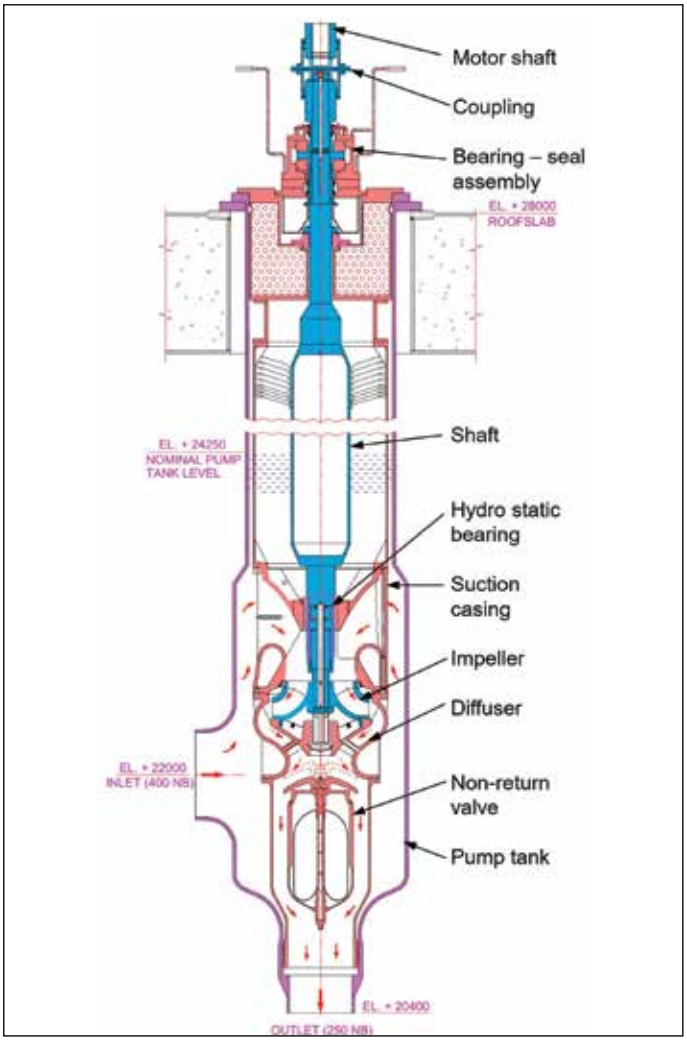

Fig. 1: Schematic of PSP in loop configuration of FBTR-II

III-07 Experimental and Numerical Evaluation of Sodium Aerosol Characteristics in the Cover Gas of a Sodium-Filled Test Vessel

Sodium-cooled Fast Reactors (SFRs) employ an inert cover gas to isolate the liquid sodium pool; however, temperature-driven evaporation, nucleation, and condensation produce sodium aerosols, which are then convectively transported within the cover gas space. These aerosols affect cover gas thermal hydraulics, deposition on top-shield structures, annular gaps, and affect the cover gas purification systems, all of which are relevant to reactor engineering safety. A mechanistic model is necessary to comprehensively understand the thermal hydraulics and aerosol dynamics in the cover gas region, and its verification through simulated experiments remains essential. For this purpose, a numerical model is developed based on a mixture-based Eulerian approach, which is validated against in-house experiments conducted at the SILVERINA loop. The governing equations are solved in the modified AeroSolved, in the OpenFOAM framework.

Experiments were previously conducted in the SILVERINA loop, and the characteristics of aerosols in the cover gas of the test pot (TP-1) were analyzed. The inner diameter and cover gas height of the TP-1 vessel were 760 mm and 820 mm, respectively. Aerosol sampling was taken at three elevations (near pool: 715 mm, mid: 415 mm, and near top: 215 mm) and analyzed for aerosol concentration and size distribution. Reactor operating conditions (pool temperature: 823 K, bottom of top shield temperature: 413 K) were imposed to mimic operational thermal gradients.

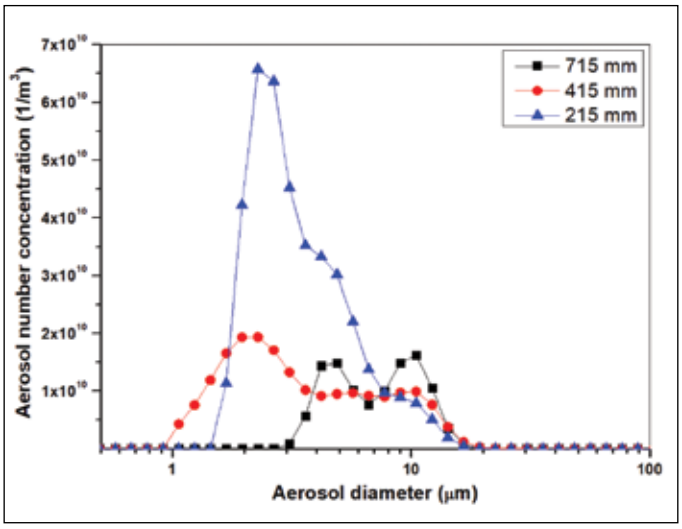

Fig. 1: Aerosol size-dependent concentration at three heights of cover gas space

Experimental measurements (Fig. 1) show that the aerosol distribution ranges from 1 to 20 μm, with a count median diameter (CMD) of ~7.7 μm (near the pool), 3.9 μm (middle), and 3.8 μm (near the top), with the highest total number concentration found adjacent to the pool. Larger particles concentrate near the pool due to gravitational force and high local condensation rates. However, smaller aerosols are transported upward by natural convection and are distributed throughout the cover gas.

The estimated temperature distribution (Fig. 2a) within the cover region varies from 413 K to 823 K, with an average cover-gas temperature of ~600 K. The estimated average convective velocity is around 0.4 m/s, peaking near the vertical walls at ~0.8 m/s.

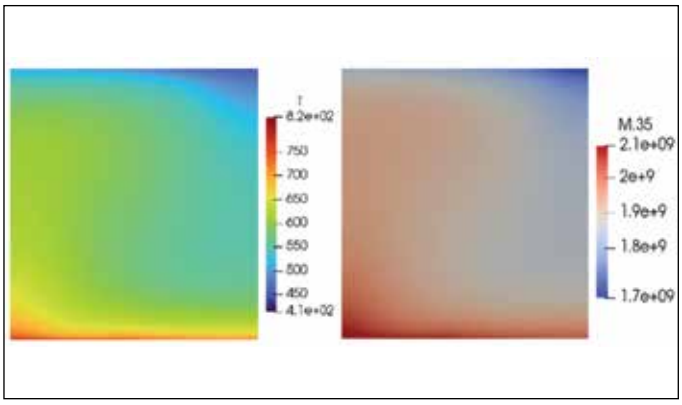

Fig. 2: (a) Temperature contour inside the cover gas space and (b) sodium aerosol distribution of diameter 23 μm

Fig. 2(b) shows the distribution of 23 μm sodium aerosol in the cover gas space. The mechanistic model reproduces the key experimental trends: (i) larger diameter aerosols remain confined near the pool (Fig. 2), (ii) smaller aerosols are distributed across the cover gas, and (iii) predicted CMD (~7 μm near the pool) aligns well with measurements. The observed vertical distribution of aerosol sizes suggests that deposition rates on top-shield penetrations will be strongly dependent on the size of the aerosol.

The combined experimental and numerical study demonstrates consistent sodium aerosol characteristics in a representative cover gas geometry. In the future, validated numerical models can be extended to estimate aerosol deposition in annular penetrations of the complex top shield.

III-08 Performance Assessment of Irradiated Enriched U-6%Zr Metal Fuel and T91 Cladding

As part of the R&D program on metal fuel cycle development for FBRs, Post-Irradiation Examinations (PIE) of sodium bonded Enriched Uranium-Zirconium (EU-6Zr) metal fuel pins test irradiated in FBTR to 26.5 GWd/t (peak) burn-up at a peak linear heat rating of 155 W/cm, was taken up. The non-destructive examinations of metal fuel pins such as X-ray & neutron imaging and Gamma scanning had revealed an axial fuel swelling of ~10% and complete closure of fuel-clad gap. The salient results of the Fission Gas Release (FGR) measurements, microstructural examination of fuel pin sections, and tensile properties & swelling measurements of the mod 9Cr-1Mo steel (T91) clad, are presented in this article.

Fission gases were collected from the fuel pins inside the hot cell using a customized puncturing set up. FGR measurements & analysis were done using gas chromatography and mass spectrometry in tandem. The maximum fission gas pressure measured inside the fuel pins was ~1.15 MPa and the Fission Gas Release (FGR) was in range of 48-52%. Subsequently, bond sodium was removed from the fuel pins using an in-house developed remotely operable Vacuum Distillation System (VDS) (Fig. 1) inside the hot cell.

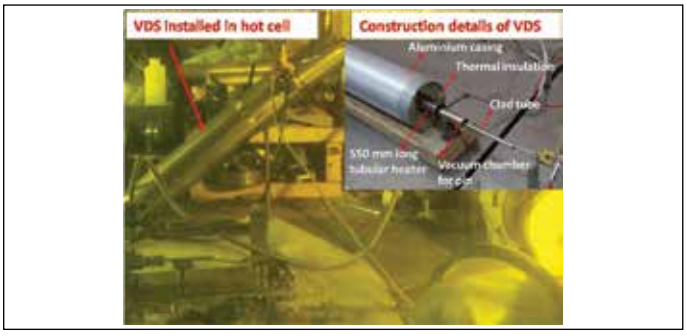

Fig. 1: Vacuum distillation system (VDS) installed inside the hot cell. Inset shows the construction details

Microstructural studies were conducted on transverse sections of the fuel-clad extracted from the peak-power location, as well as from positions 64 mm and 140 mm below the peak-power zone of the U-Zr slug. Samples were metallographically prepared and examined in a glove interfaced scanning electron microscope facility.

Microstructure of all the cross sections indicated complete closure of the fuel-clad gap indicating a radial swelling of 15%. The average volumetric swelling of the fuel was ~45% which corresponded to swelling of ~17% per at% burn-up. Micrographs at peak power indicated isolated fission gas channels at the center of fuel matrix and interconnected channels at the periphery (Fig. 2), consistent with the FGR measurements. The size and number density of gas channels was relatively higher at peak power location.

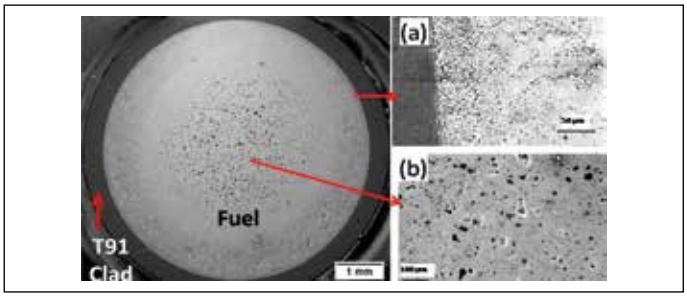

Fig. 2: Scanning electron microscope image of Enriched U-6%Zr metal fuel pin irradiated to 26 GWd/t in FBTR, revealing closure of fuel-clad gap and fission gas channels (a) interconnected at fuel periphery and (b) isolated at fuel centre

Micro-chemical analysis using Energy Dispersive Spectrometer (EDS) did not indicate any significant redistribution of fuel constituents or formation of Fuel Clad Chemical Interaction (FCCI) products. However, a discontinuous Zr-rich segregation was found in the periphery of section at 140 mm below peak power zone. Incipient segregation of lanthanides (near fuel slug periphery), and metal fission products (inside fuel matrix) was observed in all the cross-sectional samples.

Two 60 mm long clad segments were extracted from plenum region having neutron damage of 60 dpa (adjacent to peak power location) & 38 dpa. These samples were tensile tested at 420 °C using the in-cell universal testing machine. Stress-strain curves of irradiated T91 cladding, as shown in Fig. 3 reveals hardening and reduction in ductility as compared to the unirradiated clad. The ductility (uniform elongation) of the clad has reduced from 12% to 8 % at 60 dpa. The density of T91 clad samples from various locations, measured using immersion density technique, indicated negligible swelling (ΔV/V) for neutron damage up to 60 dpa.

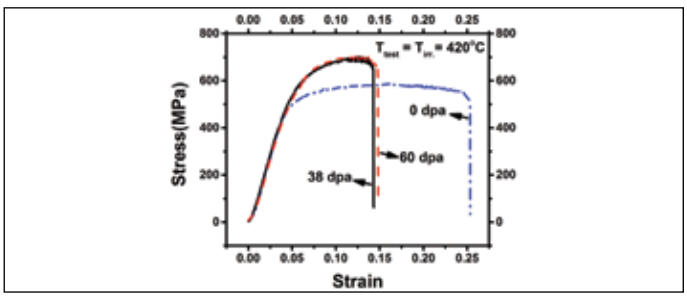

Fig. 3: Stress strain curve of T91 clad tubes

To summarize, the test irradiation of EU-6Zr fuel pins has indicated that fuel swelling, fission gas release and microstructural changes are commensurate with the burn-up of 26.5 GWd/t and in line with the reported literature. The residual ductility and swelling of the T91 clad do not pose any concern for enhancing the burn-up of other ternary metal fuels pins under test irradiation in FBTR.

III-09 Development of Ag-Al Fusible Plug for SGDHR System of FBR

As a part of passive safety feature in future FBRs, high temperature fusible plug was developed to act as electric circuit breaker in SGDHR system enabling heat removal through an air damper, if Na temperature exceeds 833 ± 5 K (565 ± 5 °C). Requirements for the fusible plug material include: (1) Melting point – 833 to 838 K , (2) Thermal conductivity – 20 W m^{-1} K^{-1} (min) and (3) uniformity in microstructure. Photograph of the fusible plug assembly is shown in Fig. 1.

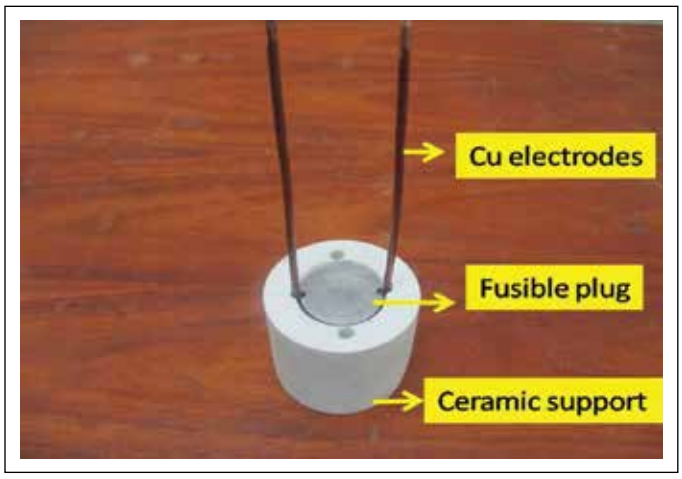

Fig. 1: Photograph of the fusible plug assembly

Melting point requirement for the fusible plug is met by the eutectic composition i.e. Ag-32.27 wt%Al. Hence trial experiments were conducted with 10 g buttons in order to optimize holding temperature and time to achieve uniform composition in the final melt. Photograph of the Ag-32 wt%Al fusible plug fabricated by the stir casting method is given as Fig. 2a.

Microstructure of the plug was analyzed using both BSE and X-ray imaging in EPMA. Microstructure was found to be uniform across the plug with eutectic mixtures of Ag-Al solid solution (SS) and δ-Ag_2Al phases (Fig. 2b,c). In Fig. 2b, SS and δ-Ag_2Al phases appear as dark and bright phases respectively. Chemical composition of the phases and average composition (in wt%) of the alloy were obtained as Ag-55Al (SS), Ag-14Al (δ) and Ag-(32)Al respectively.

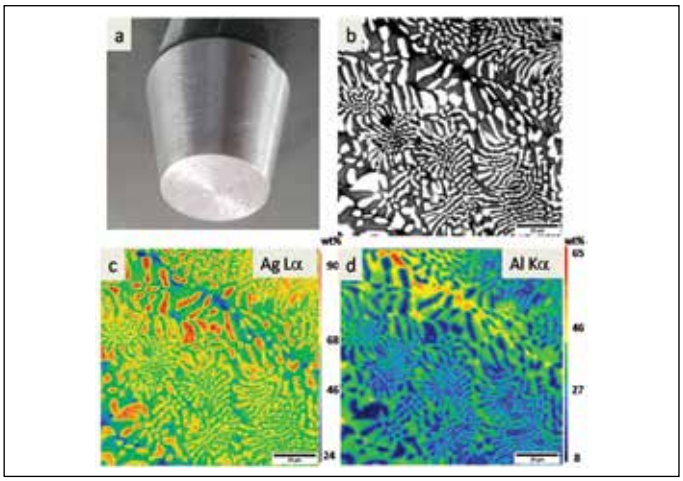

Fig. 2: (a) Photograph of the fusible plug, (b) BSE image, (c,d) X-ray maps showing eutectic Ag-Al SS+δ-Ag_2Al structure

Melting point was measured using DSC by heating the sample at a rate of 1 K min^{-1} up to 1273 K then cooling to room temperature (RT) at 30 K min^{-1}. Peak melting temperature was 840 K (Fig. 3a). From experimentally measured thermal diffusivity (α), heat capacity (C_p) and density (ρ), thermal conductivity (k) was calculated from RT up to 723 K using the expression $k = \rho\alpha C_p$. Temperature dependent variation in k is shown in Fig. 3b. Uniformity with respect to microstructure and properties was ensured through multiple measurements. Experimentally measured k was 3.7 times more than the design specification of 20 W m^{-1} K^{-1} at RT.

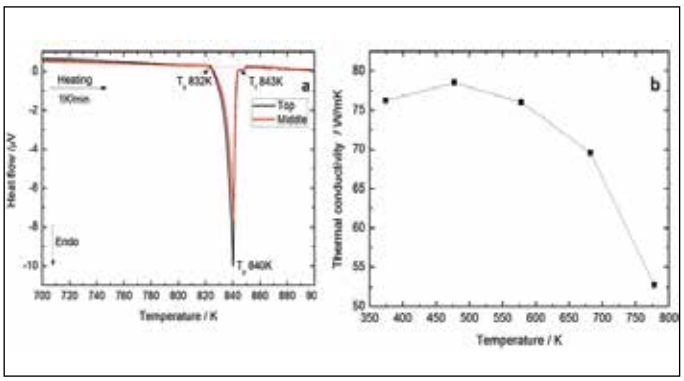

Fig. 3: (a) DSC thermo gram for melting point measurement, (b) Thermal conductivity variation with temperature

III-10 Study of Sintering Path and Densification Mechanism during Spark Plasma Sintering of Tungsten Carbide Powder for Lower Axial Shielding of FBTR

To extend the residual life of FBTR, stainless steel pellets used for bottom axial shielding in the fuel SA are being replaced with Tungsten Carbide (WC), to reduce the neutron fluence experienced by the grid plate. Accordingly, indigenous development and fabrication of binderless high-density WC pellets are being regularly carried out by Spark Plasma Sintering (SPS) method at the Physical Metallurgy Division. The objective of this study is to analyze and understand the sintering path and densification kinetics of WC powder in achieving a high density.

Consolidation of WC powder with particle size of 2-5 µm as discs of 40 mm diameter and ~9.5 mm thickness was carried out at a temperature of 0.64T_m (2013 K) and dwell time of 15 min under uni-axial compaction pressure of 35 MPa (44 kN).

Fig. 1(a) shows the time-temperature-pressure profile used to sinter the WC powder at 2013 K. The events and phenomenon responsible for the densification during heating cycle is indicated in Fig. 1(b). The 1st sharp peak is attributed to initial re-arrangement of powder particles and 2nd sets of peaks appear, when powder undergoes localized deformation at the contact points under fixed compaction pressure.

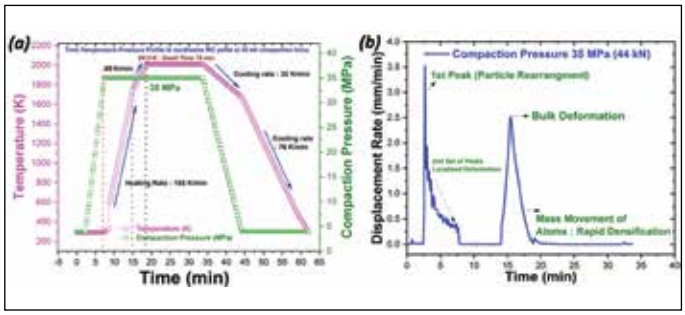

Fig. 1: (a) Time-temperature-pressure profile used to sinter WC powder, (b) Punch displacement rate vs time during densification

It is observed from Fig. 2(a) that, during initial compaction for 15 min, 45% theoretical density is achieved at 35 MPa. While heating from 1773 to 2013 K (0.64T_m) along with application of pressure and for the soaking time of 15 min, the localized deformation extends to the core (bulk deformation) resulting in mass movement of atoms throughout the volume of the pellet promoting higher densification. The bulk deformation appears as the 3rd peak in Fig. 1(b).

The final relative density achieved during this process is 99.5% of theoretical density (15.63 g/cc). The curve exhibits accelerated densification at the beginning and saturation in densification in the end, following the well-known “S” shape curve. Fig. 2(b) shows the typical variation of relative density and densification rate as a function of temperature for the compaction pressure 35 MPa.

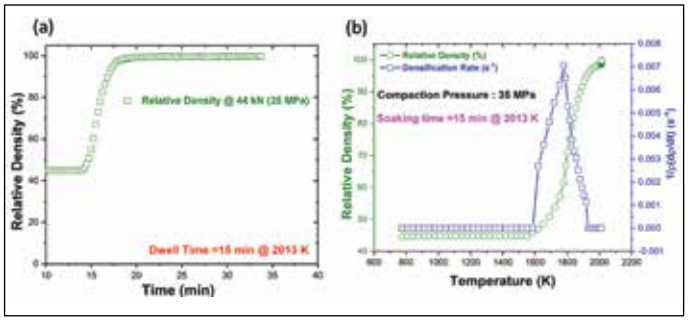

Fig. 2: (a) Variation of relative density with time, (b) Relative density and densification variations with temperature

Densification starts at 1573 K, reaches a maximum at 1773 K and plateaus beyond 1973 K. To elucidate the steps controlling densification, the densification rate, stress exponent (n) and activation energy (Q) were evaluated using the analytical model proposed by Bernard-Granger and Guizard as, n (2.91,1.02,0.14) and Q (489 kJ/mol for n = 1.02) (Fig. 3). The n-value suggests, densification proceeds by boundary/lattice diffusion, grain boundary sliding and dislocation gliding for values close to 1 (n ≤ 1), 3 (2 < n < 3) and above 3 (n >> 3), respectively.

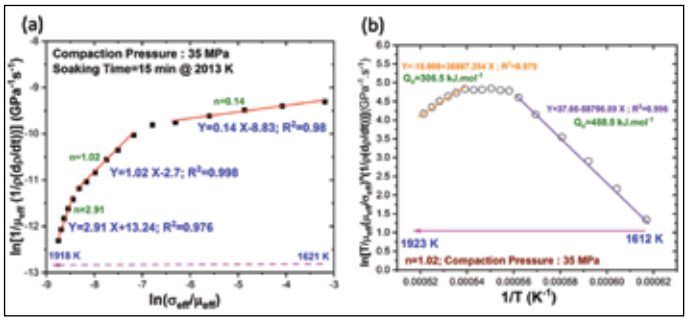

Fig. 3: (a) Stress exponent and (b) Activation energy

Based on this study, SPS parameters for synthesis of WC discs of high density (99.5%) have been optimized to be 2013 K and 35 MPa with a holding time of 5 min. Pellets of 13.1 mm were carved out from the discs by EDM cutting to be loaded into the bottom of fuel sub-assemblies for grid plate shielding in the 33rd and future campaigns of FBTR.

III-11 Demonstration of carbon removal from sodium at engineering scale

Sodium is commercially produced by the electrolysis of fused sodium chloride in a Downs cell, which employs a carbon anode and iron cathode. During this process, erosion of the graphite anode introduces carbon impurities into liquid sodium. Carbon in sodium beyond a limit may carburize low carbon austenitic stainless steel structural material, which would adversely alter the material properties. Hence, carbon concentration in nuclear grade sodium is limited to a maximum of 30 ppm to ensure the safe and reliable operation of sodium circuits in Fast Breeder Reactors (FBRs).

Carbon exists in sodium as (i) dissolved species and (ii) suspended particulates. Since carbon solubility is very low (~2.5 ppm at 550°C), most carbon is present in particulate form. Two kinds of carbon removal techniques are effective: microfiltration for particulates and hot trapping for dissolved carbon. Microfiltration uses a sintered metallic filter to retain carbon particles, while hot trapping uses low-carbon martensitic steel getter at ~650°C to absorb dissolved carbon by diffusion and carbide formation. Multiple static sodium experiments with SS410 getter material were carried out to evaluate the mass transfer coefficient of carbon. The size and shape distribution of Carbon particles in sodium could also be found through analytical techniques. With these input data a hot trap and micro filter were designed to remove carbon from 10t of sodium inventory of SOWART facility, which has got 25ppm of carbon in it.

A carbon trap loop was integrated to the SOWART facility, where a bypass line at 400°C houses the microfilter. Another parallel line houses hot trap operates at 650°C and associated heater circuit. Microfilter and hot trap were operated independently. Photograph of major components of carbon trap loop are shown in figure 1.

Two-phase purification was performed: 360 hours of microfiltration at 400°C, to remove undissolved carbon Particulates followed by extended hot trapping at 650°C to remove dissolved carbon. After 14 days of circulation through the microfilter, the concentration dropped to 9.3 ppm from 25 ppm. Nearly 68% of carbon was removed after microfiltration process.

Fig.1 Components of carbon trap loop

During the subsequent hot trap operation, carbon content further reduced to 6 ppm after 750 hrs of hot trapping. The combined operation resulted in an overall reduction of approximately 75 % in carbon concentration.

The results confirm that the combined purification approach, mechanical filtration followed by hot trapping is effective for achieving nuclear-grade sodium purity. The microfiltration process, being purely mechanical, operates efficiently even at lower temperatures (~400 °C), does not require getter replacement making it operationally simpler and more effective than the hot trapping process.

Future work includes metallurgical examination of getter and filter elements, optimization of microfilter pore size and development of a standalone particulate-based carbon trap to eliminate the need for high-temperature hot trapping.

III-12 Design Qualification of Indigenously Developed Sodium Service Valves for Indian FBRs

In Indian FBRs, sodium service valves of sizes 100 NB and below are typically selected as Bellows Sealed Globe Valves (BSGVs). Since hot sodium is highly pyrophoric, preventing external leakage is critical. To ensure leak-tightness, the valve is provided with a hydroformed metallic bellows as the primary sealing element. A secondary seal of GRAFOIL gland packing is provided to offer temporary leak tightness in the event of bellows failure until leak of bellows detected. The annular space between the primary and secondary seals is continuously monitored using a sodium leak detection system, enabling early identification of breach in primary seal and allowing timely safety actions. Historically, most sodium valves used in Indian FBRs, as well as key critical components such as bellows assemblies, were imported from Europe. For long-term sustainability, a dedicated valve development program focusing on complete indigenization was implemented. Program addressed several technological challenges including hermetic sealing in sodium, precise metal-to-metal plug-seat contact, robustness under thermal shock and seismic loads. Leveraging the experimental feedback from sodium facilities and operational experience of two decades, several design improvements were implemented. BSGVs feature a specialized Y-shaped forged body to minimize hold up volume and pressure drop.

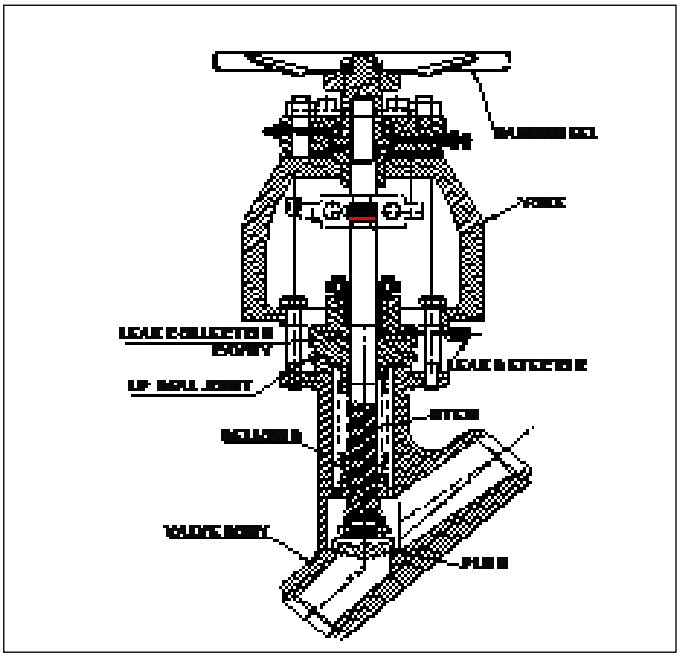

Fig.1 Schematic of indigenously made Bellows sealed globe valve

Fig.2 Testing of Inconel 625H bellows in sodium (left) and seismic testing of indigenously developed sodium valves (right)

Fig.3 Indigenously developed BSGVs from size 15NB to 100 NB

The design of valve body was optimized and finalized by experimental studies in sodium, water and air, and parametric studies using FEA and CFD tools. Indigenously designed BSGV is shown in fig.1.

The structural design of valve has been significantly enhanced through improvements in primary seal and engineering measures to withstand thermal shock, flow-induced vibration (FIV), and seismic loads. Flow tests in water were performed to evaluate flow characteristics and qualify flow coefficient. The integrity of bellows due to stem vibration against FIV loads was demonstrated experimentally. Indian make Inconel 625H bellows were qualified by in-sodium creep-fatigue tests (fig.2). Finally, sodium service BSGV was tested on seismic table to qualify the valve for reactor application (fig.2). With successful completion of qualification activities, the sodium service BSGVs from size 15NB to 100NB (fig.3) are now fully developed and manufactured within India, contributing significantly to the indigenization and sustainability goals of the Indian fast reactor program.

III-13 Commissioning and Operation of a New Sodium Facility at Sodium Technology Complex

Sodium Technology Complex (STC) of Fast Reactor Technology Group is located in the southwest sector of the newly developed IGCAR North Site. The facility spans 40 m × 21 m × 43 m and houses major infrastructure, including a high bay, a sodium dump pit, a material storage area, Sodium Removal Facility, and a sodium cleaning and disposal bay. The sodium dump pit measures 12 m × 7 m × 7 m (below FFL), while the storage area measures 12 m × 8 m × 15 m. A large experimental sodium facility (Fig 1) has been established to validate and optimize design concepts and to provide critical inputs for future Fast Breeder Reactor (FBR) development.

Safety Review Committee for Operating Plants has recommended stage-wise clearances for commissioning. The total planned sodium inventory for the facility is 100 tonnes. A major design feature of STC (Fig 2) is the ability to isolate either of the two test vessels, enabling independent control of test conditions and vessel-specific operations—such as filling, draining, heating, and cooling—while maintaining uninterrupted operation of the other vessel.

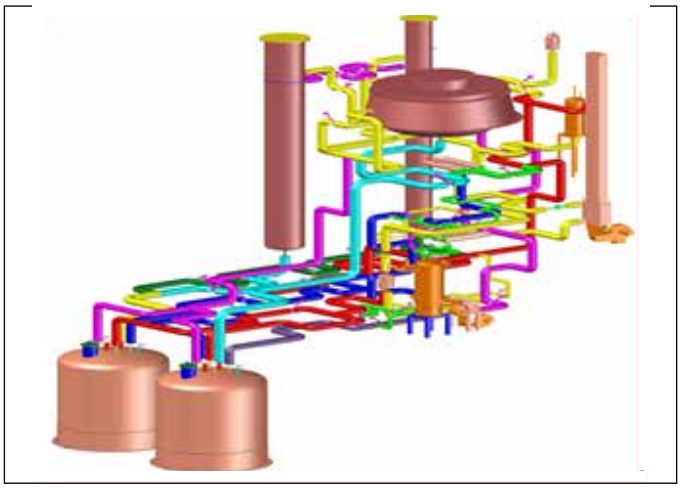

Fig.1 Sodium Loop in Sodium Technology Complex

Commissioning of STC is being carried out in sequential phases, including sodium charging of the storage tank and commissioning and operation of the sodium loop at intermediate temperatures (up to 300 °C) and subsequently at rated operating conditions (630 °C).

All auxiliary systems—including cover gas, compressed air, preheating, DACS, leak detection, level detection, fire alarms, ALIP, and additional support systems—were individually tested, verified, and integrated with the sodium loop.

Fig.2 Inauguration of commissioning of sodium loop

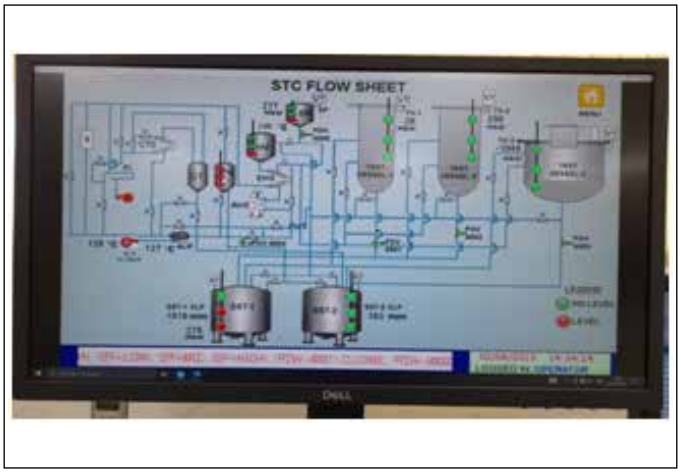

Fig.3 Flow sheet of sodium loop

The loop was subsequently commissioned up to 300 °C, operated successfully for a cumulative duration of 856 hours, demonstrating satisfactory performance (Fig 3).

Preparations are underway to qualify the loop at the rated operating temperature in line with design specifications. The primary objectives of the facility include qualification and testing of shutdown mechanisms with enhanced safety features, the third shutdown system, in-house–developed ultrasonic transducers, and other long-component testing requirements. The facility is also being augmented to support performance evaluation of the indigenously developed SGDHR Annular Linear Induction Pump for next-generation FBRs. Overall, STC sodium facility is progressing toward full operational capability and a key sodium facility for supporting future FBR development.

III-14 Studies on Evaluation of Soundness of Butt Welds during Qualification of Welding Procedure – An ASME Codal Perspective

ASME Section IX Boiler & Pressure vessel code is used for qualification of welding procedure and personnel to give direction to welder to make sound weld deposit. Root and Face bend/Side bend tests are used to ascertain soundness of weld coupon qualitatively as per QW-451. As per this code, there is no mandatory requirement for volumetric Non-Destructive Testing (NDT) such as Radiographic Testing (RT) or Ultrasonic Testing (UT) of weld coupon for procedure qualification. However, in codes such as RCC MR-X, BS 5500 volumetric NDT is specified as mandatory requirement in addition to bend test for procedure qualification. This study intends to highlight the limitation of guided bend tests as sole acceptance criteria.

Towards this, butt welded (using GTAW and SMAW

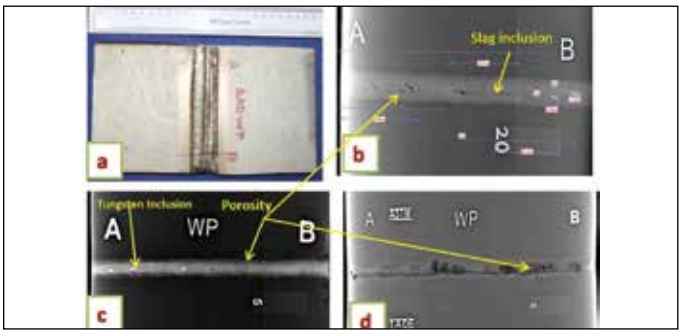

Fig. 1: (a) Weld pad, RT image of (b) 14 mm, (c) 6 mm and (d) 3 mm coupons. Characterization of flaw using RT image analysis and PAUT

process) samples of thickness (3 mm, 6 mm, 10 mm, and 12 mm) containing different artificial defects (such as porosities, slag and Tungsten inclusion) at different depths were fabricated (Table 1). These defects are not acceptable by radiography examination in accordance with ASME section IX QW-191.1.2 as shown in Fig. 1. Characterization of the defects in the weld samples was performed using Radiography (for defect length) and Ultrasonic phased array examination (for defect depth)

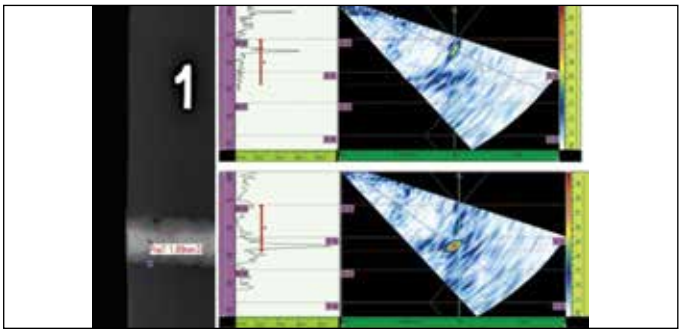

Fig. 2: Characterization of flaw using RT image analysis and PAUT

as shown in Fig. 2. After characterization of flaws in weld samples, the Transverse Face (FB), Root (RB) and Side Bend (SB) coupons were prepared by cutting the weld samples to form specimens of rectangular cross section. Angle of wrapping is 180° with bend diameter of four times the thickness of specimen as shown in Fig. 3.

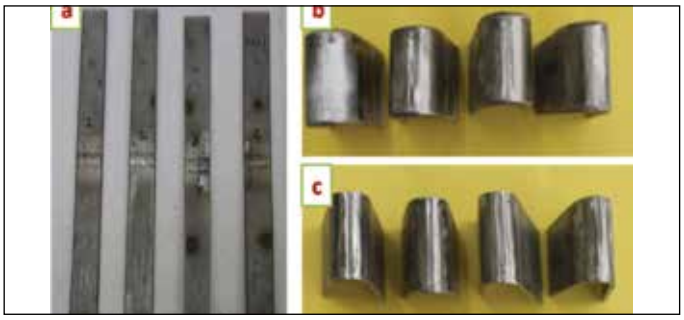

Fig. 3: (a) Typical bend test specimen, FB & RB of (b) 6 mm and (c) 3 mm

Spec. No.	Weld Specimen Thickness	Nature of flaw	Depth from weld face	Depth from weld root	Types of bend test	Result
1a	6 mm	porosity Φ 1.9 mm	–	2 mm	Root bend	No open discontinuity
1b	6 mm	Ti, L=3.03 mm	–	4 mm	Root bend	No open discontinuity
1c	6 mm	Ti, L=4.0 mm & L=3.4 mm	1.2 mm & 3.2 mm	–	Face bend	Ti 4.0 mm open to surface
1d	6 mm	porosity Φ 0.7 mm	1 mm	–	Face bend	No open discontinuity
2a	10 mm	Slag, L=20 mm		2.5 mm-3 mm	Root bend	No open discontinuity
2b	10 mm	Slag, L=6 mm	7 mm-9.5 mm	–	Face bend	No open discontinuity
3a	14 mm	porosity Φ 3.6 mm	12.5 mm	–	Side bend	Pores open surface
3b	14 mm	porosity Φ 4.0 mm	8.5 mm	–	Side bend	Pores open surface
3c	14 mm	Ti, L=4.6 mm	7.5 mm	–	Side bend	No open discontinuity
3d	14 mm	Ti, L=6 mm	8 mm	–	Side bend	No open discontinuity
4a	3 mm	porosity Φ 3.0 mm	–	–	Root bend	No open discontinuity
4b	3 mm	porosity Φ 1.5 mm	–	–	Root bend	No open discontinuity
4c	3 mm	porosity Φ 3.5 mm	–	–	Face bend	No open discontinuity
4d	3 mm	porosity Φ 0.7 mm	–	–	Face bend	No open discontinuity

Table 1: Details of defects and bend test results

Table 1 also summarizes the bend test results on different thickness of weld coupons with defects positioned at various depths within weld volume. It can be inferred from Table 1 that some of weld coupons have cleared bend test in spite of having unacceptable flaw in radiography. Hence, it is recommended that RT/UT requirement may be considered for welding procedure qualification in addition to the bend test requirement for ascertaining soundness in ASME Section IX, in line with other international codes such as RCC-MRx and BS5500.

III-15 Design & development of indigenous hardware based mutual inductance type leak detector instrument for FBR

Mutual inductance based leak detector (MILD) is used for sodium leak detection in safety vessel, IHX, DSRDM and sodium pipelines in PFBR. MILD sensor has a primary coil excited with an AC current and a separate secondary coil wound on a magnetic core. Eddy currents are generated in the leaked sodium surrounding the sensor. Theory of eddy currents indicate that magnitude and phase of the induced secondary coil voltage is affected by presence of conductive target. The field generated by eddy current opposes the primary field decreasing the magnitude of inducted voltage. The time taken for the diffusion of primary field in the conductive target manifests as phase lag in the secondary coil voltage in reference to the primary coil excitation current.

The electronic instrument deployed in PFBR is a micro-controller based embedded system. The sensor primary coil is excited with a sinusoidal current of magnitude 100 mArms at a frequency of 5250 Hz. The setting of magnitude of current, frequency, detection threshold and calibration is performed using application software. The secondary coil voltage is acquired and change in the secondary voltage magnitude is processed to detect & annunciate sodium leak. Spurious alarms have been reported when there is a change in process temperature.

An indigenous hardware instrument was developed to excite the primary coil and to acquire the secondary coil voltage magnitude and phase difference. The hardware-based instrument is simpler, reliable and easily amenable for verification & validation. The photograph of the unit is shown in Fig. 1. It consists of exciter, voltage controlled oscillator, pre-amplifier, phase detector & power supply module. The unit can source primary coil excitation current in the range of 25 to 125 mArms at a frequency of 1 to 10 kHz. The receiver module measures magnitude

Fig. 1: Photo of prototype electronics hardware

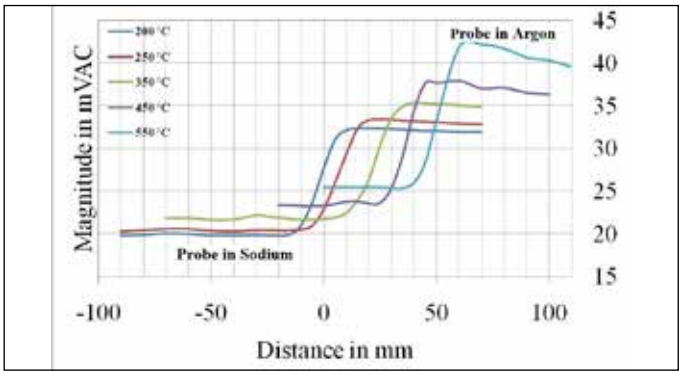

Fig.2: Magnitude at different sodium temperature

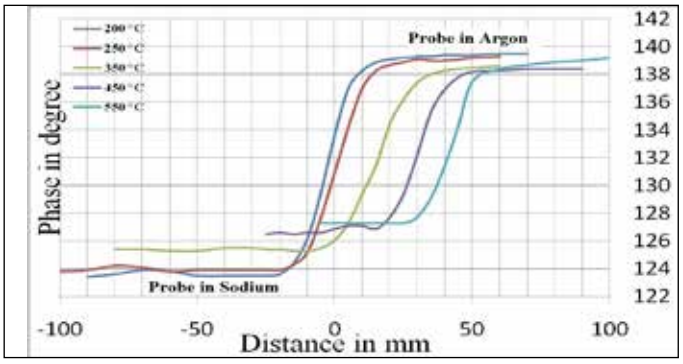

Fig 3: Phase angle at different sodium temperature

and phase of the secondary coil voltage with a resolution of 1°. Experiments were conducted with the instrument along with MILD sensor at the sodium pot test facility in Hall-III at FRTG, IGCAR. Data was recorded at different sodium temperature from 200 °C to 550 °C. The plot of magnitude and phase change at different temperature is shown in Fig 2. & 3. At temperature of 200 °C the change in magnitude is 12 mVrms and 16 ° for phase change with the sensor fully surrounded by sodium. It is observed that magnitude change is around 10 mVrms in argon atmosphere at different process temperature. This variation is probe dependent and increases the probability of false alarm if calibration is not carried out at correct sodium temperature. In comparison, the phase angle change in argon atmosphere at different process temperature is only 2° which provides an advantage of temperature independent calibration for any probe. Further, it is observed that phase based signal processing is relatively in-sensitive to variation in excitation current amplitude (less that 1° change for 50 % change in amplitude). In comparison magnitude change is directly proportional to % change in current amplitude. It is concluded that phase change provides a clear indication of leaked sodium.

III-16 Development of Control System using NUCON PLC for SILVERINA facility FBR

For monitoring and control of process parameters in SILVERINA facility, NUCON PLC based distributed control system architecture has been developed as shown in Fig.1 and tested. DAE units have developed an industrial strength PLC (NUCON PLC) with in house developed GUI based application development environment.

As a part of sodium technology development, the existing SILVERINA facility is modified to conduct studies on sodium impurity monitoring and purification components for FBRs. The envisaged loop has a storage tank with sodium of known purity feeding to another transfer tank through the test section, eliminating mixing of sodium.

The signals from the modified SILVERINA sodium loop are terminated at the Field Instrumentation Panels (FIPs) located in the loop area, where they are processed by the NUCON PLC-based control system.

A scaled down model test facility was setup in RTSD lab

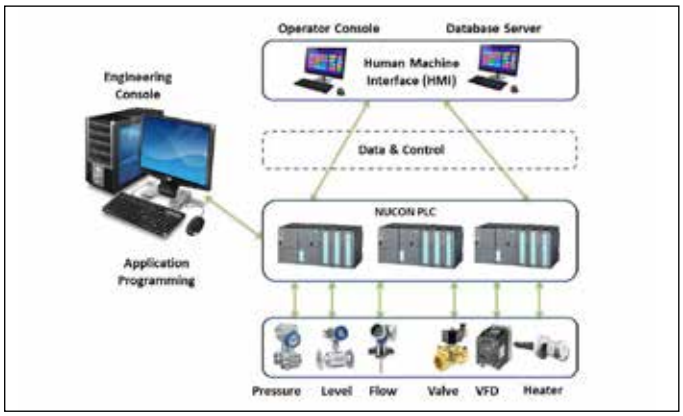

Fig.1: Architecture of NUCON PLC System

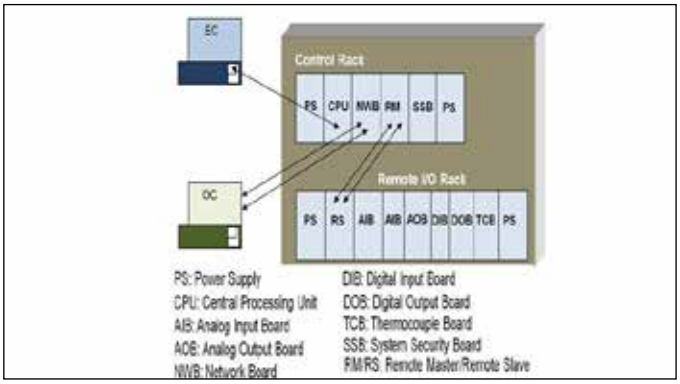

Fig.2: NUCON PLC Programming Configuration

with two PLC nodes, signal simulators, network switches, Operator Console (OC) & Engineering Console (EC) as shown in Fig.3. The NUCON PLC based control system generates control/interlock outputs, window alarm outputs and sends the data to operator console.

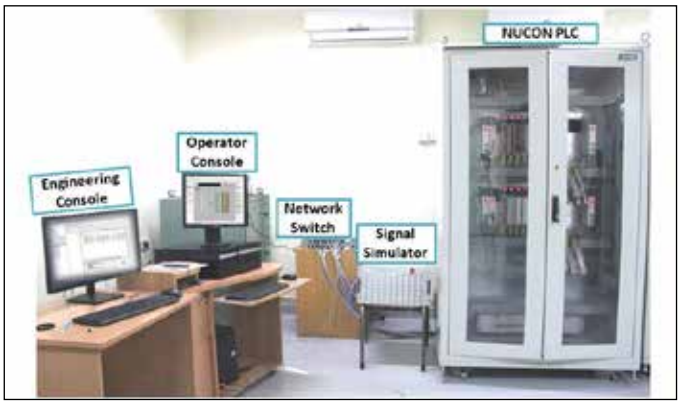

Fig.3: NUCON PLC Test Setup in Lab

NUCON PLC node was configured through engineering console as shown in Fig.2 using CODESYS software (IDE for PLC application development) and SCADA front end was developed using EC-SCADA (an indigenous SCADA package developed by ECIL) for lab demonstration as a proof of concept. Requirements document and architecture document were prepared & released with the inputs received from end user.

Plant database design for all signal parameters of SILVERINA was completed and interfaced with SCADA software.

GUI for SILVERINA Loop was developed with mimics, signal information, alarms & popup control as shown in Fig.4 and tested in lab by simulating inputs through signal

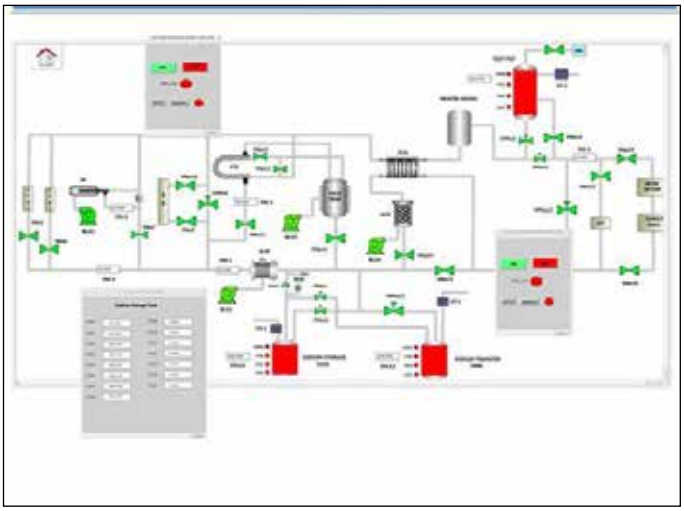

Fig.4: GUI Mimic Screen (SCADA)

simulators. Control/ interlock logic development in PLC was completed and tested alongside the requirements.

III-17 Design and Development of Centralized Event & Data Analysis System (CEDAS)

The Centralized Event & Data Analysis System (CEDAS) has been envisaged as part of the I&C infrastructure of PFBR to provide a unified platform for integrated log analysis. The Distributed Digital Control System (DDCS) of PFBR comprises 840 control nodes, six servers and thirty display stations. Presently, independent mechanisms exist for logging history data, alarms, events and system performance. CEDAS consolidates these into a single system to provide operators and maintenance personnel with a comprehensive view for enhanced situational awareness, efficient troubleshooting and predictive maintenance.

CEDAS (Fig. 1) interfaces with existing logging systems to collect real-time data from DDCS components through the plant network and organizes them into a structured event–data repository. The system architecture provides time-synchronized correlation between process parameters, alarms and operator actions.

The application software has been developed using a modular, scalable framework with analytical utilities for event correlation, sequence tracing, alarm clustering and trend visualization. Among its key functional modules are the Operator Action Log and the Trip Analysis Module.

The Operator Action Log records all human–machine interactions in DDCS components, including set-point modifications, command issuance, mode changeovers and login/logout activities. Each event is time-stamped with millisecond precision and tagged with operator ID, system source and destination. The data are correlated with history and alarm logs for root-cause analysis and post-event review.(Fig2)

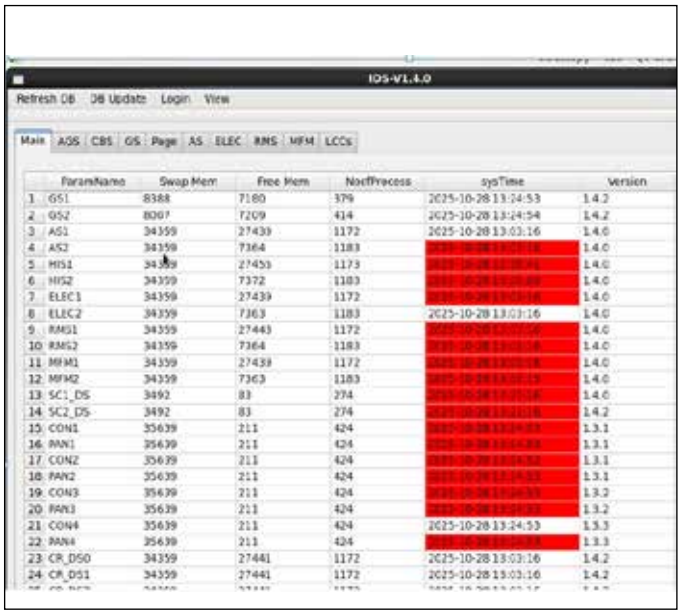

Fig. 1 : CEDAS Prototype Dashboard – System Health View

Fig. 2 : Operator Action Log Records

The Trip Analysis Module facilitates detailed study of major equipment related events such as PSP, SSP and EM Pump trips. Historical process data corresponding to the selected event are automatically retrieved from the Historian Server, enabling visualization of signal trends before, during and after the trip. This assists in identifying the initiating cause, sequence of operations and response of critical systems.

CEDAS provides significant operational benefits such as complete traceability of operator actions and events, enhanced root-cause and post-event analysis, and the ability to correlate multiple data sources for holistic diagnostics. It also supports predictive maintenance by detecting anomalies early, and strengthens auditability and regulatory compliance by maintaining synchronized, comprehensive logs of system and operator activity.

In contrast to conventional log viewers, CEDAS provides a unified analytical interface across multiple subsystems, enabling comprehensive assessment of plant performance. A prototype version has been deployed at PFBR site and features such as data acquisition, operator action logging and event visualization have been demonstrated successfully.

III-18 Pilot Deployment of Hybrid Energy Harvesting Wireless Sensor Networking node at INSOT

The Energy Harvesting technique is a good power option for energy-constrained Wireless Sensor Network (WSN) applications, where energy is derived from non-conventional but accessible external sources. However, the amount of energy harvested is unpredictable. To overcome the limitation, Hybrid Energy Harvesting (HEH) which provides energy solution from multiple sourceswas selected. It was tested at the laboratory level to evaluate whether the harvested energy was sufficient for WSN operation. To analyse the HEH WSN performance in plant atmosphere, IN SOdium Test (INSOT)facility has been selected for pilot deployment. INSOT consist of creep & fatigue loop. These loops are designed to study the creep&fatigue properties of the PFBR component materials under the influence of flowing sodium.

Site survey for INSOT facility was conducted to identify non-conventional, accessible energy sources to power on HEH-WSN node. Thermal, wind and indoor light sources were identified for the purpose. Thermo Electric generator (TEG) is used to harvest the thermal energy released from sodium pipes. Wind turbine is used to harvest power from wind released from blower. Plant indoor lighting is utilized to harvest power through solar panels. Block diagram of pilot HEH WSN setup is shown in Fig1. Mounting of TEG, Solar panel and wind turbine at INSOT facility is shown in Fig 2

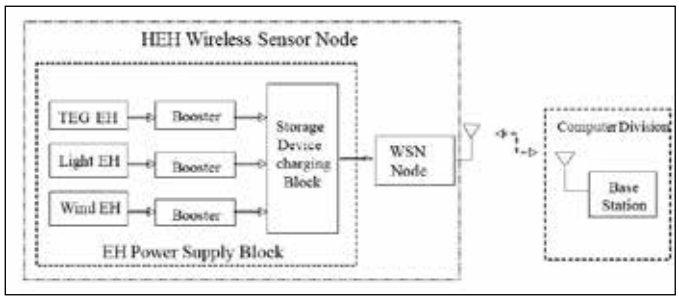

Fig 1 Pilot HEH WSN Block Diagram

Three numbers of HEH WSN nodes were configured at 2.445GHz frequency. To utilize the limited harvested power, they were configured in sleep state by default. Based on the harvested power by individual HEH WSN node, packets with on board sensor (temperature and humidity) values were transmitted to the Ethernet based Base Station (BS) located at Computer Division via router nodes. In addition, to ensure the WSN network availability&and to distinguish between node power loss and network unavailability, 2 numbers of solar powered health nodes were deployed at INSOT facility. They transmit periodic network health data at 1min interval to BS. Data from HEH WSN collected by BS are forwarded to Unified WSN server. Pilot HEH WSN Deployment at INSOT is shown in Fig 3.

Harvested energy varies with location and time, depending on the availability of ambient sources.The packet transmission rate of HEH WSN nodewas manually varied at different times to identify a sustainable sleep/active duty cycle. Based on this experiment, node's optimized sleep/active duty cycle was determined considering the ambient energy available in INSOT facility during loop running condition. During this pilot deployment, it is observed that HEH is able to establish sustainable network with 60 min sleep with 1sec active duty cycle.

Fig. 3: HEH WSN node developed in INSOT fatigue loop

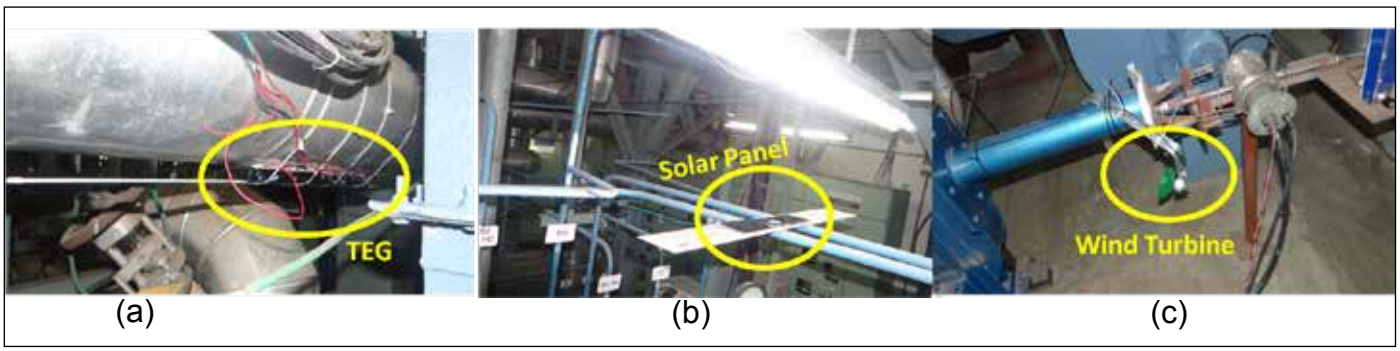

Fig 2: (a) TEG mounted on Sodium Pipe; (b) Solar Panel mounted below the Tube light; (c) Wind Turbine Mounted near Blower

III-19 In-house developed pulsating type turbidity meter for online measurement

Turbidity measurement is crucial in industries that depend on clear water for their operations. Continuous monitoring of turbidity ensures consistent product quality by detecting the presence of suspended particles or impurities in real time. An opto-resistive quasi-digital sensor for online turbidity monitoring has been designed and developed at Innovative Sensors Section. The turbidity meter can measure from 0 NTU to 400 NTU with an accuracy of ± 3 NTU. The unit has a 2.4" TFT display and is powered by 5 V DC (0.5 A current). The response time of the instrument is 1 s and uses multipoint calibration. The sensor consists of a LED, two Light Dependent Resistors (LDR) and a logic gate oscillator (LGO) circuit. Figure 1 shows the working principle of the system schematically.

The light from a LED is made to fall on the sample. Depending on the level of turbidity, either the scattered light or the transmitted light is measured. The degree of light scattering/ absorption is directly related to the

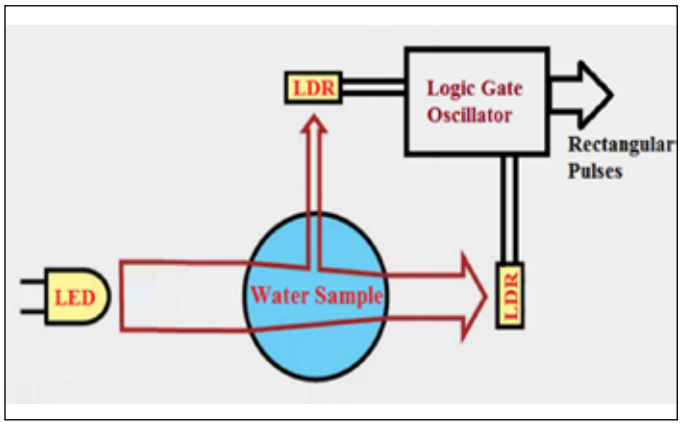

Fig.1. Working principle of turbidity sensor

concentration, size and distribution of suspended particles in the sample. Thus, the water turbidity reduces the light intensity and the same is reflected through a change in the resistance of the LDR. Further, a change in resistance

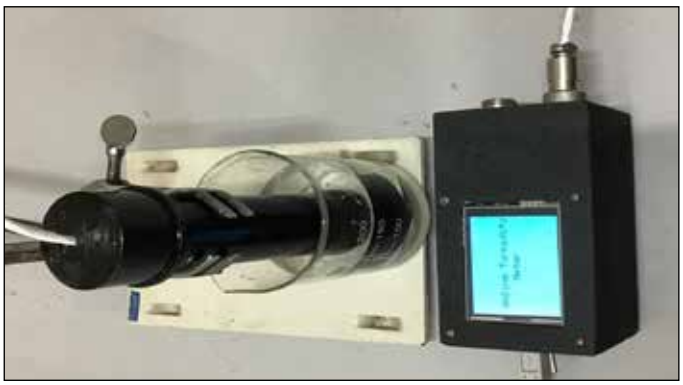

Fig. 2 Photograph of the online Turbidity Meter

shifts the output of the LGO circuit which is in the form of a train of rectangular digital pulses of 5V amplitude. Counting these pulses for a fixed duration gives the frequency and frequency carries information on the turbidity of the water.

A mathematical relationship between frequency and turbidity is established by taking turbidity standards of known NTU and the same is stored into the instrument's firmware.

All the components of the turbidity meter, viz., micro controller based embedded system, PCB and the sensor were designed and developed in-house. An Atmel SAM3X8E ARM Cortex-M3 microcontroller is employed to read, process and display the final turbidity data in terms of NTU on a TFT display. The Arduino sketch open source tool was used to develop the firmware. The PCB layout was carefully engineered as a two-layer design to ensure optimal signal integrity, compactness, and reliable electrical connections among the sensor components. This configuration facilitates seamless integration of the sensor with the overall monitoring and data acquisition system. The turbidity meter was tested in our laboratory and was found to work satisfactorily. The turbidity meter is compact, rugged and can easily be configured as per the end users requirement. Figure 2 shows the photograph of the online turbidity meter.

III-20 Design, fabrication, testing and commissioning of multiple pin sodium bonding furnace

Metal fuel fabrication facility is being setup for fabrication of wire wrapped sodium bonded metal fuel pins of 932 mm long for sub-assembly level irradiation in fast breeder reactor at IGCAR. Metallic fuel pin is designed with smear density of 75% to accommodate the irradiation induced fuel swelling and it enhances burnup of fuel upto 10 at.% by preventing the fuel clad mechanical interaction. Sodium bonding process is incorporated in the metal fuel pin fabrication for wetting of sodium on T91 steel clad tube and fuel slug and venting voids to plenum space. In Experimental breeder reactor-II, various sodium bonding techniques were evaluated by experimental investigations like furnace bonding, submerged canning, ultrasonic bonding, centrifuging, pressure pulsing and vibratory bonding. Vibratory bonding technique has high yield and is suitable for adaption in glove box line and remote fuel fabrication in shielded facility. Hence, a glove box facility with vibratory bonding technique for sodium bonded metal fuel fabrication and multiple pin bonding furnace (Fig.1) has been developed to increase the productivity.

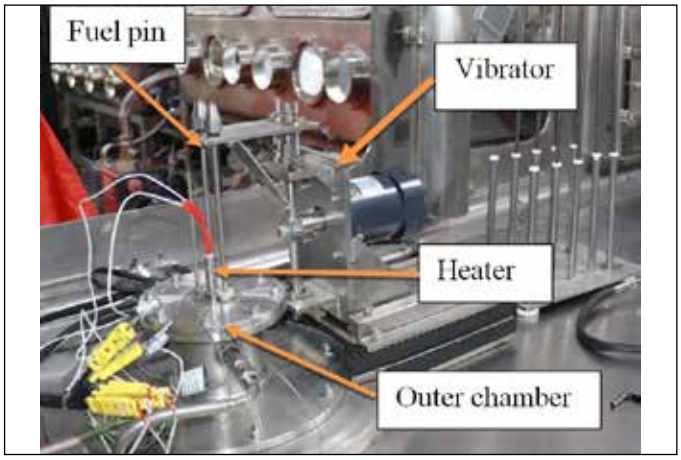

Fig.1 : Multiple pin sodium bonding furnace

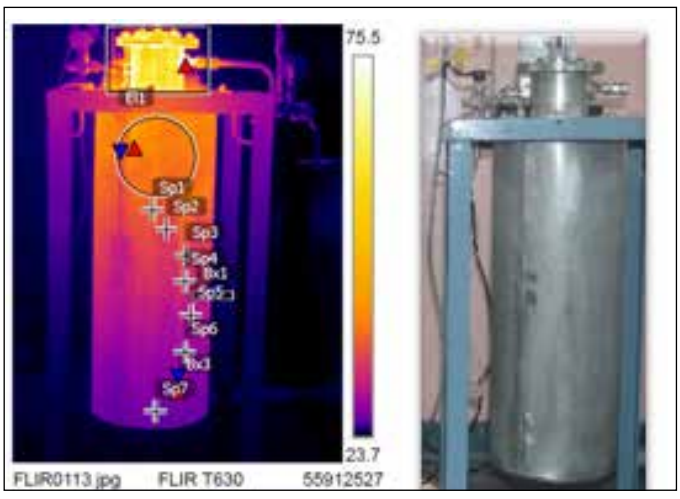

Fig.2a & 2b: IR and actual image of furnace during heating

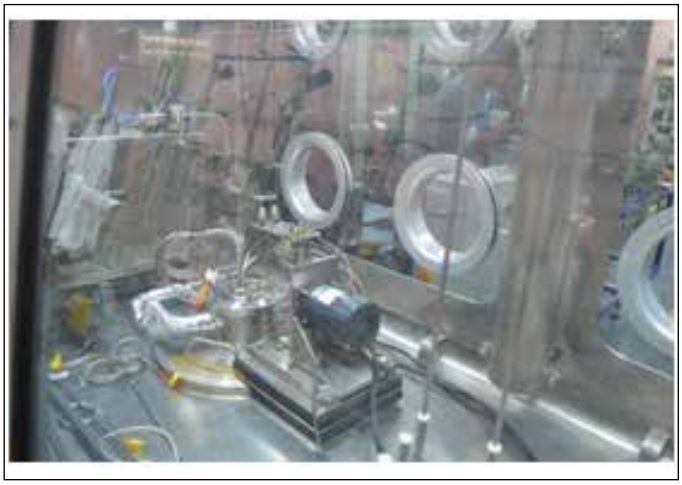

Fig.3: Sodium bonding furnace inside GB

During sodium bonding process, fuel pins filled with sodium and fuel slug is heated upto 500°C and vibrated at this temperature to remove the void pockets trapped inside sodium metal in the annular gap. Finally, it is purged with argon gas for directional solidification of liquid sodium inside fuel pins to avoid shrinkage void defects.

Cartridge type resistance heating system with PID based controller (Fig.2a & 2b) is designed to maintain the hot zone of length 600 mm at temperature of 500°C. Furnace inner chamber has top flange with inconel tubes at PCD of 30 mm for supporting the fuel pins (2Nos.) and multi-point thermocouple and cartridge heater is mounted at center using cover flange

Scotch yoke mechanism was designed for transforming rotary motion of motor to linear oscillating motion of plunger with flange for vibrating the fuel pins after heating to high temperature. All furnace components were designed as modular for easy operation and replacement during maintenance inside glove box. Dimension control of inner chamber during fabrication is important to prevent scratch marks during heating and vibrating the fuel pins for bonding process. Performance of the sodium bonding furnace was tested by heating upto 500°C and temperature distribution along fuel pin length was measured by multipoint thermocouple and IR image was captured to identify the hotspot on enclosure shell. Furnace along with vibrator was installed inside the glove box and then tested using dummy fuel pins filled with sodium (Fig.3)

III-21 Design and development of Air-cooled solid coil Vacuum Induction melter for cathode processing in hotcell environment

Spent fuel reprocessing forms a critical and challenging step in the nuclear fuel cycle. During metal fuel reprocessing, the cathode product obtained from electrorefining contains uranium metal in dendritic form, with occluded LiCl–KCl eutectic salts. The occluded salt in cathode deposit has to be separated by heating the metal deposit in vacuum furnace to evaporate the volatile components in a cathode processor. The cathode processor is an induction furnace where vacuum distillation and consolidation is carried out. The system has been designed and developed for adaptation inside a hot cell environment.

The developed system is a compact, air-cooled, solid-coil vacuum induction melter, designed for handling up to 100 of metallic deposit (cathode product). The major components include the cylindrical shell, induction coil, graphite crucible,

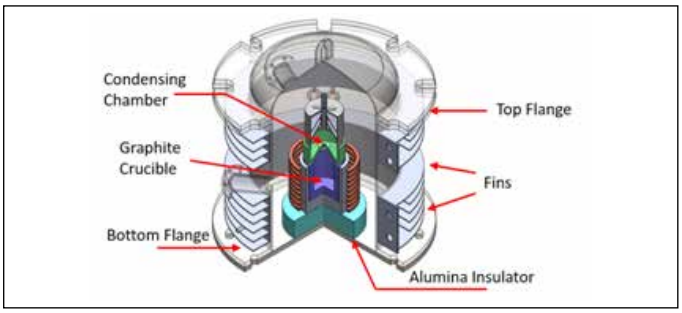

Fig. 1 Solid Modelling of Air-cooled solid coil Vacuum Induction melter

Fig. (2) (a) Vacuum Induction melter commissioned inside glove box. (b) Electrical feed through

electrical feedthroughs, and distillation chamber were sized based on detailed temperature profiling and thermal simulations. Adequate spacing between critical components was optimized to achieve uniform heating, effective salt evaporation and cathode product consolidation. The outer shell is provided with external fins and forced-air cooling to maintain its surface temperature below 100°C during operation. The complete compact assembly has been configured to fit within double module glove box for initial trial runs prior to hot cell deployment.

Fig. 3 (a) Copper strips used for consolidating. (b) Consolidated Copper meta

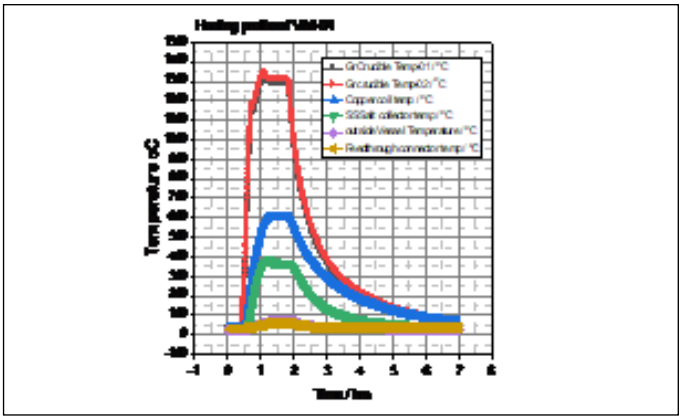

Fig.4 Heating Profile fo vacuum

The system is designed by keeping the shell along with copper coil suspended from the top flange which is in turn fixed to glove box roof with sufficient reinforcement. The Bottom flange (consisting of alumina insulator, alumina susceptor, yttria coated graphite crucible, SS316L baffle chamber) will be lifted by two linear actuators working in tandem as shown in Fig.2 (a) and aligned to the suspended vessel to establish leak tightness to a vacuum of 10^{-2} mbar. A Few experimental runs were successfully carried out using copper as a surrogate material (Fig. 3) chosen for its melting point close to that of uranium. These trials demonstrated efficient metal consolidation at 1300°C, validating the performance of the system under simulated conditions. The system is commissioned inside a double-module glove box, an important step toward adapting the system in hot cell for for uranium metal recovery from electrorefined cathode deposits.

The power source was designed to deliver kW power to the solid copper induction coil. Heating profiles were recorded by plotting temperature as a function of time to evaluate the thermal performance of the induction melter and to study its cooling behavior after system shutdown. The results confirmed stable heating characteristics and effective cooling through the finned shell.

III-22 Ensuring Radiation Safety in FBTR operations and Fuel Cycle activities at IGCAR

Radiological services are being provided to different radioac¬tive facilities viz., FBTR/IFSB/KAMINI, RML, RCL, CORAL, and DFRP at IGCAR. Radiological status, Work place monitoring (radiation level, contamination in air and area), environmental monitoring (stack release, borehole samples) and personnel monitoring (TLD, DRD and neutron badge) are being car¬ried out in the nuclear and radiological facilities based on the AERB approved radiation protection procedures and under Radiological Work Permits (RWPs). Radiation safety measures during routine and special operations were effectively implemented throughout the reporting period. No personnel received any occupational radiation dose in excess of regulatory limits. Some of the major radiological operations carried out in the facilities are highlighted below:

FBTR: Reactor was operated at 40 MWt, irradiated sub assemblies (Mark 1 FSA, Ni SA, Special SA) were discharged and fresh Mark 1 FSAs and Ni SAs were loaded into the reactor core. Calibration of neutron detectors of PFBR, testing of high range gamma detectors, replacement of failed bellow seal valves in RCB and Iodine retention efficiency test of RCB filter banks, primary sodium sampling, assembling of fresh FSAs were carried out. Maintenance of BSC sub loop A2 coil, liquid effluent pump, servicing of OFT valve in B cell, inspection of primary sodium pipe line support hangers in B cells and decontamination of guide tube were performed. Total 335 RWPs was cleared and collective dose is 2.08 PmSv.

KAMINI: Reactor was operated for activation analysis of samples. The mixed bed resin was replaced. Detailed gamma spectrometric analysis of water samples were carried out by HP team and reported.

RML: SEM examination of metallic fuel pin sample, clad sample, irradiated MOX fuel pin cut section were performed. Fatigue testing of irradiated grid plate sample, radiometallography testing and micro-hardness measurement of MAPS irradiated failed feeder pipe section; fatigue testing and bend testing of MAPS specimen were some of the major works performed. Maintenance work of Hot cell 1 and 2 in-cell crane, Vertical transfer system, MSM were completed. 625 RWPs were cleared and collective dose is 11.09 PmSv.

RCL: Characterization and moisture estimation of LiCl/KCl eutectic salt used for electro-refining of irradiated U-6 wt.% Zr, Separation of 89Sr, remote replacement of hot cell HEPA filters, assay of all the old filters and transfer of alpha waste NDE of plutonium in MOX pellets, fabrication of U-10 wt.% Zr alloy slug were the salient works. Traceable level of soil contamination was observed during Zone-1 survey. Dose mapping was done by HP team in detail and reported. The area was decontaminated later. 250 Nos of RWPs were cleared and collective dose was 4.78 PmSv..

CORAL: 67th campaign for reprocessing of the spent fuel from FBTR was carried-out. In-cell crane maintenance, replacement of LLW HDPE line, erection of SS pipe line in CSA and AAL and LLW-2 HDPE tank replacement with SS tank, maintenance of Airlift 102 and MSM, transfer of alpha waste, replacement of HEPA filters are the other highlights. 940 Nos of RWPs were cleared and collective dose is 47 PmSv.

DFRP: DFRP successfully completed hot commissioning activities involving the reprocessing of spent fuel from FBTR. Four campaigns have been successfully completed. Establishment of flow sheet for the separation of Np-237from radioactive waste, extraction of 90Sr and minimizing Plutonium (Pu) losses are the other highlights. 595 RWPs were cleared and collective dose is 3.5 PmSv.

Chapter - IV

Fuel Cycle

IV-01 Process and analytical improvements relevant to FBR spent fuel reprocessing

Destruction of HDBP using Ozone as Oxidant

Metal ions (U, Pu, and traces of FPs) present in the carbonate waste generated during the lean solvent clean-up of Dibutyl phosphate (HDBP) require quantitative removal before waste disposal. But HDBP must be removed first to avoid the formation of any undesirable floating mass. Investigations were conducted to remove HDBP using ozone. Results indicate the feasibility of removal to satisfactory levels at a faster rate than the conventional methods.

DFRP flow sheet simulation using in-house code

Dynamic simulation of the first stripping cycle (HC) of DFRP using the indigenous computer code SEESPEC revealed that Pu retention in the lean organic phase is mainly due to the unsteady condition at startup. It also pointed out that the addition of U(VI) to the 4 M strip stream would aid in reaching steady state rapidly and minimise Pu retention. This was experimentally validated using an actual solution at CORAL with 1 g/L of HDBP. Simulation was also carried out for partitioning (2B) and U stripping (2C) cycles of DFRP to optimise the A/O feed ratio for achieving desired product purity and reduce aqueous & organic wastes. This was validated experimentally and successfully executed in the DFRP.

High throughput studies in 40 mm CE

The feasibility of increasing the throughput of the DFRP plant was investigated using a six-stage 40 mm CE setup. The extraction and stripping of U(VI) using 30% TBP/n-DD with flow rates at five times the design flow sheet was tested. No flooding was observed during these studies, indicating the feasibility of increasing the DFRP process throughput, which would reduce the process time and solvent degradation.

Distribution data generation for Nd(III)

The distribution coefficient (Kd) of Nd(III) under typical PUREX conditions was determined as a function of acidity, [Nd(III)], temperature and HDBP. K_d was found to decrease in the presence of HDBP, but temperature did not affect it. The results would be beneficial for MA separation studies, which are in progress.

Development of analytical methods

Simultaneous analysis of U(VI) & Zr(IV) is essential but very challenging. A spectrophotometry-based method using Br-PADAP as the chromogenic agent was developed to determine Zr(IV) in the presence of high U(VI).(U(VI) interference was eliminated by ascorbic acid). Linearity was acquired at 585 nm, in the concentration range of 0.1-1 ppm of Zr(IV) with a molar absorptivity of 89574 $L.mol^{-1}.cm^{-1}$ and Sandell's sensitivity of 0.003 $\mu g.cm^{-2}$. The results were in good agreement with those of ICP-OES analysis. The method was employed satisfactorily to analyse the samples generated during the dissolution of U-Zr metal in nitric acid.

Feasibility studies for uranium removal from waste streams using Cr- based porous material

To evaluate the feasibility of removing heavy metals from low-level radioactive streams, Cr-based porous materials were tested. One such compound was synthesised in-house and evaluated for U(VI) removal from a concentrated HNO_3 stream. It was found that the U(VI) extraction capacity of the material was 944 mg/g and 115 mg/g at 0.1 M and 0.5 M $HNO_{3,}$ respectively.

Evaluation of the WACT system for assaying used HEPA filters

The used High Efficiency Particulate Air (HEPA) filters from the vessel off-gas (VOG) and evaporator off-gas (EOG) systems of the DFRP were assayed for the detection of various radionuclides using the Waste Assay Computed Tomography (WACT) system. The gamma spectra recorded using a High Purity Germanium (HpGe) detector clearly indicated the presence of ^{137}Cs, ^{134}Cs, ^{154}Eu, ^{125}Sb and ^{241}Am nuclides in the HEPA filters of both EOG and VOG systems. The spectra also suggest that there is no ^{239}Pu (below its detection limit of 35 mg) in either of the HEPA filters. The passive neutron-based assay confirmed this. Hence, the WACT system was evaluated for assessing the used HEPA filters. The results indicate that the HEPA filter of the EOG system contains radionuclides in relatively higher quantities than the HEPA filter of the VOG system.

IV-02 Recovery and Purification of Strontium-90 from FBTR Reprocessing Waste and Production of Carrier-Free Yttrium-90

The utilization of radioisotopes for the diagnosis and therapy of various diseases is a key program of the Department of Atomic Energy. Several radionuclides are produced using research reactors and particle accelerators for applications in nuclear medicine. The high-active waste (HAW) produced during the reprocessing of high-burnup fast-reactor spent fuel is considered as a valuable source of medically important radionuclides. This stream contains significant quantities of radionuclides such as ^{137}Cs, ^{90}Sr, ^{106}Ru, ^{144}Ce, ^{237}Np, ^{241}Am, and ^{242}Cm, making it a potential resource rather than a waste. One of the most significant radionuclides present in HAW is ^{90}Sr, which decays to ^{90}Y, a pure beta emitter (β_{max}= 2.28 MeV, $T_{1/2}$= 64.1 h), possess therapeutic application in nuclear medicine. With its availability in large quantities in HAW, ^{90}Sr serves as a

Fig. 1 Hot cell operation for the separation of ^{90}Sr form HAW of fast reactor reprocessing

long-lived parent for generating carrier-free ^{90}Y. However, separation and purification of such radionuclides from HAW is highly challenging. To isolate ^{90}Sr from high-level liquid waste (HLLW), several techniques have been developed, including precipitation, liquid–liquid extraction, extraction chromatography, and ion exchange chromatography. Among these, solvent extraction has gained considerable attention due to its established application in spent fuel reprocessing and its multiple advantages such as ease of handling, remote operability, flexibility in stage design, and scalability.

In Reprocessing Group, IGCAR, An attempt has been made to selectively recover ^{90}Sr from HAW using a solvent-extraction method inside the hot cell. The extractant used was 0.1 M 4,4',5-di-(t-butylcyclohexano)-18-crown-6 in a

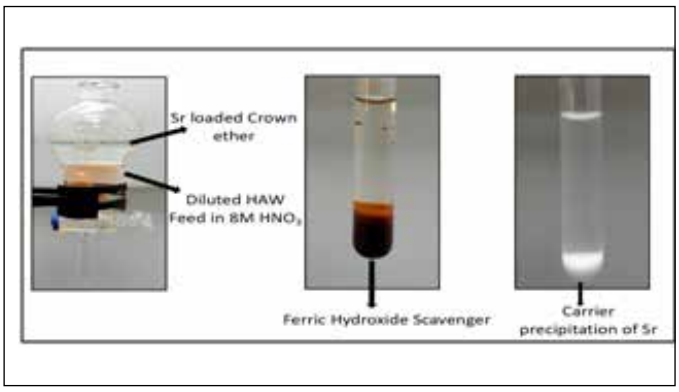

Fig. 2 Purification of Sr from alpha impurities

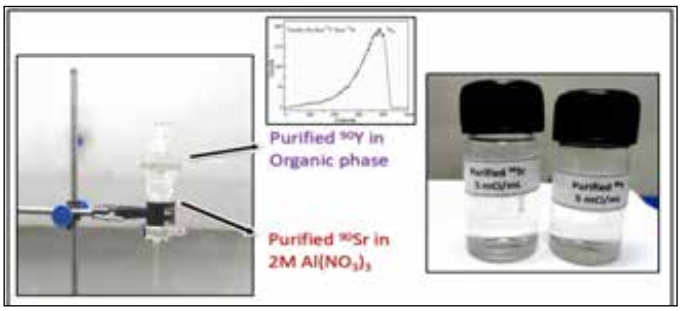

Fig. 3 Milking of ^{90}Y from Purified ^{90}Sr

mixture of 1:1 n-octanol and dodecane. The conditioned feed solution was equilibrated with above solvent, allowed to settle, loaded organic phase containing ^{90}Sr was separated. This ^{90}Sr was stripped using dilute nitric acid, and the resulting strip solution was further purified through repeated precipitation to remove alpha-emitting and other fission-product nuclides.

Upon separation and purification, ^{90}Sr can serve as a long-lasting source for the generation of carrier-free ^{90}Y. A solvent extraction-based separation method was developed in our laboratories for the separation of ^{90}Y from ^{90}Sr, and it has been proven to be a convenient method for milking ^{90}Y. Extensive studies have shown that the generator system is suitable for obtaining clinically acceptable ^{90}Y, with a breakthrough level of ^{90}Sr less than 10^{-6} Ci/Ci of ^{90}Y. The alpha contamination and gross gamma activities in purified ^{90}Y are found to be below 10^{-9} Ci / 1.0 Ci of ^{90}Y and 0.0015% of total gross beta activity. The metallic impurity present in purified ^{90}Y solution was analyzed by ICP-OES and was found to be within the acceptable limit.

IV-03 Recovery of neptunium-237 from spent nuclear fuel discharged from FBTR

The radioisotope ^{237}Np does not occur naturally. Its only practical source is nuclear reactors, where it forms as a by-product in irradiated nuclear fuel. In fast reactors, the formation of ^{237}Np is higher compared to thermal reactors primarily because of the higher neutron flux and the harder neutron spectrum. These conditions significantly enhance the (n,2n) and successive neutron-capture reactions on uranium (U) isotopes. In view of its potential application as the target nuclide for the production of ^{238}Pu, an isotope of considerable importance in space power systems, the separation of ^{237}Np has become a subject of significant

Table1: Predicted MA inventory in the fuels from various reactors

Nuclide	PHWR (UO$_2$ -6.7 GWD/t) (g)	FBTR (155 GWD/t) (g)	PFBR (MOX-100 GWD/t) (g)
^{237}Np	23.7	350	250
^{241}Am	38.8	1030	4600

interest. In addition, the recovery of ^{237}Np from spent nuclear fuel (SNF) is considered an essential step in actinide management at the back end of the nuclear fuel cycle, due to its long half-life and higher alpha toxicity.

In general, the PUREX process is followed for the recovery of unused U and Pu from SNF. The SNF discharged from FBTR contains nearly 350-400 mg of Np/ kg of it. Therefore, it is considered to be an ideal source for Np. In solution, Np exhibits different oxidation states, such as Np(IV), Np(V), and Np(VI). Among these oxidation states, Np(IV) & Np(VI) are extractable with an organic phase consisting of TBP/n-DD. Under high acid flow sheet conditions, as in DFRP, Np mainly exists in oxidation states IV and VI. More than 90% of the Np is found to be extracted in the organic phase. Analytical methods were established and implemented for the systematic monitoring of 237Np in the plant streams. The analytical report clearly shows that more than 80% of the extracted ^{237}Np follows the uranium route and is concentrated in the uranium product stream. Therefore, attempts were made to separate 237Np on a laboratory scale from the U product, and a significant quantity of 237Np was successfully isolated from the U_3O_8 product.

In the present work, the U_3O_8 product was dissolved in nitric acid. Aqueous phase acidity was adjusted to 1 M. Subsequently, the reduction of Pu to Pu(III) and Np to Np(IV) was accomplished with a reagent mixture consisting of ascorbic acid and hydrazine nitrate, followed by the extraction of Np(IV) selectively in the organic phase, which consisted of HTTA in xylene. Then, it was back-extracted with concentrated nitric acid, and an ion exchange separation process further purified the Np in the strip product. The composition of U_3O_8 and purified neptunium nitrate is provided in Table 2.

Table 2: Composition of U_3O_8 and $Np(NO_3)_4$

Element	U_3O_8 (%)	Np product (%)
U	99.68	< 0.2
Pu	0.21	<0.07
Np	0.045	99.8
Fe	0.03	< 0.001

The neptunium nitrate solution thus obtained was then subjected to hydroxide precipitation and calcined at 550°C to obtain neptunium oxide. It has been planned that the resultant Np-oxide will be fabricated as an MOX pellet using a suitable oxide matrix and irradiated in the desired neutron flux in FBTR to produce ^{238}Pu, thereby validating the method for the effective conversion of ^{237}Np to ^{238}Pu.

Fig.1 Purified Np nitrate and Np oxide

Studies are in progress at Reprocessing group, IGCAR to establish methodology for the plant scale recovery of Np from spent fuel.

IV-04 Development of a Glove Box-Adaptable Continuous Precipitation and Sedimentation System for Plutonium Reconversion

The plutonium reconversion operation in the PUREX process is conventionally performed by a series of batch or semi-continuous systems. These systems have some limitations, such as low throughput, inconsistent product quality, and extensive manual intervention, leading to worker exposure, which are unfavorable and inefficient for large-scale reprocessing plants. In contrast, a continuous process typically offers higher throughput, reduced cycle times, reduced manual interventions, and consistent product quality, making it a safer, more efficient and reliable to the conventional batch or semi-continuous systems.

In this context, a glove box-adaptable continuous precipitation and sedimentation system, as shown in

Fig.1 Continuous precipitation and sedimentation system

Figure 1, was developed for plutonium oxalate precipitation and separation. The system consists of a stirred-tank precipitator equipped with a standard impeller and a sedimentation column having a slow-rotating rake. A comprehensive evaluation of the new system was carried out using Cerium(III) as the non-radioactive surrogate for plutonium. The effects of critical process parameters, such as residence time, metal ion concentration, and rake

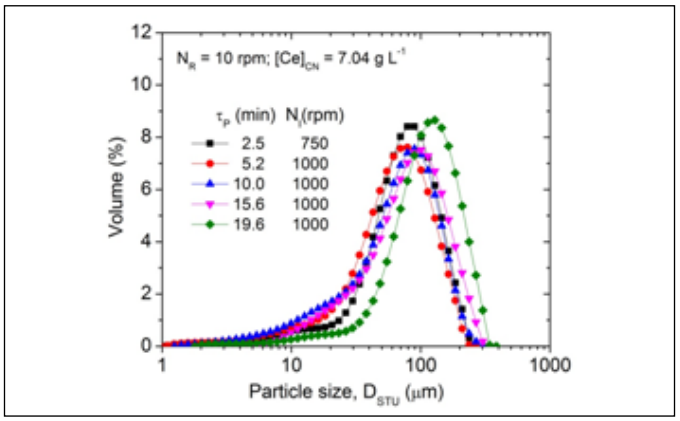

Fig.2 PSD of cerium oxalate as a function of residence time

speed, on the key performance indicators of the system, such as throughput, conversion, median particle size, solid recovery, and volume reduction, were assessed in detail to optimize the system. The results showed that 10 min residence time in the precipitator, cerium concentration of 7-21 g L^{-1}, and a rake speed of 50 rpm, at a constant impeller speed of 1000 rpm are optimum for this precipitator. These conditions ensured the continuous steady-state operation of the system, achieving a throughput of 60-152 g Ce per hour, >99% conversion, cerium(III) oxalate particles with a median size of 60-70 μm, >99.5% solid recovery and 87-94% volume reduction by gravity sedimentation.

Lower cerium concentrations (<2.7 g L^{-1}) led to decreased conversion (<97%) and increased solid carryover (>1.5%), affecting overall performance of precipitation. Figure 2 shows the particle size distribution as function of resident time. The median size of cerium(III) oxalate particles increased from 61 to 111 μm, and bulk density of the cerium(III) oxalate sediment increased from 0.28 to 0.43 g mL^{-1}, while increasing the residence time from 5 to 20 min, which indicated the strong influence of residence time on the relative rates of growth and nucleation mechanisms and the density of the cerium(III) oxalate particles.

IV-05 Developments for Higher Reliability and Reduced Maintenance Downtime of Mechanical Systems

1.TC-200 Compressor Water Ingress Solution

The TC-200 vertical, water-cooled reciprocating compressor faced recurrent issues due to water leakage from punctured after-cooler tubes or minor seepage through the cylinder head and eventually contaminate the lubricating oil in the

sump, forcing complete dismantling of the compressor for maintenance. Since the OEM design did not include any provision for draining such ingress water, an auxiliary tubing arrangement was developed in-house. This modification collects and drains the accumulated water above the scraper area before it can reach the oil sump. The simple intervention has greatly reduced maintenance requirements and enhanced the availability of the compressed-air system.

2. Compact Handling System for In-Cell Crane Drive Motors

In the 177 cell, the in-cell drive system—comprising CT, LT, and hoist motors—is housed inside a glove box. Each motor, combined with its reduction gearbox, weighs about 16 kg. Limited space and restricted handling through gauntlet gloves made maintenance difficult and ergonomically unsafe. To address this, a compact 50-kg-capacity material-handling system was developed using a manually operated brake winch, stainless-steel rope, and a horizontal (X-axis) channel with a pulley-assisted vertical (Z-axis) movement. This arrangement allows safe lifting, lowering, and positioning of the motor units entirely through the glove-box ports. The solution significantly improved safety and maintainability within the glove box.

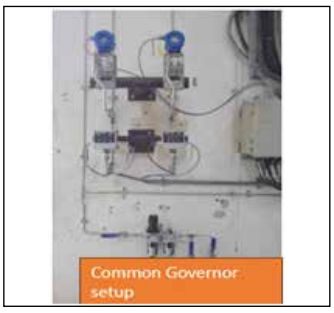

3. Gear-Locking for In-Cell Crane Limit Switches

In-cell cranes (250–500 kg capacity) rely on drive units located inside glove boxes for maintenance accessibility. Frequent changes in limit-switch settings during in situ maintenance increased equipment downtime and man-rem exposure. An in-house gear-locking mechanism was developed to prevent unintended limit-switch adjustments. Its successful installation across crane drive glove boxes enhanced radiological safety and reduced retrofit costs.

4. Common Governor System for Six Compressors

Six compressors—three essential and three non-essential—were originally operated individually with identical pressure governor. Minor sensing variations over time caused one compressor to remain loaded continuously, leading to repeated failures. A dedicated tubing line and common governor system were designed and implemented to synchronize compressor operation. This modification has reduced breakdowns and significantly improved compressed-air system reliability.

5. Anti free fall mechanism for in-cell crane

An anti–free-fall mechanism was developed for the in-cell crane to enhance reliability and safety during hoist motor maintenance. A locking system for the hoist shaft was designed, fabricated, tested, and commissioned. This mechanism prevents unintended hook fall and significantly improves the overall safety of the system.

These mechanisms reduced maintenance downtime of mechanical Systems and increased reliability.

IV-06 Development of a Reliable Mechanical System for Overload Protection for Hot Cell Cranes

Most of the hot cells in DFRP are equipped with in-cell cranes for the operation and maintenance of in-cell equipment. The in-cell crane is a critical tool, and many activities inside the cells depend on its availability. Therefore, failure of an in-cell crane is not only irreversible & would severely impact vital operations and may even result in a permanent shutdown of the plant, which would be catastrophic.

In-cell cranes generally use stainless steel chains for long travel and cross travel inside the cells, while stainless steel ropes are employed for handling loads along the vertical axis. The hot cells are designed to be highly compact to meet requirements related to economic considerations & nuclear material accounting. Consequently, these cells

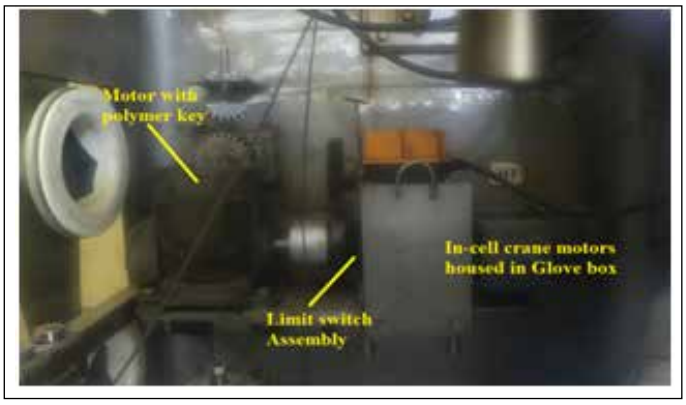

Fig.1 Maintenance glove box with In-cell crane motors

accommodate a large number of equipment, vessels, piping, supports, etc., in close proximity. In such a constrained environment, accessing specific locations with the in-cell crane to perform remote material-handling operations becomes highly challenging.

Material-handling operations have to be performed remotely, which is an exhausting task that getsfurther complicated by the restricted visibility available through the viewing window. This limitation creates numerous blind zones for the operator, making meticulous and highly skilled crane operation indispensable. Under these conditions, there is a significant risk of the lifting hook becoming entangled with structures inside the cell, and any inadvertent hoisting thereafter may lead to snapping of the stainless steel rope, an irreparable and potentially catastrophic event. To eliminate this risk, a customized, foolproof overload-protection device was developed and validated in-house.

Fig.2 Polymer key samples & Mock testing arrangement

The electrical motors for the in-cell cranes are housed in a glove box located outside the cell to facilitate maintenance, while the drive shafts and other components such as couplings, chains, and ropes are installed inside the cell to achieve the required crane functions. However, the maintenance glove box does not have sufficient space to accommodate any standard overload-protection device & electrical devices for overload protection is understood to be less reliable for in-cell crane, hence was dismissed.

In view of the said limitations, a simple, reliable, and cost-effective strategy was developed. The metal key of the first coupling connecting the driver and driven shafts of the power-transmission line was replaced with a non-metallic key, designed to fail well below the safe load limits of the chain or rope. The maximum payload in one of the cells is 20 kg, while the crane's design capacity is 250 kg and the tensile strength of the chain is around 1200 kg. In this rationale, a polymer key with a shear strength of approximately 75 kg was selected. Multiple

Table 1: Proof load of key samples made from virgin grade

SL. NO	Key Material (Virgin)	Proof Load in KG			
		1	2	3	Avg.
1	Derlin	63	63.8	56	61
2	Nylon	53	54	63	57
3	PEEK	85	85.5	91	87

proof tests using different key materials and key designs were conducted, and the results are presented in Table-1.

By customizing keys using reinforced polymers or suitable metals with low UTS, keys with optimized proof strength can be developed to meet the actual payload of in-cell crane. Since in-cell crane is a life line tool for the seamless operation & maintenance of hot cell equipment, the robustness of the crane is pivotal to the plant & the same has been ensured by a simple but effective above detailed technique.

IV-07 Current Operation Status of DFRP

Hot commissioning of the Demonstration Fast Reactor Fuel Reprocessing plant (DFRP) facility was accomplished in April 2024. The spent carbide fuel discharged from the Fast Breeder Test Reactor (FBTR) with a burn-up of 155 Gwd/Te was reprocessed at the DFRP facility in a limited hot-run campaign mode before performing regular reprocessing campaigns. The primary objective of the limited hot-run was to validate the process flow sheet and assess the performance of all the equipment installed in DFRP.

In the limited hot-run campaign, the reprocessing campaign of Mark-I FBTR carbide fuel was progressively increased from 20 pins to 40 pins and then to the full batch capacity of 60 pins per campaign, demonstrating the validation, performance, and efficiency of the plant at all levels, from fuel inventory to processing, recovery, and waste generation.

Fig.1. Fuel handling area and sampling cell area of DFRP

The plant operation was performed strictly in accordance with the protocols and safety guidelines approved by the regulatory authority. The process parameters and performance of the equipment were monitored during the limited hot-run, and they were found to be exceptional, with negligible loss of heavy metals in the raffinate and lean organic streams. Additionally, the radiological status of the plant was well below the limits of the approved guidelines,

Fig. 2. Solvent Extraction Unit in DFRP

confirming the successful hot commissioning of DFRP.

After the limited hot run, a performance report for the plant was prepared, analysing all critical components for the next level of operation of DFRP. The hot commissioning report was submitted to the regulatory body for review and approval to conduct additional hot-run campaigns. Based on the report, the regulatory body consented to two additional hot-run campaigns. The 4^{th} and 5^{th} campaigns were performed with improved parameters at each step of operations, starting from dissolution, solvent extraction, stripping, and partitioning, among others. Before changing any operating parameters in the 4th and 5th campaigns, process simulation, modelling, and laboratory studies were conducted to mimic the plant conditions. After getting sufficient confidence in the lab simulation study, it was implemented in DFRP operations. These results obtained were again excellent and improved the process performance.

In conclusion, the five hot-run campaigns performed so far at DFRP successfully validated the design intent, equipment performance of the plant and readiness for regular and sustained operations.

IV-08 Sustained operation of CORAL for the reprocessing of high burn-up fuel discharged from FBTR

CORAL (Compact Reprocessing of Advanced Fuel in Lead Cell) is a test facility, set up by the Reprocessing Group, IGCAR, for the reprocessing of spent carbide fuel discharged from the Fast Breeder Test Reactor (FBTR). The objective of CORAL is to establish the reprocessing technology of irradiated carbide fuel discharged from FBTR. It is capable of reprocessing the FBTR fuel on an experimental basis and can accommodate improvements in process and equipment. It has provided the operating experience and technical inputs for DFRP and FRP of FRFCF. CORAL has been operating since 2003 and has received a second re-licensing for the reprocessing of FBTR spent fuel from AERB for a period of 5 years, commencing on September 1, 2023. A total

Fig.1 CORAL facility

Fig.2: shipment of organic waste to WIP

Fig.3 Neutron Drum Monitoring System

of 67 campaigns of reprocessing FBTR spent fuel were completed, with various burn-ups (low, 25, 50, 100, and 155 GWd/t).

During the last year, two reprocessing campaigns (66th & 67th) of FBTR fuel with a burnup of 155 GWd/t were received at CORAL. Reprocessing campaigns were carried out successfully, and U & Pu have been recovered with the required DF from a single cycle of solvent extraction operation, yielding an excellent recovery.

The generated lean organic from the reprocessing campaigns showed a significant amount of Pu & U, which was treated with 0.2 M oxalic acid. Pu & U were recovered from the same, with a loss of Pu & U in the organic waste within the waste disposal limit.

CORAL ventilation is catered to by Exhaust, supply, and off-gas fans. A total of 48 active filters associated with the filter banks of the Exhaust fan have been replaced safely with new filters due to a higher pressure drop.

Due to space constraints in the organic storage tank of the CORAL waste vault, the generated organic waste from the reprocessing campaigns could not be stored in the tank. After obtaining clearance from AERB, a shielded tank with a capacity of 350 L was designed and fabricated for transferring organic waste from CORAL to the WIP of BARCF, Kalpakkam. One shipment of organic waste was moved safely to the WIP in tanker mode.

To collect low-level liquid waste from the analytical laboratory, a separate collection facility with line modifications was implemented in the existing LLW system, and the facility was successfully commissioned. Additionally, a 3 m^3 HDPE tank for collecting low-level liquid waste has been replaced with an SS tank of the same capacity.

Mercury vapour lamps were used to illuminate the inside of the hot cell; however, the brightness and longevity of the light fell short of the required level. All the existing hot cell lamps (36 in number) were replaced with LED lamps to improve lifespan, enhance illumination, and reduce power consumption.

Fig.4 Two-stage 200 CFM compressor

Highly active alpha-bearing solid waste, such as CE bowls, damaged cameras, and tongs, generated in the hot cell during reprocessing campaigns, was removed safely through two La-Calhene containers and transferred to CWMF for interim storage. Also, low active alpha-bearing solid waste from the hot cell, glove boxes and fume hoods was removed periodically through the bagout technique and collected in a 200 L SS drum. Ten drums of alpha-bearing low-active solid waste were transferred to CWMF, BARCF, Kalpakkam, after the Pu assay using a helium-based Neutron Drum Monitoring system.

The liquid flow testing of the waste transfer lines for acidic waste, alkali waste, thorium waste and organic waste from CORAL WV to DFRP WV was carried out with DM water, and the result of the testing was found to be satisfactory.

One new 200 CFM capacity compressor (two-stage horizontal type) has been installed at CORAL to cater to the additional need for compressed air in the plant, and it was commissioned successfully.

IV-09 Immersive VR-Based Systems for Mapping of Cell Internals and Operator Training for Hot Cells

Knowledge management and operator training are critical for the sustainable and safe operation of nuclear energy programs. Access to radioactive areas in nuclear facilities is often restricted due to the considerations of safety, security, and operational constraints, which limit the opportunities for practical training and knowledge capture. The work here can be divided into parts: The first part of the work provides details of the methodology for creating and using 360-degree images and videos inside the Plant before hot commissioning to produce immersive virtual views and walkthroughs for knowledge preservation and operator training. A simple and generic workflow was developed, consisting of: Cell Layout Mapping – Using CAD layout drawings as a reference to mark key vantage points inside the cells for image recording. Image / Video Capture –

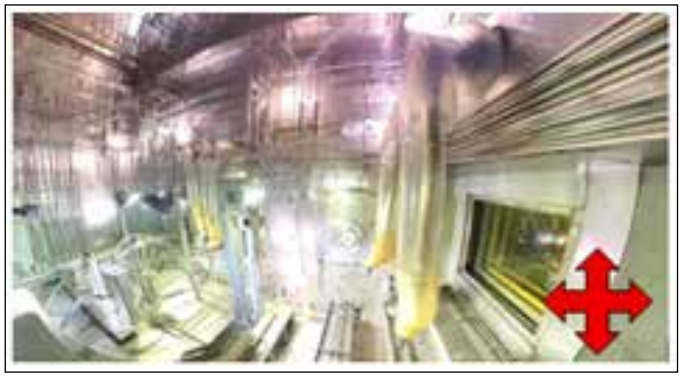

Fig.1 360° video of typical hot cell

Utilizing a commercial off-the-shelf (COTS) 360° camera, and providing the required lighting conditions for optimal image / video clarity. The hot cells of a Reprocessing Plant, often densely packed with equipment and piping, were captured by this camera. Videos are used for walkthroughs. Offline Video Stitching – Processing and stitching video files using standalone software to maintain confidentiality and avoid internet connectivity. Content Deployment – Converting stitched videos to MP4 format and porting them to VR/AR headsets for immersive viewing. The MP4 videos can be rotated 360 degrees to view the internals (Fig. 1).

The resulting immersive content allows operators to virtually explore high-radiation and remote areas, improving their understanding of equipment layout, and complex piping arrangements. This methodology is applicable to any nuclear facility.

The second part of the work is Virtual Reality (VR) based training system designed for personnel involved in hot-cell material handling operations. The platform allows users to perform virtual object manipulation tasks such as picking, lifting and placement, thereby minimizing the need for initial training within hazardous workspaces. A physical master arm from a Master–Slave Manipulator (MSM) setup is employed as the primary input device to control a corresponding virtual slave arm displayed on a VR computer screen (Fig. 2) simulating a hot cell viewing window. The master arm is instrumented with rotary encoders to measure joint angles, and these signals are transmitted to the host computer via a microcontroller interface. The simulation environment (Fig. 3) processes this real-time joint data to animate the virtual slave arm with accurate kinematic mapping. A motor-driven haptic feedback system provides resistance or assistance based on interaction forces, enabling the trainee to perceive load variations, contact forces and grip response similar to real operations. The overall architecture is modular, allowing integration of additional sensors, feedback channels or tool attachments for advanced scenarios.

Fig. 2 VR training system for hot cell equipment manipulation

Figure 3: Virtual environment display on the computer screen

IV-10 Automation of Centrifuge Operation for Liquid Clarification in the Hot Cell

In DFRP, spent fuel pins are chopped and dissolved in the dissolver. The dissolver solution generally contains fine solid particles of size 0.5 to 500 microns, which are mainly clad fines. These particles not only lead to choking of the liquid transfer lines, but also accumulate in the interfaces in the solvent extraction step leading to solvent degradation. Hence, high-speed centrifuges are used in DFRP to remove these fines from solution before further processing.

The centrifuge is rotated using an air turbine. The solution from the dissolver is transferred by an airlift to the rotating centrifuge from which the clarified solution comes out. To get the required separation of solid fines, the unit has to be operated at about 18000 rpm.

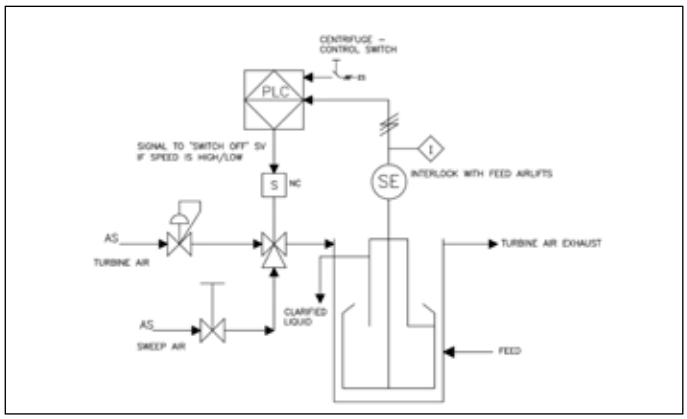

Fig.1 Conventional Manual Control System sensors.

As the speed of the equipment largely depends on turbine air pressure, factors including liquid feed flow rate, submergence ratio and mechanical failure, also contributes to the challenge of maintaining optimum rotation per minute (RPM). To maintain the required speed, the plant operators have to monitor speed and liquid flow rate in the control room and communicate to operators in service area to throttle and regulate turbine air header pressure using Pressure Regulating Valve (PRV) (Fig. 1). This manual operation leads to personnel fatigue, failure of required optimum clarification and thereby increasing other operational challenges.

To overcome the operational difficulties, the centrifuge speed control system was automated.(Fig. 2). For monitoring pressure from operator desk in control room, a blind pressure transmitter is installed in turbine air header and EPRV is wired to an analog output channel

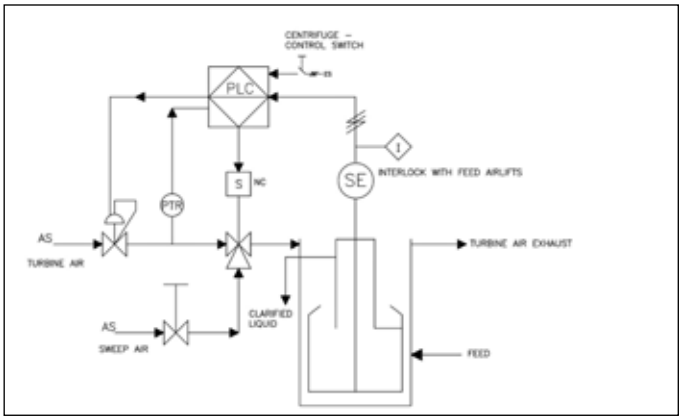

Fig. 2 Automated Control System of Centrifuge in DFRP

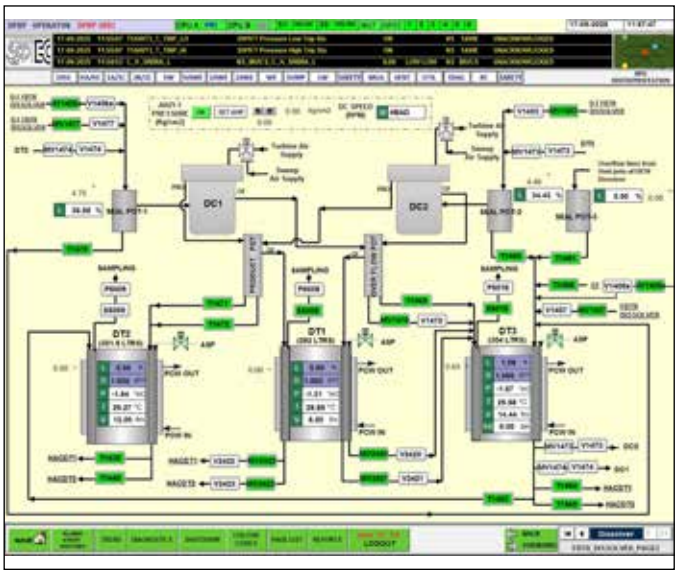

Fig. 3 Centrifuge Control Operator Screen

and controlled by corresponding 4~20mA current output through a ramp logic in the PLC. To monitor and control all parameters related to the centrifuge, operator screens are also developed in SCADA application. The operator can either directly set required header pressure or in incremental pattern in SCADA. (Fig. 3)

Due to this implementation of automation in the control system, a high accuracy speed control in centrifuge could be achieved. As all parameters are available in SCADA, the plant operator could take timely reaction to every process change, providing better control of the equipment, and also reducing the manpower requirement. The SCADA also has data logging for future study for analysis related process optimization.

IV-11 Voltammetric Investigations on Distilled LiCl-KCl Salt from PPRDF

Pyroprocessing is considered to be the best method for reprocessing of short cooled high burn up metallic fuel. In this process irradiated fuel is taken as anode, SS430/ liquid Cd as cathode and LiCl-KCl-UCl_3 as electrolyte. U is selectively electrodeposited at SS430 cathode and U, Pu, minor actinides are co-deposited at liquid Cd cathode at 773 K. Purification of used electrolyte is mandatory when fission product concentrations in the electrolyte reach to a certain level. Purification of spent electrolyte is carried out by ion exchange using Li/K-tagged zeolite and ADDP method using Li-Cd alloy. Deposit at cathode contains occluded salt. During distillation of liquid Cd cathode, salt is also distilled out along with Cd.

The current study is about electrochemical investigation of LiCl-KCl salts obtained after vacuum distillation of liquid Cd and solid SS430 cathode at PPRDF facility in PPED. Vacuum distillation of cathode deposits was carried out at 1223-1273 K using vacuum of 1-5 Torr. The current study aims the qualitative analysis of the salt by cyclic voltammetry technique and quantitative analysis by ICP-OES. Also to check the feasibility of re-using the distilled salt back to head end step of Pyro process.

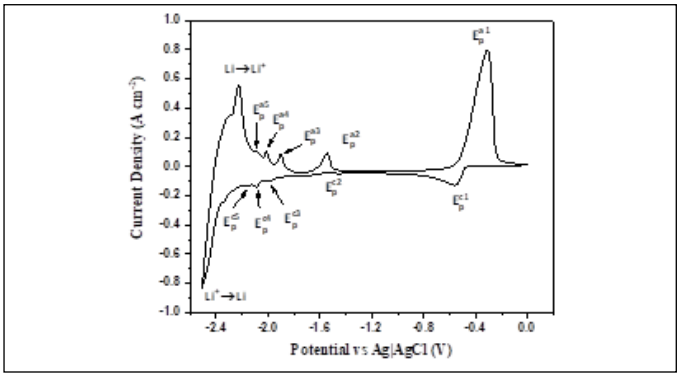

Fig. 1: Cyclic voltammograms of distilled LiCl-KCl salt at tungsten WE at 723 K at 100 mV/s scan rate.

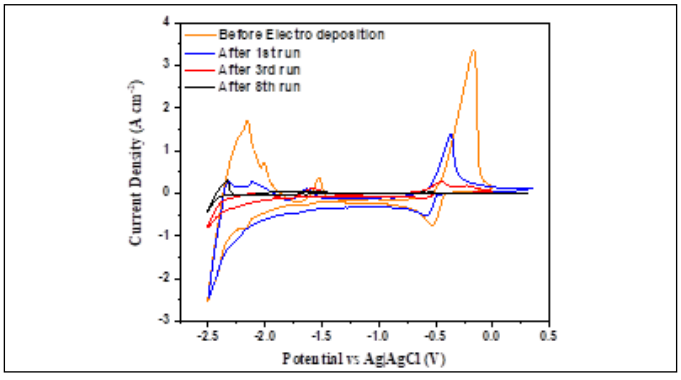

Fig. 2: Cyclic voltammograms of distilled LiCl-KCl salt at tungsten WE before and after pre-electrolysis on Ta-foil at 773 K, Scan rate: 100 mV/s.

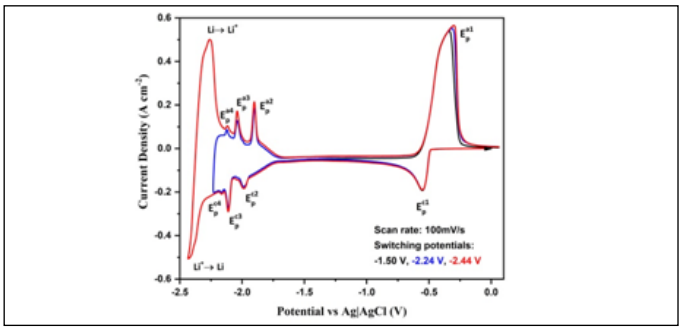

Fig. 3: Cyclic voltammograms of LiCl-KCl-CdCl2 (1wt%) salt at tungsten WE at 723 K.

150g of distilled salt was re-melted and cyclic voltammograms of the molten salt was recorded at tungsten working electrode at 723 K. The voltammograms (Fig. 1) were characterized with multiple cathodic and anodic peaks. The major redox couple E_p^{c1}| E_p^{a1} at -0.55 V was characterized to be Cd^{2+}|Cd, which was further validated by ICP-OES analysis of the salt.

Additionally, four redox couples (E_p^{c2}| E_p^{a2}, E_p^{c3}| E_p^{a3}, E_p^{c4}| E_p^{a4}, E_p^{c5}| E_p^{a5},) were appeared in potential range of -1.65 V to -2.2 V prior to the lithium deposition peak. The peaks can be assigned to under potential deposition of Li due to formation of Li-Cd alloy. To further confirm the Li-Cd alloy formation, pre-electrolysis of melt was carried out on tantalum foil applying cathode potentials of -0.6, -0.7, -0.95 for 3600 s and voltammetric (Fig. 2) features at tungsten electrode was checked. It was observed that cathodic and anodic current intensity of all those four redox couples have decreased. Cyclic voltammogram recorded after pre-electrolysis run-8, has no additional voltammetric peaks in the same potential range, which confirms that the aforementioned peaks are associated with formation of Li-Cd alloys.

To further verify the formation of Li-Cd alloys, a fresh LiCl-KCl-1wt%$CdCl_2$ salt was prepared by mixing $CdCl_2$ with LiCl-KCl eutectic salt. Cyclic voltammograms (Fig. 3) recorded at tungsten electrode displayed distinct redox couples within the potential range of -1.97 V to -2.2 V, alongside a cadmium peak at -0.55 V. These observations confirm that, due to the presence of $CdCl_2$ in the LiCl-KCl melt, lithium undergoes underpotential deposition over cadmium and Li-Cd alloys were formed.

IV-12 Electrorefining of U-Zr alloy and cathode deposit consolidation at PyroProcess R&D Facility (PPRDF)

Pyroprocessing is best suited for reprocessing of metal fuel from future FBRs. Towards development of pyrochemical reprocessing technology, research is being carried out at IGCAR. Pyroprocess R&D Facility (PPRDF) is set up to carry out electrorefining and cathode deposit consolidation at 10 kg of heavy metal per batch scale.

Electrorefining of U-Zr fuel was carried out in engineering scale at PPRDF. Un-irradiated sodium bonded U-6Zr fuel pins were chopped and distilled to remove bond sodium. Chopped fuel segments with total weight 2.22 kg (including clad) was loaded in anode basket of High Temperature Electrorefiner (HTER). Electrorefining operation was carried out in galvanostatic mode, Anode potential was limited to prevent dissolution of Zr from the fuel. The applied current was manually reduced whenever anode potential reached cut off value (Fig. 1). Accurate anode polarisation was evaluated by incorporating ohmic drop correction.

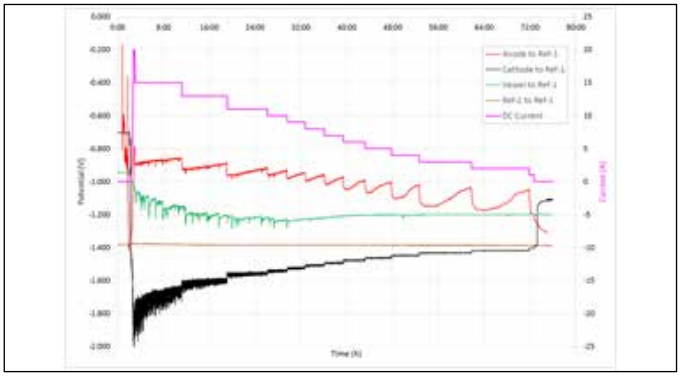

Fig. 1 Potential vs Ag|AgCl reference electrode

Fig.2 Photos of fresh cathode and cathode with U-deposit

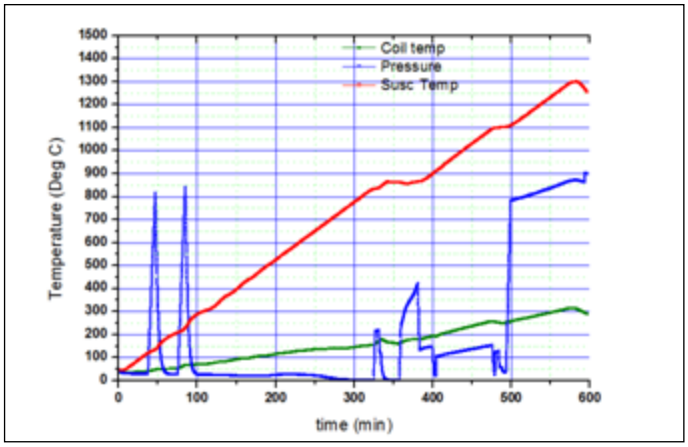

Fig.3 Temperature and pressure plot of Distillation and Melting

Fig.4 Photos of graphite crucible, collected deposit and consolidated Uranium metal

Maximum cell current 15 A with anode polarisation limit of +300mV. Cell current was subsequently reduced because of material reduction in anode. Cathode deposit (Fig. 2) was scraped and collected. Graphite crucible with collected deposits was transferred to Automated Vacuum Distillation and Melting System (AVDMS). Crucible transfer mechanism was used to pick and load the graphite crucible from scraping station to vacuum distillation unit. Adhering salt was distilled at 1100°C and <10 torr pressure (abs) for 15 minutes duration. Subsequently uranium melting was carried out at 1300°C and 600 torr pressure (abs) (Fig. 3 & 4).

Denser uniform deposits were observed due to low current density at cathode. Metal dissolution at anode and deposition at cathode was estimated from weight measurement data. Uranium ingot (Final product) weight was 1.370 kg. Current efficiency at cathode was 96.0%. Collection efficiency of overall process was 92.2%.

IV-13 Studies on cadmium distillation for recovery of actinides from cadmium- actinides alloy

Metallic fuel and reprocessing of spent metallic fuel by pyrochemical reprocessing has drawn significant attention in nuclear industry due to several advantages in comparison to existing oxide fuel and its reprocessing via aqueous reprocessing flow sheet. In pyrochemical reprocessing flow sheet, process steps have not been industrially established yet. Hence, lab scale and engineering scale studies are in progress by several countries. Present study discusses about cathode consolidation process step involving high temperature distillation of Cd metal from cadmium-actinide (Uranium) alloy. Alloys were prepared by electro-refining process (ER) at 773 K. High temperature distillations have been carried out at 1078 K and 0.32 mbar vacuum. Studies are in context of pyro-chemical reprocessing of spent metallic fuel related to cathode consolidation process step.

Fig. 1a shows high temperature distillation experiment set up for salt and Cd distillation experiments attached with vacuum pump and located inside 2 m^3 Ar atmosphere glove box along with the split type resistance furnace.

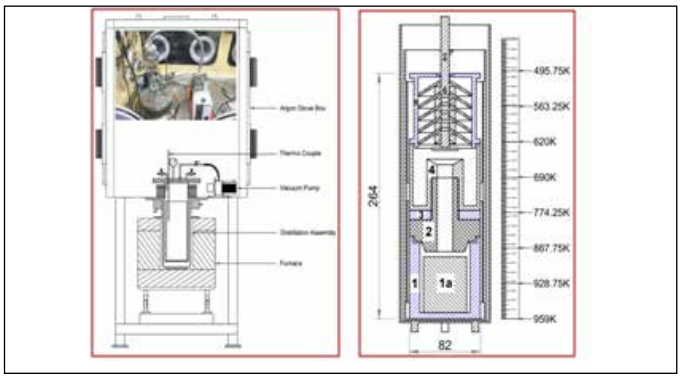

Fig.1a Cadmium and cadmium-actinide alloy distillation set up attached at the floor of argon glove box, Fig.1b Part 1 to 6 and Temperature profile for distillation setup during distillation

Fig. 2a U-Cd alloy prepared by LCC Electro-refining before distillation experiments Fig. 2b Cd distillate after distillation at 1078K

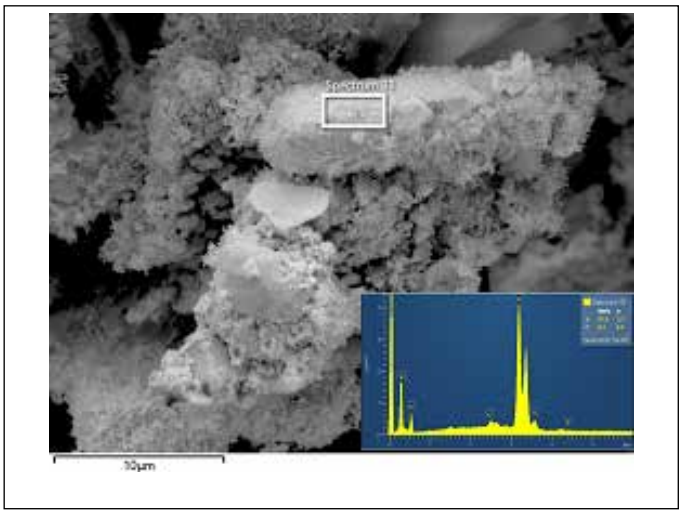

Fig.3. SEM – EDX analysis of actinide / uranium residue after distillation experiment at 1078K

Table 1, Summary for distillation efficiency determination

Expt.	Initial weight	Wt. of distillate Cd	Wt. of residue	Loss in vapours	Efficiency/%
Runl Cd	90.06g	87.52g	0.05g	2.49g	97.19
Run 2 U-Cd	121.83g	117.05g	2.78g	2g	98.32
Run 3 U-Cd	113.97g	106.76g	5.39g	1.82g	98.32

Fig 1b shows distillation assembly components (1-6) and temperature profile across height. Three representative Cd distillation experiment results are shown in Table 1. Run 1 was aimed for distillation of commercially obtained cadmium metal (purity - 99.5%). Two different set of ER experiments were carried out for preparation of U-Cd alloys where(i) U was present close to the solubility limit of Cd (Run-2) and (ii) U was present more than the solubility limit of Cd (Run-3). Fig. 2a represents loading of U-Cd alloy in part 1a (fig. 1b) and Fig. 2b shows distilled Cd at the bottom of part 5 (fig. 1b).

Feasibility of Cd and U-Cd alloy distillation experiments were studied and separation of uranium was demonstrated at 1078 K. Based on the weight difference and material balance, distillation efficiencies were estimated. Wet chemical, SEM-EDX (Fig. 3) and XRD analysis confirms efficient U and Cd separation. About 97-98% distillation efficiency was observed in all the runs.

Chapter - V

Basic Research

V-01 Optimization of Process Parameter for the Manufacturing of IHTA Tubes

Indian Advanced Ultra Super Critical Power Plant (AUSCPP) is being designed to achieve efficiency exceeding 45%. To meet the operational requirements of the super-heater tubes of the AUSCPP, IGCAR, in collaboration with MIDHANI and NFC, has developed an indigenous nickel based super alloy based on the Ni-Cr-Co system. This alloy named as "Indian advanced High Temperature Alloy" (IHTA) is designed for operation at nominal temperature of 720 °C and 35 MPa pressure. Billets manufactured at MIDHANI were used as input material to carry out experiments required for optimization of hot extrusion process, which is considered as a crucial step in seamless tube manufacturing.

Hot deformation experiments were carried out in a thermo-mechanical simulator, in a temperature range of 1050-1220 °C for various combinations of preheating temperature, soaking time and strains rate. Extensive microstructural investigation was carried out on the deformed specimens. Analysis of these results helped to understand the intrinsic behaviour of the alloy, the adiabatic temperature rise and melting characteristics under thermo-mechanical loading. Calculations were made to determine the influence of friction factors for various extrusion temperatures. Numerical simulations were carried out to predict the temperature profile across the blank during hot deformation. Flow behaviour, adiabatic temperature rise, friction factors, lubrication and heat dissipation etc were considered for the simulations. Fig. 1(a) shows the results obtained from the simulation carried out to predict the temperature across cross-section of an extruded blank.

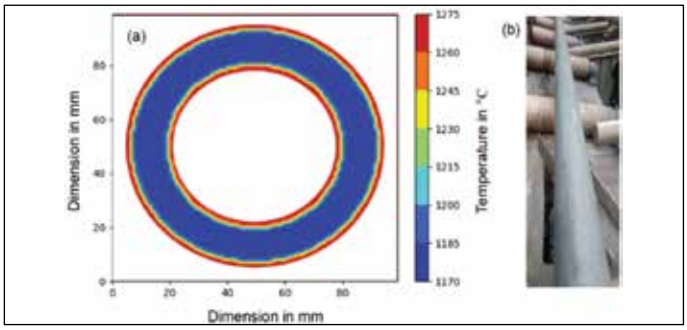

Fig. 1: (a) Temperature profile across the cross-section of the extruded blank, (b) Extruded blanks of IHTA

Following comprehensive analysis of the results obtained from the simulations, parameters for the industrial hot extrusion were optimized in collaboration with NFC, Hyderabad. The blanks extruded using the optimized extrusion parameters are shown in the Fig. 1(b).

The specimens were extracted from the extruded blanks for the multi-stage cold deformation with intermediate heat treatment to simulate the pilgering processes. Solution annealing heat treatment experiments were carried out on cold deformed specimens and the resulting microstructures were evaluated to identify the potential solution annealing temperature domain. Selected solution annealed specimens were imparted with different levels of cold deformation, to physically simulate the strain experienced during tube straightening process. These specimens were aged and subjected to creep tests.

The microstructure of crept specimens primarily comprised γ/γ' phases along with $M_{23}C_6$ and MX precipitates. Crept microstructures exhibited intergranular cracks, as shown in Fig. 2. These results aided to optimize the final heat treatment at the laboratory scale. The solution annealing temperature that resulted in requisite creep properties and microstructure was selected for industrial validation.

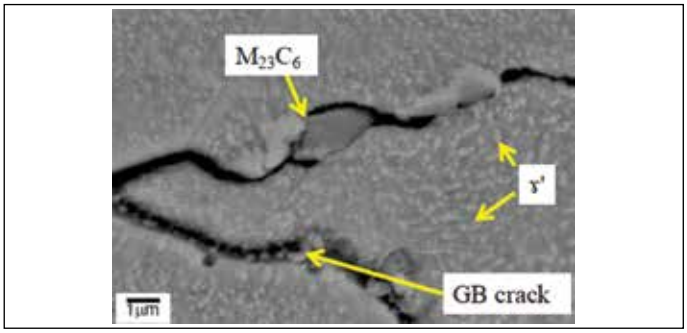

Fig. 2: Grain boundary cracks in crept specimen

An industrial heat treatment experiment on pilgered tube segments was carried out to understand the characteristics of the industrial furnace. Based on the creep test results, laboratory heat treatment and the capabilities of the industrial furnace, the final solution annealing parameters were optimized. The microstructural and mechanical properties of the solution annealed tubes were:

Grain size	Hardness (HV_{30})	YS (MPa)	UTS (MPa)	% El.
ASTM 2	149 ± 10	292	739	67

In collaboration with NFC and MIDHANI, the first batch of IBR certified IHTA tubes (Fig. 3) has been successfully produced for the Indian AUSCPP.

Fig. 3: The first batch of indigenously produced IBR certified IHTA tubes.

V-02 Evaluation of Diffusion Bonded Ti/304L SS Dissimilar Joint for Reprocessing Application

Diffusion bonding is a promising alternative over the currently employed explosive bonding, for joining of spent fuel dissolver vessel (Ti) to plant pipings (304L SS) in a reprocessing plant. The objective of this work is to study the effect of diffusion bonding parameters and interlayer on the properties of diffusion bonded Ti/304L SS joints fabricated by direct joining and by using tantalum (Ta) as intermediate piece (interlayer) between Ti and 304L SS. The integrity of the joint was evaluated by ultrasonic examination, macro and microscopic observation of the joint interface followed by cross-weld tension test and three phase corrosion test in 11.5 M boiling nitric acid.

The surface finished commercially pure Ti (CP Ti), and 304L SS rods were diffusion bonded in the temperature range of 850-950 °C for holding time of 1 h/2 h with the imposed pressure of 5-7 MPa. For diffusion bonding using Ta interlayer (Ti/Ta/304L SS), Ta foil of 100-150 µm was used in between Ti and 304L SS. The ultrasonic C-scan of Ti/304L SS and Ti/Ta/304L SS diffusion bonded samples revealed good bonding. The optical microscopic studies of the joints confirmed good metallurgical bonding. The partial solubility of Fe, Cr, Ni in Ti and vice versa results in the formation of brittle intermetallic phases at the joint interface in case of direct Ti/304L SS joint (Fig. 1-diffusion bonded at 850 °C for 1 h). Fig. 2 presents the FESEM microstructure of the diffusion bonded joint with a Ta interlayer (900 °C-1 h). The interface between 304L SS and Ta shows limited secondary phase formation, as seen in Fig. 2(a), while β-titanium is present across the Ti-Ta interface, as shown in Fig. 2(b).

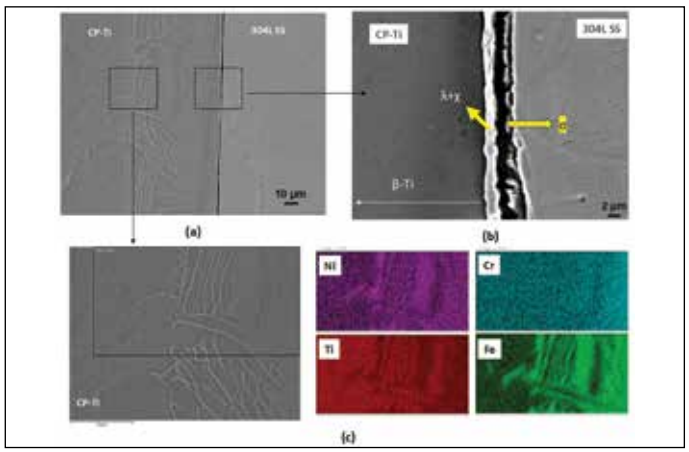

Fig. 1: FESEM microstructure across the interface of Ti/304L SS direct diffusion bonded joint

Three-phase 11.5 molar boiling nitric acid testing (liquid, vapour and condensate) was performed on Ti/304L SS and Ti/Ta/304L SS diffusion bonded samples and the average corrosion rate calculated for a total test duration of 240 h (5 cycles of 48 h each). Both the joints (direct and with Ta interlayer) showed more corrosion rate in the liquid phase (5-8 mpy) in comparison to vapour and condensate phases where corrosion rate is less than 1 mpy. The microscopy study of corrosion tested specimens indicating preferential corrosion in the vicinity of the joint interface. The hardness measurement of the samples showed higher hardness at

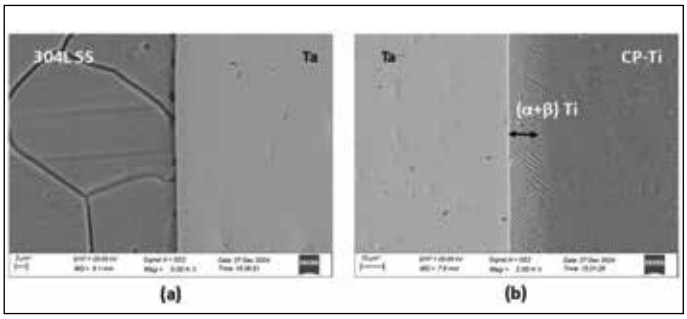

Fig. 2: FESEM Ti/Ta/304L sample - (a) SS304L-Ta interface and (b) Ta-Ti interface

the interface due to formation of brittle phases in Ti/304L direct joint and hardness increases with increases in bonding temperature (Fig. 3a), and lower hardness of Ta interlay in case of Ti/Ta/304L sample (Fig. 3b). The cross weld tension test of the Ti/304L SS direct joints showed maximum tensile strength of 244 MPa (bonded at 850 °C/1 h), while the Ti/Ta/304L SS joints showed maximum tensile strength of 252 MPa (bonded at 900 °C/1 h) with fracture at the joint interface and are found to be lower than the titanium base metal tensile strength of 314 MPa. The lower tensile strength of the Ti/304L SS & Ti/Ta/304L SS joints are due to presence of brittle phases at the joint interface. From the present studies, it is concluded that the diffusion bonding process produces sound & leak tight joints between Ti and 304L SS with adequate corrosion resistance and strength.

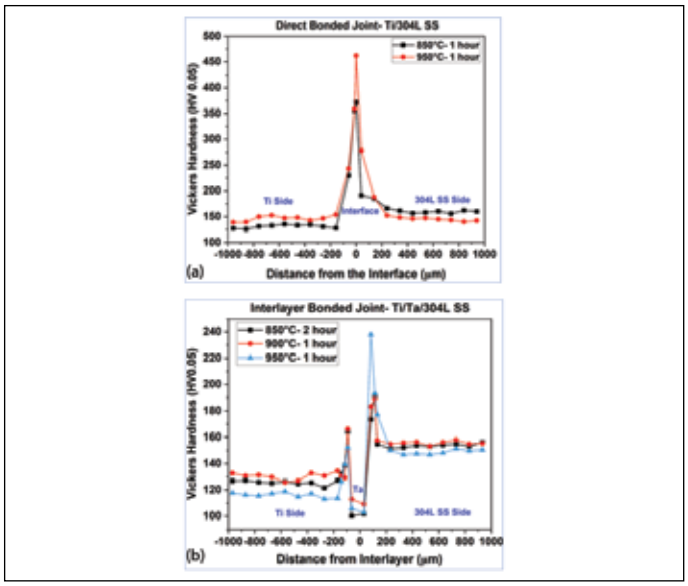

Fig. 3: Hardness measurement across the joint interface. (a) Ti/304L SS joint and (b) Ti/Ta/304L SS joint

V-03 Creep-High Cycle Fatigue Interaction in Type 316L(N) SS under FBR Operating Conditions

The normal operating conditions in Fast Breeder Reactors (FBR) introduce varied thermo-mechanical load cycles during reactor startup, shutdown, and power transients. Thermal striping, free level oscillations in sodium, and stratification generate low-amplitude stress fluctuations, which are the primary sources of High Cycle Fatigue (HCF). In addition to these, the static loads at high temperature induce significant creep damage, thus intensifying the HCF damage leading to the accumulation of creep-HCF damage, which is a major concern for long-term component reliability. In the present work, the Creep-HCF Interaction (CHCFI) has been examined on type 316L(N) austenitic stainless steel, in the solution annealed condition. Accelerated total axial stress-controlled HCF tests were conducted at 973 K in accordance with the ASTM standard E466-15, using the RUMUL electromagnetic resonance HCF testing machine. The HCF endurance limit of the steel at 923 K was observed to be 135 MPa.

The creep-HCF interaction tests were performed as sequential blocks of HCF loadings followed by blocks of creep loadings, as schematically depicted in Fig. 1. The HCF blocks consist of fully reversed (i.e., R = −1), stress controlled cyclic loads of stress amplitudes, σ_a, below the endurance limit, and the size of the HCF block is denoted as N_B cycles.

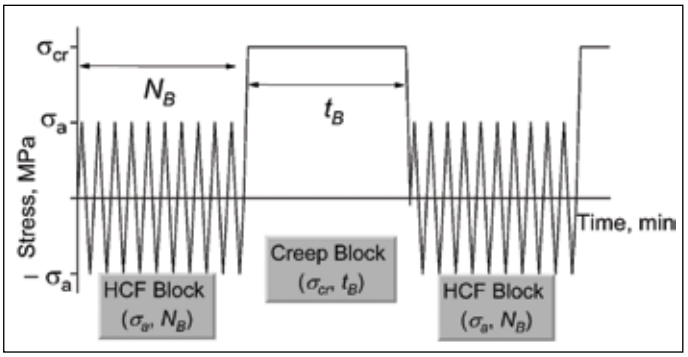

Fig. 1: Test scheme employed in the sequential CHCFI tests

The creep block consists of only mean load of stress values (referred as creep stress), σ_{cr} (σ_a = 0) for creep block size of time period t_B. The creep dwell time, $\sum t_B$, is defined as the total time spent on creep load during the complete CHCFI test. The Creep-HCF interaction in the type 316L(N) austenitic stainless steel is shown in Fig. 2 as the plot of HCF life (N_f), normalized with the run-out life of 10^7 cycles, against the creep dwell time ($\sum t_B$), normalized with the specific creep rupture time, at 923 K.

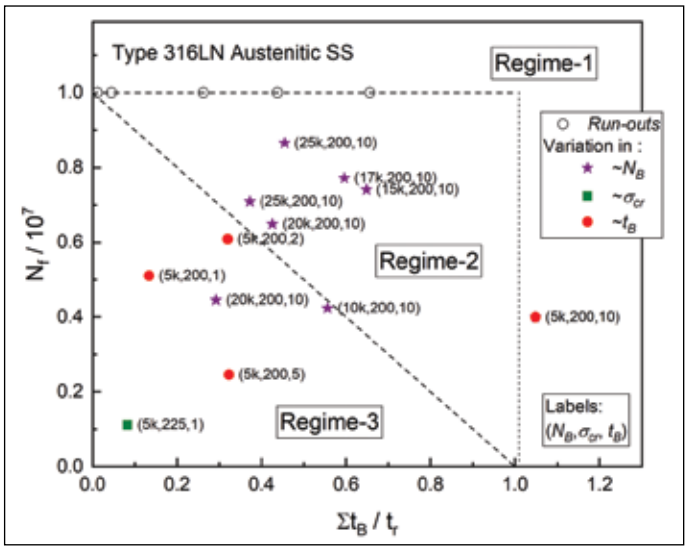

Fig. 2: Creep-HCF interaction diagram for the type 316L(N) austenitic stainless steel at 923 K

It may be observed that the C-HCFI plot exhibits three distinct regimes: Regime-1 relates to a safe zone, where the observed life is above either the pure creep life or the pure HCF life. Regime-2 represents the region where the life under C-HCFI condition is below both the isolated creep life and the isolated HCF life. However, the C-HCFI life is observed to be safe within the Robinson's life fraction rule with damage summation >1. Regime-3 constitutes a region of concern, where the observed life under C-HCFI condition falls much short of the pure creep life and the pure HCF life, and as well as the life predicted by the damage summation rule.

Results obtained in the current investigation highlight the critical need to include the creep-HCF interaction in the design consideration of structural components prone to these coupled damage mechanisms.

V-04 Influence of Thermo-mechanical Treatment on Creep Properties of Austenitic 316LN Stainless Steel

Thermo-Mechanical Treatment (TMT) is an important means of enhancing the high temperature strength of 316LN SS, which is currently used for primary side components of PFBR, Kalpakkam in India. The present study is aimed at evaluating the influence of TMT on creep properties of 316LN SS with 0.07 wt.% N. TMT adopted in this study is a 'strain annealing' based methodology under grain boundary engineering concept which consists of single-stage cold rolling (with 5%, 15%, 20% cold work) followed by solution annealing heat treatment at 900, 950 & 1000 °C for 30 minutes & then water quench. The selection of TMT conditions was based on earlier studies on mapping of Coincidence Site Lattice (CSL) boundaries at various degrees of cold work (CW: 3-25%) and annealing temperatures.

The TMT samples were creep tested at 650 °C and 140 MPa stress. The creep properties obtained on the same compared with as-received (ASR) and only Cold Worked (CW) conditions. The selected conditions of TMT samples are: (1) 5TMT1: 5%CW + 900 °C, (2) 5TMT2: 5%CW + 1000 °C, (3) 15TMT: 15%CW + 950 °C, (4) 20TMT1: 20%CW + 900 °C and (5) 20TMT2: 20%CW + 1000 °C. In reference to creep life of ASR condition (2023 h), the creep tests on only CW samples revealed an improvement in creep life by 2.3-6.0 times depending on the extent of CW imparted. In CW condition, increase in creep life is attributed to the strengthening arising from the CW induced high dislocation density and associated internal stresses. However, beyond certain amount of CW, the recovery of dislocation structure by thermally activated dislocation movement assumes dominance during the creep. Hence, among CW levels of 5-20%, highest creep life of 12425 h is observed at 15% CW with an extensive steady state creep regime. The corresponding rupture lives exhibited by 5% and 20% CW samples are 4737 h and 5967 h respectively.

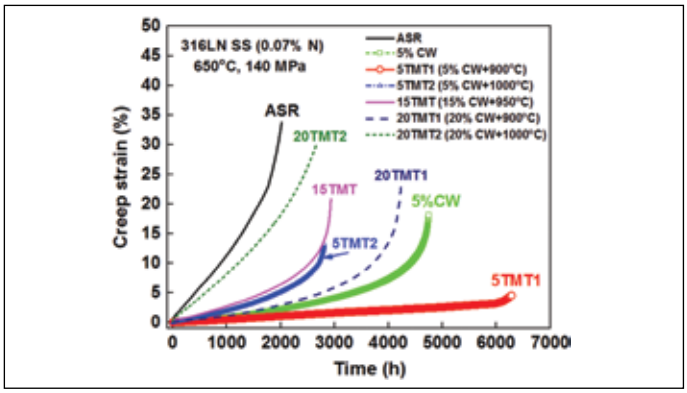

Fig. 1: Variation of creep strain with time, (h) for ASR, 5% CW and TMT treated samples

The implementation of TMT on ASR material has induced two significant beneficial effects on the creep characteristics, i.e. an extension of the steady state creep regime and a delay in the onset of tertiary creep (Fig. 1). Consequently, the creep lives of all TMT samples are higher than the creep life of ASR condition by 1.3 to 3.2 times (Fig. 2). However, the extent of creep life improvement is strongly relied on imposed TMT condition. Among all the

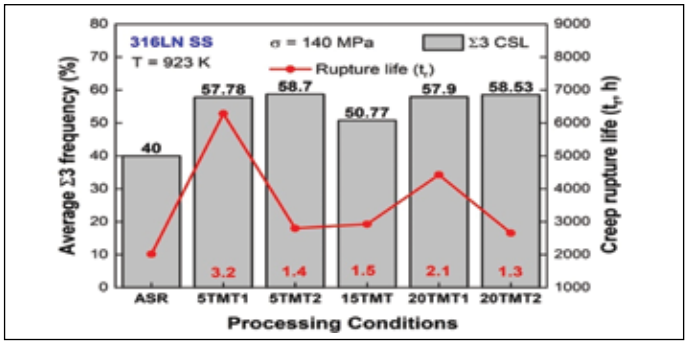

Fig. 2: Variation of average Σ3 CSL frequency and creep life as a function of TMT condition

TMT conditions, an extensive secondary creep regime is observed in 5TMT1, which showed the highest creep life of 6283 h, followed by 20TMT1 with creep life of 4230 h. Improved creep life is partially attributed to the fine $M_{23}C_6$ carbides (free from cavities) on CSL boundaries compared to the carbides which underwent preferential coarsening and cavitation on grain boundaries during creep (Fig. 3). In contrast, the fracture surfaces of all tested samples (ASR, CW & TMT) exhibited ductile transgranular fracture mode with lower density of coarse cavities in TMT samples.

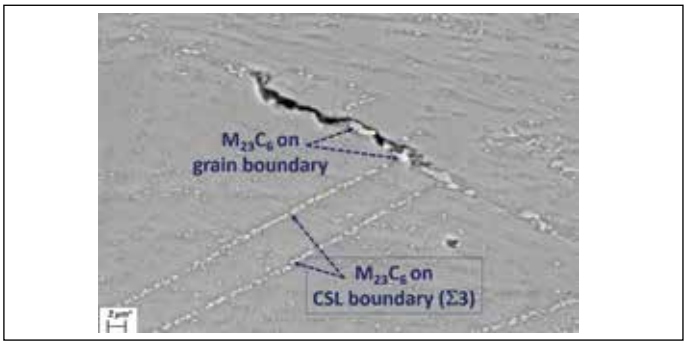

Fig. 3: Coarsening of $M_{23}C_6$ carbides in 5TMT1 condition at grain boundary compared to CSL boundaries

It must be mentioned that though the TMT has introduced beneficial CSL boundaries in material, no direct correlation could be established between the CSL fraction and improvement in creep rupture life. These results thus suggest that the creep performance of TMT-316LN SS is not a simple function of the CSL fraction alone but also influenced by precipitation kinetics of $M_{23}C_6$ carbides.

V-05 Development of Highly Corrosion-Resistant Medium Entropy Metallic Glass Ni-Nb-Ta-Zr Alloys for Nuclear Reprocessing Application

Reprocessing of spent nuclear fuel is one of the key processes in the closed nuclear fuel cycle. Nitirc acid (HNO_3) is used as a medium for the dissolution of spent nuclear carbide fuel of FBTR. The current generation of stainless steels and advanced titanium alloys in these harsh corrosive conditions are susceptible to various forms of corrosion attacks (transpassive corrosion, intergranular corrosion, active corrosion, vapour, and condensate corrosion, etc.) over prolonged exposure in HNO_3. Metallic Glasses (MGs) have been of immense interest due to various applications with superior chemical and mechanical properties under extreme conditions. The effect of Zr substitution in Ni-based MGs, highlighting its influence on corrosion behaviour and the development of versatile and new bulk metallic glassy alloys with exceptional durability and corrosion resistance in aggressive environments for nuclear applications are explored.

Medium Entropy Metallic Glass Alloy (MEMGA) ingots of $Ni_{60}Nb_{35}Ta_5$ and $Ni_{40}Nb_{35}Zr_{20}Ta_5$ alloys were prepared by arc melting and ingot was cast into ribbons of thickness ~20 µm and width of ~10 mm (Fig. 1a) using a Melt Spinner. Both the ribbons showed a broad diffuse peak, indicating a single-phase amorphous structure (Fig. 1b).

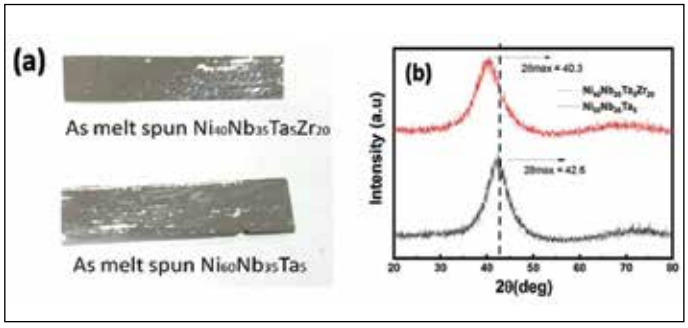

Fig.1: (a) Photograph of melt-spun ribbons; (b) XRD of $Ni_{60}Nb_{35}Ta_5$ and $Ni_{40}Nb_{35}Zr_{20}Ta_5$

Substitution of Ni by Zr increased the range of the super-cooled liquid region ΔT_x, from 25 to 44 °C. After the corrosion test of $Ni_{40}Nb_{35}Zr_{20}Ta_5$ in boiling 11.5 M HNO_3 at 120 °C, the weight loss measurement showed an insignificant weight loss of ≈0.0088 mm/y (Fig. 2). The lower E_{corr} value for the $Ni_{40}Nb_{35}Zr_{20}Ta_5$ amorphous ribbon than $Ni_{60}Nb_{35}Ta_5$ in 11.5 M nitric acid is associated with the ease of passive film formation due to the addition of Zr. The passive current density decreased by one order in $Ni_{40}Nb_{35}Zr_{20}Ta_5$ compared to $Ni_{60}Nb_{35}Ta_5$ (Fig. 3). XPS (Fig. 4) and Raman analysis showed that the passive

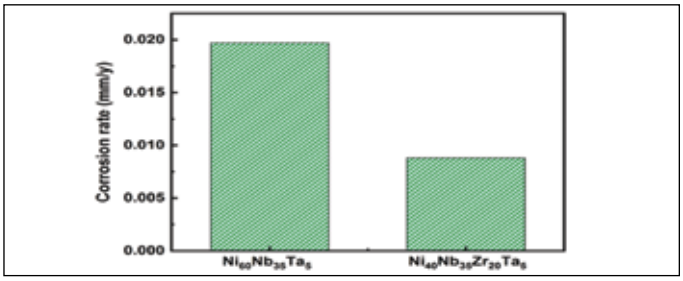

Fig. 2: Corrosion rate of $Ni_{60}Nb_{35}Ta_5$ and $Ni_{40}Nb_{35}Zr_{20}Ta_5$ ribbon samples during boiling nitric acid test

film was composed mostly of Nb_2O_5, Ta_2O_5, and ZrO_2 in $Ni_{40}Nb_{35}Zr_{20}Ta_5$. Surface characterization indicated that Zr substitution caused dense passive film formation with a wider passive region. However, in the case of $Ni_{60}Nb_{35}Ta_5$, small crystallites on the surface acted as defect sites, weakening the stability of the passive film. The incorporation of Zr reduced the oxidation of base Ni in ribbons. New MEMGA alloys were successfully cast and demonstrated to exhibit improved corrosion resistance, providing useful insights for designing corrosion-resistant materials for nuclear reprocessing application.

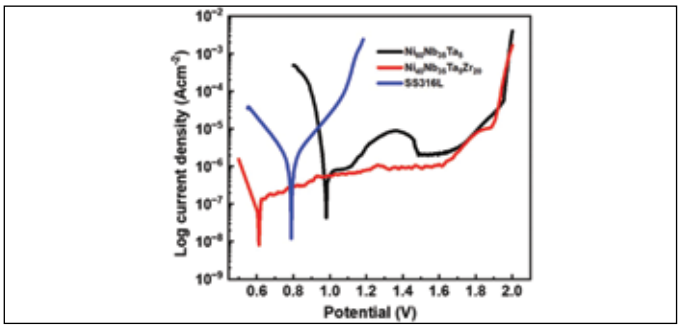

Fig. 3: Potentiodynamic polarization curves of $Ni_{60}Nb_{35}Ta_5$, $Ni_{40}Nb_{35}Zr_{20}Ta_5$ and 316LSS in 11.5 M HNO_3 solution

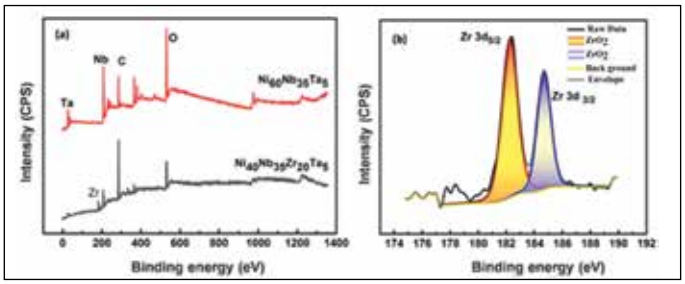

Fig. 4: XPS survey spectrum of $Ni_{60}Nb_{35}Ta_5$ and $Ni_{40}Nb_{35}Zr_{20}Ta_5$ post immersion tests in boiling 11.5 M HNO_3 and the corresponding high-resolution spectra of (b) Zr

V-06 Durable Ce-Ni Myristate Superhydrophobic Coating on Steel with Corrosion and Biofouling Resistance

Superhydrophobic (SHP) coatings have emerged as an effective solution, offering corrosion resistance along with additional benefits such as self-cleaning and anti-biofouling. In this study, a Ce-Ni myristate based SHP coating was fabricated on carbon steel via electrodeposition resulting in a water contact angle (WCA) value of 166.8° ± 0.9° after 60 s of deposition. SHP coating exhibited a combination of thread-like and cauliflower-like features. Notably, both structural types consist of small petal-like morphologies, indicating that the petal-like structures serve as the building blocks for both thread-like and cauliflower-like structures (Inset of Fig. 1). Potentiodynamic Polarization (PDP) and Electrochemical Impedance Spectroscopy (EIS) showed the corrosion protection property of Ce-Ni myristate SHP coatings on carbon steel in 3.5% NaCl solution.

SHP samples prepared with a deposition time of 90 s exhibited the highest E_{corr} value and the lowest i_{corr} value (Fig. 1), resulting in lower corrosion rate and better corrosion protection efficiency. EIS studies (Fig. 2) revealed that the SHP coating provided corrosion protection for up to 192 h while maintaining a WCA above 150° in 3.5% NaCl solution.

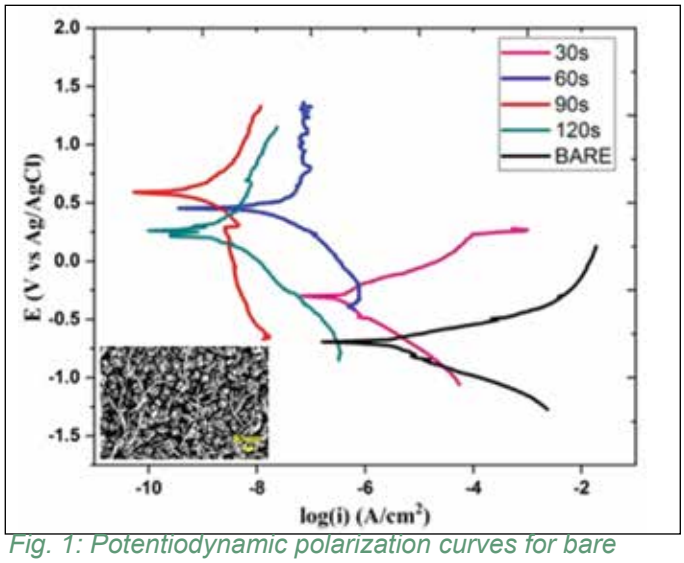

Fig. 1: Potentiodynamic polarization curves for bare and Ce-Ni myristate coated SHP carbon steel samples at different durations of electrodeposition in 3.5% NaCl solution.

Ce-Ni myristate SHP coating is ranked 5B as inferred from cross-hatch tape adhesion test (ASTM D3359) and the coating is intact and adherent on the substrate. SHP coating was found to be stable in different pH solutions ranging from 0 to 14 and also exhibited remarkable self-cleaning properties (Fig. 3).

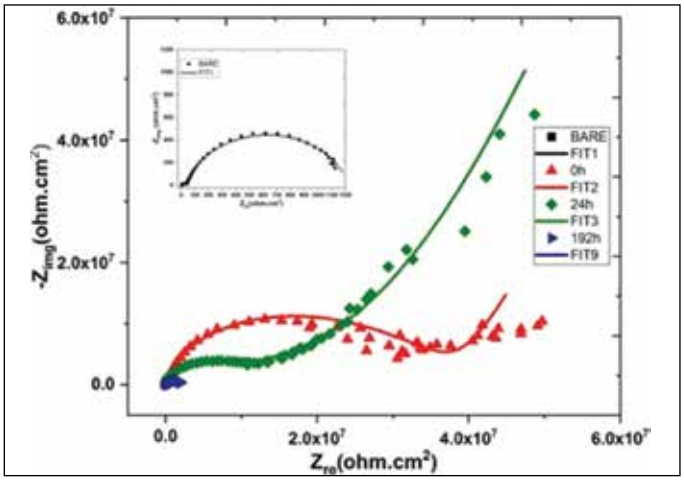

Fig. 2: Nyquist plots for the bare and Ce-Ni myristate coated SHP carbon steel samples exposed in 3.5% NaCl solution

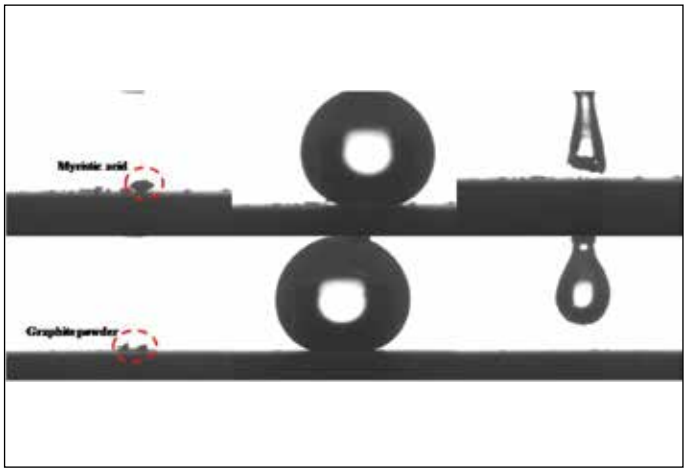

Fig. 3: Goniometer images of different stages of self-cleaning process on SHP carbon steel surface

SHP coating has been demonstrated to exhibit an impressive biofouling resistance up to 120 h in *Pseudomonas* sp. (Gram-negative) and *Bacillus* sp. (gram-positive) bacterial cultures, that are prevalent in the coastal waters of Kalpakkam. The present study indicates that the SHP coating offers a strong potential for long-term corrosion and biofouling protection in harsh seawater environments as a functional material for practical application.

V-07 Comparative Study of the Dosimetric Parameters of Multifiller Nanocomposites for Lead-Free Diagnostic X-Ray Shielding

Lead-free lightweight polymer nanocomposites are being developed as alternate diagnostic X-ray shielding materials. Towards this, attempt has been made to prepare multifiller loaded polymer nanocomposites for diagnostic X-ray shielding. Experimental analysis earlier revealed ~95-71% attenuation for 50-120 keV X-ray energy. However, there is a need to probe the effect of additional filler elements and optimization of filler concentrations. Towards this, the Mass Attenuation Coefficients (MAC) of various multifiller nanocomposites (SGB) of silicone polymer containing Gd_2O_3 and Bi nanoparticles are theoretically compared in the present study. Further, the dosimetric parameters of multifiller nanocomposites containing 0.025 to 2.5 wt.% tungsten nanoparticles (SGBT) are also estimated. National Institute of Standards and Technology-photon cross section database (NIST-XCOM) was utilized.

Fig. 1 shows the MAC for (a) lead, (b) SGB, (c) SGBT-2.5, (d) SGBT-0.25, (e) SGBT-0.025, and (f) pristine polymer samples. The MAC for lead was found to be 7.29, 4.43, 2.01 and 5.24 cm^2/g at 50, 60, 80 & 100 keV. For SGB, the corresponding MAC values were found to be 3.38, 6.09, 2.82 & 2.60 cm^2/g, respectively. For SGBT-2.5, the MAC values were 3.58, 6.29, 3.06 and 2.76 cm^2/g, which decreased to 3.39, 6.10, 2.84, 2.61 cm^2/g respectively, when W content was reduced to 0.25 wt.%. Further, for SGBT-0.025, the MAC values slightly reduced to 3.38, 6.09, 2.82 and 2.60 cm^2/g. The pristine polymer did not exhibit any attenuation in the studied photon energy range.

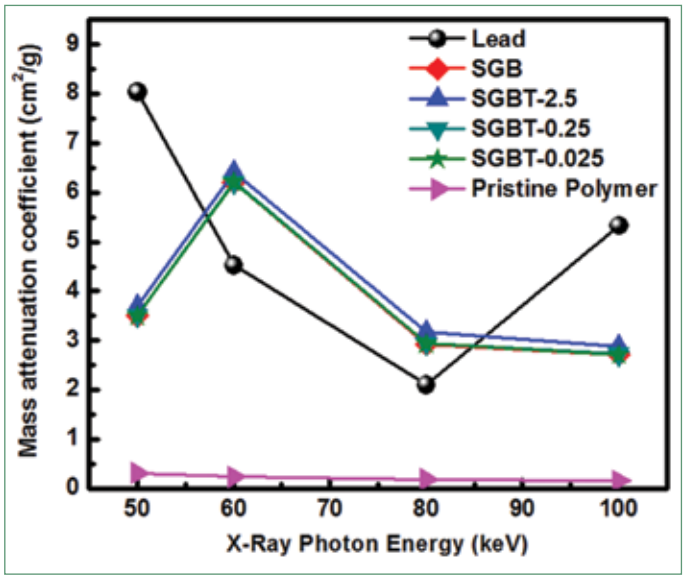

Fig. 1: MAC of multifiller silicone polymer based nanocomposites and lead for 50-100 keV X-ray photon energy

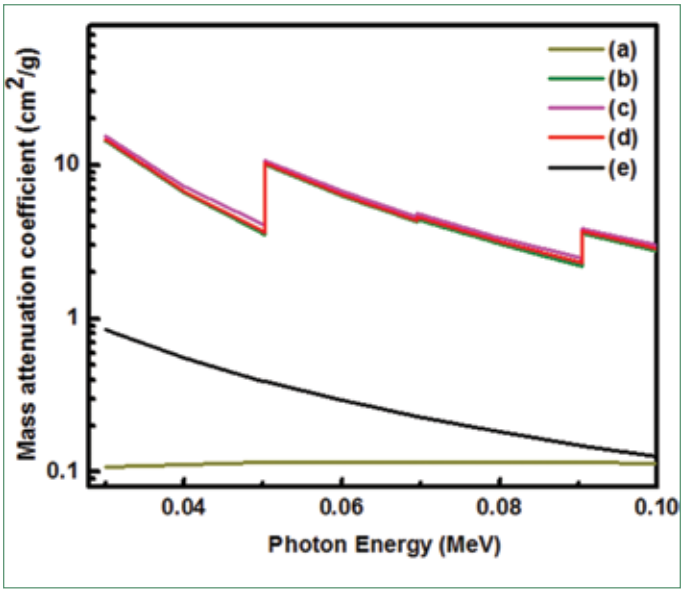

Fig. 2: Contribution of various attenuation mechanisms, viz., (a) incoherent scattering, (b) photoelectric effect, (c) total attenuation with coherent scattering, (d) total attenuation without coherent scattering and (e) coherent scattering, in the MAC of multifiller nanocomposite (SGBT-2.5)

A comparative analysis confirmed that the SGB nanocomposite is a better X-ray attenuating material than lead in the X-ray photon energy range of 50.2 to 85 keV, which is also a lead-feeble energy range, as shown in Fig. 1. The X-ray attenuation of SGB was found to improve slightly with the addition of 2.5 wt.% tungsten (SGBT-2.5). The mechanism of attenuation was probed in detail, and the contributions from incoherent scattering, photoelectric effect, and coherent scattering were calculated. Fig. 2 shows the contributions from various mechanisms to the MAC of SGBT-2.5 nanocomposite. It was observed that the attenuation was primarily due to the photoelectric absorption. Thus, silicone polymer nanocomposites containing Gd_2O_3, Bi & W is an ideal candidate for lead-free diagnostic X-ray shielding applications.

V-08 Electronic Axial Gradiometer to Suppress Background Magnetic Noise for Magnetocardiogram (MCG) Measurements

Cardiac electrophysiology involves the electrical activity of the heart, associated with the generation of time-varying electric and magnetic fields that can be respectively measured using electrocardiogram and magnetocardiogram (MCG). Cardiac magnetic fields are extremely weak of the order of 10 to 100 pico Tesla (pT) and provide valuable diagnostic information about cardiac function and pathology.

However, detecting such weak magnetic signals is challenging due to strong ambient magnetic noise. The most significant disturbances originate from power-line interference (50 Hz and its harmonics) and electromagnetic interference (EMI) from surrounding electrical equipment, and power sources in the vicinity. It is also possible that some of these noise sources share the same frequency band as the cardiac signal and vary dynamically, making conventional filtering techniques inadequate.

Measurements are traditionally performed in multi-layer magnetically shielded rooms (MSRs) to minimize noise, but such setups are bulky, costly, and impractical for wider clinical use. Hardware-based axial gradiometers relying on measuring the spatial gradient of the magnetic field by two spatially separated coils, wound in such way that it eliminates common-mode disturbances. Since uniform magnetic fields produce nearly identical signals at both positions, their difference effectively cancels out, leaving only the spatially varying component due to the cardiac source. Despite its effectiveness, the conventional hardware approach faces several constraints:

1. A fixed baseline, which limits reconfigurability once assembled.
2. Analog-only subtraction, restricting precision and tuning flexibility.
3. Baseline drift, due to mechanical or thermal instability.
4. Lack of digital signal processing, preventing adaptive noise cancellation.

Fig. 1: Electronic axial gradiometer

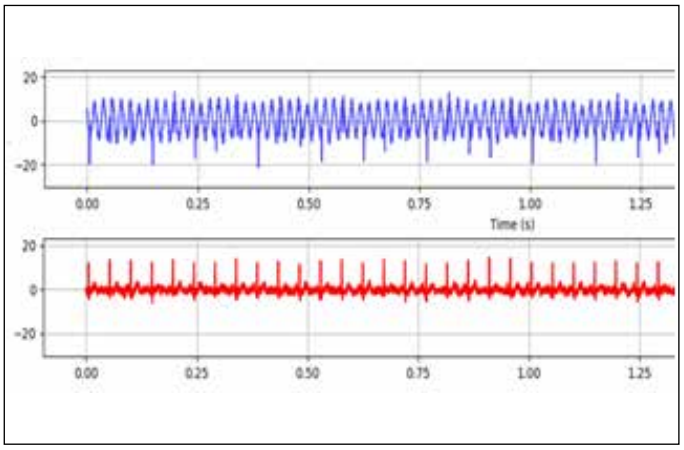

Fig. 2: Top: Raw simulated weak cardiac activity masked by noise, Bottom: Extracted signal by electronic axial gradiometer.

To overcome these issues, an electronic axial gradiometer using two fluxgate magnetometers operating in an unshielded environment has been attempted. Though the fluxgate sensors are known to have limited sensitivity in measuring MCG, the arrangement tried to evaluate the feasibility of the software gradiometry for MCG. The baseline between the sensing and reference units is adjustable, allowing optimization according to the noise profile and the cardiac source depth. Figure 1 illustrates the experimental arrangement, where the measuring fluxgate is positioned near the source coil (which mimics the actual cardiac signal measured from a human subject) and the reference sensor is placed farther along the same axis on a sliding rail.

This accurate collinearity between the sensing and reference fluxgate magnetometers ensures effective common-mode noise rejection by minimizing geometric misalignment and thus to facilitate the suppression of uniform environmental magnetic fields that are common to both measurement and reference sensors. As illustrated in figure 2, this configuration demonstrates the system's capability to isolate simulated MCG signals in an unshielded environment through combined spatial and digital noise suppression techniques, thereby offers scope for its further assessment for affordable bio-magnetic diagnostic systems for cardiac activity.

V-09 Indigenous development of a Faraday cup for large ion beam flux measurement in ion irradiation experiments

MSG is involved in radiation-damage research that includes alloy screening and fundamental studies of defect production using ion accelerators. One of the primary aspects of radiation damage studies is the displacement damage, expressed in DPA, which in ion irradiation experiments is determined from accurate measurements of the ion current and integrated charge. These measurements become more challenging when samples are subjected to additional processes such as high-temperature exposure, applied stress, in-situ corrosion, and electrical and mechanical property testing. This has resulted in several indirect beam current measurement techniques, including beam choppers, current transformers, transmission Faraday methods, and intermittent beam sampling approaches.

The UHV beam line of the 1.7MV Tandetron accelerator used for radiation damage studies employs an intermittent beam flux measurement system. The main component of the current measurement is the retractable Faraday cup. An indigenous development of a Faraday cup was undertaken and the details of its design, fabrication and commissioning are presented here. Fig. 1a shows the components of the Faraday cup, which consists of a solid OFHC copper cup with a tantalum cone-insert to promote uniform heat distribution and minimize beam hotspots.

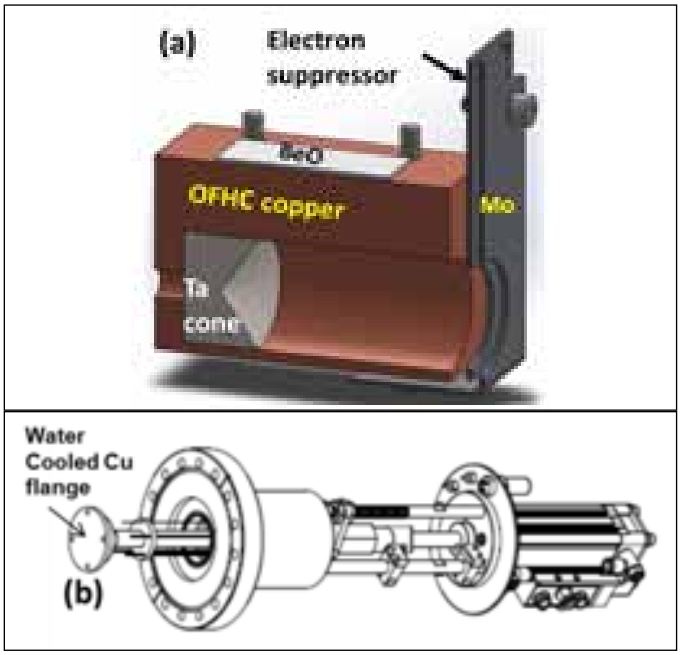

Fig.1 (a) The details of the Faraday cup (b) retractable assembly showing the water-cooled copper flange

Fig.2 The photograph of the Faraday cup assembly

The Faraday cup is mounted on a water-cooled copper flange with an inter-layer of BeO between the cup and the cooling flange to ensure efficient thermal dissipation while simultaneously providing electrical isolation. The entire assembly is mounted onto a retractable shaft sealed by edge-welded bellows, allowing it to be precisely inserted into or withdrawn from the beam path for beam sampling and irradiation, respectively (Fig. 1b).

A thermal analysis was conducted to evaluate the temperature rise in the components of the Faraday cup when subjected to a 200 W beam uniformly distributed over a 5mm^2 area. The results demonstrated that with water cooling, temperature rose up to 292 ºC at the tantalum insert and was less than 60 ºC in the copper cup in immediate contact with the tantalum insert.

Following the simulations, the engineering drawings were finalized, and suitable domestic fabricators specialized in ultra-high vacuum (UHV) technology were identified for fabrication. The resulting Faraday cup assembly was leak tested achieving a leak rate of better than 10^{-10} mbar.litres. sec-1. The photograph of the Faraday cup assembly is shown in Fig. 2.

The Faraday cup was installed in the beam-line of a 200 kV accelerator and Ar^+ ion currents of different energies and intensities were benchmarked against a standard 600 mm long Faraday cup.

Agreement within 5% was found. The development marks a major contribution to import substitution.

V-10 Atomic Scale Study of Defects in $Co_2FeAl_{(1-x)}Si_{(x)}$ Heusler Compounds: Promising Spintronic Materials

Heusler compounds have been theoretically reported to be half metallic predicted to exhibit 100% of spin polarisation (SP) having wide applications in spintronics based devices. In spite of promising high value of SP, multiple types of lattice disorders such as B2, DO_3 and A2 may coexist with the most desired $L2_1$ ordered structure in these compounds.Ternary full Heusler compound is represented as X_2YZ (with X, Y are transition metals and Z is any sp block element). While X, Y play a crucial role for magnetic properties, Z element of X_2YZ plays a key role in the stabilization of appropriate crystal structure as well as improvement in SP. Therefore, in this study, the role of defects/disorders occurring at submicron level & affecting the local structural, magnetic and hence SP properties of ferro-magnetically ordered $Co_2FeAl_{1-X}Si_X$ has been carried out using X-ray diffraction (XRD), vibrating sample magnetometer (VSM) and Mössbauer spectroscopy. XRD pattern of $Co_2FeAl_{1-X}Si_X$ is shown in Fig.1. Due

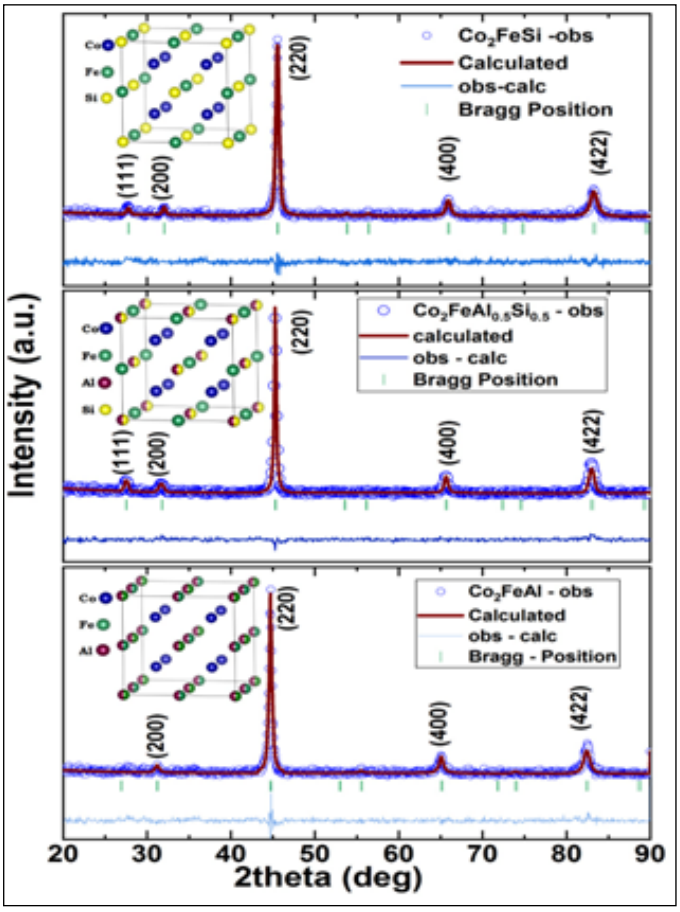

Fig.1 Rietveld refined X-ray (Cu K_α) diffraction pattern with schematic of possible major crystal structures in $Co_2FeAl_{1-x}Si_x$.

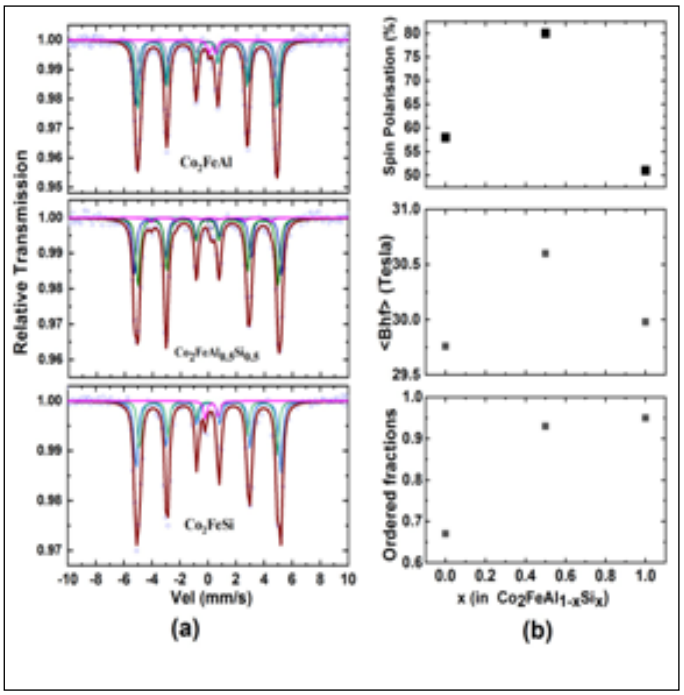

*Fig.2 **(a)** Mössbauer spectra recorded at room temperature & **(b)** Variation of the ordered fraction, the mean hyperfine field $<B_{hf}>$ and spin polarisation as function of x in $Co_2FeAl_{1-x}Si_x$.*

to very small intensity of (111) peak for Co_2FeAl, Rietveld analysis has been performed with B2 structure by assigning Fe & Al atoms at 4a & 4b Wyckoff sites with equal probability whereas $L2_1$ structure has been considered for Si substituted Co_2FeAl due to presence of both (111) & (200) peaks in the XRD pattern. Lattice parameters following Rietveld refinement analysis for $Co_2FeAl_{1-X}Si_X$ (x = 0, 0.5 & 1) have been found to be 5.73(2) Å, 5.68 (1) Å & 5.65 (3) Å respectively. The saturation magnetization has been found to be 5.1, 5.5 & 6μ_B per formula unit in $Co_2FeAl_{1-x}Si_x$ for x = 0, 0.5 & 1 respectively. Mössbauer results are presented in Fig. 2(b) in terms of the variation of the ordered fraction and the mean magnetic hyperfine field $<B_{hf}>$ for $Co_2FeAl_{1-X}Si_X$. These results indicate that there is a significant increase in the lattice ordering at atomic level resulting in an increase in the value of B_{hf} as experienced by Fe atoms with enhanced substitution of Si atoms at Al sites in Co_2FeAl. This is ascribed due to stronger hybridization of Co/Fe with Si atoms as compared to Al. Hence, the results of this study elucidating the enhanced lattice ordering in $Co_2FeAl_{0.5}Si_{0.5}$ as compared to Co_2FeAl and Co_2FeSi, might lead to extensive applications of $Co_2FeAl_{0.5}Si_{0.5}$ in the field of spintronics.

V-11 Studies on the Structural, Magnetic and Magneto-Caloric Properties of $La_2Ni_{1-x}Cu_xMnO_6$ Systems

The $RE_2BB'O_6$ type double perovskites materials are highly promising from both fundamental as well as technological aspects. La_2NiMnO_6 and La_2CuMnO_6, both belong to the lanthanum (La) based double perovskite oxides have interesting crystallographic, electronic and magnetic properties. In the present work, the evolution of structural, magnetic and magneto-caloric (MCE) properties of $La_2Ni_{1-x}Cu_xMnO_6$ series is evaluated.

The $La_2Ni_{1-x}Cu_xMnO_6$ samples were synthesized by conventional solid-state reaction method. Powder XRD diffraction measurements indicate monoclinic unit cell (space group P21/n) for all the samples. Figure 1 presents the variation of unit cell volume with composition. The unit cell slightly expands with increase in the copper content. Slightly larger ionic size of the Cu^{2+} compared to Ni^{2+} in the octahedral environments is the reason for this.

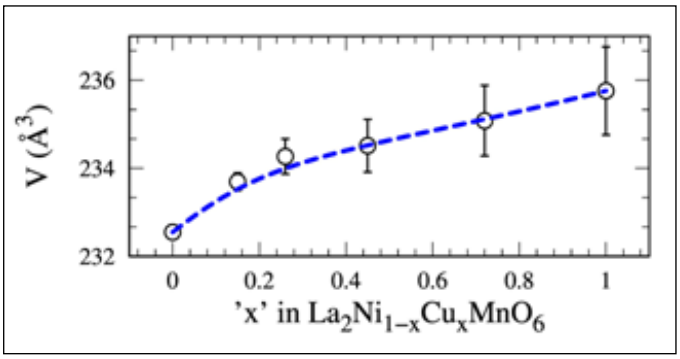

Fig.1 Variation of monoclinic (space group P21/n) unit cell volume (V) with nominal composition (x). Symbols represent the experimental data and the broken line is guide to the eyes.

Figure 2 presents the magnetic transition temperature versus composition ('x') phase diagram for the $La_2Ni_{1-x}Cu_xMnO_6$ series, which clearly shows gradual reduction of ferromagnetism and evolution of the spin glass state with the increases in copper content in the $La_2Ni_{1-x}Cu_xMnO_6$ series. The La_2NiMnO_6 shows T_C around 270, which gradually falls to ~ 200 K for x = 0.6 composition. The x = 0.8 and x= 0.9 compositions exhibits Griffiths phase also. Griffiths phase occurs due to the formation of small ferromagnetic (FM) clusters without any long range ordering in the paramagnetic main phase.

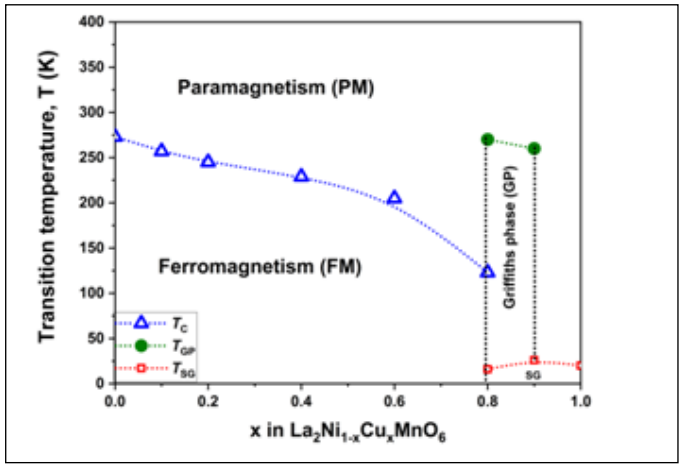

Fig. 2 T-x phase diagram for La2Ni1-xCuxMnO6 system comprising paramagnetic (PM), ferromagnetic (FM), Griffith's phase (GP) and spin glass (SG) phases.

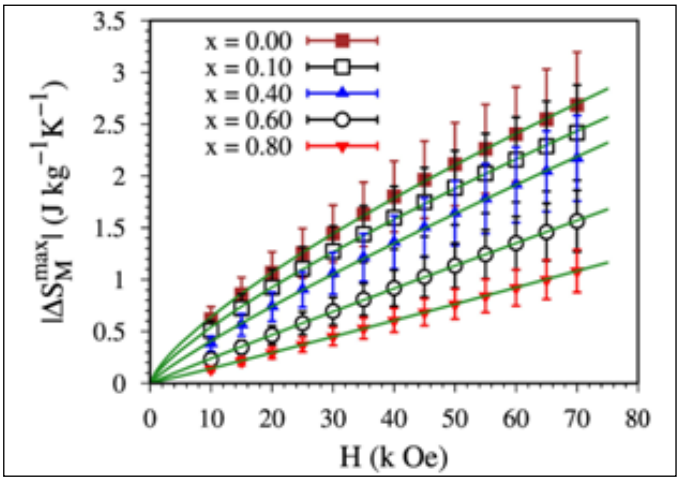

Fig.3 Magnetic field (H) dependence of the maximum isothermal entropy change for the $La_2Ni_{1-x}Cu_xMnO_6$ systems.

For the ferromagnetic composition of the series (ie. for x <=0.8) the magneto-caloric properties were also studied from the experimental magnetization measurements. Characteristic MCE parameters such as the isothermal magnetic entropy change (ΔS_M) and refrigerant capacity (RC) are evaluated using the Maxwell's thermodynamic relations. The $La_2Ni_{1-x}Cu_xMnO_6$ system has moderate MCE characteristics. The systems shows isothermal magnetic entropy change of 1.0–2.7 J kg^{-1}K^{-1} and refrigerant capacity of 110–200 J/kg for the field changes from 0 to 70 kOe, depending on the chemical composition.

V-12 Surface Plasmon Heating in monolayer MoS_2 Probed by Tip-Enhanced Raman Spectroscopy (TERS)

Surface plasmon resonance (SPR) of metal nanoparticles is frequently employed to enhance Raman scattering and photoluminescence (PL) emission in semiconductors. However, the extreme confinement of light around the nanoparticles induces localized heating, which may adversely affect this enhancement. In particular, PL emission is strongly dependent on the local temperature due to thermally activated non-radiative recombination processes. Recently, two-dimensional (2D) semiconducting materials such as monolayer MoS_2 (1L-MoS_2) have attracted significant attention because of their intriguing optical properties. SPR from metal nanoparticles is commonly used to enhance the PL intensity of monolayer MoS_2 owing to its intrinsically low PL quantum yield. However, SPR-induced heating can significantly influence the PL intensity of 1L-MoS_2 due to its atomic-scale thickness. Therefore, understanding the effect of SPR heating on the PL intensity of monolayer MoS□ is essential.

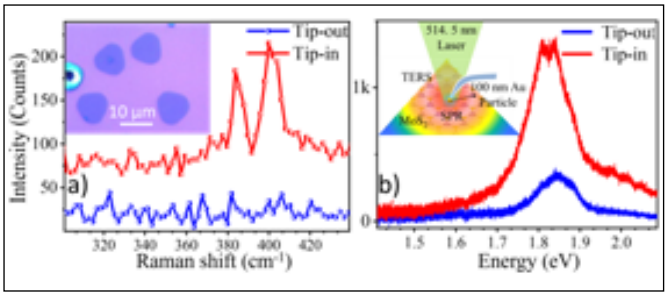

Fig.1 a) Raman spectra recored in presence and absesnce of TERS tip. Inset figures as-grown 1L-MoS2 flakes on SiO2 sustrate. b) PL spectra recored in presence and absesnce of TERS tip. Inset figure shows shcematic of TERS measurements procedure.

Tip-enhance Raman spectroscopy (TERS) and Tip-enhanced PL can exclusively delineate the impact of SPR heating. Figure 1a and 1b show the Raman and PL spectra recorded with and without tip, respectively. The 1L-MoS_2 samples were grown on SiO_2/Si substrate using the CVD (Inset of Fig. 1a). Au nanoparticle of size < 100 nm attached to the AFM tip was used for the TERS measurements (Inset of Fig.1b).

The Raman and PL spectra were clearly enhanced in the presence of Au nanoparticle (Tip-in). The enhancement factor (EF) is calculated for different laser powers and plotted in Fig. 2a. It is revealed that PL EF is closely one order less than Raman EF (Fig. 2a). It is also revealed that both EFs are reduced with laser power.

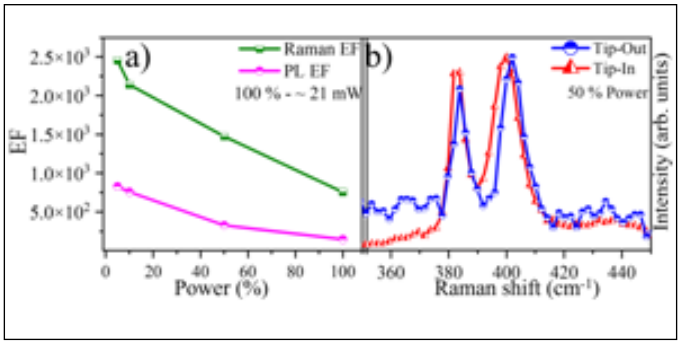

Fig. 2 a) Variation of EF with laser power. b) Tip-out and Tip-in Normalized Raman spectra.

A significant redshift (2.4 cm^{-1}) of A_{1g} mode is observed in the presence of the TERS tip compared with the absence of it (Fig. 2b), indicating the rise in the local temperature. Using, first-order temperature coefficient, the additional rise in the local temperature in the presence of the TERS tip is approximated to be 147 °C. Thus, the low PL EF compared to Raman EF is attributed to additional local temperature rise in the presence of the TERS tip.

To study the substrate effect, as-grown 1L-MoS_2 flakes were transferred onto Cu-substrate (Inset of Fig. 3a). The total PL intensity is enhanced by 4.7 (Fig. 3a) in the presence of a TERS tip, which is 2.5 times higher the SiO_2 supported flakes. In addition, the Cu-supported flake shows a negligible shift in the A_{1g} mode with and without the TERS tip (Fig. 3b), suggesting that near-field heating effects are negligible on the Cu substrate. Our results demonstrate that near-field heating and local temperature play a significant role in influencing the EFs associated with SPR. Selecting substrates with higher thermal conductivity could mitigate SPR heating effects.

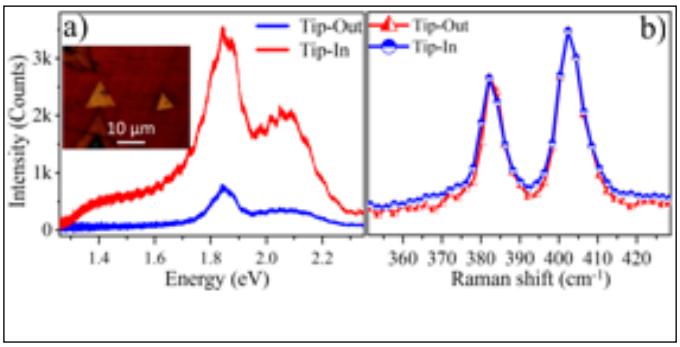

Fig.3 Tip-in and Tip-out PL (a) and Raman spectra (b) of 1L-MoS2 flake supported by Cu-substrate. Inset of (a) shows optical image of transferred flakes on to Cu-substrate.

V-13 Behaviour of molybdenum diphosphide at high pressure

Mo-P binary system includes stable phases like Mo_3P, MoP, and MoP_2 (orthorhombic), with high-pressure synthesis revealing new phases such as α-MoP_2 (monoclinic), and metastable Mo_4P_3 and Mo_8P_5. They are attractive because of their catalytic properties with properties improving with higher phosporization, making MoP_2 more interesting. Moreover, orthorhombic MoP_2 is identified to host long-awaited Weyl quasiparticles and exhibits exotic magneto-transport properties. At low temperature, MoP_2 exhibits high magnetoresistance. The stability range of MoP_2 has been theoretically predicted to lie below 40 GPa, with a phase transformation into Mo_2P_3 and elemental phosphorus occurring around 38 GPa. Interestingly, monolayer Mo_2P_3 has been computed to exhibit good electrical conductivity and excellent electrocatalytic activity for water-splitting reactions. However, experimental synthesis of Mo_2P_3 is not yet reported. Hence we aimed to investigate the structural transformation of MoP_2 under pressure and

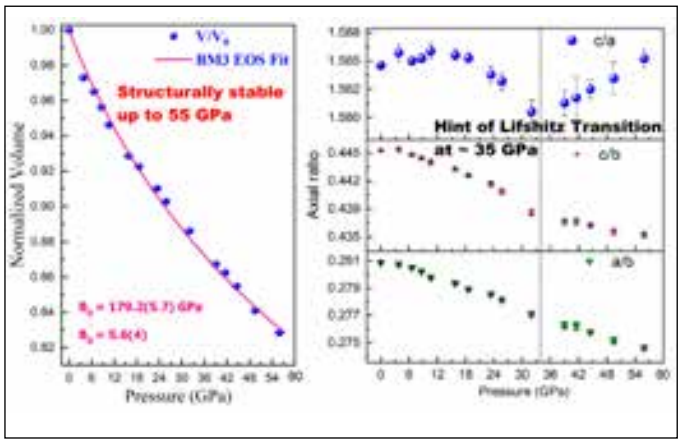

Fig.1: Pressure evolution of unit cell volume of MoP_2 (left) and axial ratio (right)

elucidate the compressibility mechanism of both its ambient and high-pressure phases. MoP_2 was synthesized from MoO_3 and red P in a vacuum sealed quartz tube at 850 °C. High pressure X-ray diffraction experiments were performed at the synchrotron facility at BL-11, Indus-2, RRCAT, India with λ = 0.6668Å using Mao-Bell type diamond anvil cell. The ambient crystal structure was obtained as orthorhombic with space group $Cmc2_1$. Mo and two types of P atoms designated as P1 and P2 are at Wyckoff positions 4a with coordinates (0, 0.093, 0), (0, 0.297, 0.809) and (0, 0.428, 0.115) and form a singly capped triangular prismatic polyhedra. Contrary to prediction, the $Cmc2_1$ structure remained stable up to 55 GPa and no structural transformation to

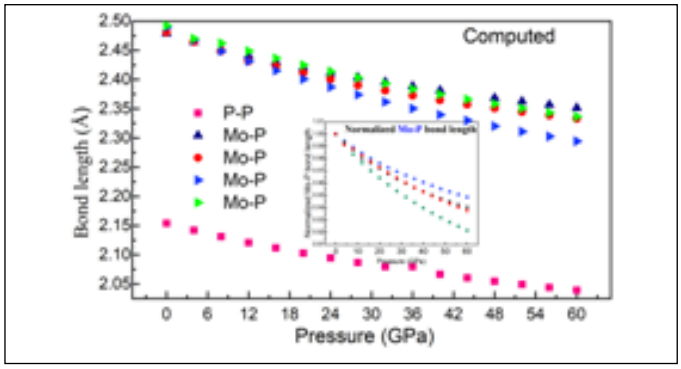

Fig.2. Pressure evolution of Mo-P bond lengths indicating polyhedral distortion around 12 GPa

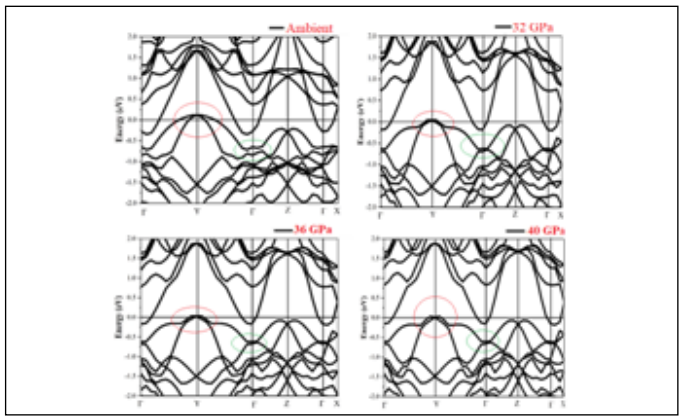

Fig 3: Electronic band structure of MoP_2 at selected pressures.

Mo_2P_3 was observed at 38 GPa. Further substantiation of the structural stability was obtained by checking the Born stability criteria for computed elastic constants. The pressure vs. unit cell volume is shown in fig. 1. The bulk modulus was estimated to be 180(6) GPa.

However, despite structural stability, we observed a slope change in axial ratio c/a around 12 GPa and 36 GPa (fig. 1). Analysis of the bond length constituting the polyhedra, indicated a variation in Mo-P bond compression rate around 12 GPa as presented in fig. 2 and its inset showing normalized Mo-P bond length. Pressure evolution of electronic band structures of MoP_2 exhibited that the band that crosses the Fermi level (E_F)at Y point, goes below E_F at around 36 GPa (fig. 3) suggesting a change in Fermi surface topology which is indicative of Lifshitz transition.

In summary, MoP_2 is structurally stable up to 55 GPa. The polyhedral distortion around 12 GPa and electronic transition around 36 GPa get reflected in the pressure evolution of axial ratio c/a.

V-14 Demonstration of Deutsch Algorithm on the Polarization States of Light

Given a Boolean function , f:{0,1}→{0,1} Deutsch algorithm aims at distinguishing whether the function is constant or balanced with just one query. Classical computation requires two queries. But quantum superposition allows both inputs to be probed simultaneously demonstrating a fundamental advantage of quantum computation over classical methods. In this work, we present a novel experimental realization of the Deutsch algorithm using only the polarization states of light as the physical qubit. Traditionally, implementation of Deutsch algorithm uses an XOR oracle, requiring two registers: |x› (input) and |y› (output), ensuring unitarity by encoding the function's output through XOR with the second register. Instead, we use a phase oracle where the result of the function evaluation is encoded in the phase of the quantum state:

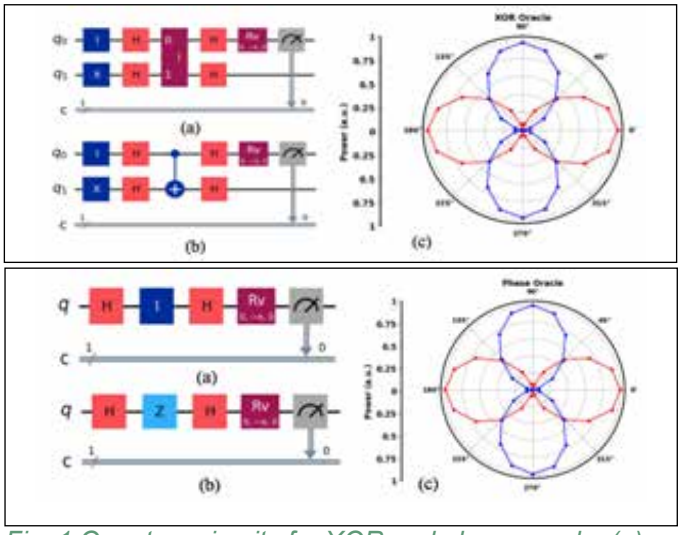

Fig. 1 Quantum circuits for XOR and phase oracle: (a) Constant function 0 (b) balanced function I (c) polar plot between projection angle θ and number of counts in state |0›. Red and blue curves denote the constant and balanced functions.

$$O_P|x\rangle = (-1)^{f(x)}|x\rangle$$

This approach removes the need for a second qubit, allowing the algorithm to be performed with a single physical qubit- the polarization states of light. Although phase oracles cannot distinguish all four possible Boolean functions- 0,I,X,1 individually due to global phase ambiguities, they are perfectly suited for differentiating constant from balanced functions, which is the only requirement of Deutsch's problem. Towards this, we develop the mathematical framework for both XOR and phase oracles and show their operational equivalence in the context of the algorithm.

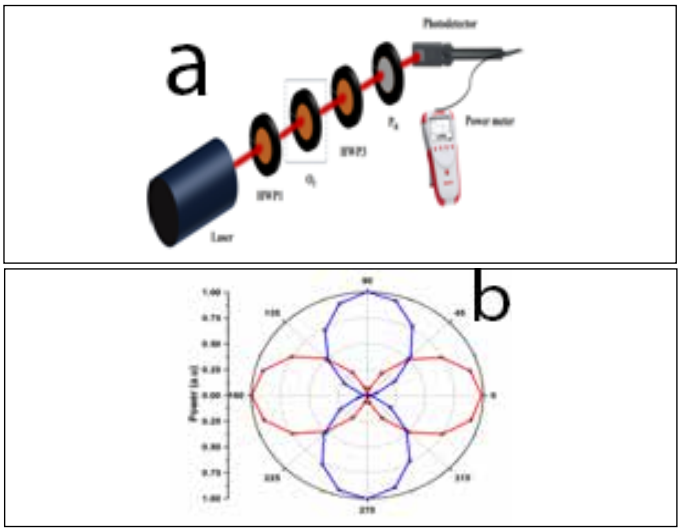

Fig.2 (a) Schematic for the experimental implementation of Deutsch algorithm. (b) Polar plot of normalized power measured experimentally at different orientations of analyzer.

Implementation of Deutsch algorithm follows the steps: qubit initialization, Hadamard transformation, followed by oracle operation encoding the function information and finally another Hadamard transformation. If measurement of the resulting state is same as input, the oracle function is constant and if it is orthogonal to input, the function is balanced. We have performed simulations using Qiskit on IBM's cloud-based quantum computer to verify our experimental results. The simulation results confirm that both the oracles yield identical measurement pattern emphasizing the equivalence of XOR and phase oracles.

Experimentally we demonstrate the algorithm using a He-Ne laser at 632.8 nm with horizontal and vertical polarization states serving as |0› and |1›. Half-wave plates (HWP) oriented at appropriate angles serve as Hadamard gates and oracle operations are realized by associating the four Boolean functions onto a physical optical component- empty, HWP at 0^0, 90^0 and phase plate respectively. Measurements are performed using a rotating analyzer which reveal that constant functions return the polarization state |H›, while balanced functions return |V›. The experimental polar plots are identical to the numerical plots.

To conclude, we have successfully demonstrated that Deutsch algorithm can be implemented using only the polarization degree of freedom of light, eliminating the need for a second register or additional degree of freedom.

V-15 A Simple and Novel Method for Determining Boron Isotopic Composition in Boron Carbide using Inductively Coupled Plasma Optical Emission Spectroscopy

A simple, fast, and cost effective analytical approach compared to the conventional mass spectrometry techniques for determining the isotopic composition (I_C) of boron, ($^{10}B/^{11}B$), using inductively coupled plasma optical emission spectroscopy (ICP-OES), by monitoring the emission peak of the BII ionic line at 345.13 nm was developed. The atomic line of boron at 208.96 nm was also considered for the calculations.

First derivative of emission spectra (Fig. 1) were recorded for various B_4C samples with 20 %, 53 %, 70 %, and 95 % ^{10}B enrichment levels and a calibration plot (Fig. 2) was established between wavelength at zero crossing against

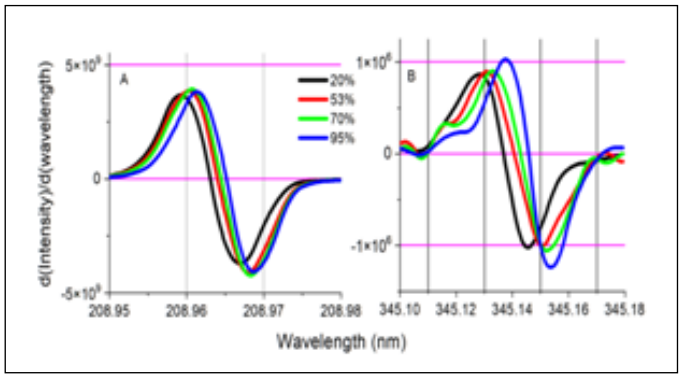

Fig. 1 First derivative spectra of B4C with different 10B enrichment recorded at (A) 208.96 nm and (B) 345.13 nm

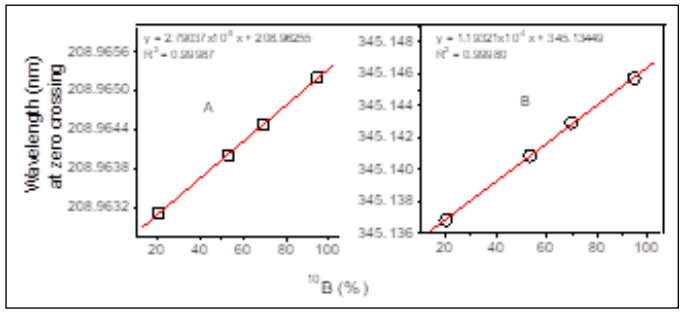

Fig. 2 Calibration plot between first derivative peak maxima and 10B enrichment for (A) 208.96 nm and (B) 345.143 nm

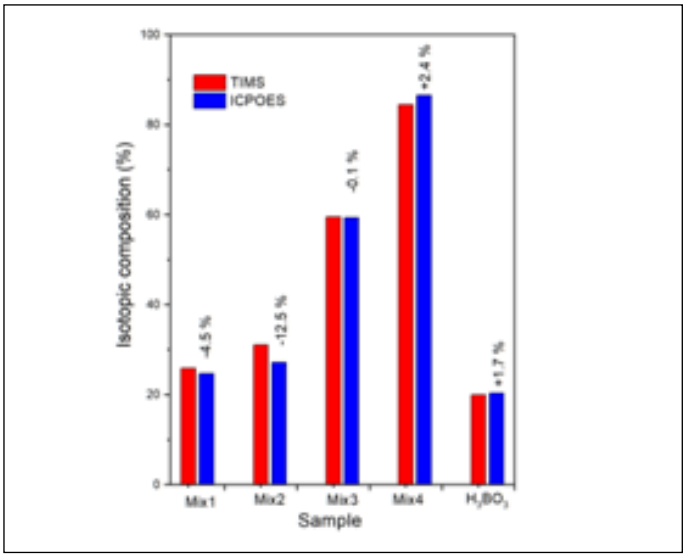

Fig. 3 Comparison of isotopic compositions obtained from ICP-OES and TIMS values given in % indicate the deviation from TIMS value

^{10}B enrichment percentage for both 208.96 and 345.13 nm. An excellent linearity with $R^2 > 0.999$ was obtained for both boron lines with the 345.13 nm line proving more sensitive and thus was selected for isotopic analysis.

Unknown isotopic concentrations (Mix1 to Mix4 and Nat. H_3BO_3) were analyzed under the same experimental conditions as calibration standards. Their isotopic compositions were calculated using the regression from the first derivative calibration curve at 345.13 nm. A paired t-test was performed to evaluate the statistical significance between ICP-OES and Thermal Ionization Mass Spectrometry (TIMS) results across five test samples at 95% confidence level, the critical t-value is found to be 2.78. The calculated t-values at 345.13 nm and 208.96 nm in the present case are 0.59 and 3.28 respectively. The t value calculated at 345.13 nm indicates no statistically significant difference between the two methods unlike t value at 208.96 nm. Fig. 3 compares the ICP-OES and TIMS results, showing agreement within 0.1 – 12.5% with no systematic bias.

V-16 Development of a compact standalone instrument for the hydrogen measurement using a proton exchange membrane sensor

A compact standalone instrument was uniquely designed and developed for the measurement of hydrogen concentration in percentage range using a proton exchange membrane sensor for the cleaning of sodium in fast reactor components.

Hydrogen is an inflammable gas in the 4-75% (V/V) concentration range in air. Hence, for the purpose of safety, it is required to be monitored such that the concentration is maintained within safe limits. Hydrogen is liberated during the cleaning of sodium from fast reactor components and is required for the precise measurement. A proton exchange membrane based hydrogen sensor was developed to measure the hydrogen liberated during sodium cleaning. The hardware and software of the

Fig. 1 Photograph of the PHS instrument for the measurement of hydrogen

instrumentation setup were designed and developed. It has various features for the analysis of the sensor response for online measurement of hydrogen generated. A sophisticated algorithm for online calibration and measurement using four points for nonlinear sensor response was developed and applied to the sensor response to measure the data precisely.

The compact hardware measures and processes the sensor response from 10 nA to 200 µA current and displays

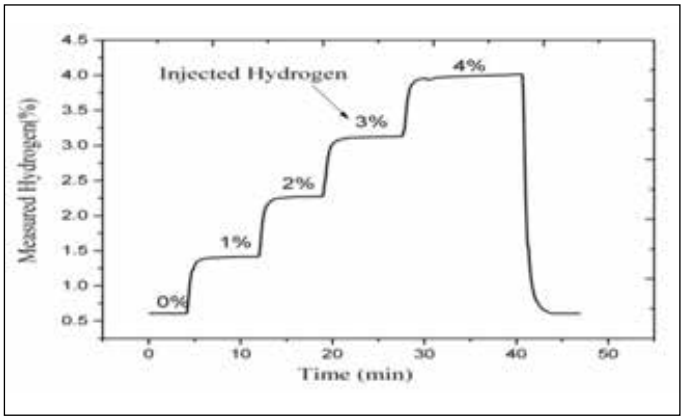

Fig. 2 The graph between measured and injected hydrogen

the data in a standalone touch panel display. The software has various unique features of different screens for the online calibration and measurement of current and hydrogen with manual and auto mode and diagnosis of the various signals and sensors with safety features. The concentration of hydrogen and current are displayed in an online graph in real time, and the corresponding data is saved into the internal memory of the instrument. The data is also sent to LAN for remote monitoring and acquisition. The instrument also provides programmable analog output from 0 to 10 V for recording the data with various other modules for the safe operation of nuclear reactors/allied facilities. The photograph of the PHS instrument for the measurement of hydrogen is shown in Fig. 1. The instrumentation setup was calibrated, tested, and validated online in the laboratory with a sensor by passing different known concentrations of hydrogen for their long-term performance, and it was found that the results were satisfactory. The graph between measured and injected hydrogen from 1-4 % hydrogen is presented in Fig. 2.

The setup was successfully deployed on-site for sodium cleaning of fast reactor components and weight of by sodium using water vapor methodology resulting in the evolution of hydrogen.

V-17 Hybrid Polymer-Supported Graphene Oxide Microspheres: Next-Generation Adsorbents for Selective Uranium and Zirconium Separation

Separation chemists have increasingly recognized graphene oxide (GO) as a promising material for solid-phase, separation-based metal ion recovery due to its large surface area and ability to incorporate diverse functional groups. The integration of functionalized GO into polymeric microspheres enhances the structural stability of the adsorbent and facilitates efficient metal ion separation, a task that would be considerably more challenging without the supportive polystyrene framework.

Polystyrene (PS)-incorporated functionalized graphene oxide (GO) microspheres was studied as a suitable adsorbent for uranium recovery from low acidic aqueous solutions. The functionalized GO prepared by incorporation of diethylenetriamine (DETA) moiety by chemical

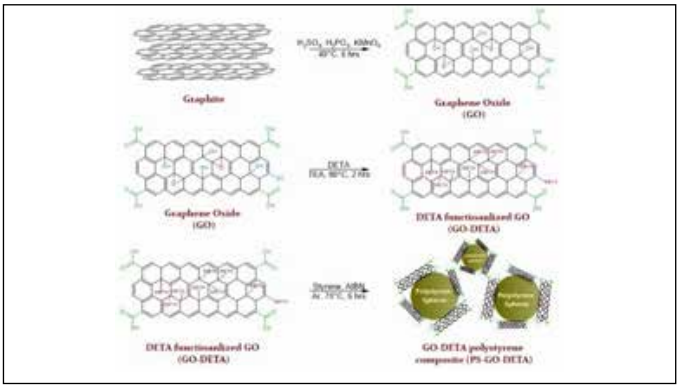

Fig1. Synthesis scheme adopted for the preparation of PS-GO-DETA microspheres.

modification of GO which was prepared by a oxidative chemical exfoliation specially designed using a modified Hummers' oxidation approach. The microspheres was finally obtained by making a composite of the above with polystyrene (PS) through an in situ polymerization, resulted PS-GO-DETA microspheres. (synthetic scheme shown in Fig. 1).PS-GO-DETA showed good extraction of U throughout the pH ranging from 2 to 7 with maximum extraction at pH 5 with the maximum uptake capacity was estimated to be 104 mg g^{-1}, and a rapid uptake within 50 minutes The extracted U can be successfully recovered

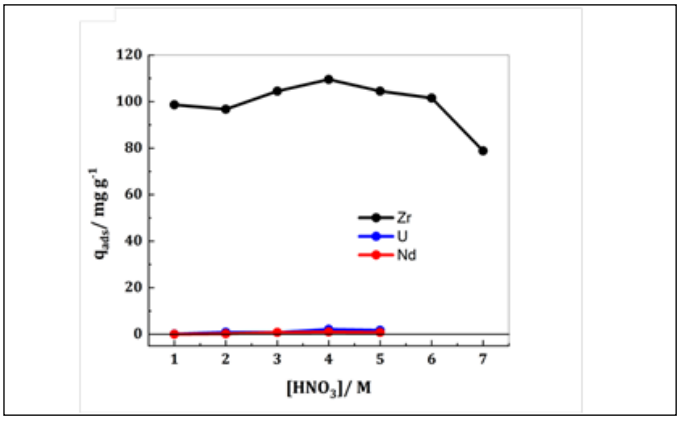

Fig. 2. Adsorption of Zr, U and Nd by PGOA.

using 2 M nitric acid that needs 2 stages of elution for complete U recovery.

For the selective removal of Zr from PUREX originated acidic aqueous waste of metallic fuel, an adsorbent based on graphene oxide (GO)-polystyrene composite functionalized with amide functional group was developed (PS- PGOA). Amide moiety was incorporated to GO by reacting with thionyl chloride followed by amination reaction, and the subsequent polymerization reaction (as discussed before).

It have shown the extraction of Zr in all the nitric acid conditions ranging from 1 M to higher acidity (~ 7 M), as seen in Fig. 2. It is also seen that the GO-amide composite exhibited a superior adsorption preference towards Zr with negligible U/Nd extraction and it can therefore be used for large-scale Zr removal from the PUREX raffinate.

With minimal interference from other metal ions, PS-GO-DETA microspheres underscores the superiority and scalability of GO-based microspheres for uranium recovery, and PS- PGOA showed superior selectivity towards Zr, which could play an important role in future fast reactors based on U-Pu-Zr fuels wherein Zr removal using the above method could reduce its interference for further processing.

V-18 Phosphonate based solvents for the extraction of U: Insights from DLS, EXFAS and DFT

Phosphonates are found to be superior to phosphates for the extraction of actinides. Phosphonates were examined for the extraction of uranium from nitric acid medium. Mixer-settler runs, aggregation behavior, EXAFS analysis and complexation behavior of uranium with DBBP, DAAP and TBP were investigated using DFT computations. Counter-current extraction of U was performed by feeding uranyl nitrate solution as the aqueous feed from first stage and 1.1 M DAAP/n-DD solution as the solvent from 16th stage in mixer-settler bank. Results indicate that the concentration of uranium in the organic phase is found to be about 85-100 g/L from stage 1 to 10 and it decreases from thereafter and it was found to be below detection limit (0.2 mg/L) in 16th stage indicating the quantitative extraction (>99.9%) of uranium was achieved with 1.1 M DAAP/n-DD in mixer-settler runs (Fig.1). Back-extraction of U(VI) from the

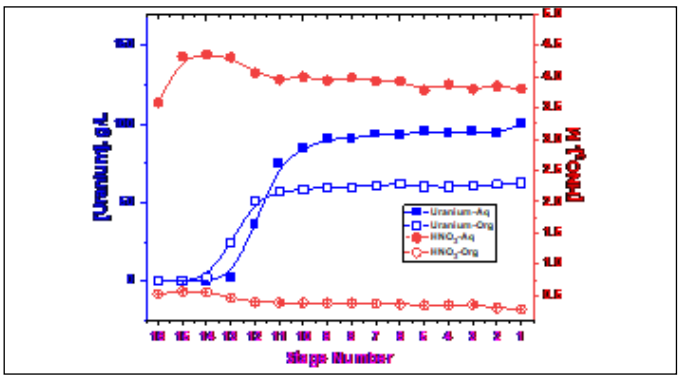

Fig. 1. Organic and aqueous stage profiles for Uranium and HNO3 in the extraction run-U(VI)-4M HNO_3-1.1M DAAP/n-DD system.

loaded organic phase was performed by passing loaded organic from 16th stage and 0.01 M HNO_3 from 1st stage in a counter-current mode.

Results demonstrate that both, i.e. HNO_3 and uranium decline towards 1st stage, and it is an indication that both are back-extracted from the loaded organic phase. Nevertheless, the concentration of U in organic phase is found to be noteworthy and it is around 13.6 g/L. This indicates that more stages (>16) required for back-extraction of uranium from loaded 1.1 M DAAP/n-DD.

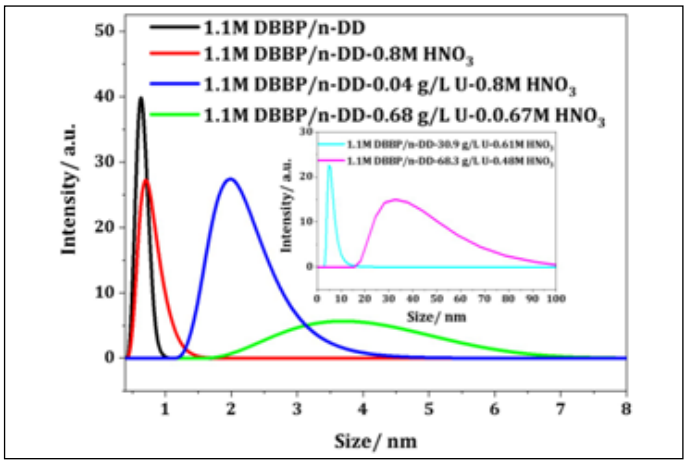

Fig. 2. Aggregation size of U-DBBP system as a function of nitric acid and uranium concentration at 298 K.

Results of the DLS studies (Fig. 2) showed that the aggregate size of the uranium-phosphate system (measured as hydrodynamic size) increased with the increase of nitric acid and uranium concentration. Overall, based on the DLS experiments, it has been understood that the phosphonates, DBBP and DAAP, exhibited a higher uranium loading capacity (>60 g/L) without the formation of a third phase. The higher uranium loading capacity of the above phosphonates, without the formation of a third phase, suggests the possibility of considering them as suitable alternate candidates to TBP.

EXAFS analysis of U loaded phosphonate based solvents indicated that U was coordinated to 8 oxygen atoms (two axial O's, four O's from nitrate groups, two O's from ligand). Computational studies reveal that phosphonates exhibit stronger interactions with uranyl nitrate compared to phosphates. EDA results indicate that the nature of interaction is nearly identical across all three ligands. This study demonstrates that the experimental solvent extraction results of uranium using DBBP and DAAP are in good agreement with the DFT-computed complexation energies. Additionally, DLS and EXAFS studies confirm the aggregation and coordination behavior of uranium complexes with DBBP and DAAP.

V-19 Revamping and requalification of the Analytical Sodium Chemistry Loop

The Analytical Sodium Chemistry Loop (ASCL) was commissioned at Materials Chemistry Division in 1987 to, a) test in-house developed online sensors for hydrogen, oxygen and carbon b) study transport and trapping of radioactive isotopes c) serve as a facility for research works in sodium chemistry like sodium corrosion of materials as function of temperature and sodium velocity. ASCL consists of two experimental sections, namely Main Loop (ML), Auxiliary Loop (AL) along with Dump Tank (DT), Expansion Tank (ET) plugging indicator (PI), cold trap (CT) and sodium sampler (SS). ML has test section and AL has meter section to test five sensors simultaneously along with a foil equilibration facility. ASCL is provided with 63 surface heaters, 144 thermocouples, 130 leak detectors and 10 each flow meters and level detectors.

Fig. 1 Photograph of upgraded Analytical sodium chemistry loop

ASCL has an inventory of 150 kwwwg of total sodium and during the operation, the experimental section, DT, ET will hold the liquid sodium quantity of 75, 25 and 50 kg respectively. The loop was operated in round the clock shifts for about 15 years and after that, it was maintained in argon atmosphere.

Accurate measurement of distribution of hydrogen in, liquid sodium and cover gas at various operating temperature is gaining more importance and is essential safe operation of sodium cooled fast reactors. In order to cater the need, it was planned to revamp, upgrade and make use of ASCL for the purpose. The pipelines and signal cables of the ASCL are about four decades old and the ASCL does not have provision for measurement of hydrogen in cover gas and in-sodium using sputter ion pump (SIP). Hence, the revamping of ASCL was planned in a five-step process. i) Requalification of existing pipelines, ii) Development of SCADA based control system, iii) replacement of signal cables and iv) Making incorporation of nickel coil assembly and nickel diffusers in cover gas and in sodium hydrogen measurements. i) ASCL pipeline re-qualification was carried out using the NDT techniques like ultrasound wall thinning, radiographic examination on weld joints, in situ. metallographic tests and in situ XRF analysis for elemental composition by on selected 10 sample points. The test were done in co-ordination with Quality and Assurance Division. The pipelines successfully passed the quality control tests. ii) A dedicated SCADA system (SCS) was developed by CFED for ASCL operation. SCS has five operation modes like ML, AL, CT PI and altogether. In all the modes, the SCADA system will measure, supervise, and control field parameters from the thermocouples, leak detectors, flow meters level detectors in the field and log the data as function of real time. The SCS measures the sodium leak and give alarms. iii) All the field signal cables were replaced and connected with SCS. iv) In the electrochemical hydrogen meter (ECHM) and electrochemical carbon meter (ECCM) sections, two numbers of nickel diffusers were weld joined by tungsten inert gas (TIG) welding and were qualified with radiographic examination. v) Similar way new expansion tank with of nickel diffuser was replaced, qualified to facilitate the hydrogen in argon measurements using in-house developed sensors. All the up-gradation works were completed and successfully inaugurated the upgraded ASCL on 17-09-2025.

Fig.2 Director, IGCAR inaugurate the ASCL-U

V-20 Installation and testing of H_2S senor in Heavy Water Plant, Manuguru

HWP in Manuguru produces D_2O, the moderator and coolant for PHWR, using H_2S-H_2O Bithermal process. Large quantities of H_2S is used in this process. However, H_2S is a toxic gas with a threshold limit value (TLV) of 10 ppm and 1000 ppm of which being the lethal dose. Multilayers made of thin film of Sb-SnO_2 and CuO integrated with suitable substrate heaters were used for sensing H_2S at 503 K in air. The sensors respond from 80 ppb to 100 ppm of H_2S and their performance is evaluated with respect to the imported sensors currently used for monitoring H_2S in HWP(M). The performance of in-house made sensors is comparable to that of the imported sensors of HWP(M) as evident from nearly close response patterns as shown in Fig. 1. Responses were also measured in resistance mode for both sensors and were compared.

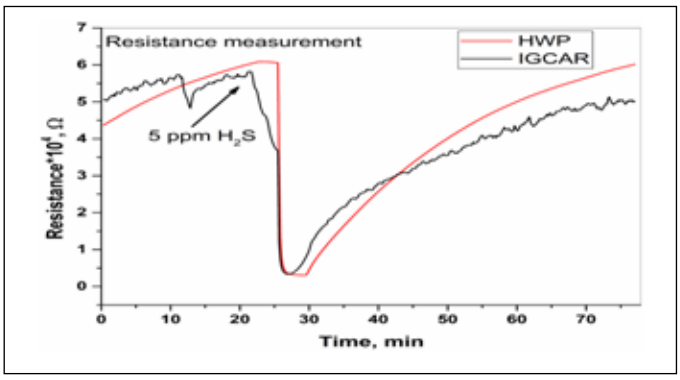

Fig.1Comparison of signals from HWP(M) and IGCAR sensors.

Fig.2 Sensor Head XU II

Two IGCAR made sensor heads were placed in the exchange unit I and II (XU I and II) of Heavy Water Plant, Manuguru (HWP(M)). The photograph of the sensor head in XUII is shown in Fig. 2.

The integrated electronics module of both the units comprising display and temperature control boards were placed in the control room and the photograph of which is shown in Fig. 3

Fig. 3 Photograph of electronics display and temperature control in the control room of HWP(M)

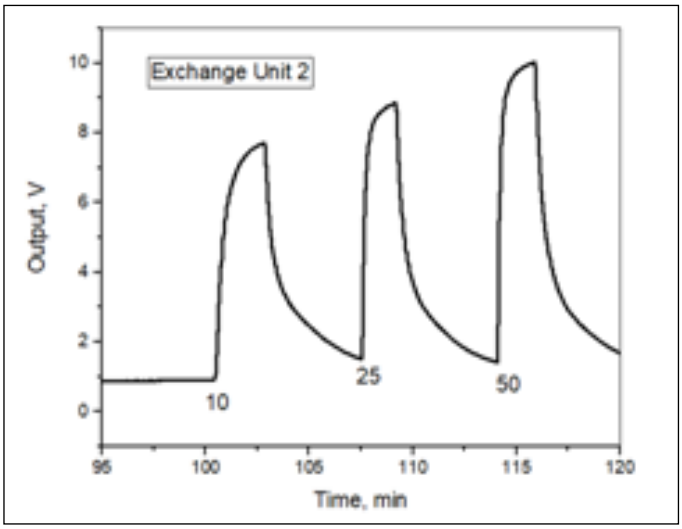

Fig.4 Typical transient of the sensor towards 10-50 ppm H2S in XU(II)

The sensors were tested for the range of 10-50 ppm of H_2S and their performances in XU(I) and XU(II) were evaluated. Fig. 4 shows the output in voltage mode recorded from IGCAR sensor located in XUII towards 10 (± 2), 25 (± 2) and 50 (± 2) ppm H_2S. The response and retrace time was around 10 sec and 10 min respectively.

The composition of the sensing material, concept of nanotechnology and the design of configuration collectively contributed to the realisation with a linear behavior in H_2S sensing performance from 1 to 50 ppm. The baseline stability of the sensor placed in XU(II) was satisfactory over a period of 7 days. Adaptations in sensor head and electronics module as per the specifications of HWP(M) is in compliance with industrial grade senor housing are being implemented for next testing.

V-21 Integration of Source Term Estimation Model using Kalman Filter Technique in Online Nuclear Emergency Response System (ONERS)

Introduction

The Source Term (ST) is a critical input for dose projections using atmospheric dispersion models during accident conditions. A Kalman Filter (KF) method is developed and integrated into the Online Nuclear Emergency Response System (ONERS) to enable real-time source term estimation using environmental radiation monitors data.

Methodology

The KF algorithm is developed using Gaussian Plume Model (GPM), based on Eqs. (1) & (2):

$$q_t = q_{t-1} + w_t \ldots (1)$$

$$q_t^+ = q_t^- + K_t[d_t - q_t^- D_t^{GPM}(q_t = 1)] \ldots (2)$$

A Python-based in-house KF algorithm is integrated into ONERS. The algorithm is executed via a shell script every 10 min to update the real-time source term. The model has been extensively validated under various flow conditions using routine releases of Ar-41 from the Madras Atomic Power Station (MAPS).

Results

The algorithm uses 10-min averaged real-time meteorological data and measurements from 28 radiation monitors (27 AGDLs and 1 Data Buoy) to estimate the source term, as shown in Fig. 1.

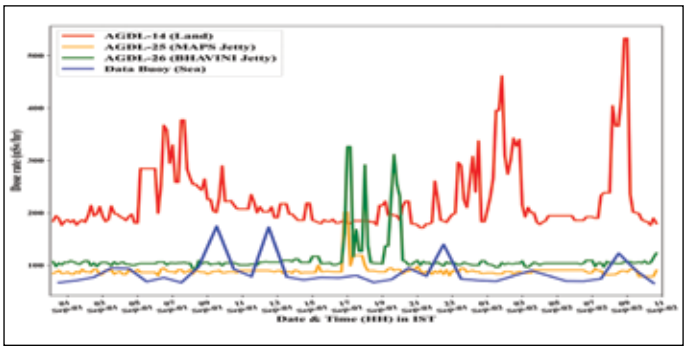

Fig. 1: Real time radiation monitors data

The time series of the estimated source term using the KF model (red line) and the existing GPM model (green line), along with the actual ST (black line) for the period 21-25 October 2024, is shown in Fig. 2.

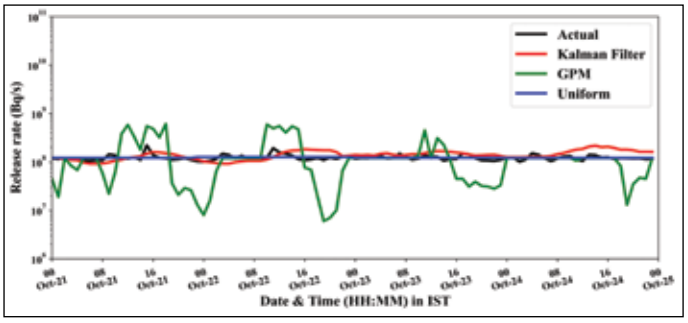

Fig. 2: Time series of actual and model estimated ST

The noise filtering method in the KF reduces fluctuations in the release rate by a factor of 3 (Fig. 2) and improves the correlation and overall agreement index by a factor of 4 (Fig. 3), compared to the existing GPM method (Table 1).

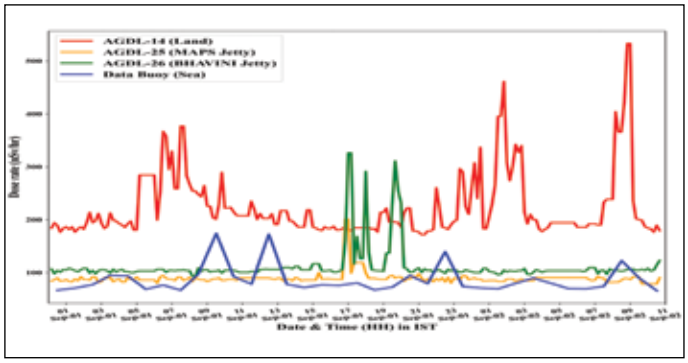

Fig. 3: Scatter plot of KF estimated and actual release rate during Nov-Dec 2024

Hypothesis testing reveals that, with a 95% confidence interval, the KF-estimated average source term is approximately 1.4 times higher than the actual value, whereas the GPM method overestimates it by a factor of 2.2.

Table 1: Statistical parameters

	KF	GPM
MBE (GBq/s)	0.05	0.07
RMSE (GBq/s)	0.12	0.31
CC	0.80	0.21
IOA	0.63	0.19

The forward model using the KF-estimated source term successfully captures the dose rate and concentration patterns observed by OIMS, achieving a correlation of approximately 0.40.

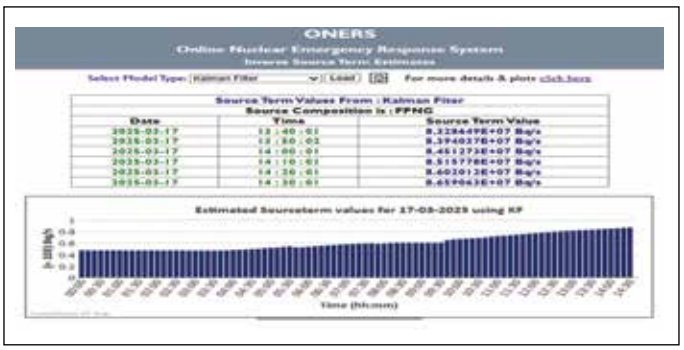

Fig. 4: Time source term page in ONERS

Conclusion

The KF-estimated release rate in ONERS (Fig. 4) provides more accurate source term estimates compared to the existing GPM inversion method and can therefore be advantageously used during accident scenarios.

V-22 Measurements of Radiocarbon Concentrations in Plant Leaves using Carbon Dioxide Absorption Method

Introduction

Radiocarbon (^{14}C) is a pure beta emitter with endpoint energy of 156 keV. The half-life of ^{14}C is 5700 ± 30 years. The ^{14}C is produced in the reactors due to neutron activation of target elements like ^{13}C, ^{14}N and ^{17}O present in the coolant, moderator, fuel and other structural materials. The ^{14}C also produced due to natural cosmogenic production, atmospheric nuclear weapon testing. The released carbon-14 from the nuclear power plants is integrated into the natural carbon cycle in the environment and then enters into the food chain. Hence, monitoring carbon-14 in the vicinity of nuclear power plants is essential to observe any increase in natural background levels. The present study focuses on the measurements of activity concentration levels of ^{14}C in the plant leave samples using the carbon dioxide absorption method.

Materials and Methods

The total carbon content in the samples was measured using the multi-N/C 2100s Model TOC/TN analyzer. Quantification of radiocarbon levels in the environmental samples are carried out using liquid scintillation counter (LSC). In this study, the carbon dioxide absorption method is used as a pre treatment technique used for quantification of ^{14}C activity levels. In the Carbon dioxide absorption method, the carbon dioxide (CO_2) is produced from the carbon present in the sample either by acidification or by combustion techniques. The Parr Oxygen bomb (USA, 1121) was used in this study for combustion of plant leaf samples. The produced CO_2 was absorbed in the Carbo-Sorb E and Permaflour absorption mixture and measured in LSC for ^{14}C activity levels.

Results and Discussions

Five different plant leaf samples with total of 25 No's were collected within the IGCAR campus. The samples were dried at room temperature and grounded to homogenous powder form using mixer and grinder. The total carbon present in the leave samples were measured using TOC analyzer. The average percentage of total carbon is found to be 39.2 ± 4.0 in 25 plant leaf samples. The experimental set up for combustion and trapping of carbon dioxide is shown in the Fig. 1. The carbon dioxide released in combustion is absorbed in two bubblers containing 2 N sodium hydroxide solutions. It is observed that an average of 83% of carbon is trapped in bubbler 1 and 17% of carbon is trapped in bubbler 2. The carbonate formed is precipitated as barium carbonate using barium chloride. The barium carbonate formed is used in carbon dioxide absorption method for measurement of radiocarbon levels using liquid scintillation system. The liquid scintillation counting system was calibrated using NIST Oxalic standard. The method was validated using IAEA certified reference material and the relative bias in measured and actual values was found to be 2.1%. The variation in measured ^{14}C activity concentration levels is shown in the Fig. 2. The measured ^{14}C activity concentration levels in the plant leaf samples ranged between the 70.7 and 110.3 Bq/kg an average activity concentration of 93.9 ± 10.5 Bq/kg.

Fig. 1: Experimental set up for combustion and trapping of carbon dioxide

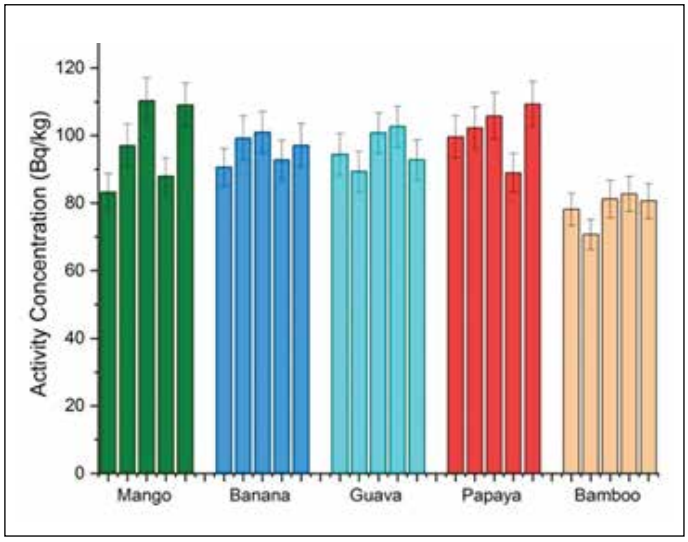

Fig. 2: Variation of specific activity levels in different plant leaf samples

V-23 Active Thermography Approaches for Detecting De-laminations of Steel Plates in Concrete Beams

Infrared Thermography (IRT) is one of the advanced NDE methods, used to inspect large areas in a short period and in a non-contact manner. While predictive condition management using IRT is based on passive thermography, defect characterization utilizes active thermography. Pulsed Thermography (PT) and Step Heating Thermography (SHT) are most widely used active thermography techniques. PT utilizes a short and high-energy optical pulse to heat the surface of the object whereas SHT utilizes a continuous and low-energy light beam. Underlying surface and sub-surface defects alter the rate of heat diffusion, resulting in change in surface temperature, which can be detected using an IR camera. In nuclear facilities, it is proposed to strengthen the deficient reinforced concrete beams with external plate epoxy-bonded retrofitting and post-installed anchors to withstand different levels of vibratory ground motion and other effects arising from earthquakes. The most common problem associated with an externally bonded plate is premature failure due to de-lamination. There is a need for inspection of these concrete structures after the completion of reinforcement procedure and during the service to evaluate their quality and integrity. In this study, the feasibility of using PT and SHT for detecting de-laminations of Stainless Steel (SS) plates in externally retrofitted concrete beams is reported.

For the present study, two concrete beams, each with dimensions of 425 mm x 120 mm x 120 mm, are externally strengthened with SS plates of thicknesses 1.6 mm and 3 mm. After the epoxy bonding, the concrete beams are subjected to tensile deformation to induce cracks, resulting in the development of de-lamination between the SS plate and the concrete surface. PT and SHT inspections are performed on the SS side of the sample. The surface temperature of the samples during the experiment was recorded using an IR camera with a pixel resolution of 640 x 480 and thermal resolution of 30 mK. For PT, two flash lamps of energy 3 kJ each and for SHT, two Halogen lamps of power 1000 W each are used.

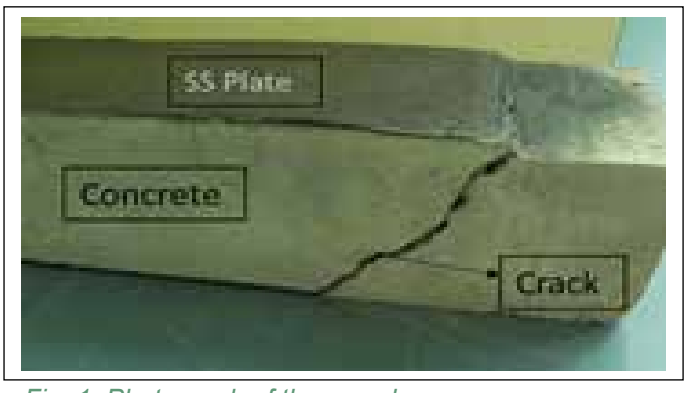

Fig. 1: Photograph of the sample

The photographs of the sample and schematic diagram of the experimental setup are shown in Figs. 1 and 2, respectively.

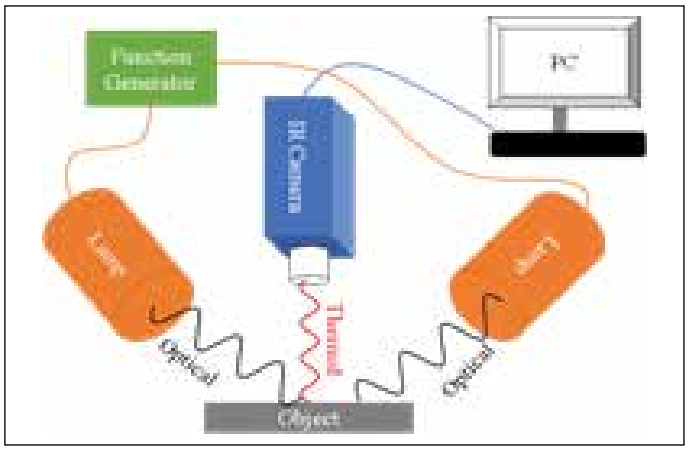

Fig. 2: Schematic diagram of the experimental setup

Fig. 3 shows the thermal images of the concrete sample bonded with 1.6 mm thick SS plate following both pulse and step heating. The images clearly show the de-lamination as a hot spot. The thermal contrast – defined as the temperature difference between the defect-free region and the de-laminated region – was calculated for both methods and is tabulated in Table 1. It can be observed that SHT gives higher thermal contrast when compared to PT technique.

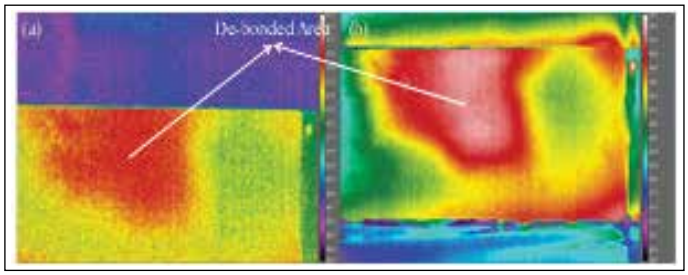

Fig. 3: Thermal images obtained using (a) PT and (b) SHT

Table 1: Comparison of thermal contrast

Technique	Thermal Contrast (K)	
	1.6 mm	3.0 mm
PT	0.83	0.34
SHT	4.25	2.02

The study demonstrates the ability of PT and SHT techniques for detecting de-laminations of SS plates in externally retrofitted concrete beams. The SHT technique offers superior thermal contrast making it well suited for field inspections.

V-24 Establishment of Neutron Reference Fields for Calibration of Neutron-Measuring Instruments

A semi-automated neutron calibration system is being established for the calibration of neutron measuring instruments used in research, reactors, radiation protection, and safety applications, by the Radiological Applications & Technology Division (RATD). As a prerequisite, it is essential to establish standardized neutron reference field. RSSD–BARC, the Designated Institute for Ionising Radiation Metrology, carried out the onsite calibration of a ^{241}Am-Be neutron source using their calibrated transfer standard. The source has a nominal strength of 185 kBq (5 Ci) and dimensions of 30 mm in diameter and 60 mm in height.

The standardization work was performed in the neutron calibration laboratory, with internal dimensions of 8 m (L) × 8 m (W) × 5 m (H). The transfer standard which used for standardization consists of a BF_3 proportional counter (LND-24120) positioned at the centre of a moderator assembly comprising two concentric cylinders of High-Density Polyethylene (HDPE). A 1-cm thick cylindrical borated-rubber thermal neutron shield separated these two moderator layers. This portable transfer standard is traceable to the $MnSO_4$ bath, primary standard for neutron emission rate measurement. Its effective centre is located at r_0 = 6.71 ± 1.03 cm, and it has an intrinsic detection efficiency of ε = 3.24 ± 0.07 counts per n·cm².

The source was placed at the centre of the laboratory to minimize room-scatter contribution. The transfer standard was mounted on the calibration bench with the centre of the detector front face positioned at a height of 117.5 cm from the floor. A laser mounted on a tripod at the same height was used for precise alignment of the source and transfer standard. Fig. 1 illustrates the experimental setup used for standardizing the neutron source.

The measured count-rate data were plotted (count rate vs. distance) as shown in Fig. 2 and fitted to obtain the

Fig. 1: Experimental setup for the standardization of Neutron source

response factor (K_i) and scattered neutron component (S_i). Using these fitted parameters, the neutron emission rate was evaluated.

The scattering contribution was estimated using the reduced-fitting method, in accordance with ISO 8529-2 (2000), wherein both the geometric correction factor and air-attenuation factor were taken as unity. The final emission

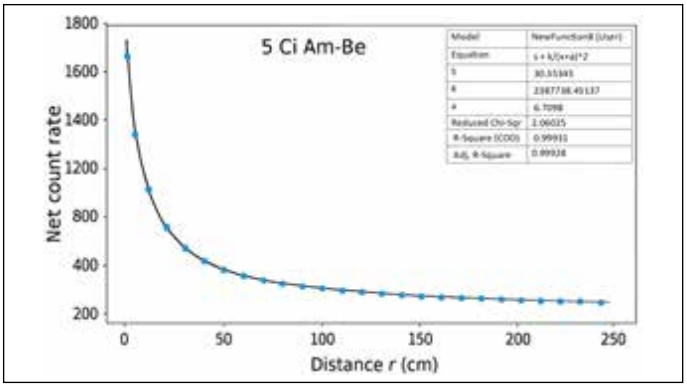

Fig. 2: Variation of net count rate as a function of distance (r)

rate, observed with a coverage factor k = 2, was 8.85 × 10^6 n/s ± 4.76%. This standardized emission rate serve as the reference neutron field valuefor establishing the neutron calibration facility.

Chapter - VI

Infrastructure and Resource Management

VI-01

Condition Monitoring & Structural Assessment towards Ageing Management of REL Building

Reactor Engineering Laboratory (REL) was constructed in the early 1970 and it houses office rooms and AHU rooms at ground floor and first floor. The structure was designed 55 years ago with prevailing design codes. As seepage of water through the roof slab and wall was observed during the monsoon season, based on user request visual inspection of the building was undertaken. Main observations were, concrete spallation in the roof slab and exterior column, damage of waterproofing on the inaccessible terrace. From the structural drawings,it was clear that there were no plinth beams and external masonry wall at ground floor level was found to be constructed on random rubble masonry and the inner partition walls were resting on PCC grade slab; so REL is combination of load bearing masonry and RCC frame.

Fig.1 Overview of REL Building

Fig.2 Distressed areas on the structural members

In view of this, a decision was taken to undertake ageing management exercise as per BSC safety manual consisting of condition survey, seismic revaluation and requalification of civil structure, which was not meeting codal requirement.

A comprehensive condition assessment plan was developed, encompassing relevant non-destructive, semi-destructive, electrochemical and chemical tests. Main distress in the building was assessed to be due to damaged waterproofing in addition to the cracks from long

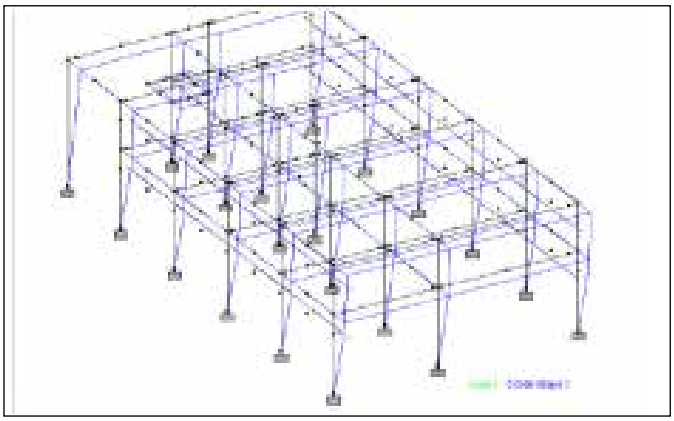

Fig.3 First mode of vibration -Frequency 1.05 Hz

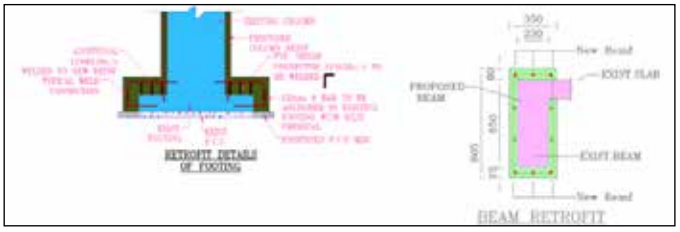

Fig.4 Retrofit scheme for footing & beam

term deflection of the slabs, Other than that the concrete quality was good and the structure was in good condition.

Further a detailed analysis including seismic loads and capacity assessment was done as per IS 456-2000 considering realistic loads and in situ strength as evaluated from semi destructive core test. Columns and beams were found to be apparently failing in seismic load combination whereas slab was not meeting the serviceability condition.

Hence it was decided to undertake local retrofitting measures and strengthen footings, columns and beams through concrete jacketing as per IS 15988-2013 and slab by providing additional support using FRP pultruded beams.

After deciding upon the retrofitting scheme a re-analysis was performed with strengthened sections. The extended life of structure is assumed to be 25 years in the analysis. Water proofing also will be replaced using biaxial polymer reinforced APP membranes and anti-carbonation coating is recommended for all RCC elements.

In accordance with the safety manual, the estimate of the complete repair and retrofit was confirmed to be economically viable.

VI-02

From Concept to Care: Sustainable, Efficient & Human-Centered Architectural Strategies of 100-Bedded Healthcare Facility

DAE Hospital at Anupuram demonstrates a holistic design approach that integrates sustainability, operational efficiency, and human-centered principles. The architecture of the hospital building establishes a balance between built and natural environments through climate-responsive planning, façade design, ensuring long-term performance and user well-being.

Sustainable External Envelope & Double-Skin Façade:

A key innovation in this project is the adoption of a double-skin façade system, developed to minimize heat gain, and enhance energy efficiency .High-performance solar-control glass, external shading devices, and controlled openings enable glare-free natural lighting in patient rooms, OPDs, and workspaces. Combined with landscape-driven microclimate enhancement,

Fig.1 Double skin face design plan and cross section

the façade strategy significantly improves environmental quality as mentioned in Fig.1. Internally, the hospital planning follows a Tri-Integrated Framework comprising operational safety, cognitive ergonomics, and environmental control, ensuring smooth circulation, infection-controlled zoning, and user well-being. The modular planning methodology and flexible structural grid allow future expansion without disruption to ongoing healthcare services. In complex areas such as Operation Theatres, architectural interventions including ceiling-mounted equipment booms, aseptic zone differentiation, and acoustic finishes act as proactive engineering controls that reduce clutter, minimize noise propagation, lower infection risks, and decrease cognitive load on surgical teams. Sun path analysis is carried out to achieve goals like passive solar heating, natural daylighting, and energy efficiency, indicated in Fig. 2 Sustainable resource management strategies such as rainwater harvesting, wastewater recycling, low-flow fixtures, LED lighting systems, and automated building control are undertaken to reinforce operational efficiency and long-term performance.

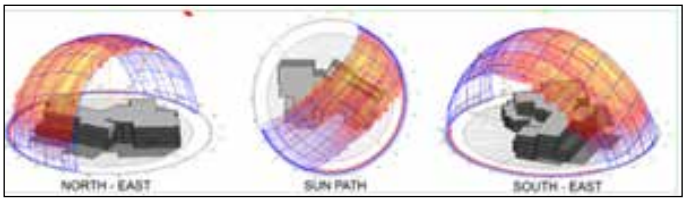

Fig.2 Sun path analysis model of the hospital building

Key Highlights

Double-skin façade reduces heat load by ~30% and lowers HVAC energy demand

- Daylight optimization improves visual comfort and reduces dependency on artificial lighting
- Rainwater harvesting, recycling systems, and low-flow fixtures support resource conservation
- Landscape integration improves thermal comfort and creates healing outdoor spaces
- Patient-centered design enhances recovery outcomes and staff wellbeing

Project Achievements

Energy-efficient and climate-responsive hospital facility

- Improved operational efficiency and safety in clinical environments
- Strong balance between nature, technology, and human experience
- Future-ready model aligning sustainability with healthcare excellence

Overall, the project exemplifies how Architecture of a health care facility can achieve a harmonious balance between natural environment integration and advanced medical functionality, establishing a future-ready benchmark in institutional healthcare design.

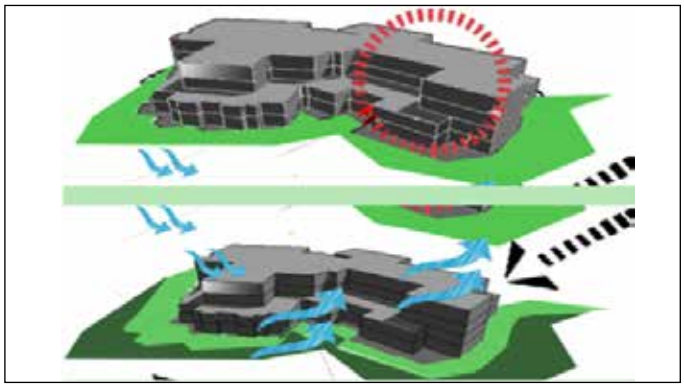

Fig.3 Hospital Model

VI-03

Construction & Commissioning of Nisargruna Biogas Plant at IGCAR: Creation of Wealth from Waste

The Nisargruna Biogas Plant established at IGCAR represents a significant step toward sustainable waste management and renewable energy generation within the campus. This plant efficiently converts kitchen waste generated from various canteens located on the IGCAR premises into clean biogas and nutrient-rich slurry/manure. Based on BARC- Nisarguna Technology for a biogas plant is 500 kg per day, layout development, civil & structural design and construction are undertaken at IGCAR. The plant is commissioned in June 2025 and has been running smoothly since then. The biogas produced is utilized as a clean energy source for the central canteen of IGCAR, reducing dependence on LPG and lowering the overall carbon footprint of the campus. In addition to energy production, the plant generates high-quality organic manure, which is effectively used for horticultural activities across IGCAR.

Fig.1 View of Bio gas Plant during construction

Fig.2 View of Bio gas Plant

This not only reduces need for chemical fertilizers but also supports the Centre's commitment to promoting eco-friendly landscaping and soil enrichment practices.

Primary components of the plant are Waste Processing Room, Pre Digester, Main Digester, Gas Storage Balloons, Blower Room and Waste collection Pit. Waste Processing Room consist of food-processing platform cum mixer grinding air compressor and water heater. Collected food waste, is shredded, and mixed

Fig.3 Commissioning of Bio gas Plant

with hot water to create slurry, which is sent to pre digester. Size of the building is 3 x 4 x 3.30 m and it is a RCC framed structure covered with Zincalume roofing. The capacity of the food waste shredder machine is 850 kg/hour. Pre Digester is a closed concrete chamber equipped with air diffuser to provide oxygen to aerobic bacteria. Here the proteins & low molecule weight Carbohydrates present in the food waste is digested to produce volatile fatty acids (organic acid) by aerobic bacteria. Size of chamber is 2.10 m dia & 2.80 m depth. The capacity of the diffuser is 6.8 CFM with 180-litre cylinder. Main Digester is a RCC circular tank partially below and partially above ground with prefabricated dome above. The dome is made of 5 mm thick MS sheet & coated with Epoxy paint. The size of RCC tank is 4 m dia & 3 m depth. Here the organic acid is converted into Bio- Gas by using anaerobic bacteria. Undigested slurry is sent to waste collections pit/drying bed. The methane-rich biogas rises and is captured at the top of the digester and it is stored in balloon of sizes 4.5 x3 x 2 m and made up of 1100 GSM PVC coated polyester yarn material, called Gas Storage Balloon. This balloon is kept in the airtight room of sizes 5.7 X 3.7 X 2.2 m with all safety provisions. Capacity of the balloon is 27 cum.

A separate blower room is made to supply stored gas with required pressure to Gas burner kept in the Central Canteen. The capacity of the blower is 29 cum / hour @ 1354 RPM. Waste collection Pit is a RCC rectangular open tank with filter media. After the digestion process, excess water and indigested slurry is separated into final effluent and manure using the filter media. The size of pit is 3.6 x 3.2 x 2.0 m.

CEG's commitment towards achieving bio-degradable zero solid waste managed IGCAR campus is being realized by constructing & commissioning of Nisarguna technology based biogas plant converting vegetable and food waste to wealth by generating renewable energy.

VI-04

Establishment of 33 kV Ring main and North node at North plant site, IGCAR

As part of the electrical infrastructure expansion at the North Plant Site, a 33 kV Switching station (33 kV Northern node) has been established to enhance power reliability for the entire campus and support future load growth. The substation is designed to receive power from two switching stations, 33 kV Central Switching Station (CSS) and NCSS-2 (33 kV Southern node) located near the Desalination Plant, and is fully integrated into the 33 kV Ring Main System (RMS). The installation includes a complete set of 33 kV indoor HT switchgear panels, one 12.5 MVA 33/11 kV power transformer with provision for installing two additional 12.5 MVA transformers, and a dedicated OFC-based communication network linking all nodes of the ring for SCADA connectivity for real-time monitoring and controlling.

The 33 kV RMS comprises three major cable connectivity: 4.5 km

Fig. 1: 33kV Cable and OFC cable on Service corridor near UGC

Fig. 2: 33 kV HT switchgear panels at the Northern Node

of 33 kV cable between Southern and the Northern Nodes, 3.65 km between CSS and the Northern Node, and 2.0 km between CSS and Southern Node. To maximise reliability and ensure long-term maintainability, the majority of the 33 kV cable system has been installed in RCC built-in trenches or mounted on a dedicated over-ground service corridor, as illustrated in

Fig. 3: 33 kV transformer and associated HT panel connections at the Northern Node.

Fig. 4: 33kV Northern Node at the North Plant Site

Figures 1. This approach minimises interference from future civil works or underground services and ensures the uninterrupted performance of the ring system.

A complete set of 33 kV indoor switchgear has been installed at the Northern Node forming the primary switching and protection interface for the RMS. The switchboard comprises incomers from CSS and Southern Node, transformer feeders, bus-coupler panels, and outgoing feeders. Each panel is fully compartmentalised for breaker, busbar, cable termination, and protection/control equipment, ensuring operational safety, reliability, and compliance with IS/IEC 62271-200. All necessary electrical and mechanical interlocks, SCADA-ready relays, and control wiring have been incorporated for safe and reliable operation.

A 12.5 MVA, 33/11 kV power transformer has been installed as part of the first phase of development. The transformer feeder is fully integrated with the HT panels and SCADA system, enabling real-time monitoring and protection.

Conclusion: With the establishment of 33kV Northern Node and RMS the reliability, capacity and flexibility of the IGCAR power distribution system is improved. This will help in introducing radial feeders without compromising the reliability.

VI-05

Retrofit of UF Skid for Reuse of Desalination Membranes in Tertiary Water Treatment

The process of the Tertiary Treatment Plant (TTP) is to convert treated sewage water into industrial-grade potable water through tertiary treatment. The core process involved is Reverse Osmosis (RO). IGCAR's Sewage Treatment Plant (STP) had a surplus of about 700 m^3 of treated sewage water per day after meeting all gardening requirements. To meet the fresh water demand of 300–400 m^3/day for the make-up of the condenser water system of the Central Water Chilling Plant (CWCP), the TTP was commissioned in 2023 with the objective of treating the excess STP water and making it suitable for industrial use.

The TTP incorporates state-of-the-art technologies, comprising an Ultrafiltration (UF) system followed by an RO system. The plant consists of two independent streams, each capable of

Fig1: TTP with Original UF Membranes in Skid-2

producing 10 m^3/h, providing a total capacity of 400 m^3/day. The plant was established as a green initiative to reduce fresh water consumption from the IGCAR reservoir.

The 2 MIGD Seawater Reverse Osmosis Desalination Plant at IGCAR has been in continuous operation since 2015, catering to the potable water requirements of all DAE installations. The desalination plant also employs the Reverse Osmosis (RO) process, supported by a similar Ultrafiltration (UF) system as part of its pre-treatment. Due to aging and the gradual reduction in flow rate performance of the UF pre-treatment system, the desalination plant discarded and replaced 58 UF membranes after completing nine years of service life.

Although these discarded UF membranes were no longer suitable for seawater desalination applications and had no scrap value or viable recycling technologies, it was observed that the permeate quality still met the RO feed water requirements of the TTP. Based on this observation, the desalination plant team

Fig.2: Discarded UF Membranes of Desalination Plant

Fig.3: Reused Membranes in Service at UF Skid-2

conceived the idea of utilizing these discarded UF membranes in the Ultrafiltration skid of the TTP, against replacement of detoriated 4 nos. of membranes in UF Skid – 2 at TTP.

With the suitable flow rate balancing for sewage water application, eight discarded UF membranes from the desalination plant were successfully reused in the existing TTP. The necessary modifications to the headers, pipelines, and supporting structures were carried out in UF skid-2 to facilitate this integration.

The modified Skid-2 equipped with discarded UF membranes is performing on par with the skid fitted with new membranes. Following the successful integration of eight UF membranes, another set of 50 discarded membranes are being preserved for future use. This initiative has eliminated the need for new UF membrane procurement for the TTP, resulting in a cost saving of approximately ₹7 lakh per replacement. Furthermore, as Polyethersulfone (PES) membranes are non-biodegradable and no recycling technology is presently available, the effective reuse of these discarded membranes also contributes to environmental protection by preventing polymer contamination.

VI-06 Mobile based Employee Authentication System

In-house developed Handheld RFID readers were being used by CISF personnel to authenticate the credentials of employees coming by their own vehicles (two wheeler / four wheeler) to gain entry into the DAE Kalpakkam complex at Main gate. It was decided to replace with highly rigid mobile(android) based RFID readers for the ease of use by CISF personnel.

To achieve the objectives, mobile app has been developed to read the credentials of Identity cards of the employee and present the information read in a desired format along with the photograph of employee in the mobile display. Mobile app uses NFC(Near Field Communication) protocol facility to communicate with the mifare card.

The MIFARE card follows the ISO/IEC 14443 Type-A 13.56 MHz contactless smart card standard. The mobile application makes the mobile acts as an RFID reader. It reads the details stored in the ID card using the mobile's NFC features, i.e., NDEF(NFC Data Exchange Format) communication protocol. The mobile app along with the sqlite database is developed to store employee credentials acquired from employee Identity card in the mobile locally. Only DAE programmed cards will be read and information will be displayed. The employee transactions are stored locally and then transferred wirelessly using Bluetooth via Raspberry pi Gateway to server.

Asymmetric encryption, also known as public-key cryptography, is a cryptographic method that uses a pair of keys—a public key and a private key—to encrypt and decrypt data. The public key stored in the mobile is used for encrypting the transaction data, while the private key stored securely at the server is used for decrypting the transaction data. This allows secure communication where only the intended recipient can decrypt the transaction, even if the encrypted data is intercepted.

Security features implemented in the mobile app are listed below-

- Mobile application is designed to work in kiosk mode.
- Mobile application takes the device to admin privilege to take control of whole device.
- Blocking wifi / Bluetooth / volume control / SIM enable/ disable / SMS facility
- Blocking Camera / Mic.

Fig. 1: Mobile based Employee Authentication System

- Blocking outgoing calls / Airplane mode / Factory Reset / Add user
- Blocking File transfer from mobile to other devices.
- Blocking Mount physical media.

The intermediate Gateway is designed using Raspberry Pi 4 Computer Model B with 4GB LPDDR4 RAM. It facilitates communication between the remotely located server and a Bluetooth-based system. The transaction and health data generated by mobile based RFID readers reach up to gateway wirelessly using Bluetooth, and from gateway to the remote server via Ethernet LAN. A web-based application was developed and hosted from the server to monitor the Mobile based RFID readers from any client on successful login within the intranet using a web browser. It supports Bluetooth version 5.0 and Gigabit Ethernet.

The Mobile based Authentication Systems(MAS) are deployed in DAE Main gate, Kalpakkam and Kokilamedu Gate for authenticating the employees, trainees and contract employees of various units of DAE Kalpakkam complex commuting either by Bus or by their own vehicle. MAS deployed at IGCAR Gate and IGCAR material gate is used for monitoring the movement of the employees, trainees and contract employees through these facility gates.

VI-07

DAE Hospital Kalpakkam – Online Hospital Appointment System

Introduction

DAE Hospital Kalpakkam managed by General Services Organization (GSO) provides healthcare services to serving and retired employees and their dependent family members of DAE Units located at Kalpakkam, viz., Indira Gandhi Centre for Atomic Research (IGCAR), General Services Organization (GSO), Bhabha Atomic Research Centre Facilities (BARCF), Madras Atomic Power Station (MAPS), Bharatiya Nabhikiya Vidyut Nigam (BHAVINI), Directorate of Purchase & Stores (DPS), Central Industrial Security Force (CISF) and Atomic Energy Central Schools (AECS). Presently the hospital provides medical services at four locations, i.e., Kalpakkam, Anupuram, Institute of Mathematical Sciences (IMSc) campus and DAE nodal centre Pallavaram campus serving more than 26000 beneficiaries. The hospital is covered under Contributory Health Services Scheme (CHSS) of DAE since 1993.

Need of the System

At present the appointment of specialist doctors at these locations are provided manually. This system poses challenges like long queues at the registration counters, long waiting time to secure appointment and inconvenience of unnecessary travel simply to book an appointment by the beneficiaries. To address these challenges and provide seamless access to the medical facilities, it was decided to initiate providing online services to the beneficiaries. As an initial step online appointment system was planned to be rolled out. The goal was to develop in-house a user friendly, robust and transparent system of booking appointments for all the locations.

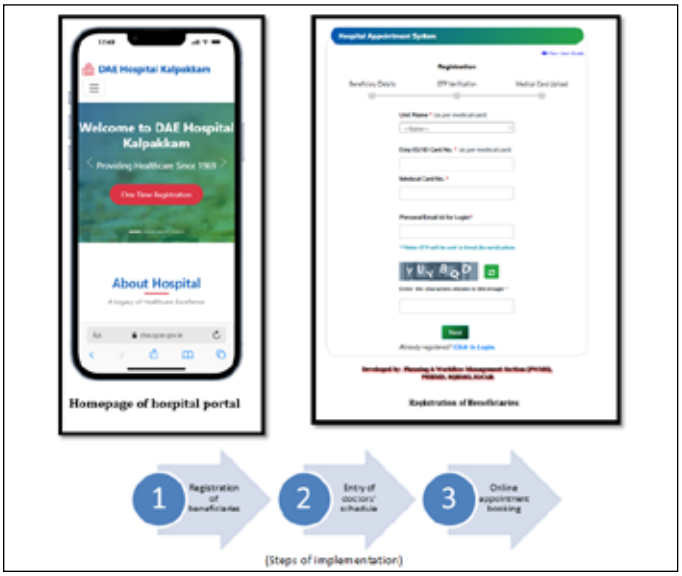

About Hospital Appointment System

Development of online services for DAE Hospital Kalpakkam was split into three parts.

The first part contains development of portal for the hospital showcasing services offered by the hospital and details of specialists, links to the online services and emergency contact numbers.

The second part of the development was to provide registration facility to the beneficiaries. The online registration includes filling of registration form, verification of email id using one time password, and approval of registration application by the DAE Hospital office. Online registration process facilitated seamless registration of the beneficiaries at their convenience without visiting the hospital. The registration process links the employee and all dependent family members with the email id provided during the registration process. After successful registration, the registered email id is used for login to the online services. About 2000 primary beneficiaries have already registered on the portal.

The third part of the development was to provide online appointment services to the registered beneficiaries. To provide online appointments following steps were followed.

(a) Maintenance of specialists master data
(b) Entry of doctors schedule
(c) Booking of appointments

All the three provisions have been made available in the online system. Master data of specialist doctors and daily schedule entry is done by the Hospital office which enables the beneficiaries to book appointments online.

The system has been developed in-house using open source technologies like Apache, MariaDB, PHP and JQuery. It can be accessed using any latest browser from PC, laptop and smart phone.

Benefits to the Stakeholders

The system provides following benefits to the beneficiaries and management.

- 24 / 7 accessibility
- Booking at convenience from home or office without visiting hospital
- Information about availability of specialist doctors
- No waiting in the queue
- Better planning and resource optimization
- Increased user satisfaction

VI-08

Towards a Safer Workplace: Industrial, Fire, and First Aid Initiatives at IGCAR

The Industrial & Fire Safety Section (IFSS) has supported management in fulfilling its statutory obligations and ensuring the prevention of personal injuries by maintaining a safe work environment. This has been achieved through detailed Job Hazard Analysis for critical activities, aiming for a zero-harm workplace. Additionally, IFSS has conducted regular industrial and fire safety inspections, along with physical hazard surveillance, at all R&D labs and construction sites of IGCAR, ensuring the quality and proper use of personal protective equipment provided to workers.

The Industrial & Fire Safety Section (IFSS) has been issuing various Industrial Safety Work Permits through the online platform Atoms 2.0. In 2025, a total of 379 permits were issued, with the category-wise distribution as follows: Hot Work Permit (236), Height Work Permit (121), Excavation Work Permit (13), and Confined Space Entry Permit (9). The implementation of the Safety Related Deficiency Reporting (SRDR) system, in conjunction with the online work permit system, has significantly enhanced the monitoring of critical activities, facilitated timely correction of deficiencies, and reduced the time required for permit issuance.

Fig. 1: Industrial safety work permits statistics

Hydraulic A Hydraulic Pressure Testing facility for portable fire extinguishers has been established at IGCAR to serve the needs of all DAE units within the Kalpakkam complex. During this period, a total of 59 portable fire extinguishers of various types were hydraulically tested in accordance with IS 2190:2024 standards, of which 7 extinguishers failed the hydraulic pressure test. Additionally, 79 Self-Contained Breathing Apparatus (SCBA) cylinders were periodically checked and refilled based on requests received from various units within the DAE Kalpakkam complex.

As per the AERB guidelines, Industrial Safety, Fire Safety and First Aid training programmes have to be conducted annually for IGCAR employees and contract workers. A two day Industrial, fire safety training and first-aid training programme was organized to enhance the awareness of safety among officers/engineers, supervisors of IGCAR during Feb-2025, March- 2025, Jul-2025 and Sep-2025. Total 253 nos. of participants were attended for this training programme.

All 829 contract workers received safety induction training before being deployed for work. Height-pass tests and training were conducted for 179 workers involved in working at heights. A one-day training programme on the authorization of crane operators and signalmen was successfully conducted on June & September 2025, with the participation of 50 personnel.

Job-specific training programs were conducted, including Safety in Operation and Maintenance of HT & LT Electrical Cables with 64 participants and Scaffolding Safety with 53 participants. In collaboration with the CISF Fire Wing, hands-on fire extinguisher training was also provided (Fig. 2), covering various types of portable extinguishers and demonstrating their use in different fire scenarios.

Fig. 2: Fire safety training by CISF fire wing

First-aid training programs were conducted with the support of doctors and paramedical staff from Apollo Hospitals, Chennai. Participants received training in CPR techniques using a mannequin and were briefed on essential life-saving procedures.

VI-09 Design, Development and Commissioning of the Registration Authority (RA) System for IGCAR CA Facility

IGCAR had obtained license to function as a Certifying Authority (CA) by CCA-INDIA to issue Class 3 Digital Signature Certificates and Encryption Certificates for DAE employees. To facilitate this process, employees have to submit certificate request applications through a Registration Authority (RA) System. In a typical Public Key Infrastructure (PKI) setup, the RA acts as an intermediary between end-users and the CA. It performs identity verification of individuals requesting digital certificates, receives and validates certificate applications together with the requisite documentation, forwards the verified requests to the CA for issuance, issues user tokens, and facilitates certificate revocation whenever required. To enable the IGCAR CA facility to issue digital certificates, an RA system was developed. It consists of two modules:

- RA portal, a web application for interaction with end-users
- RA Agent, a desktop application for interaction with USB Crypto tokens

RA Portal

The RA Portal, shown in Fig. 1, is a web-based application developed using React JS, with Express JS and MySQL as the web technologies. Access to the portal is restricted to authenticated users assigned one of the following roles: RA Administrator, CA Administrator, CA Coordinator, Site Coordinator, or Applicant. The digital certificate issuance process begins when the Applicant submits an online application. Upon successful submission, a certificate requisition form (in PDF format) is generated. The Applicant prints, signs, and forwards the physical copy of the form to the Approving Authority through the Site Coordinator for approval. Once the application is approved, the Site Coordinator issues a Crypto Token to the Applicant. Using the token, the Applicant generates a Certificate Signing Request (CSR) and submits it to the CA Administrator via the CA Coordinator through the web application. Upon receiving the CSR, the CA Administrator uses the CA facility to generate a digital signature certificate, and an encryption certificate and corresponding private keys. Finally, the Applicant downloads the issued certificates and the private key to the Crypto Token through the portal.

Fig. 1: Home page of the RA portal

IGCAR RA Agent

The IGCAR RA Agent is a cross-platform desktop application built on Electron framework and can interact with crypto tokens using the PKCS11JS library. The RA portal can communicate with the agent through a secured & encrypted web socket connection. The RA agent is responsible for executing token-related operations initiated through the RA portal like CSR generation, fetching the token serial number, changing the token pin and downloading the issued certificates and private key. A screenshot of the IGCAR RA Agent displaying the certificate stored in a crypto token is shown in Fig. 2.

The IGCAR RA agent also provides a web API that enables authorized third-party web applications to digitally sign PDF documents using the certificates issued by IGCAR CA.

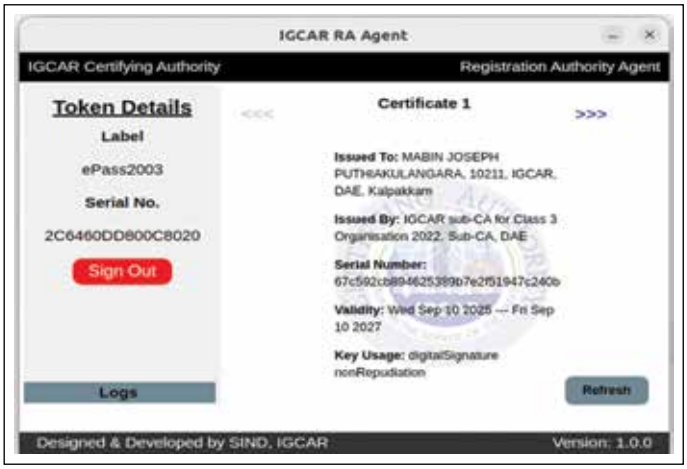

Fig. 2: Agent displaying the certificate from crypto token

VI-10

Implementation of an Open-Source Software-Defined Storage System for HPC Facility

The increasing storage demands of the HPC facility comprising of HPC clusters, high-end graphics workstations, private cloud setup, and Virtual Desktop Infrastructure (VDI) necessitated the deployment of a unified, highly available, and scalable storage system. A key motivation for this implementation was to eliminate dependence on proprietary storage solutions by adopting Ceph - a free and opensource, software-defined storage (SDS) system. SDS architecture decouples storage software from hardware, offering greater flexibility, cost-effectiveness, and eliminating vendor lock-in. This approach offers more efficiency and faster scalability by making storage resources programmable. Ceph is designed to support block, file, and object storage, making it well-suited for diverse storage scenarios.

A Ceph-based storage cluster was designed and deployed using five high-end x86 storage servers. Each server is having dual Intel Xeon Silver 4214R processors (12 cores), 128 GB DDR4 ECC memory, and 288 TB raw storage capacity. The architecture of the implemented Ceph-based Unified Storage Cluster with 10G network backbone is shown in Figure 1.The first phase of implementation involved setting up the servers by installing the required Linux operating system, and configuring network interfaces in the commodity hardware. Three dedicated networks were established: a 10G network for the Ceph storage cluster, an administrative network for server's management, and an IPMI network for out-of-band access.

A containerized Ceph storage system was then deployed to build a robust five-node unified storage cluster. Ceph software packages were installed on the Linux OS using Cephadm, which handles the cluster initialization, node addition, service orchestration and monitoring through an agentless architecture using SSH. The installation process was started on Server 1, which was designated as the bootstrap node for the Ceph storage cluster. This server initializes the cluster and later manages the orchestration of services across other servers. The deployment included the configuration of the core Ceph services: (1) ceph-mon (Monitor): Maintains critical cluster maps (OSD map, monitor map, CRUSH map) and ensures cluster quorum and health. (2) ceph-mgr (Manager): Provides real-time monitoring, performance metrics, and coordination with the Ceph Dashboard for visual management. (3) ceph-osd: Handles actual data storage, replication, rebalancing, and recovery across the cluster. (4) ceph-mds (Metadata Server): Enables the Ceph File System (CephFS) by managing directory hierarchies and file metadata. In this setup, each Ceph service runs inside a Docker container, isolating components for better reliability and ease of upgrades. Once the ceph software packages were installed, bootstrap operation was initiated which configures Server 1 as the monitor node using the 10G interface and sets the cluster network for backend replication and OSD communication to the 10G subnet. Once the bootstrap process was completed, the remaining four storage servers were added to the Ceph storage cluster. Then, OSD configuration, cluster management and monitoring was done through the Ceph Dashboard.

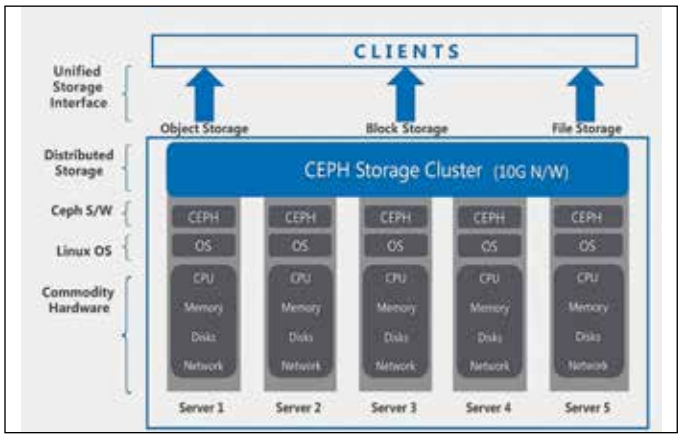

Fig. 1 Architecture of a Ceph-Based Unified Storage Cluster

The cluster was deployed using the Reef release of Ceph, which provides improved stability and better memory utilization. After the service orchestration was completed, the Ceph storage was configured at both block and file levels, offering flexibility for integration with various applications—block devices for VM or database workloads, and file storage for HPC and collaborative environments. Thus, Ceph acts as a distributed storage system built on commodity hardware.

The storage benchmark tool 'fio' was used to evaluate IOPS, bandwidth, and latency on Ceph File System (CephFS) and Ceph Block volumes across different file sizes, ranging from 1 MB to 10 GB. The tests covered four primary scenarios: (1) Sequential Read, (2) Sequential Write, (3) Random Read, and (4) Random Write. Table 1 shows the Random write performance where CephFS achieved 345K IOPS (Input-output operations per second) and 1,412 MB/s, outperforming Ceph Block and Local FS.

Table 1: Random Write Performance in Ceph Block Device, Ceph FS & Local FS

Storage Type	IOPS	Bandwidth (MB/s)	Latency (µs)
Ceph Block	137K	563	2.31
CephFS	345K	1412	2.50
Local FS	136K	558	2.21

Awards & Honours

- Akhil G. Nair, Chanchal Ghosh, Indradev Samajdar, Arup Dasgupta received the Best Poster Award for the paper titled "Exploring the influence of Cr on bond characteristics in $(Fe,Cr)_2B$: A comprehensive experimental and computational investigation" at the advanced microscopy and its applications in materials science problems (AMAMS 2025) symposium held at IIT Madras, Chennai, January 15-18, 2025.
- Mrs. M. Margret from SQRMG received the IARP Award for the Best Poster presentation at the 35th IARP National Conference held at Mangaluru during January 29-31, 2025 for the paper titled "Parametric evaluation of matrix influences on detector response across broad range of photon energies".
- Mrs. M. Sowmya from Radiological Applications and Technology Division (RATD), SQRMG, IGCAR has been awarded the second prize for technical paper presentation for the paper titled "Annual variations in air quality parameters at Kalpakkam Site (East Coast of India) in the 9th International Conference on Air Quality Management (IICAQM-2024) held at IIT Madras, Chennai during December 18-21, 2024.
- Dr. Usha Pujala from Health Physics Section, Health and Industrial Safety Division, SQRMG received the best poster award (First Prize) for the paper titled "Charged aerosol dynamics behaviour for improving the fast reactor safety assessment during severe accident: Modeling aspects" during 35th IARP National Conference, Mangalore, January 29-31, 2025.
- Shri K. Palani, B.P. Arun, G. Elaiyaraja, Vasanthi Sekar, S. Manickam, Pratik Bhardwaj, R.V. Satheeshkumar, C. Murugesan, J.W. Reuben Daniel, A. Palanivel, N. Subramanian, A.K. Karthi, M.S. Gopikrishna, M. Dhananjeyakumar, M. Mathews Geo, K. Rajan, received First Prize for Poster Presentation titled "Development, Installation and Commissioning of Modular Remote Sampling Station Title for Sampling Cell of DFRP" in the 4th Triennial DAE-BRNS National Symposium on Recent Advances in Nuclear Fuel Cycle activities (NUFUC-2025), February 6–8, Tarapur, India.
- R. Anbarasan[1], R. Ramar, Varsha Roy, Subham Dhyani, R. M Sarguna and S. Ganesamoorthy has received best poster award for the paper titled "Development of portable Direct reading dosimeter based on in-house grown CdZnTe Single Crystal" in the 27th National Seminar on Crystal Growth and Applications held at BARC, Mumbai during February 7-9, 2025.
- Amit Kumar, Shobhit Verma, Vijay Anand R, Sujatha P N, Sarangapani R, Thangamani M, John Arul A and Suresh Kumar K V from IGCAR has received the best presentation award (Third Prize) for the paper titled "A feasibility study on radioactive aerosol characterization in the cover gas region of primary sodium" during NSRP-24 National conference held at the DAE Convention Centre, BARC, Mumbai during March 27-29, 2025.
- Dr. Anees P., MMS, DDSD, MSG delivered an invited talk at the International Conference on "Electronic Structure Theory and Applications" held at IISER Pune during May 18–21, 2025.
- Shri S. Shyam Kumar bagged the STT-Hillert Scholarship for presenting a poster titled "Isopiestic Vapour Pressure Measurements and Thermodynamic Modelling of the La-Te System" by S. Shyam Kumar, Soumya Sridar, Rajesh Ganesan at the CALPHAD 2025, 52nd International Conference on Computer Coupling of Phase Diagrams and Thermochemistry, conference in Paradise Hotel, Busan, South Korea held between May 25–30, 2025.He won the Best Poster Award for presenting a poster titled "Vapour Pressure Measurements in Nd-Te System" by S. Shyam Kumar, Rajesh Ganesan at the Thermans–2024, BARC, Mumbai, held between January 16–18, 2024.
- Ms V. Athulya, SRF, CSTD/MCG/MMMG was awarded the Best Paper Award for the poster presentation in ICECORR 2025 during 20th to 22nd at Le Meridien Kochi, Kerala, India organized by ASNT India Section, AWS and AMPP Chennai Chapter.
- Ms S. Sofia, CSTD/MCG/MMMG (Amazonians Quality Circle of MMG) participated in the Quality Circle Annual Meet (QCAM 2025) organized by IGCAR Kalpakkam on 3rd September 2025 and received the Gold Certificate of Merit for the QC case study presentation.
- Dr. M. Vasudevan, AD, MDTG name appeared in the top 2% world ranking of scientists in career and year wise rankings published on 19th September 2025 by Stanford University and Elsevier publications. His name is listed in the rankings since 2020 every year.
- Shri V. Vinod, Scientific Officer-H, Head, Experimental Thermal Hydraulics Division, Fast Reactor Technology Group, IGCAR is elected as Fellow of National Academy of Engineering (F.N.A.E.) with effect from 01-11-2025 by Indian National Academy of Engineering.
- Yasotha E, Madhusmita Panda, Shailesh Joshi, Annalakshmi O, EAD/SQRMG, Presented a poster in " National Conference on Luminescence And its Applications - 2025 (NCLA- 2025) during 07th to 09th December 2025" held at SSN College and received best poster award (Third Prize).
- Dr. Gopinath, SO/E, CSTD received the IIM Kalpakkam Chapter - Best Journal Paper for the paper titled "Improvement

of intergranular corrosion resistance of SS 304L by grain refinement followed by gamma-ray irradiation treatment for the application in the back end of the nuclear fuel cycle", Materials Chemistry and Physics 313, 128750. Authors: Gopinath Shit, A. Poonguzhali, S. Ningshen.

- Dr. Chanchal Ghosh, SO/F, PMD received the IIM Kalpakkam Chapter - Best Journal Paper for the paper titled "Atom column analysis of (Fe,Cr)2B phase in high B containing ferritic steel", Materialia, 33, 102007, Chanchal Ghosh, Akhil G. Nair, Arup Dasgupta, R. Mythili, R. Divakar.
- Dr. Veerababu J, SO/E, MMD received the IIM Kalpakkam Chapter - Best Journal Paper for the paper titled "Slip to twinning to slip transition in polycrystalline BCC-Fe: Effect of grain size", Physica B: Condensed Matter, 694, 416465. Veerababu J, A. Nagesha, Vani Shankar.
- Ms. Athulya V, SRF, HBNI received the IIM Kalpakkam Chapter Best Paper Award (Young Researcher Category) for the paper titled "Electrodeposition of myristate based superhydrophobic coatings on steel with enhanced corrosion resistance and self-cleaning property", Surface and Coatings Technology 489, 131114. Authors: Athulya V, S.C. Vanithakumari, A. Ravi Shankar and S. Ningshen.
- Ms. Aishwary Vardhan Pandey, SRF, HBNI received the IIM Kalpakkam Chapter Best Paper Award (Young Researcher Category) for the paper titled "Development of a novel approach to correlate small punch fatigue with uniaxial ratcheting fatigue", International Journal of Fatigue 190 (2025) 108585, Aishwary Vardhan Pandey, K. Mariappan, V. Karthik, Vani Shankar, R. Divakar.
- Dr. C. Sudha, SO/G, PMD/MCG/MMG received the Fellow of EMSI Award for the Year 2024 in the Materials Science category at the International Conference on Electron Microscopy and XLIII Annual Meeting of Electron Microscope Society of India (EMSI-2025) held at Indian Institute of Science, Bangalore during July 12-14, 2025
- Dr. Chanchal Ghosh, SO/F, MSSCS/PMD/MMG/IGCAR was awarded the prestigious DAE Homi Bhabha Science and Technology Maanpatra for the year 2025
- S. Murugesan, R. Mythili, G. V. Prasad Reddy, V. Ganesan, R. Thirumurugesan, Arup Dasgupta won the SAIL TIIM BEST Technical paper award 2025 in Ferrous Category for the paper titled "X-ray Diffraction Analysis of Creep-deformed Nitrogen-added 316LN Stainless Steels" in Transactions of the Indian Institute of Metals 77 (2024), 3537-3546

Colloquium, Lectures & Nurturing Activities

IGC Colloquium

- "Breaking Barriers, Shattering Limiting Beliefs" by Shri. Satyarup Siddhanta, Indian Mountaineer on January 17,2025.
- "Green Energy Technologies in Combating Environmental Pollution and Climate Change & Combating Plastic Pollution" by Dr. R. Arun Prasath, Head, Department of Green Energy Technology, Pondicherry University on June 5,2025.

Special Lectures

- Total Quality Management Through Quality Circles by Shri.S.Anil, DGM, M/s. JK Tyre & Industries Ltd, Chennai Plant on January 3,2025.
- Special talk on "Health: Our First Priority in the Pursuit of Life" by Dr. G. Sivaraman, Managing Director & Chief siddha Physician, Arokya Healthcare, Chennai on April 8,2025.
- Special Lecture on "Democrasting Proton therapy for cancer treatments: How and Why?" by Dr. Sapna Nangia Radiation Specialist Oncologist, Apollo Proton Cancer Center, Chennai on May 21,2025 .
- Special Lecture on "Civil Engineering Aspects in NPPs- Experience Sharing" by Shri Y.T. Praveen Chandra AD, Civil, NPCIL, Mumbai on August 8,2025.
- Special Lecture on " Changing Role of Materials for Advanced Nuclear Reactors in India" by Dr.Raghvendra Tewari, Distinguished Scientist & Director, Materials Group Head, Materials Science Division, Bhaba Atomic Research Centre, Mumbai on October 6,2025.
- Special Lecture on Sexual Harassment - A Brief Understanding & Discussion by Dr. Kitheri Joseph, Regional Director, MRPU, Chennai on December 04,2025.
- Special Lecture on "Aspects of Weather Forecasting" by Dr. B. Amudha, Director, Regional Meteorological Centre, Chennai and "Know Your Risk – Cancer Awareness" by Dr.S.Rajeswari MBBS, DNB (OG) Preventive Oncologist, Iswarya Hospital, Chennai on December16,2025.

Seminars, Workshops and Meetings

- All India Hindi Scientific Seminar, January 10-11, 2025
- Workshop on "Electromagnetic Nondestructive Evaluation", March 4-6, 2025
- Author workshop by M/s Wiley and M/s Springer May 16, 2025
- Theme Meeting on "Radiation Metrology and National Standards for Ionising Radiation", May 21-22, 2025

- Workshop on "Geospatial and Radar Technologies for Improved Weather Modelling and Effective Disaster Management (GRADM 2025)", IGCAR, Kalpakkam 12-14 June, 2025
- Theme Meeting on "Role of Safety Research in Nuclear Regulation: Current Status and Future Directions", June 20-21, 2025
- Awareness Programme on “Intellectual Property Rights" July 11, 2025
- Online webinar, Author Workshop – Publishing Open Access in Wiley Journals Under the DAE Consortium's Agreement, October 23, 2025

Nurturing Activities

- Brilliant Bharath Hackathon -2025 program on February 28- March 1,2025.
- International Women's Day celebration by IGCAR and IWSA-K on March 6,2025.
- Technical Talk on New 7 QC Tools and their application in Quality Circles on April 24,2025.
- IGCAR Foundation Day celebration on April 30,2025.
- Career guidance program for neighborhood TN Government school students on May 17,2025
- Summer Training Programme in Physics and Chemistry (STIPAC -2025) on June 2-July 9,2025.
- Rashtriya Karmayogi Large Scale Jan Seva Programme on July 24- September 11,2025.
- Teachers Day Celebration on September 8,2025.
- 33rd Prof. Brahm Prakash Memorial Materials Quiz on September 13,2025.
- Gyan Samvardhan Programme by Shri C.G. Karhadkar Director IGCAR& GSO Kalpakkam on December11,2025.
- As part of DAE Platinum Jubilee Celebration school students have visited IGCAR. About 1167 students and 62 faculties from 28 different schools have visited during 2025.

Administrative Seminars / Workshop / Events

- Swachhata Pakhwada 2025 Skit Competition for IGCAR employees on the theme 'Plastic se Raksha' on February 25, 2025.
- Awareness program on CLRA Provisions for contractors and contract employees on March 3-4, 2025.
- International Women's Day celebration by IGCAR on March 10, 2025.
- Meeting with PFMS Team-Officials from Ministry of Finance on April 16, 2025
- Technical Talk-NPS Vs UPS on April 28, 2025.
- "Instruction to Indenting Officers" by MRPU Purchase Team on June 12,27,July10, August 21 2025.
- “Tax player Outreach/Tax Literacy Programme” by Income tax Department, Tambaram on August 28,2025.
- Hindi Month – 2025 on September 22 and October 16 – 31, 2025.
- Vigilance Awareness week on October 16 – 31, 2025.
- Awareness Programme on Unified Pension Scheme by ATI on November 20, 2025.

IGCAR Publications during the year 2025

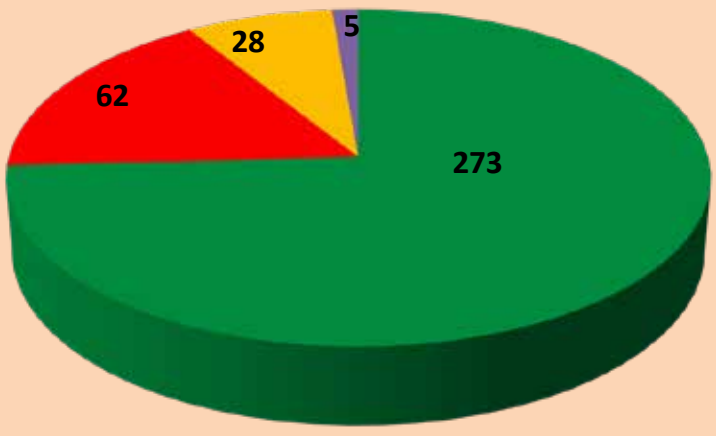

H-Index

Scopus : 134 | Web of Science : 127 | Google Scholar : 137

Anu Yatra 2025 Report

January 21, 2025

As part of the Department of Atomic Energy's (DAE) Platinum Jubilee celebrations and the PRIS(G) activities of SQRMG for 2024-25, Anu Yatra (Phase-3) was organized to highlight India's advancements in nuclear technology, aligning with the vision of Atmanirbhar Bharat. The program aimed to create awareness about nuclear science and technology, particularly among the youth in rural areas across Tamil Nadu and Karnataka.

Inauguration – Flag Off Ceremony

The 2025 edition of Anu Yatra was flagged off on 21st January from AECS, Anupuram, with an inaugural ceremony graced by Shri C. G. Karhadkar, Director, IGCAR; Dr. B. Venkatraman, Former Director, IGCAR; Shri M. Seshaiah, Station Director, MAPS; Dr. T. V. Krishna Mohan, Facility Director, BARC(F); Shri Gopal Parthasarathy, State Secretary, Tamil Nadu Ariviyal Sangam; Shri C. N. Srinivasa Ragavan, Principal, AECS, Anupuram along with other senior officials from IGCAR, MAPS, BARCF, and GSO.

Atoms on Wheels and Details of Exhibits

Shri C. G. Karhadkar, Director, IGCAR & Dr. B. Venkatraman, Former Director, IGCAR during Flag off event at AECS, Anupuram.

A special bus "Atoms on wheels" arranged for carrying the exhibits, standees, digital display and models showcasing various activities of Department of Atomic Energy to all nodal colleges along the route.

The Yatra commenced from Kalpakkam, Tamil Nadu on 20th January 2025 and covered 1,116 km, concluding at Kaiga, Karnataka, on 7th February 2025. The journey passed through key locations such as Vellore, Uthangarai, Dharmapuri, Bengaluru, Tumkuru, Hubballi, and Belagavi, with a team in each district organizing the awareness program.

Atoms on wheels

VIT, Vellore

SVMC, Uthangarai

SVMHSS, Palacode

RVC, Bangaluru

MSRC, Bangaluru

SIET, Tumakuru

PCJC, Hubbali

KLE's Tech. University, Belgavi

Glimpses at various nodal institutions

Grand Conclusion:

The culmination event on 7th February 2025 at Kaiga brought together distinguished personalities, including: Shri B. Vinod Kumar, Site Director, KGS; Shri Shriram, Station Director, KGS 1&2; Shri J. L. Singh, Project Director, KGS 5&6; Shri K. Rajan, Director, RpG, IGCAR and Shri Prasad Gokhale, Principal, AECS, Kaiga.

Culmination event at AECS, Kaiga

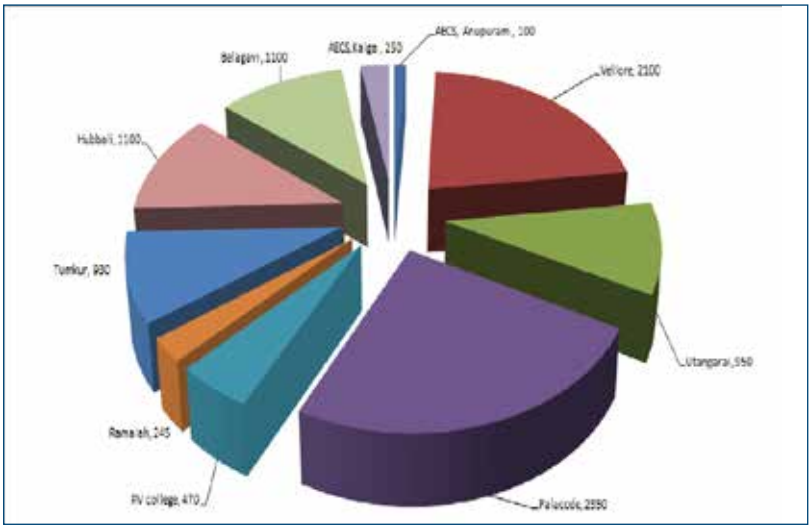

Concluding Remarks

The initiative of Anu Yatra 2025 was jointly organized by IGCAR along with Indian Association of Radiation Protection (IARP), Indian Association of Nuclear Chemists and Allied Scientists (IANCAS), and Vijnana Bharati, Tamil Nadu Chapter (Tamil Nadu Ariviyal Sangam). It covered a distance of 1,116 km from Kalpakkam to Kaiga with 08 nodal institutions across Tamil Nadu and Karnataka state. Overall, around 10,000 students and more than 500 faculty members and teachers actively engaged in Anu Yatra 2025.

One Day Theme Meeting on Embracing the Digital Age: Re-imagining Library Resources Management

January 24, 2025

Scientific Information Networking Division (SIND) of SQRMG, IGCAR has organized a one day theme meeting on "Embracing the Digital Age: Re-imagining Library Resources Management" on 24th January 2025 at Sarabhai Auditorium, IGCAR. Eminent information professionals from various DAE units, Anna University, NIAS University, IIT-M and Pondicherry University have participated the meeting.

The theme meeting started with the welcome address of Dr. Vidya Sundararajan, AD, SQRMG; Shri E. Soundararajan, Head, DRTS, briefed about the workshop and highlighted the points to be addressed. The Presidential address was given by Shri C. G. Karhadkar, Distinguished Scientist and Director, IGCAR. Director emphasized the importance of the library in the digital era. Shri J. Rajan, Head, SIND gave the vote of thanks.

Presidential address was given by Shri C. G. Karhadkar, Distinguished Scientist and Director, IGCAR

In the Technical Session-I, Prof. M. Sai Baba, NIAS, Bengaluru and Former Director, RMG, IGCAR, delivered the keynote address on Information Resources Management in the Era of Evolving Digital Age. He elaborated the current trends of Information Resource Management in the digital library era. Dr. M. Saravanan, Deputy Librarian, Anna University, Chennai, gave the lecture on Best Practices and Resources Management at AU Library. In the end of the Technical Session-I, Dr. Deepaali Kuberkar, Librarian, Tata Memorial Hospital, Mumbai, delivered the technical talk on Digital Renaissance of Libraries. Technical Session-II began with the invited talk on Text and Data Mining – Licensing in the Digital World by Dr. Mahendra Jadhav, Librarian, IIT-M, Chennai. The various technical steps towards the text and data mining in the era of making digital library and licensing issues were addressed by him. Shri Manoj Singh,

Head, SIRD, BARC, Mumbai gave the lecture on Digital Resources Management: Current Status and Future Trends of Libraries. The various advance digital resources management activities of BARC libraries have been explained by him. Finally, Prof. R. Sevugan of DLIS, Pondicherry University, delivered the lecture on Research Data Management: A Perspective of Developing Country.

The Panel discussion was chaired by Dr. M. Sai Baba. All the experts who gave the lectures on the technical sessions were part of the panel discussion along with Smt. S. Rajsewari, Former AD, SIRD and Shri J. Rajan, Head, SIND. The ONOS (One Nation One Subscription) scheme, Licensing issues, the digital enhancement etc., were discussed in the panel discussion. In the end, concluding summary of the deliberations was given by the Dr. M. Sai Baba.

Reported by:
Dr. Vidya Sundararajan, Associate Director, SQRMG

Tamil Nadu BEAT EXPO 2025

January 25-26, 2025

Incubation Centre of IGCAR participated in TN BEAT EXPO 2025, a flagship event organized by the Tamil Nadu Government Corporation, TAHDCO on January 25-26, 2025 at Chennai Trade Centre in Chennai. Focus of this two-days Expo was to build entrepreneurs from the marginalized communities such as the Adi Dravidars and Tribals. A stall was up by IC-IGCAR Team to showcase IGCAR's technology incubation and licensing opportunities through videos and posters. The event had a reported footfall of around 37,000 visitors and IGCAR's stall was well attended.

Dr. M. Mathiventhan, Honaurable Minister of Adi Dravidar Welfare, Tamil Nadu, handing over a memento to Head, IC-IGCAR for IGCAR's participation in Tamil Nadu Government's TN BEAT EXPO 2025 January 25-26, 2025 at Chennai to build entrepreneurs from Adi Dravidars & Tribals.

Reported by:
Dr. N. Subramanian, Head, Incubation Centre-IGCAR

8th National Conference Urjavaran – 2024-25

February 06, 2025

Air-Conditioning & Ventilation System Division (AC&VSD), ESG, IGCAR in association with Indian Society of Heating Refrigerating & Air-Conditioning Engineers (ISHRAE) - Kalpakkam Chapter organized the 8th National Conference URJAVARAN – 2025 at Sarabhai Auditorium, IGCAR on 6th Feburary 2025. The theme of the conference was "Policy and Regulatory Frameworks for Sustainable HVAC Practices". Two hundred and fifty delegates attended the conference from various DAE units, academic institutions, industries and leading consultancies.

Shri Biswanath Sen, Convener, Urjavaran 2025 delivered the welcome address and also made brief introduction about the conference. Shri N. Suresh, Associate Director, CEG delivered the inaugural address highlighting the significance of energy conservation for sustainable environment. Chief guest of the conference, Dr. T. V. Krishna Mohan, Facility Director, BARCF addressed the forum on sustainable HVAC, smart technology integration and workforce development and training in his presidential address. Dr. K. Anantha Sivan, Former Director, RpG

Releasing of souvenir during inaugural function

Dr. K. AnanthaSivan, Former Director, RpG, delivering the keynote address on "Climate change and the change in climate"

has delivered the keynote address on "Climate change and the change in climate", which emphasized the importance of policy and regulatory frameworks for sustainable HVAC practices. The address was well received by the participants. The conference souvenir was released by Dr. K. Anantha Sivan, Former Director, RpG along with the dignitaries. At the end of the inaugural session, Shri T. Manikandan, Organizing Secretary, URJAVARAN – 2025 has proposed the vote of thanks. Dr. R. Divakar, Director, MMG and Dr. Sandip Kumar Dhara, Director MSG have inaugurated the exhibition stalls of the exhibitors of the conference.The conference discussed latest technologies, products and ongoing research on sustainable buildings. It included invited talks by eminent speakers from academic institutions, industries, R&D organizations and leading consultants in the areas of HVAC. The conference had six contributed papers presentation from DAE units (IGCAR and BARC) covering wide spectrum such as regulatory requirements of nuclear facilities and energy efficiency improvements in various HVAC areas such as air filters, unitary air conditioners, smart HVAC systems, mechanical seals, centrifugal chillers etc. Product presentations from reputed industries were also a part of the conference. The conference facilitated good interactions among delegates and experts in the area of HVAC.Shri S. Francis Wilfred, Co-Convenor & Head ACWPO&MS delivered the welcome address of valedictory session. Shri Faizan Ulla Khan, Head PLAS, RDG presented the summary of the technical sessions of the entire programme. Convenor Urjavaran, in his valedictory address, described how the policy and regulatory bodies govern the production of energy efficient equipment, improve the indoor air quality etc. He emphasized the importance of standards to improve equipment performance and sustainability. Shri V. Marudhupandiaraja, BARCF and President Elect., ISHRAE Kalpakkam chapter proposed the vote of thanks.

Reported by:
Shri Biswanath Sen, Head, Air-Conditioning & Ventilation System Division

Celebration of World Environment Day 2025 at IGCAR

June 05, 2025

World Environment Day, celebrated annually on June 5th is a global platform for raising awareness and encouraging action for the protection of the environment. In line with this year's theme focusing on sustainable living and Ending Plastic Pollution, the Safety, Quality and Resource Management Group (SQRMG) of IGCAR organized tree plantation activities to mark the occasion within the DAE Campus. As a key highlight of the celebration, an IGCAR Colloquium was conducted, featuring an invited talk by Prof. R. Arun Prasath, Department of Green Energy Technology, Pondicherry University. The talk, titled "Green Energy and Waste/Plastic Management Technologies to Combat Climate Change and Pollution", focused on the pressing need for sustainable energy solutions and effective waste management practices. He elaborated on various technological advancements in renewable energy, the circular economy, and the environmental implications of plastic usage. His insights offered a scientific perspective on how institutions and individuals can contribute to mitigating climate change and reducing pollution. Following the colloquium, a tree plantation program was organized as a symbolic and practical step towards environmental conservation. The plantation activity was held within the DAE Campus, covering a dedicated area of approximately 4000 square meters. A total of 500 saplings, comprising a mix of native perennial plants, were planted to enhance the campus greenery, improve air quality, and contribute to biodiversity enrichment. The event witnessed active participation from all employees of SQRMG, IGCAR, who collectively engaged in the plantation activity. This program showcased IGCAR's continued efforts in promoting environmental awareness and sustainable practices.

Tree plantation on the occasion of World Environment Day 2025, and active participation by the employees

Reported by:
Dr. C. Venkata Srinivas & Colleagues, EAD

Theme Meeting on "Quantum Frontiers: Mechanics, Information & Entanglement: QMINENT-2025"

June 19-20, 2025

A two days theme meeting titled “Quantum Frontiers: Mechanics, Information & Entanglement: QMINENT-2025” was held on 19th to 20th June 2025 and was jointly organised by Materials Science Group (MSG) & Engineering Physics Group (EPG) of RDG in association with Kalpakkam chapter of Material Research Society and Indian Physics Association at Sarabhai Auditorium, IGCAR, Kalpakkam. Prof Emeritus V. Balakrishnan, IIT-Madras was the chief guest of the event. This theme meeting was organized to commemorate the centenary year of the development of foundational theories and mathematical frameworks of quantum mechanics, established around 1925. The year 2025, declared by the United Nations as the International Year of Quantum Science and Technology to mark this significant milestone in scientific history.

The theme meeting brought together leading researchers and experts from premier institutions such as IIT Madras, IGCAR Kalpakkam, and KREA University. The event featured keynote lectures and insightful talks covering a broad spectrum of topics, including quantum optics, information theory, quantum simulations, entanglement, error correction, and cutting-edge developments in quantum materials and technologies. With engaging discussions on foundational aspects like symmetry principles, Bell’s inequalities and Wigner functions, as well as practical themes like quantum tomography and polarization qubits. The meeting concluded with a panel discussion on the future of quantum science in the coming decades. The panel explored questions related to the direction of quantum computing, the most promising types of quantum bits (qubits), the potential for task-specific quantum machines, and whether the current excitement around quantum technology is justified. While acknowledging the surrounding

hype, the discussion highlighted the value of public interest and emphasized the need for more research,regular scientific gatherings, collaboration between institutes, and active participation by young scientists to support the goals of the National Quantum Mission.

Reported by
Dr. John Arul A, Engineering Physics Group, Reactor Design Group
Dr. Sandip Kumar Dhara, Materials Science Group

Workshop on Advanced Scanning TEM based Techniques and EPMA

July 09-10, 2025

An International Workshop on Advanced Scanning TEM-based Techniques and EPMA was conducted during 09-10th July, 2025 in IGCAR, Kalpakkam. The inaugural program was addressed by the Shri C.G. Karhadkar, Director, IGCAR; Dr. R. Divakar, Director, M\MG, IGCAR; Dr. R. Tewari, Director, MG, BARC; Dr. Anish Kumar, AD-MCG, IGCAR and Dr. Arup Dasgupta, Head-PMD, IGCAR. Renowned electron microscopists delivered lectures covering Advanced Scanning TEM based techniques including magnetic domain imaging using Lorentz TEM and LMSTEM-differential phase contrast imaging; Orientation Imaging Microscopy using Precession Electron Diffraction (PED-OIM). The workshop also included invited talks from several eminent speakers from India covering the principles and practices on TEM and Electron Probe Micro Analysis (EPMA) along with their application to advanced

materials development and characterization. Practical live demonstrations on aberration corrected TEM and EPMA facilities were held during the workshop. The workshop was attended by more than 100 participants from IGCAR and from across India. Participants included, scientists, faculties, a doctor and a number of Ph.D. students.

Reported by:
Dr. Arup Dasgupta, Physical Metallurgy Division

Workshop on "Advances in Environmental and Radiological Monitoring, Radiation Dosimetry and Emergency Preparedness (AEMRDS 2025)"

August 25-26th, 2025

A 2-day workshop on "Advances in Environmental and Radiological Monitoring, Radiation Dosimetry and Emergency Preparedness (AEMRDS 2025)" was conducted by SQRMG, Indira Gandhi Centre for Atomic Research in association with the Indian Association for Radiation Protection during 25-26 August 2025 at IGCAR, Kalpakkam. The workshop was attended by about 75 Scientists and Engineers from BARC, IGCAR, AERB, NPCIL, Bhavini, KARP, PRL, faculty and research scholars from Sri Ramachandra Institute of Higher Education and Research (SRIHER), Andhra University, SRM University, GITAM University and Satyabama University.

Inauguration of AEMRDS-2025 workshop

The workshop was inaugurated by Shri Dinesh Kumar Shukla, Chairman, AERB. The newly commissioned C-Band Doppler Weather Radar and Mid-Tropospheric Wind Profiler facilities were inaugurated by the Chief Guest Dr. D.K.Shukla during the workshop. The workshop comprised 4-technical sessions and detailed interactions. The presentations covered various aspects. On the first day 25 Aug'25, the talks covered Perspectives of Health, Safety and Environment at IGCAR and BARC, High-Throughput In Vivo and In Vitro Approaches for Emergency Radiation Monitoring System Development, Latest developments in Nuclear and Radiological Emergency management at DAE, application of LNT model in occupational exposure and radiation therapy, physical and biological techniques of external exposure assessment, radiation dose measurements using luminescence techniqures from natural minerals, Internal dosimetry techniques and computer models for rapid dose assessment, effects of ionizing radiation in biota from high back ground radiation in Kerala, diagnostic radiation biology and low dose effects of ionizing radiation in Drosophilla. The talks on the second day 26 Aug'25 covered application of photonic crystals in pollution sensing and radiation detection, radionuclide transfer factor studies for public dose estimation, environmental radioactivity measurements in Tamil Nadu, regulatory perspectives of environmental assessment, environmental assessment at NPP sites and within Kalpakkam site, environmental aspects of radon and thoron, radioactivity measurements in marine organisms, perspectives of emergency preparedness, lessons learnt from Chernobyl nuclear accident, radiation monitoring network at Kalpakkam, source term estimation, chemical emergency preparedness at HWB sites, and radiological emergency response systems during last two decades at Kalpakkam. The research gaps, for future course of action towards promoting their application for effective environmental surveillance, dosimetry and response are also discussed. Overall, the need of advanced methodologies for environmental assessment, dosimetry techniques for routine monitoring and emergency scenarios and realistic assessment of the radiological risk during accidents for recommendation of optimum protective actions was acknowledged by all the experts.


Delegates of the AEMRDS-2025 workshop

Reported by:
Dr. C. Venkata Srinivas & Colleagues, EAD

33rd Prof. Brahm Prakash Memorial Materials Quiz Programme (BPMMQ-2025)

September 12-13th, 2025

The 33rd Prof. Brahm Prakash Memorial Materials Quiz (BPMMQ) was conducted at Indira Gandhi Centre for Atomic Research, Kalpakkam during September 12-13th, 2025 for school students of class XI and XII. A total of 45 teams from across the country participated in this programme, along with nearly 35 escorting teachers and professionals. All participants visited the Fast Breeder Test Reactor (FBTR) and Madras Atomic Power Station (MAPS) as part of the 'Metal Camp' programme during this event.

The winners of BPMMQ-2025 with the chief guest

The participants were also addressed by Dr. S.V.S. Narayana Murty, Chairman & Managing Director, MIDHANI, Hyderabad, who delivered the Prof. Brahm Prakash Memorial Lecture on "Current Achievements and Challenges for Indian Metallurgists Towards Atmanirbharta in Strategic Materials". In this lecture, he enthused students with various stories of technological excellence, and materials-based advances in India, especially in the strategic sectors. He exhorted the students to work with national spirit and contribute towards making the nation self-reliant, as laid out in the Viksit Bharat-2047 mission.

The quiz commenced with drawal of lots for the preliminary rounds, which were held in six parallel sessions. The winner and runner-up of each session contested in semifinal round held in two parallel sessions. In the Grand Finale of BPMMQ-2025, six teams, representing Trichy (2 teams), Varanasi, Bhubaneswar, Durgapur and Mumbai engaged in a spirited competition. The questions in the Grand Finale ranged from societal applications of nuclear industry to advancements in Indian materials manufacturing/production, quantum materials, lightweight materials, etc.

Reported by:
Dr. V. Karthik, HMTD & PIED, MMG

14th National Conference on Recent Advances in Information Technology (READIT-2025)

September 24-25th, 2025

Scientific Information Networking Division, IGCAR in association with Madras Library Association – Kalpakkam Chapter (MALA-KC) organized the 14th Biennial National Conference on Recent Advances in Information Technology (READIT) during September 24-25, 2025 at Sarabhai Auditorium, IGCAR, Kalpakkam, with the theme 'Envisaging the Libraries of the Coming Decades'.

The conference was organized as two days event with participation from various academic, R&D and DAE Institutions. About hundred delegates from the academic and public domain, Information Technology Professionals and Research scholars attended the conference.

In the inaugural function, Dr. Vidya Sundararajan, Associate Director of SQRMG delivered the welcome address. Shri E. Soundararajan, organising secretary READIT and Head DRTS, SIND, IGCAR presented about the READIT conference. The function was presided over by Shri C.G. Karhadkar, Distinguished Scientist & Director, IGCAR. In his presidential address, Shri C.G. Karhadkar highlighted the importance of the libraries in the digital era. A book on the Genesis of READIT was released by the director. Inaugural address was given by Prof. (Dr.) Sudha Seshayyan, Director, Sastra University & Former Vice Chancellor, Dr. MGR Medical University where she mentioned challenges before the librarians in the Artificial Intelligence world and presented about the importance of oral tradition in preserving the knowledge.

Shri J. Rajan, Convener READIT and Head, SIND proposed the vote of thanks. The conference included invited talks by domain experts in Information Science & Technology and oral presentations by Research Scholars & Professionals. The sub-themes of the conference included Digital Infrastructure and Accessibility of Information, Libraries as cultural hubs and preservation of heritage, AI and the Role of Advanced technologies, Libraries as learning spaces, Personalized User Services through Adaptive Technologies and Government policies and global collaboration to enhance access to information resources.

Special technical session was organised for the contributed presentations by Research Scholars and Delegates which included oral and poster presentations. The conference facilitated good interactions among young researchers, students, professionals and well-known speakers in the area of future technologies for libraries.

There was a panel discussion moderated by Prof. M. Sai Baba of NIAS Bengaluru and Former Director, RMG, IGCAR. Dr. Anup Kumar Das, Jawaharlal University, New Delhi, Dr. V. Gopakumar, Digital University, Kerala, Shri J. Rajan, Head, SIND, and Dr. M. Vijayakumar, Pondicherry University, participated in the panel discussion on 'Role of Libraries in the Coming Decades'. The conference concluded with the valedictory function. Shri J. Rajan delivered welcome address, Shri E. Soundararajan presented the conference summary. The valedictory address was given by Prof. M. Sai Baba. He has also presented the best paper awards of READIT 2025. Shri K. VijayaKumar, Head, LISS, SIND, IGCAR proposed the vote of thanks.

Reported by:
Shri E. Soundararajan, SIND, SQRMG

IGC COUNCIL

Chairman

Shri C. G. Karhadkar
Distinguished Scientist & Director, IGCAR

Shri Chandrashekhar Gaurinath Karhadkar, Mechanical Engineer, is from the 31st batch of BARC Training School, Mumbai. He then joined the Reactor Operations Division of Reactor Group of Bhabha Atomic Research Centre at Trombay, Mumbai, in 1988. Shri C. G. Karhadkar has thirty-six years of experience and served in various capacities from Shift Charge Engineer and took charge as Director, Reactor Group.

As Director, Reactor Group, BARC, he was piloting the Research Reactor Programmes of BARC. The programmes encompasses safe and efficient operation, utilization, upgradation, enhancing safety aspect, decommissioning and planning of new research reactors, at BARC. He has extensively contributed towards, operation of Dhruva at its rated full power and improving the fuel performance of Dhruva reactor. Shri C.G Karhadkar has extensively contributed in sustaining the isotopes supply for the medical fraternity, after shutdown of Cirus reactors and COVID-19. Under his leadership Dhruva was refurbished innovatively without core unloading, thereby repair was completed well ahead of the schedule. He has initiated programs for enhancing utilization of the Research Reactor for industrial applications like Neutron Radiography, Neutron Activation Analysis, Accelerated life testing of detectors, material irradiation studies etc.

Under the leadership of Shri C.G. Karhadkar, commissioning and First Approach to Criticality of Apsara-U (2 MW reactor), and decommissioning plan for a large reactor like Cirus have been successfully accomplished. He also extensively contributed towards de-regulation of the old Apsara for converting it into a DAE museum.

Shri C.G. Karhadkar has chaired several Administrative, Financial, Technical and Regulatory Committees. He has been instrumental in reforming the procurement procedures, this has simplified procurement process for speedy execution of projects in BARC. He is also a member of various Strategic Committees in BARC.

Presently Shri C.G. Karhadkar is a Distinguished Scientist and Director, Indira Gandhi Centre for Atomic Research, Kalpakkam & Director, General Services Organization, Kalpakkam.

Members

Shri Vivek Bhasin is presently the Director of BARC, Mumbai. Shri Bhasin joined the Reactor Engineering Division, in 1988 after successfully graduating from the 31st Batch of BARC Training School. He is widely recognized for his expertise in the development of nuclear fuels, nuclear reactor component designing and structural integrity assessment of power reactors..

In a career spanning more than three decades, he contributed significantly towards several programs and activities to ensure the longevity of power reactor fleet, including rehabilitation and structural integrity assessment of RAPS-1, TAPS-1&2, MAPS and TAPS-3&4 alongside reactors operating in Kaiga, Kakrapar and Narora.

Shri Bhasin played a leading role in setting up of facilities for fabrication of fuel for APSARA-U Reactor and a novel plant for production of Fission-Moly (a radioactive isotope with extensive applications in healthcare) in Trombay. He was also instrumental in improving the rate of production of Plutonium-Uranium carbide fuel for Fast Breeder Test Reactor (FBTR) in Kalpakkam.

Shri Bhasin is a recipient of several honours, including Indian Nuclear Society Medal (2002), DAE Science & Technology Award (2006), and Homi Bhabha Science and Technology Award (2014). He is a Fellow of Indian National Academy of Engineering and has more than 300 publications to his credit in the field of nuclear science and engineering.

Dr. V. Jayaraman joined Indira Gandhi Centre for Atomic Research (IGCAR), Kalpakkam in the year 1989. He is from the 32nd Batch of BARC Training School. His areas of research interest includes materials chemistry, chemical sensors, novel soft-chemical synthesis, actinide chemistry, metal fuel development, pyrochemical process, radiopharmaceuticals, burn-up measurements, etc. He is a recipient of Homi Bhabha Science and Technology Excellence Award (2018). He is also Professor of HBNI and supervising PhD scholars. He is presently Outstanding Scientist and Director, Materials Chemistry & Metal Fuel Cycle Group.

Shri K. P. Kesavan Nair Graduated in Electrical engineering from Govt. Engineering Collage, Trichur in 1988 and joined BARC in 1990. After completing 34th batch of training school, he joined RPD, BARC in 1991. He was a member of the team responsible for the PRP Electrical System comprising of power generation & distribution with islanding capability. At PRP he has made substantial contribution towards the development of compact Nuclear Reactor for strategic application. After the commissioning of PRP, he was transferred to IGCAR in Nov 2007 and joined Engineering Services Group.

His expertise includes design, construction and O & M of various infrastructure systems related services. He is presently an Outstanding Scientist and Director, Engineering Services Group.

Ms. Nidhi Pandey, IInfoS (1991 Batch) currently appointed in Department of Atomic Energy, Mumbai as Additional Secretary (R&D). Ms. Nidhi Pandey joined Department of Atomic Energy on 26th September 2025.

Dr K. Natesan is a graduate in Mechanical Engineering and joined Department of Atomic Energy at BARC Training School in Mumbai (40th batch) in 1996. After successful completion of one year training, he joined IGCAR and was involved in the thermal hydraulics analysis of fast reactor systems. He has enhanced the analysis capabilities of in-house developed plant dynamics codes used for carrying out safety analysis of fast reactor plant. Code modifications for adopting this code for development of operator training simulator for PFBR has also been carried out. The safety analyses carried out by him for FBTR has been instrumental for obtaining regulatory clearance for various campaigns and also for the current 40 MWt power operation. He got his PhD degree from Homi Bhabha National Institute in 2020. Currently he is an Outstanding Scientist and Director of Reactor Design Group of IGCAR. The group is responsible for supporting BHAVINI in commissioning and regulatory clearance for PFBR, and design of future reactor systems, viz., FBR 1&2 and FBTR 2. In addition to his responsibility in Reactor Design Group, he is also involved in the review of various regulatory documents and member of several review committees. He has co-authored more than 150 publications including 43 in reputed journals. He is a fellow of World Nuclear University and recipient of Scientific and Technical excellence award for the year 2011 from the Department of Atomic Energy.

Shri K. V. Suresh Kumar is a graduate in Chemical Engineering and joined Department of Atomic Energy at BARC Training School in Mumbai as a trainee (29th batch) in1985. After successful completion of one year training, he joined in FBTR operation in 1986. Initially he was involved in the commissioning of various system of FBTR such as Sodium heated Steam Generators, Steam & Water system and Turbo-Generator. He was involved in the first raising of reactor power and carried out physics & engineering tests for validating the assumptions made in the design. He has got vast experience in Reactor operation, operation of sodium systems, steam and water system, turbine & its auxiliaries and all other auxiliary systems in FBTR. He was instrumental in carrying out many plant modifications and contributed in improving the availability factor of the plant. He shouldered many responsibilities in the plant

and was Director, Reactor Facilities Group from March 2016 to November 2022 and was responsible for operation of FBTR, KAMINI Reactor and PFBR Fuel Fabrication Facility. During his tenure, FBTR power was raised to its design power level of 40 MWt feeding electricity to the grid. In addition to his responsibility in Reactor Facilities Group, he was also involved in the review of commission procedures/ reports and Technical specifications for PFBR Operation. He was the chairman of Project Design Safety Committee (PDSC) constituted by Atomic Energy Regulatory Board (AERB) for issuing stage wise clearance for commissioning of PFBR. He is a Distinguished Scientist and presently the Chairman and Managing Director (CMD), BHAVINI.

Dr. T. V. Krishna Mohan was born in 1966. He graduated in Chemical Engineering from Osmania University and pursued his Masters in Business Administration (MBA) from the same university. He got his PhD degree from Homi Bhabha National Institute in 2016. He is from 34th batch of BARC training school and presently Facility Director, BARC Facilities, and Head, Water and Steam Chemistry Division. His field of specialisation is Design, Procurement, Installation, Commissioning, and Operation of Simulated Engineering loops to carry out water chemistry, biology and heat transfer experiments. His contributions are towards Bioremediation, Flow Accelerated Corrosion, Biological Denitrification, Aerobic Granulation, Wastewater Engineering. He is recipient of DAE Group Achievement Awards. He has more than 100 publications and one patent to his credit.

Dr. Kitheri Joseph is a Gold Medalist in M.Sc Chemistry, from Loyola College, Chennai. She is from 33rd Batch of BARC Training School and joined IGCAR in 1990. She is a doctorate in Chemistry from University of Madras. She gained experience in the field of sodium chemistry, thermal analysis, solid state nuclear materials and nuclear waste management. She took the lead role and developed a new electrolyte and reference material for electrochemical hydrogen meter, used for sensing hydrogen in sodium. Dr. Kitheri Joseph as Associate Director, Metal Fuel & Reprocessing Group, led the team on metal fuel fabrication, pyrochemical reprocessing both at lab & plant scale level and towards conversion of uranium oxide to metallic uranium by Direct Oxide Electrochemical Reduction (DOER) process. She leads the team from IGCAR in Indo-UK civil collaboration in the field of nuclear waste management. Presently, she is the first women Regional Director, MRPU, DPS, DAE. She caters to the purchase and stores activities of IGCAR & others units of Kalpakkam and HWP, Tuticorin.

Shri S. A. Murugesan, IAS, Uttarakhand cadre -2005 Batch. Currently on deputation to Department of Atomic Energy serving as Internal Financial Advisor (IFA) in IGCAR and GSO.

Shri Paresh Nath Mahadani joined the Department of Atomic Energy on January 18,1999 with degree in Commerce (Hons.) from Vinoba Bhave University and ICWA(I) from ICWAI, Kolkata. He has completed 27 years of service in the Department serving in various capacities in different Units like DAE Secretariat, AMD, HWB, BARC, IGCAR, BARC (F), Kalpakkam and presently in IGCAR thus gaining vast experience in all matters relating to administration. He is holding the post of Chief Administrative Officer (CAO) in IGCAR. As administrative head of the Unit he provides service, advice and support with the highest level of professionalism valuing rules and procedures as a tool to achieve the objectives of the Organization and the desired outcome, contributes towards smooth internal functioning of the organization through dissemination of information, extensive use of automation and information technology, updating and simplifying procedures and instructions to the changing environment, proper record and data management systems, developing standard process sheets to ensure procedural compliance, periodical training of Officers and staff to enhance the knowledge and skill, secure better focus and ownership of task and increase their yield, monitoring delays, identifying bottlenecks and implementing remedial measures, promoting transparency and accountability in decision making process, mentoring subordinates and building teams, promotes harmonious relations and secures maximum amount of cooperation from the employees.

Organisation and Activities of Various Groups

Civil Engineering Group

Shri C G Karhadkar
Director, CEG

Shri N. Suresh
AD, CEG

Shri H. I. Abdul Gani
Head, A&SED

Shri Sudipta Chattopadhyaya
Head, CED

Smt. R. Preetha
Head, CM&QCD

Shri Hari Kumar
Head, C&MWD

The Civil Engineering Group (CEG) has a very important role for development, construction, and civil maintenance of various facilities, laboratories in IGCAR as well as common infrastructure for all units of the Department of Atomic Energy (DAE) located at Kalpakkam. Mandate of CEG is design & construction of several laboratories, buildings and services beginning with the conceptual design to construction and its associated maintenance, for IGCAR's mission of 'Fast reactor development and its associated fuel cycles'. The group is continuing the path of realizing center's vision and ably supported by dedicated Architectural, Design, Estimate & Contracts and Construction, Operation & Maintenance team of engineers. CEG undertakes in-house and collaborative research projects in civil engineering aspects of Fast Breeder Reactor (FBR). Apart from achieving durable concrete, special types of concretes have been developed and now the group has proved itself in providing technical support in design of major projects like PFBR and associated fuel cycle facilities. The group has developed expertise in characterization of site for safety related structures including geotechnical investigation, site specific flood level studies. Now CEG has undertaken a mandate of conducting periodic condition survey, assessment and formulating repair and retrofitting methodologies of Reinforced Concrete Structures of existing radiological facilities, major laboratories, and infrastructure buildings at IGCAR including other DAE units at Kalpakkam.

As in previous years, CEG has given support to PFBR commissioning activities like completion of PSI of safety related buildings along with BHAVINI in priority basis. CEG has also completed periodic condition assessment of FBTR buildings and submitted report to AERB through user group. Presently CEG is actively participating in FBTR 2 & associated Metal Fuel Cycle Demonstration Facility (MFCDF) through several task forces and working groups such as siting & site evaluation aspects, conceptual civil design, plant Layout and identification of pre-project activities of FBTR 2 & MFCDF. Subsequent to completion of seismic margin assessment of DFRP main plant buildings and associated safety buildings including RC stack, associated retrofit schemes is undertaken based on experimental validation. CEG, IGCAR is also collaborating with concerned groups in BARC & NPCIL to develop high temperature concrete for reactor applications.

Presently architectural & structural design works for identified projects in upcoming vision proposals from CEG Civil Infrastructure

Augmentation & Enhancement of Facilities at IGCAR is under progress. For ongoing GSO Vision Scheme 3 projects, architectural planning, design works are completed for Atomic Energy Central School 4 (Phase 2), Convention Centre, Operation theatre with balance phase for DAE hospital at Anupuram Township, UG sumps and steel bridges across water ways at neighbouring villages around Kalpakkam Township and vertical extension of dispensary building at DAE Nodal Centre, Chennai. CEG has also undertaken construction of new RO plant buildings at NDDP, BARC, DAE, Kalpakkam for which timely estimates & tendering actions from CEG are completed apart from E& C works other civil works at IGCAR. Apart from sustained quality control activities for IGCAR, BARCF (Major Works: DDUO of WIP, Engineering Hall of PRP, RCCT & Tile Hole of CWMF) & GSO common infrastructure, as a part of ageing management, condition survey, assessment and repair methodologies for RCL, RML, VNAS and WSCD building are completed. Several special repair works like 2 MIGD RO Plant, CDO Building, Refurbishment of Brown Room, HBB and CDO Lecture Hall are completed for close in coordination with concerned Groups in IGCAR.

With proper planning maintenance of buildings, roads within IGCAR are being carried out smoothly and public health services such as water supply and sewerage are functioning 24X7 basis smoothly. CEG is also responsible for maintaining dedicated Fire Water System (FWS) 24X7 basis for FBTR and other radiological laboratories and plants including CORAL, DFRP and other infrastructure buildings within IGCAR with required minimum pressure at those furthest points.

The group has put forward substantial efforts for sustainable water conservation by introducing efficient water management scheme by recycling treated water. Towards that, entire treated water from existing STP daily around 13.5 lakh litre are already used in development & maintenance of garden & lawn at IGCAR and STP water treated through a tertiary water treatment plant is being used as makeup water for central water chilling plant, which provides centralized air conditioning for majority of building in IGCAR premises. CEG's commitment towards achieving bio-degradable zero solid waste managed IGCAR campus is being realized by constructing and commissioning of Nisarguna technology-based biogas plant using kitchen waste and Dry Leaves manure Plant utilizing garden waste. The Group has maintained an aesthetic & sustainable green environment at the plant site. Presently modification of toilets in existing common infrastructure buildings are undertaken for achieving DIVAYANG compliance in line with "Harmonised Guidelines and Space Standards for Universal Accessibility in India" under Swatchta Action Plan.

Electronics and Instrumentation Group

Shri N. Sridhar
Director, EIG

Shri. G. Venkat Kishore
Head, ED

Shri M. Sakthivel
Head, I&CD

Shri R. P. Behera
Head, RTSD

Shri M. Sivarama Krishna
Head, SISD

Shri R. Jehadeesan
Head, CD

Shri A. Shanmugam
Head, DDCSD

Electronics and Instrumentation Group is focused on design and development of indigenous technology in the areas of Electronic Instrumentation & Control systems for fast breeder reactors and reprocessing plants that include Development of Distributed Digital Control System, Safety Critical and Safety Related Systems, Safe & Secure PLC, Virtual Control Panel based Control Room, Full-scope Operator Training Simulator, 3D modeling, animation & visualization of FBR subsystems and VR walkthrough of structures, Cyber Security Management for IT and I&C systems. Design and Development of advanced equipment and technology such as, indigenous Wireless Sensor Networks for nuclear facilities, strategic and societal applications, Time Domain Electromagnetic for Deep Seated Atomic Minerals Exploration, Plutonium Condition Air Monitoring System for reprocessing plants, Test Instrument for

Steam Generator Tube Inspection, Radar Level Probe for Liquid Sodium Level Measurement, radiation resistance MEMS based sensor for nuclear applications and innovative sensors and instruments for nuclear facilities have been completed. Considerable expertise exists in designing, building and maintaining state-of the-art high-performance supercomputing facility that continues to meet large scale compute- and data-intensive requirements in multi-disciplinary domains. Implementation of IT-enabled Nuclear Knowledge Management system for Fast Reactors and associated domains, computational intelligence systems, cryptography, cyber security solutions, knowledge management and development and deployment of modern security systems for access control and physical protection of nuclear complexes are initiated.

Engineering Services Group

Shri K. P. Kesavan Nair
Director, ESG

Shri Biswanath Sen
Head, AC&VSD

Shri Utpal Borah
Head, CWD

Shri L. Subramanyam
Head, ESD

The Engineering Services Group (ESG) has a very important mandate of infrastructure support for all the units of IGCAR. It spans from planning, design, engineering, execution, testing and commissioning of Electrical, Mechanical, Air-conditioning and Ventilation works for the Laboratories. ESG also extends support for high end manufacturing for FBTR, PFBR, the R & D needs as well to all DAE units at Kalpakkam. To meet the user requirements satisfactorily and considering the qualitatively different responsibilities three divisions are formed under ESG: Air Conditioning and Ventilation Systems Division, Central Workshop Division and Electrical Services Division.

The three Divisions of ESG had set the agenda for a transformative path along with growth in capabilities and capacities with the objective to modernize/establish the facilities and enhance the service delivery, quality and health of the infrastructure, which would result in net economic gains to the Department. Main milestones of the transformative path are aligned with Industry 4.0. Projects for centralised control and monitoring of processes and systems in line with Industry 4.0 takes the centre stage in activities of all the 3 Divisions. Central workshop Integrated Manufacturing (CIM), centralised monitoring of unmanned high voltage substations and centralised control of Air Handling Units (AHUs) are the 3 major elements under this scheme, which would be implemented through in house developed technology with the support of SQRMG and EIG and are in various stages of implementation. In addition, ESG has taken up a few projects under Green Initiatives and Energy and resultant Cost Savings.

During the year, the Air Conditioning and Ventilation Systems Division (AC&VSD) sustained its commitment to excellence by ensuring uninterrupted air-conditioning and ventilation services for critical and diverse facilities, including radioactive laboratories, advanced research spaces, high–density computing clusters, administrative areas, and other essential infrastructure across IGCAR. The division efficiently managed a total connected cooling load of approximately 5000 TR, supported through the operation of central chilled water plants, VRF systems, packaged systems, standalone units and other unitary equipment, thereby maintaining a consistently high level of user satisfaction throughout the year. A major accomplishment was the successful modernization of ageing refrigeration and air-conditioning assets, which involved the replacement of chillers, AHUs, and chilled water distribution pipelines with new-generation,

energy-efficient systems. This strategic revamping enhanced operational reliability, reduced downtime, and contributed to substantial energy optimization. Furthering its focus on user comfort and energy efficiency, the division commissioned 50 Variable Air Volume (VAV) units in office and meeting environments, enabling flexible zone-wise control and improved occupant comfort while optimizing energy consumption. A notable technological advancement was the commissioning of a pilot 1000 TR-hour Thermal Energy Storage (TES) system at the Advanced Ultra Super Critical (AUSC) test facility. Designed to offset a peak cooling load of approximately 250 TR, this system now supports the AUSC, RHIDS, and SGIDS buildings, marking a major step toward demand flattening, improved operational flexibility, and long-term energy management.

In addition to HVAC infrastructure, AC&VSD continued to play a critical role in the design, execution, testing, and commissioning of material handling systems such as EOT cranes and electric wire rope hoists for upcoming facilities. The division also completed scheduled annual servicing and statutory load testing of existing lifting equipment, ensuring compliance with AERB requirements and maintaining the highest standards of safety in radioactive and non-radioactive areas.

Furthermore, the ACVSD operates a 2 MIGD Sea Water Reverse Osmosis (SWRO) Desalination Plant, which serves as a vital source of safe and reliable potable water for various DAE facilities at Kalpakkam including IGCAR, BARCF, and BHAVINI. With an annual production of 8.5 Lakh cubic meters, the plant ensured uninterrupted water supply to support scientific research, institutional operations, and essential services. The division operates a Tertiary Treatment Plant (TTP) that efficiently recycles treated sewage to produce high-quality makeup water for the Central Water Chilling Plant's cooling towers, reducing fresh water use by enabling higher CoC and consistently delivering its design capacity of 20 m3/hr.

Ever since its inception in the year 1974, Central Workshop Division (CWD) continues to fulfil its mandate of in-house manufacturing/ refurbishment/repair of various critical components and systems with the highest precision, accuracy and reliability for IGCAR and other DAE units including BHAVINI, BARCF and MAPS. CWD, specializing in machining, cold plate forming, welding, hardfacing, fabrication and inspection, undertakes in-house manufacturing of various products, which are technically challenging, commercially unviable, and needed urgently to meet the project schedules. CWD routinely carries out multiple manufacturing/refurbishment/repair activities for Prototype Fast Breeder Reactor (PFBR), Fast Breeder Test Reactor (FBTR), Kalpakkam Mini Reactor (KAMINI), Reprocessing Facilities, Post-Irradiation Examination (PIE) Facilities, R&D Projects and Infrastructure Development apart from operation and maintenance requirements. Notably, the welding procedure for the PFBR Sub-Assembly (SA) in 2G position was developed by CWD welders and the first batch of PFBR Fuel/ Blanket SAs was welded at CWD successfully.

Following malfunctioning of IFTM after loading of the blanket sub-assemblies resulting in complete halt in initial fuel loading of PFBFR, CWD was entrusted to manufacture a direct fuelling machine, named as Portable Sub-Assembly Handling Flask (PSAHF) to carry out fuel loading through the In-Vessel Transfer Port (IVTP). CWD rose to the occasion and successfully manufactured and delivered the PSAHF in record time, which resulted in resumption of initial fuel loading of PFBR. PSAHF consists of ten different sub-assemblies and long and slender components of very high precision. Prior to manufacturing the PSAHF, CWD manufactured one ~14 m long in-sodium ultrasonic scanner used for precisely locating the dislodged IFTM rail followed by manufacturing, delivery, installation, commissioning and operation of a remotely operated collapsible machine to extract the dislodged IFTM rail from the sodium pool of the IFTM cavity. While completing the PFBR works of priority, CWD also completed other committed works, including manufacturing of thermal switch, Nickel coil assembly, Anti Convection Barrier (ACB) plugs, modification of ISI plug, CSRDM and DSRM sleeves, FBTR CRDM lower part assembly etc. CWD maintains the highest precision and quality standards to conform to the stringent specifications and functional requirements under various codes, viz. ASME, ASTM, RCC-MR and ISO. CWD processes nearly 400 work orders on average every year to meet the demands of various users/ projects.

Electrical Services Division (ESD) has a mandate to provide adequate, high quality, reliable and uninterrupted power required for various needs of the research activities and the infrastructural requirements of the centre. To meet this, Electrical Services Division designs, constructs, operates, maintains and upgrades Electrical distribution system keeping in mind the system reliability & safety. The division is also responsible for providing state of the art intercom telecommunication services to the plant site as well as for Energy conservation in the Electrical sphere through auditing and implementing various energy conservation measures. At present the Electrical demand is 29 MVA which is catered by Electrical distribution network consisting of two numbers of 33 kV substations and 18 numbers 11 kV substations. Thanks to the foresight of the earlier planners, MAPS has been providing adequate, safe, reliable and quality power to IGCAR, BARC Facilities and GSO till date. Starting from an operating load of about 1.5 MVA during 1977 fed by one number 33 kV substation and five number of 11 kV substations, the load on the power system has grown to a level of 29 MVA fed by two number 33 kV substations and 18 number 11 kV substations. To meet the growing demand third power source with 230 kV/33 kV/11 kV, 50 MVA transformer at BHAVINI switchyard was commissioned in 2012. To evacuate this power along with this 33kV Indoor sub-station NCSS-2 was also commissioned in 2012. Main source for FRFCF is from NCSS-2. Moving further the transformer in the Second IGCAR feeder at MAPS was upgraded to 35 MVA in 2019 to meet the growing power demand.

Electrical Services Division (ESD) takes up steps in sync with the forecasted power demand of the centre. This ensures no new

facility waits for power to start operation. The ever growing Power system has shaped into a system with 4 sources and 20 substations and has opened up new challenges. ESD is fully geared up to meet all the challenges by progressive steps especially in the areas of monitoring and safety.

As part of the electrical infrastructure expansion at the North Plant Site, a 33 kV Switching station (33 kV Northern node) has been established to enhance power reliability and support future load growth. The substation is designed to receive power from two switching stations, 33 kV Central Switching Station (CSS) and NCSS-2 (33 kV Southern node) located near the Desalination Plant, and is fully integrated into the 33 kV Ring Main System (RMS) 33 kV Ring Main System will improve the reliability of IGCAR power distribution system. The Northern node consists of one number 33 kV switchboard, one number 12.5 MVA 33/11 kV transformer, 1.6 MVA 11/0.433 kV transformer and 11 kV switchboard. SCADA connectivity is made from the Northern node to the 33 kV CSS to monitor the real time power distribution data and its control.

Also, ESD undertook a comprehensive revamp of HV and LV Electrical systems. Revamping of Electrical system of Central Workshop (Phase-2), HASL, EID and IDEAS buildings are completed. To ensure reliability and safety, very Old Aluminium wirings were replaced with Copper wiring, the fuse DBs were replaced with Per- Phase Isolation (PPI) type MCB DBs that allow for selective isolation of earth leakage faults at the downstream level, limiting disturbances. To improve safety from external surges, surge protection is introduced at building level and in distribution boards. Old industrial panels were replaced with cubicle type Form IV-B enclosure switchgears. Electromagnetic relays are replaced with the state of the art numerical relays which can be used for the SCADA connectivity. HT Paper cables are replaced with the XLPE cables. ESD has taken up many Energy Conservation activities over the years. One of the major activities being taken up under this year was to establish a 600 kWp grid connected solar plant on various building roof tops. After the commissioning of this plant, the total solar generation capacity in IGCAR is 3.6 MWp and this is expected to save 65 Lakhs units of electricity annually. Energy Conservation is a continuing activity and many innovative ideas are being implemented in the journey. In the reporting year, ESG achieved an energy savings of 13% relative to the total energy consumption of IGCAR. The PV solar system contributes approximately 9.5 % of overall energy requirement in IGCAR, Kalpakkam.

ESG as a team is well set to take on the challenges pertaining to sustenance, augmentation and establishment of power & air conditioning systems at new projects of IGCAR. With a proactive approach all along, the group has initiated several measures to modernize the systems and processes. With the steps that are being carried out, ESG will be able to meet the challenging requirements and is moving ahead with an objective to sustain the path of excellence.

Fast Reactor Technology Group

Shri C G Karhadkar
Director, FRTG

Shri S. Chandramouli
AD, FRTG

Shri G. Vijayakumar
Head, DD&RSD

Shri V. Vinod
Head, ETHD

Dr. S. Joseph Winston
Head, RH&IED

Shri Sudheer Patri
Head, SE&CDD

Shri V. Ramakrishnan
Head, MF&SD

Shri . Ignatius Sundar Raj
Head, MF&SD

Shri Sanjay Kumar Das
Head, SED

Fast Reactor Technology Group (FRTG), mainly a Multi- Disciplinary and Multi-Faceted Engineering Group is involved in design, development and testing of fast reactor components. FRTG has proven expertise in all aspects of sodium technology particularly handling of sodium, sodium instrumentation, electromagnetic pumps, sodium purification equipment, different kinds of sodium valves, special inspection devices and operation and safety procedures concerning sodium systems. FRTG carries out design, fabrication, erection and operation of sodium test facilities for the development of sodium components.

Sodium Facilities Operations Division (SFOD) in FRTG has extensive experience in operating various sodium facilities in accordance with technical specifications and experimental requirements on a 24 x 7 basis. SFOD also takes care of decontamination of sodium components, disposal of sodium waste and sodium firefighting.Starting with the 500 kW facility, FRTG has built and operated several experimental rigs, including the Mass Transfer loop, Bimetallic Loop, Large Component Test Rig (LCTR), SILVERINA loop, Sodium Water Reaction Test Rig (SOWART), Steam Generator Test Facility (SGTF), Sodium Facility for Component testing (SFCT) and a newly added facility in Sodium Technology Complex (STC). Operation of carbon trap circuit for 750h, performance evaluation of 200 NB and 100 NB frozen seal globe valves , sodium testing of DSR armature cleaning mechanism tool, automatic plugging run experiments, testing and characterization of sodium flow fluctuations with 25 NB bypass Permanent Magnet Flow Meter (PMFM), testing and qualification of diaphragm type sodium pressure sensor, ex- vessel sodium level sensors and qualification of an Eddy Current Flow Meter (ECFM) probe, which was developed for measuring the sodium flow developed by Primary Sodium Pump are a few of the recent achievements.

Studies related to high temperature creep, fatigue, creep-fatigue interaction, etc., have been carried out on different types of material specimens in In-sodium Creep and fatigue facilities. Low cycle fatigue experiments on 316LN SS with 0.14% nitrogen content base material,,experimentsrelated to optimizing the aerosol sampling circuits for Sodium Aerosol Detectors, performance evaluation of Wireless Sensor Network (WSN) systems integrated with of sodium leak detection system in parallel mode of operation to hard wired systems,sodium compatibility of Inconel 625 specimens for chemical reactorsfor hydrogen production etc., are some of the activities.

Experimental Thermal hydraulics Division (ETHD) in FRTG is responsible for development of FBR components, sensors and processes related to FBR. Sodium and hydraulic experiments are performed towards the development, optimization and design validation of various reactor components. Recent works are such as, Characterization of Safety Grade Decay Heat Removal (SGDHR) System, Development of labyrinths and Honey Comb type Orifice Plate for core subassemblies, Hydraulic performance studies of core sub-assemblies, Development of gas entrainment mitigation devices, Development of components like sodium NRV, sodium Pressure measurement device, compact SG leak detection system, Artificial intelligence-based sodium leak detection , AI based plugging indicator, Optimization and indigenization of Bellow seal valves and Frozen seal valves for FBR, etc. Develops process schemes for PFBR like Secondary Cold trap in-situ regeneration, carbon removal from sodium etc. It is also providing service for machining and manufacturing small components for experimental requirements.

Comprehensive safety research towards reinforcing the design and accident mitigation strategies is going on in Safety Engineering Division(SED) where developmental activities such as Realistic simulation of accident scenarios to ascertain design safety margins, Parametric experiments for model validation, Development and qualification of material / device for strengthening design and operational safety. Works such as Realistic estimation of sodium leak through top shield platform in case of HCDA, Investigation on sodium boiling behaviour and associated bubble dynamics, Qualification of geo polymer-based sodium resistant concrete, Development and qualification of effective sodium fire extinguishant, Development of sacrificial layered core catcher etc are the notable current activities. The division manages In-house training program on sodium science and technology at IGCAR Sodium School also.

Device Development and Rig Services Division (DD&RSD) takes care of design and development of electromagnetic devices, instrumentation & electrical systems and sodium testing of various devices related to FBR. This division is involved in development of in-sodium sensors and electronics for sodium level measurement (CLP, DLP), sodium leak detection (MILD, SAD, ESPLD, wire type leak detector), development and testing of under sodium ultrasonic scanner, Permanent Magnet Flow Meters for sodium flow measurement, Electromagnetic (EM) Pumps, etc. DD&RSD is involved in the design, commissioning and maintenance of electrical and instrumentation systems of all sodium and hydraulic testing facilities in FRTG. Installation and commissioning of electrical and instrumentation system of new sodium facility at sodium technology complex, In-house fabrication & qualification of ultrasonic transducers, Performance evaluation of revamped USUSS of PFBR, Design, manufacturing and performance evaluation of Electromagnetic devices, are the recent major achievements.

Remote Handling and Irradiation Experiments Division carries outDevelopment of an indigenous remote inspection tool for PFBR SG,Development of an Indigenous remote inspection tool for Dissimilar metal weld inspection for PFBR (DISHA), Development and deployment of a Reactor Core Viewing System (RCVS) for remote core inspection etc. RHIED is equipped with facilities include LASER welding machine (Pulsed Nd-YAG system), Glove box with welding system, Electric Discharge Machine, Precision CNC milling machine, Precision drilling machine, Precision CNC lathe etc.

Sodium Experiments & Components Development Division (SE&CDD)played central role in the successful commissioning of various reactor components such as fuel handling machines (Transfer Arm and Primary Ramp & Primary Tilting mechanisms of IFTM), shutdown mechanisms (CSRDM and DSRDM), Core flow monitoring mechanisms, Sonar device, Start-up neutron detector handling mechanism, Under Sodium Ultrasonic Scanner, Failed fuel Location module etc. in PFBR.SE&CDDcarries out design, analysis, construction, erection and inspection of large sodium loops in FRTG, development of condition monitoring systems of reactor components.Present activities are directed towards developing robust systems for future FBRs& FBTR-II, development of third shutdown system, called Hydraulically Suspended Absorber Rod Mechanism, design and construction of a dedicated test facility for Sodium testing of large pumps of FBRs.

Mechanical Fabrication & Services Division deals with design and analysis of piping systems, fabrication and erection activities required for the sodium and hydraulic facilities, mechanical maintenance of all equipment, procurement and upkeeping of inventories and consumables etc.

FRTG also extends technical support to BHAVINI for successful commissioning as well as in the trouble shooting activities of systems in PFBR. It involves; Experimental and analytical investigation to examine the root cause of various commissioning issues, Sodium cleaning of large components, in- situcondition monitoring, Calibration of sodium sensors, Installation of remote sensors and robotic vehicles and its qualification, retrofitting of components etc.Moreover, FRTG extends its arena towards works on realising thermo-chemical cycle for hydrogen co-production with Fast Reactors. FRTG is committed towards indigenisation of fast reactor technology towards Atmanirbhar Bharat.

Materials Chemistry & Metal Fuel Cycle Group

Dr. V. Jayaraman
Director, MC&MFCG

Dr. Rajesh Ganesan
AD, F&MCG & Head, MCD

Shri T. V. Prabhu
AD, MFRG

Dr. K. Sundararajan
Head, ACSD

Dr. C. V. S. B. Rao
Head, FChD

Shri V. Suresh Kumar
Head, CF&ED

Dr. S Ghosh
Head, MFPD

Shri S P Ruhela
Head, PPED

Pioneering research and development in the domain of metal fuel and nuclear fuel cycle technologies is undertaken by the Materials Chemistry and Metal Fuel Cycle Group (MC&MFCG). The core activities of the group include establishing facilities for metal fuel pin fabrication, advancing pyrochemical processes for electro-refining spent metal fuels, producing radioisotopes, developing aqueous reprocessing methods for heavy metal recovery innovating novel liquid-liquid and solid-phase extractants, and nuclear waste management specifically designed for nuclear fuel cycle applications. The group also specializes in sodium chemistry, sodium removal/cleaning and the design and deployment of sensors critical to plant operations. Infrastructure augmentation and aging management, including seismic qualification meeting regulatory requirements, have been implemented to support all the R&D endeavors.

Significant developmental milestones include the preparation, characterization of metal fuel slugs, fabrication of sodium bonded metal fuel pins along with their successful test irradiation in the FBTR & progress towards sub-assembly construction. The production of metallic uranium via a high-temperature molten salt electro-deoxidation technique has been pioneered. Within the engineering-scale pyroprocess facility, key process steps, notably electro-refining and cathode product consolidation, have been demonstrated using un-irradiated sodium-bonded U-6% Zr pins. The design and synthesis of metal-organic frameworks (MOFs), covalent organic frameworks (COFs), graphene oxide-based adsorbents, phosphate and phosphonate solvents, and task-specific ionic liquids have extended the material innovation portfolio. These novel materials are pivotal for the selective extraction of actinides and fission products, thereby addressing challenges in sustainable nuclear waste management and actinide recovery technologies. Preliminary on-field trials were performed successfully on the H_2S sensor system developed indigenously. Furthermore, a novel online electrochemical sensor for hydrogen measurement in Pb-Li alloys, a tritium breeder in fusion reactor blanket systems for Institute of Plasma Research has been designed and fabricated. Microcontroller based Instruments for Hydrogen in Argon Detector (HAD) and Hydrogen in Sodium Detector (HSD) have been developed indigenously, installed and commissioned in PFBR.

A landmark isotope production milestone was realized with the first successful production of Phosphorus-32 at FBTR, which was formally handed over to BRIT, Hyderabad, for application in various domains. The Analytical Sodium Chemistry Loop (ASCL) has been revamped and re-qualified after years of service through concerted efforts, significantly enhancing its operational reliability. MC&MFCG continues to provide essential analytical and radio-analytical support to ongoing programs within IGCAR and across DAE units. Advanced analytical methodologies capable of quantifying bulk to ultra-trace elemental compositions in complex matrices,

including metal fuel and samples from pyrochemical processing, have been developed. Isotopic compositions of boron and heavy metals from reprocessing streams are accurately measured, alongside precise assays of primary and secondary sodium. An emission spectroscopic method has been developed as an effective alternative to mass spectrometry for determining boron isotopic composition in boron carbide. Fundamental R&D is advanced through matrix-isolation spectroscopy studies exploring molecular conformations and non-covalent interactions such as pnicogen and tetrel bonding. Complementary computational studies on lanthanide and actinide complexes are being conducted to deepen understanding of their solvent extraction mechanisms, providing a foundation for future innovations in nuclear separations.

Materials Science Group

Dr. Anish Kumar
Director, MMG

Dr. R. Nagendran
Head, S&DTD

Dr. Awadhesh Mani
Head, CMPD

Dr. S. Tripurasundari
Head, S&SSD

Dr. Christoper David
Head, D&DSD

The Materials Science Group (MSG) comprises of Defects and Damage Studies Division, Condensed Matter Physics Division, Surface & Sensors Studies Division and SQUID & Detector Technology Division. Scientists of MSG work on research problems spanning from the studies of irradiated defects in nuclear materials, high pressure and temperature induced phase transitions in condensed matter systems, developing thin film coatings for tribological applications, and SQUID based MEG applications. Details of the research activities are as follows.

Defects and Damage Studies Division (DDSD) focuses on studies of defects, defect-impurity interactions in reactor structural materials, supplemented by computations. Ion beam radiation damage studies are carried out using a 1.7 MV tandem accelerator and a 400 keV in-house built linear accelerator in single or dual ion beam modes of irradiation to study defects and radiation response in materials relevant to fusion and fission reactors. Defects, particularly open volume defects such as vacancies and their clusters, are studied using positron annihilation spectroscopy. Positron beam based Doppler broadening studies have been used mainly for depth-resolved defects studies in irradiated materials. Ion beam based characterization techniques such as high-resolution RBS, channelling are being used extensively in addition to ion beam induced luminescence studies. Irradiation creep studies are being planned with proton beam of energy 2-3 MeV and high beam current. Various experimental results related to defects are analyzed using detailed computations with a variety of simulation and ab-initio codes. High speed cluster computers at IGCAR are being extensively utilized for computation of materials properties.

SQUID & Detector Technology Division (SDTD) focuses mainly on using SQUID based systems for applications. Magneto-Cardiography (MCG) and Magneto-Encephalography (MEG) have been successfully designed, assembled, standardized and used for clinical studies. Further, SQUID based measuring systems such as high field SQUID magnetometer, SQUID VSM, SQUID based set-up for Non- Destructive Evaluation (NDE) have been developed. SDTD also carries out intense research activities related to using SQUID based time domain electromagnetic measurements (TDEM) and geophysical explorations using TDEM. Another major thrust research area of this division is the development of gamma irradiation detectors. Towards this, the researchers have grown highly resistive CdZnTe single crystals and developed a gamma detector for pulse height spectroscopic studies. This research activity is being actively pursued to develop compact semiconductor based detectors with enhanced efficiency and technologically important single crystals for detector applications.

Condensed Matter Physics Division (CMPD) pursues several theme based research programs; investigation of structure and

physical properties of materials under extreme conditions such as high pressures, low temperatures, high temperatures and high magnetic fields. Recently the team of CMPD established High Pressure – High Temperature (HP-HT; ~ 25 GPa & T ~ 10000 C) XRD facility at Beamline 12, Indus-2, RRCAT to facilitate synthesis of novel phase, study kinetics of phase transition, generating phase diagram at HP-HT, and to determine thermal expansion co-efficient with pressure. The systems under investigation encompass nuclear materials, superconductors, strongly correlated systems, magnetocaloric materials, topological insulators, multiferroics, energetic materials, frustrated systems, f-electron based intermetallics and oxides, glasses and super hard transition metal borides. Research is also pursued to investigate emergent phenomena and proximity effects in heterostructures. Dynamic light scattering and confocal microscopy are utilized for studies on soft condensed matter. Optical trapping and manipulation of mesoscopic particles using holographic optical tweezers (HOT's) to study inter-particle interactions in colloidal suspensions/ biological systems are being pursued. Besides there is also an intense effort towards quantum metrology based research studies using entangled photons.

Surface & Sensors Studies Division (SSSD) focuses on studies of monolithic and multilayered thin films and nanostructures using a variety of techniques such as secondary ion mass spectrometry, nanomechanical testing, Focused Ion Beam (FIB) based nanostructuring and nanopatterning, Scanning Probe Microscopy based characterization of various electrical and mechanical properties at nanoscale, nanospectroscopy with tip enhanced Raman spectroscopy (TERS) and Nanoscopy with near-field scanning optical microscopy (NSOM) imaging at sub-diffraction limit using polarized light. The division also specializes in high temperature triblological studies of structural materials as well as novel nano- and micro-crystalline diamond thin films. Exotic carbon nanostructures of vertical graphene based supercapacitor research is also being pursued for energy research. Furthermore, development of novel nanomaterials of 0D transition metal oxide (TMO), 1D noble metals and nitrides, 2D TMOs, and transition metal dichalcogenides (TMDs) for advanced sensor applications is being carried out. Research activities relating to ultra-sensitive sensors based on micromachined silicon and silicon oxide cantilevers and surface doped diamond thin film are also being pursued.

Metallurgy and Materials Group

Dr. Anish Kumar
Director, MMG

Dr. M. Vasudevan
AD, MD&TG

Dr. S. Ningshen
Head, CS&TD

Dr. Arup Dasgupta
Head, PMD

Dr. V. Karthik
Head, PIED

Dr. A. Moitra
Head, MJ&MMD

Dr. A. Nagesha
Head, MMD

Metallurgy and Materials Group (MMG) is pursuing a vibrant research and development programme for comprehensive knowledge-based solutions to materials issues of critical importance to India's road-map for fast reactor and associated fuel cycle programmes. In addition, in the recent past, the Group has significantly contributed to the development of high temperature materials and related technologies for national programmes and has continued to support strategic sectors.

The R&D activities of MMG are manifold. They encompass the design, indigenisation and field realization of new and indigenous material choices and process modifications mandated by emerging demands on design reliability. The Group has been spearheading a mix of basic and directed cross-disciplinary research activities under various themes and is equipped with state-of-the-art research facilities on multiple fronts. The current portfolio of MMG includes:

(i) Generation of design data of nuclear and high-temperature materials towards qualification of fast reactor structural materials and their welds, and production through industry

(ii) Development of high-performance materials for enhancing target burnup, coatings & characterization techniques for FBRs & future reactor concepts, such as metallic fuel reactors, high temperature reactors and small modular reactors

(iii) Component manufacturing initiatives for current and future FBRs, including advanced materials processing and joining methods, special nuclear materials fabrication, hard-facing and coatings, and technologies for FBR and fuel reprocessing programme

(iv) Research and development on corrosion protection and advanced coating technologies for hostile environments such as liquid sodium, molten salts, nitric acid, molten lead, steam-water and sea water for applications in FBR and associated reprocessing plants

(v) Development of advanced NDE methodologies for detection and characterization of flaws, microstructure, deformation, inspection and health monitoring of structures and components of FBR and associated fuel cycle

(vi) Post-irradiation examination for performance assessment and research on fast reactor fuels and structural materials, and failure analysis of components from active facilities.

With the FBTR continuing operations at full power during the year, continuing materials irradiation has taken place with greater focus towards metallic fuels and associated structural materials. Accordingly, post-irradiation examination of Enriched Uranium-Zirconium (EU-6Zr) fuel pins test irradiated in FBTR up to 26.5GWd/t burnup revealed an axial fuel swelling of ~10% and complete closure of fuel-clad gap. Also, the residual ductility and swelling of T91 clad do not pose any concern for enhancing the burn-up of other ternary metal fuels pins under test irradiation in FBTR. The hot cell facility has also catered to dismantling FBTR sub-assemblies and providing fuel pins for the first hot run of DFRP and for sustaining subsequent campaigns. The Group has continued to facilitate progress in commissioning of PFBR with rigorous experimentation, characterization, weld process development and quality assurance procedure development, development of novel non-destructive evaluation methodologies for under-sodium inspection in PFBR, corrosion assessment / mitigation, and surface modifications. To understand the root cause of obstruction in the movement of the transfer pot, an Under Sodium Ultrasonic Scanner was designed and deployed, to visualise the internals of the Primary Tilting Mechanism (PTM) of Inclined Fuel Transfer Machine (IFTM) of PFBR, which revealed that one of the two 31° tilting rails has got dislocated. Based on the comprehensive 3D ultrasonic image generated, the dislodged rail could be extracted from the PTM without draining the sodium and the fuel loading could be initiated through vertical loading. Ag-Al Fusible Plugs as electric circuit breaker for SGDHR System and vacuum brazing technologies for dissimilar metal joints of DSRDM and Temperature-Sensitive Electric Switch components, using BNi-6 braze filler alloy have been developed indigenously for FBR applications.

Besides these activities, R&D studies pursued in MMG include (i) development of functionalised magnetic nanoparticle ensembles for a variety of technological and societal applications, (ii) materials mechanics studies for structural integrity assessment of FBR components, (iii) mechanistic understanding of damage under tensile, creep, fatigue, and creep-fatigue interactions including development of novel test set-up for performing high temperature biaxial ratcheting fatigue experiments on small specimens and in-house software to visualize the evolving nature of dynamic strain ageing (DSA) of reactor structural materials, (iv) plasma sprayed coatings for metal fuel melting and pyro-reprocessing applications, (v) development of self-cleaning superhydrophobic coatings on steel with improved bio-fouling resistance and (vi) small specimen testing for determination of tensile, impact and fatigue properties. The Group has embarked on development of medium chromium oxide dispersion strengthened steels and multi stabilized stainless steels for fuel clad tubes for future FBRs, post-irradiation examination of ternary metallic fuels, control rods and Nickel reflectors irradiated in FBTR, and qualification of various advanced structural materials through test irradiations in FBTR. Our expertise in non-destructive evaluations and consequent repair welding has been sought and provided to NPCIL plants. State-of-the-art electron microscopy facilities have been applied to cutting-edge physical metallurgy and materials research, notable being establishing the bonding characteristics of complex nanoscale magnetic materials. Under the banner of Homi Bhabha National Institute (HBNI), research scholars are pursuing doctoral and post-doctoral research on a variety of challenging topics in radiation damage, post-irradiation electron microscopy, small specimen test development, high-temperature materials and coatings, development of NDE techniques and sensors, materials and process modelling, to name a few areas. The group actively collaborates with eminent academic and research institutions in India and abroad on a range of metallurgical and materials topics. Several members of the Group have been conferred with national and international recognitions.

Reactor Design Group

Dr. K. Natesan
Director, RDG

Shri U. Parthasarathy
AD, NSDG

Shri V. N. Sakthivel Rajan
Head, CH&MD

Shri L. Satishkumar
Head, PPCD

Shri Sriramachandra Aithal
Head, RC&AD

Shri Amzad Pasha
Head, SHTD

Dr. D. Sunil Kumar
Head, RSATSD

Smt. T. Sathiyasheela
Head, RND

Shri S. D. Sajish
Head, RND

Dr. R. Sureshkumar
Head, TH&HTAD

Reactor Design group (RDG) is responsible for the design, structural & thermal hydraulics analysis, core safety & plant dynamics analysis, structural dynamics experiments including seismic testing, and manufacturing technology development of Fast Breeder Reactor (FBR) components/ systems. The RDG made wide-ranging contributions during 2025 in reactor design, safety analysis, experimental validation, and operational support for FBTR. Major activities included sustained support to PFBR commissioning, optimisation and life-extension studies for FBTR, and conceptualisation and design of FBTR-2 and future commercial fast breeder reactors, reflecting strong integration across multiple specialised domains.

With respect to support for PFBR commissioning, fuel-loading and first-approach-to-criticality calculations have been carried out. Detailed neutron and gamma shielding analyses, covering penetrations, biological shields, in-vessel and ex-vessel fuel handling systems have been performed. Level-1 Probabilistic Safety Analysis (PSA) for internal events developed for PFBR has been cleared by AERB as mandatory documentation for First Approach to Criticality. A major milestone with respect to rectification of issues in PFBR has been the redeployment of the Under-Sodium Ultrasonic Scanner following extensive damage. Core thermal-hydraulic studies established flow characteristics for the PFBR-BOC-1 core, enabling improved prediction of subassembly outlet temperatures for validation during power operation. Analytical studies carried out have evaluated containment thermal behaviour under postulated aircraft-crash-induced fuel-fire scenarios. Several operational challenges were resolved, including clearing of flow blockages in NaK bubblers, assessment and improvement of resin-transfer systems, parametric type-testing of snubbers, and refurbishment of containment isolation dampers and emergency diesel generator based fire-water systems. Continuous technical support was provided for commissioning, operation, and maintenance of sodium and auxiliary systems, including evaluation of on-site modifications and revision of alarms and trip logics. With respect to development of alternative fuel handling concept, a permanent transfer pot was designed, manufactured, tested, and installed to enable reliable in-vessel fuel handling when standard transfer routes are unavailable.

A new portable subassembly handling flask was also developed and deployed to support initial fuel-loading operations. Extensive electrical, mechanical, and balance-of-plant engineering support was provided for PFBR, including pump-foundation and piping design, power-protection and relay-setting recommendations, emergency diesel generator upgrades for regulatory compliance, seismic-qualified battery replacement, and preheating-system designs.

With respect to isotope production in FBTR, scheme for Pu-238 production from Np-237 has been established. Fuel management studies showed that optimised shuffling between the ninth and tenth rings can extend the residence time of thoria subassemblies in FBTR.

Further, RDG is evolving conceptual design of a hybrid fuelled (ternary metal and mixed carbide) test reactor FBTR-2, planned to be launched after FBTR. Optimisation of reactor core and safety analysis of the hybrid concept along with the estimation of reactivity feedback coefficients and decay-heat has been taken up. The conceptual design of loop-type reactor assembly with a main vessel diameter of 7.48 m has been finalised. An integrated layout for FBTR-2 together with its metal-fuel-cycle facility has been developed. Process design studies also examined coupling of FBTR-2 sodium systems with hydrogen co-generation using a Cu–Cl thermochemical cycle. Design-verification testing of temperature-sensitive switches and preliminary sizing of compact control and safety-rod mechanisms were completed. Preliminary layouts of turbine, boiler, and electrical buildings were prepared, condenser-cooling options evaluated, budgetary quotations obtained, and preliminary cost estimates developed.

Several R&D studies for FBR design have been taken up which include experimental and computational investigations performed on aerosol generation, transport, and deposition during sodium-fire scenarios using large-scale test facilities and CFD tools, providing a sound basis for future three-dimensional in-containment aerosol modelling. Important experimental programmes in the rector neutronics domain included self-shielding measurements, neutron and gamma shielding studies in SiC, decay-power measurements in uranium and thorium. The oxide-fuel transient analysis code ASTRA was upgraded to include thermo-mechanical fuel-pin behaviour under transient conditions. Computational tools for safety analysis under Design Extension Conditions and applied research in high-temperature structural design, addressing creep, fatigue, fracture, ratcheting, and failure analysis have been carried out through experiments and simulations. These activities were supported by the Structural Mechanics Laboratory, which houses state-of-the-art prototype-scale facilities. RDG operates India's largest multi-axial earthquake shake table and conducted seismic qualification experiments and R&D studies in support of DAE programmes. RDG also collaborated with academic and R&D institutions, supported HBNI-linked projects, and participated in IAEA Coordinated Research Projects.

Reactor Facilities Group

Shri S. Sridhar
Director, RFG

Shri P. Sreenivasa Rao
Head, QA&ISD

Shri G. Muralitharan
Head, RMD

Shri M. Thangamani
Head, ROD

Shri S. K. Prasad
Head, TSD

Shri M. S. Koteeswaran
Head, T&HRDD

Reactor Facilities Group (RFG) is responsible for safe operation of Fast Breeder Test Reactor (FBTR), KAMINI Reactor and Interim Fuel Storage Building (IFSB). FBTR has been operating at design power level of 40 MWt with 69 Mark-I subassemblies and 4 poison subassemblies (to maintain the required shutdown margin) in the core and completed four successful irradiation campaigns at 40 MWt with turbine- generator generating ~10 MWe connected to the grid. Utilizing the reactor for irradiation of advanced fuels & structural materials for fast reactors and conducting safety related experiments form major goals of FBTR. FBTR is also used for the production of Strontium-89 &Phosphorous-32isotopes for medical applications. KAMINI Reactor has been extensively used for neutron radiography, activation studies and testing of indigenously developed neutron detectors. RFG is also responsible for fabrication and safe storage of fuel, blanket, source and control subassemblies for PFBR. All the required number of assemblies for the first core of PFBR have already been fabricated and stored safely in IFSB with all security surveillance measures and safeguards. The training division of the group is responsible for training the O&M staff of FBTR, PFBR and future FBRs. RFG has also taken part in the operational safety review of PFBR project.

Reprocessing Group

Dr. V. Jayaraman
Director, RpG

Dr. K. A. Venkatesan
AD, RDRDG

Shri M. Geo Mathews
AD, RpSG

Shri N. Krishnan
Head, NSVSD

Shri J. Kodandaraman
Head, PDRHCSD

Shri P. Varadharajan
Head, TSRD

Shri. M.S. Gopikrishna
Head, RpMD-E

Shri M. Dhananjeyakumar
Head, RpMD-M

Shri Surajit Halder
Head, COTMFRD

Shri Kinkar Mandal
Head, PRCOD

The primary mandate of the Reprocessing Group (RpG), IGCAR, is to reprocess spent nuclear fuel discharged from the fast breeder test reactor and to establish the technology for reprocessing advanced fast reactor fuels, comprising both heavy metal mixed carbide and oxide. The significant activities of RpG focus on the design, construction, commissioning, and operation of fast reactor fuel reprocessing plants, which are based on extensive reprocessing experience and sustained research and development activities in this field. This group comprises a CORAL (Compact facility for Reprocessing Advanced fuels in Lead cells) facility, the Demonstration fast reactor Fuel Reprocessing Plant (DFRP), various divisions for supporting the mechanical, electrical, electronics, and instrumentation & control engineering of the plant, and a research facility for carrying out advanced research on fast reactor fuel reprocessing. The CORAL facility has been operating successfully since its commissioning in 2003, reprocessing the mixed carbide spent fuel discharged from the FBTR. The facility continues to serve as a test bed for reprocessing and provides valuable feedback for the design and construction of subsequent reprocessing plants. The mandate of DFRP is to reprocess the FBTR spent fuel at a plant scale, and also demonstrate the reprocessing of spent fuel sub-assemblies of PFBR. The facility was hot commissioned in April 2024, and so far, it has completed the limited hot run campaigns, with the approval of AERB, which involved the reprocessing of spent nuclear fuel discharged from FBTR (155 GWd/Te). It was noted that the plant systems have been performing exceedingly well. Based on this observation, the facility is gearing up to obtain the license from AERB for regular operations. The commercial-scale reprocessing plant, Fuel Reprocessing Plant (FRP), is being constructed at the Fast Reactor Fuel Cycle Facility (FRFCF) for reprocessing spent fuel discharged from the prototype fast breeder reactor (PFBR). The reprocessing group is responsible for

providing the design inputs for the first-of-its-kind equipment to FRP. In addition to the above, focused research and developmental activities are being pursued, but not limited to, the development of advanced equipment for reprocessing, improved PUREX process flow-sheets, indigenous code and software development for fast reactor reprocessing, methods and materials for minor actinide partitioning, recovery of valuables from the radioactive waste notably ^{90}Sr and ^{237}Np, which have been achieved recently, and fabrication and supply of radiation resistant materials etc., at RpG

Safety, Quality & Resource Management Group

Shri C. G. Karhadkar
Director, SQRMG

Dr. Vidya Sundararajan
AD, SQRMG

Shri Vimal Kumar
HEAD, TC&QMD

Dr. S. Ganesamoorthy
HEAD, RA&TD

Shri J. Rajan
Head,SI&IND

Dr. S. Chandrasekaran
Head,H&ISD

Dr. K. V Rajkumar
Head,QAD

Smt L. Srivani
Head, EAD

Shri S. Vijayaraghavan
Head, PHRMD

Safety, Quality & Resource Management Group (SQRMG) at IGCAR is entrusted with overseeing health, radiation, and industrial safety; conducting environmental impact assessments; managing financial and human resources; providing scientific information services and campus-wide networking support; facilitating public outreach; and delivering quality assurance and technical coordination services to IGCAR.

This group comprises of Environment Assessment Division (EAD), Health and Industrial Safety Division (HISD), Planning and Human Resources Management Division (PHRMD), Quality Assurance Division (QAD), Radiological Applications & Technology Division (RATD), Scientific Information and Networking Division (SIND), and Technical Coordination & Quality Management Division (TC&QMD).

Environment Assessment Division (EAD) is responsible for environmental modelling and impact/dose assessment for radiological and chemical contaminants in air, water, and sub-surface geological media, atmospheric dispersion modelling, internal and external dosimetry, and baseline surveys of naturally occurring radioactive materials (NORM). EAD enhances emergency preparedness by deploying the ONERS system and integrating Online Isotope and FPNG Monitors for real-time radionuclide detection, while advancing atmospheric monitoring through state-of-the-art facilities such as a C-band Doppler Weather Radar and a 200 MHz mid-tropospheric wind profiler. The division also conducts continuous monitoring of meteorological parameters, ocean waves, and currents to provide forecasts for cyclones and extreme wave events. The division provides uninterrupted TLD-based personnel monitoring services to all active facilities of IGCAR, along with need-based biodosimetry services using dicentric, CBMN, and FISH-based translocation assays. It develops methodologies for retrospective dose estimation employing both physical and biological dosimetry techniques and conducts in-vivo and in-vitro monitoring of occupational workers during routine operations and emergency situations in accordance with AERB and NDMA guidelines. An Integrated Radiation Monitoring Facility has been established at Anupuram to support these activities. EAD also pursues R&D on low-dose effects of ionizing radiation, the development of novel biomarkers for rapid dose assessment, and the creation of new dosimetry materials, tools, and methodologies for accurate and reliable dose estimation under normal and emergency conditions, including phantom development. In addition, the division undertakes environmental studies on radionuclide transfer in marine and terrestrial ecosystems, dose assessment for marine biota, and green-cover and biodiversity development, thereby supporting environmental protection, radiological safety, and sustainable ecosystem management.

Health and Industrial Safety Division (HISD) ensures radiological protection and workplace safety by providing mandatory radiation monitoring services using advanced technologies to control external and internal exposures. It carries out continuous radiological surveillance, dose assessment, workplace monitoring, and contamination control in line with AERB standards. HISD further strengthens industrial and fire safety through systematic audits, hazard and risk analyses, job-safety studies, plant safety inspections, and regular emergency drills. To promote a strong safety culture among employees, the division conducts industrial and fire-safety training, first-aid and height-pass tests, and periodic medical examinations at the Occupational Health Centre.

Planning and Human Resources Management Division (PHRMD) is responsible for formulating and monitoring capital projects towards project planning and management, preparing annual budget requirements for IGCAR and GSO, and coordinating fast-track projects. The division is mandated to conduct the academic programmes of HBNI at the Constituent Institution, conduct stipendiary training programmes for Category I & II trainees and organize orientation programmes for newly inducted officers. It also oversees the automation and integration of administrative functions, including human resources, accounts, stores, budget, and procurement, through web-based platforms for IGCAR, GSO, MRPU, AERB, and DAE HQ. This division facilitates the induction of Research Scholars, Research Associates, and Visiting Scientists; coordinates visits of dignitaries and delegations; and formulates & facilitates collaborations. It supports project work for postgraduate students, practice school programmes for students from BITS, and organizes various training and outreach initiatives, including industrial visits for students and teachers from schools and colleges across the South Indian region, as well as coordination of classroom training for work assistants. This division serves as the nodal interface with DAE for PRIS(G) and PRIS(O) targets, institutional collaborations, and responses to queries from Parliament, audit agencies, RTI, and other regulatory bodies. It is also responsible for collating and submitting documents such as monthly PM reports, quarterly DAE reports, the DAE Annual Report, allowance reports, and brief notes for parliamentary sessions, ensuring timely monitoring, record-keeping, and reporting of IGCAR's institutional and project-level achievements. Additionally, the division facilitates professional development of IGCAR employees through initiatives such as the Integrated Government Online Training (iGOT) Karmayogi platform.

Radiological Applications & Technology Division (RATD) focuses on R&D activities in the areas of, radiation safety through modelling & simulation; thermal imaging and Terahertz imaging related studies for medical / industrial applications, growth of technologically relevant single crystals towards device fabrication. The notable among them are CdZnTe single crystal based gamma-ray spectrometer with an achieved energy resolution of 2.8% at 661 keV of 137Cs and PZN-PT piezo crystal based piezo transducers. Besides the R&D activities, the other services provided by RATD includes gamma irradiation services for R&D studies in nuclear, agricultural and medical fields; radiometry services for shielding integrity evaluation; radiation calibration services to gamma and neutron measuring instruments including contamination monitors; testing the efficiency of HEPA filters for all active labs of IGCAR etc.. The other important mandate of RATD includes conducting public awareness programmes on nuclear energy and DAE's activities for schools, colleges and general public across the southern region of the country. An IGCAR-DAE information Centre is being set up at Chennai to create awareness to students and general public on the beneficial applications of Nuclear Energy.

Quality Assurance Division (QAD), is primarily responsible for catering quality assurance, inspection, Nondestructive Testing (NDT) and quality audit activities during fabrication, construction, commissioning/operation of fast breeder reactor (FBTR, PFBR) and associated reprocessing (CORAL, DFRP, FRFCF and Pyro) plants. This division provides seamless support for the technology development activities of future FBR's. QAD also provides comprehensive structural health assessment of System, Structure and Components (SSC) of these plants focusing on establishment and implementation of an effective quality management system. In addition to this, QAD also extends its expertise to various DAE units and to other strategic sectors.

Scientific Information and Networking Division (SIND) focuses on acquiring scientific resources, disseminating knowledge, and preserving information. It provides seamless access to library databases, online journals, and institutional repositories to support research and academic activities, with services available round the clock remotely and at patrons' desktops. SIND also offers reliable internet and email facilities to the scientists and engineers of IGCAR, BARC-F, BHAVINI, GSO, DPS, MRPU, SRI, and UGC-DAE CSR, maintains the campus-wide networking infrastructure, and ensures compliance with information security and cybersecurity standards.

Technical Co-ordination & Quality Management Division (TC&QMD) is primarily responsible for quality control and manufacturing process development of equipments for IGCAR, manufactured in the western region of the country. It provides Technical co-ordination services for the centre with BARC, DAE- Mumbai and its other units. TC&QMD also participates in R&D activities which are being carried out at BARC towards meeting the mandate of IGCAR, FRFCF/NRB & PFBR and Public outreach programmes in the Western region of the country.

Incubation Centre

Dr. N. Subramanian
Head, Incubation Centre

DAE Incubation Centre registered as "AIC-IGCAR-FAST Foundation"

The DAE Incubation Centre at IGCAR, registered as AIC-IGCAR-FAST Foundation, continued its activities during the year. In 2025, MoUs were established with HBNI, Startup TN, and AIC-PECF (Puducherry). An IGCAR-patented technology, remotely operated self-locking fixture for wall-mounted equipment in contaminated enclosures was transferred to a start-up firm, this year.

Accounts

Shri S. A. Murugesan
IFA

Smt Anita Suresh Kunder
SAO

Administration

Shri Paresh Nath Mahadani
CAO

Dr. V. A Lalita Prasad
A O (L, G&R)

Shri P.T. Mani
AO-III (E & V)

Organisation Chart - IGCAR

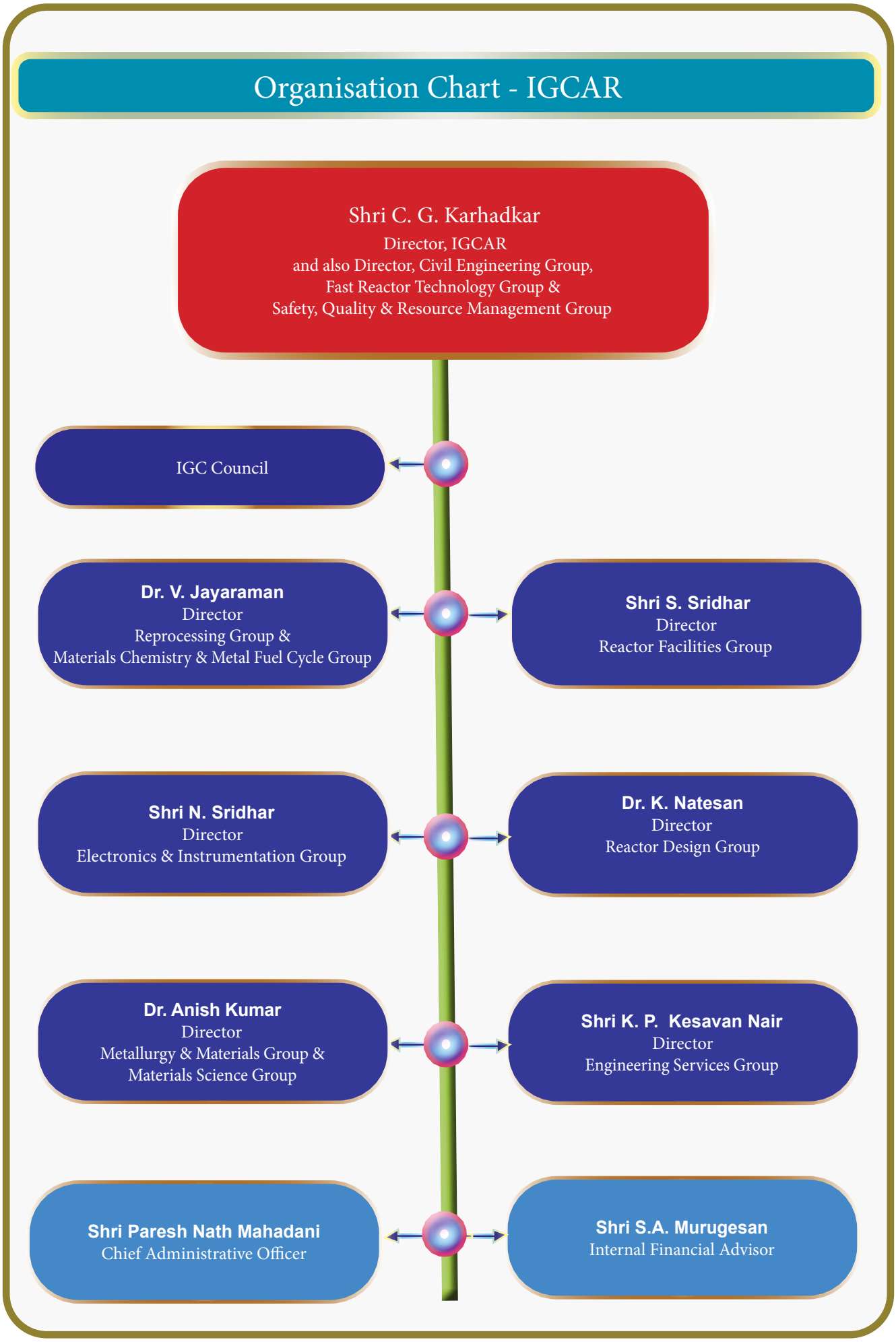

Civil Engineering Group

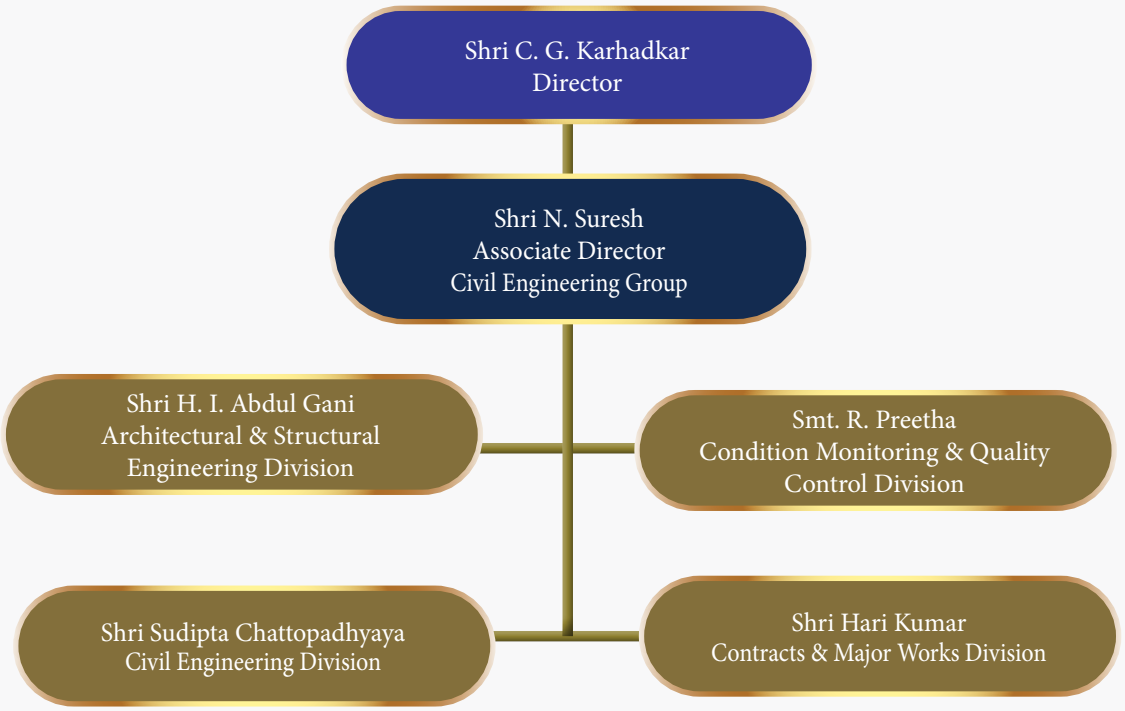

Electronics & Instrumentation Group

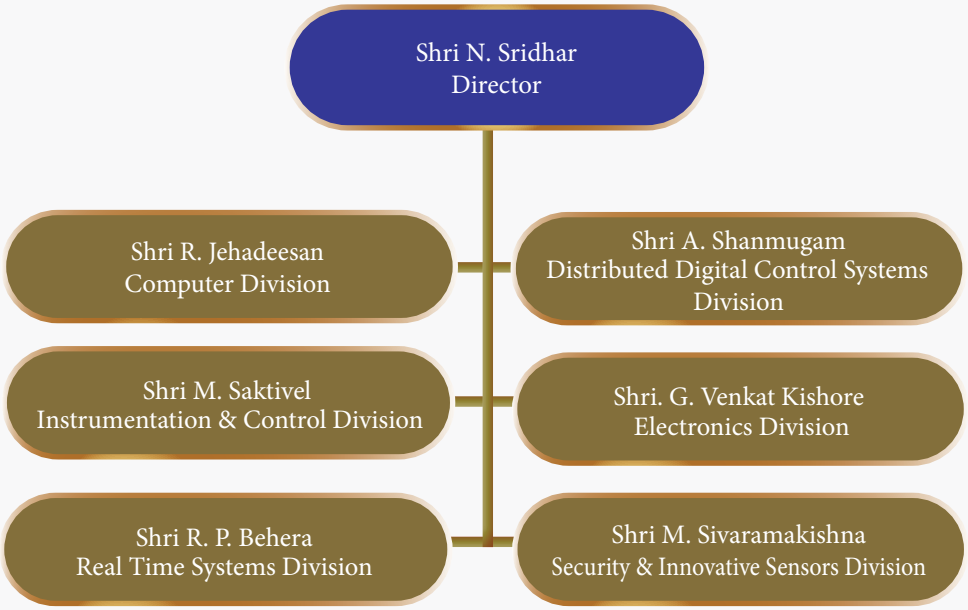

Engineering Services Group

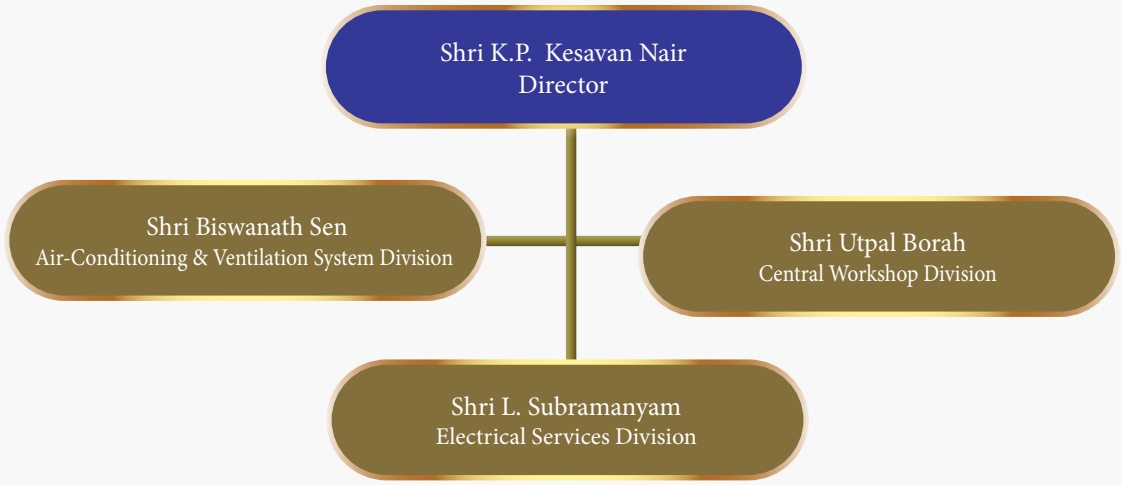

Fast Reactor Technology Group

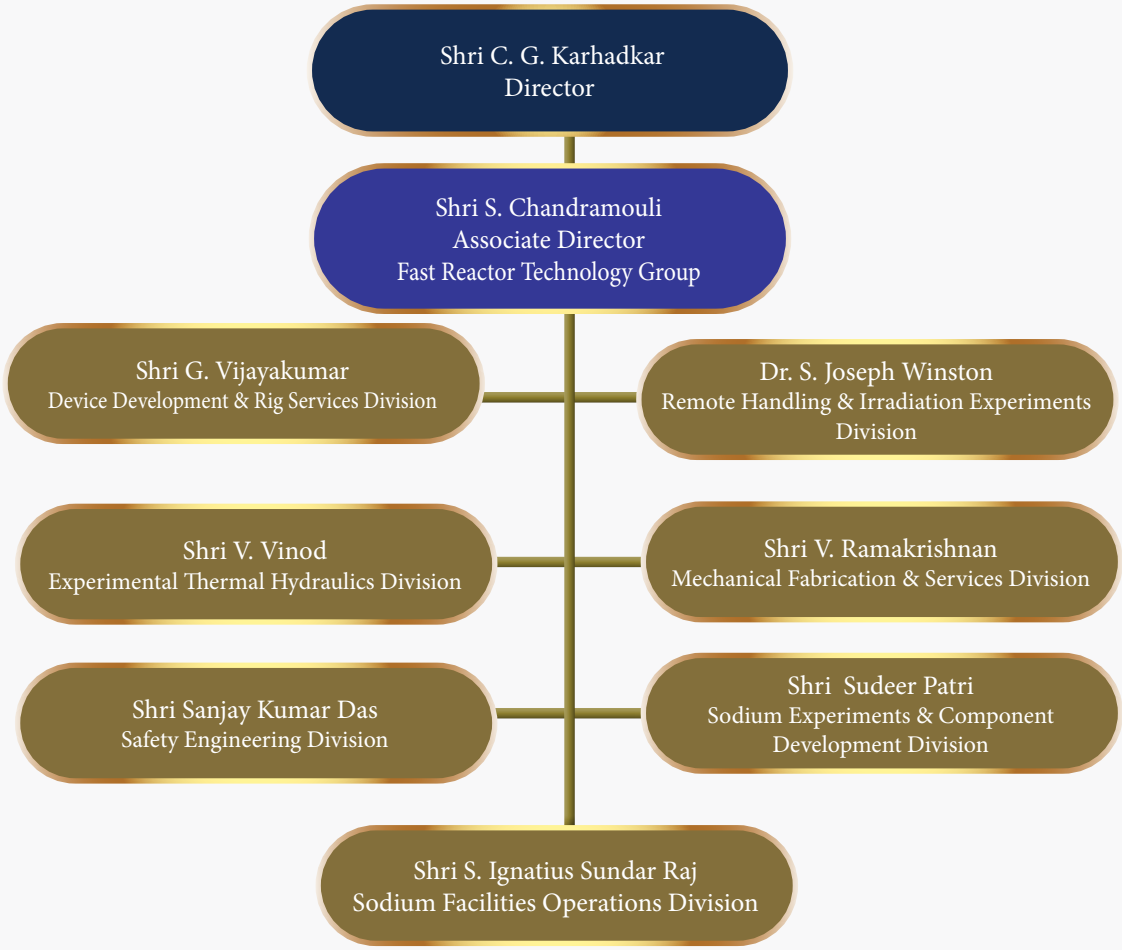

Materials Chemistry & Metal Fuel Cycle Group

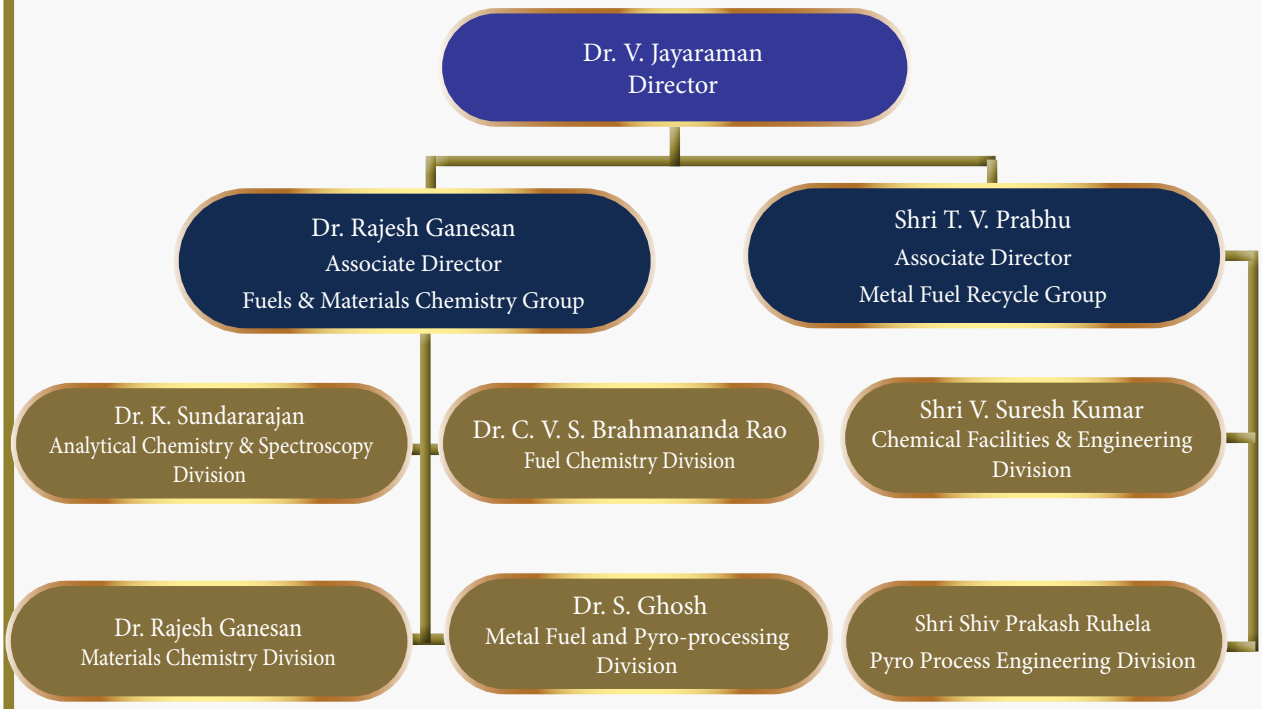

Materials Science Group

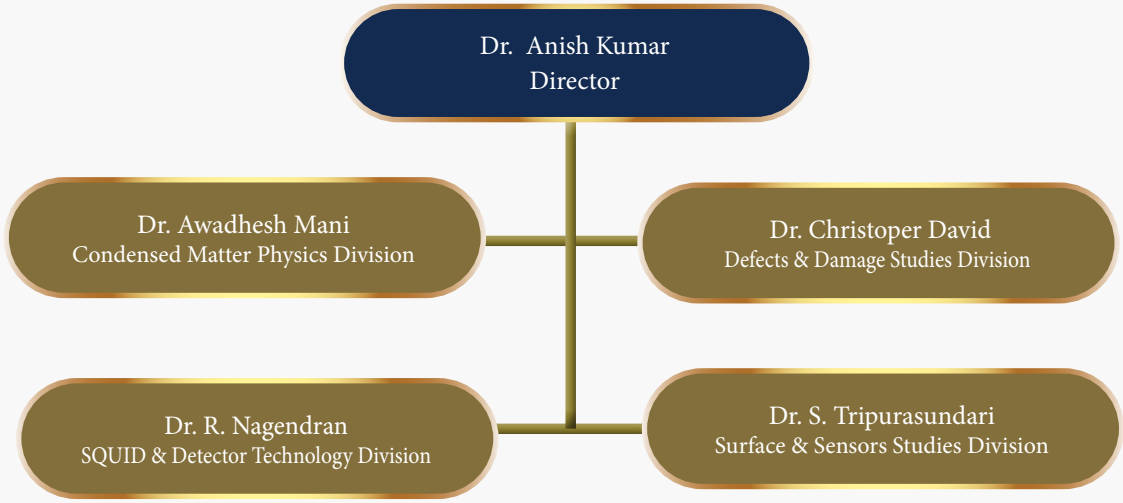

Metallurgy & Materials Group

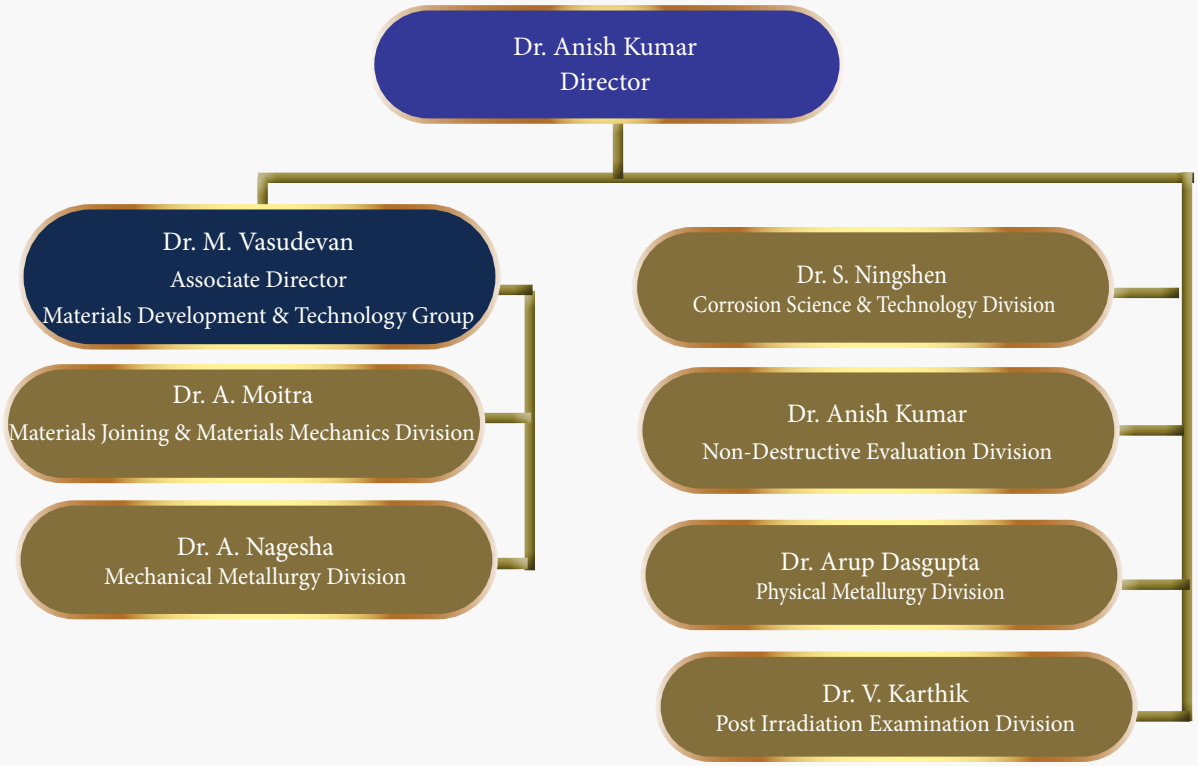

Reactor Design Group

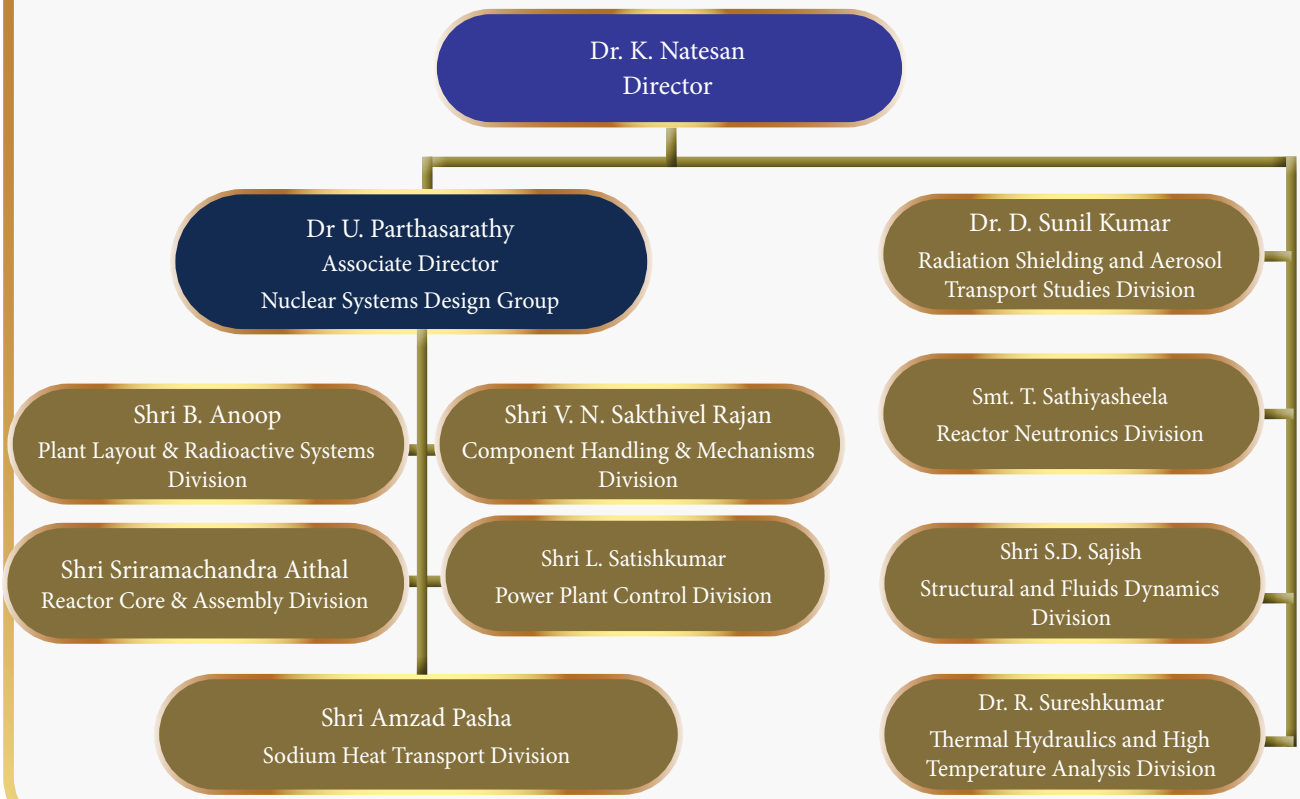

Reactor Facilities Group

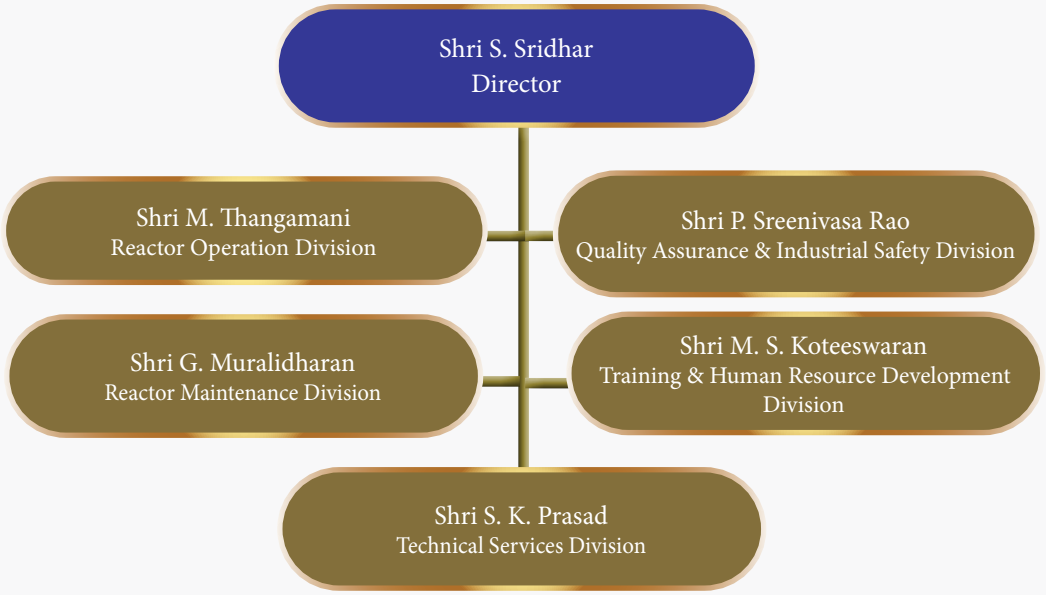

Reprocessing Group

Safety, Quality & Resource Management Group

Shri C. G. Karhadkar
Director

Dr. Vidya Sundararajan
Associate Director
Safety, Quality & Resource Management Group

- Dr. S. Chandrasekaran — Health & Industrial Safety Division
- Shri J. Rajan — Scientific Information & Networking Division
- Smt L. Srivani — Environmental Assessment Division
- Shri Vimal Kumar — Technical Coordination & Quality Management Division
- Dr. S. Ganesamoorthy — Radiological Applications & Technology Division
- Shri S. Vijayaraghavan — Planning & Human Resource Management Division
- Dr. K. V. Rajkumar — Quality Assurance Division

Incubation Centre

Shri C. G. Karhadkar
Director

Dr. N. Subramanian
Incubation Centre

Accounts

Shri S. A. Murugesan
Internal Financial Advisor

Smt. Anita Suresh Kunder
Senior Accounts Officer

Administration

Shri Paresh Nath Mahadani
Chief Administrative Officer

- Dr. V. A. Lalita Prasad — Administrative Officer (L & G) & R
- Shri P. T. Mani — Administrative Officer (Estt & Vig.)

Editorial Team

Shri J. Rajan
Chairman

Shri Biswanath Sen

Dr. R. Mythili

Dr. C. V. S. Brahmananda Rao

Dr. N. R. Sanjay Kumar

Shri M. Thangamani,

Shri M. Rajendra Kumar

Shri S. Kishore

Shri G. Venkat Kishore

Dr. P. N. Sujatha

Dr. N. Ramanathan

Dr. N. Desigan

Shri P. Vijaya gopal
Secretary

Shri K. Varathan

Birds and Butterflies of Kalpakkam

Published by PHRMD, SQ&RMG, IGCAR, Kalpakkam-603102